

LATE QUATERNARY ERUPTIVE HISTORY OF MOUNT EREBUS, ANTARCTICA
USING $^{40}\text{Ar}/^{39}\text{Ar}$ GEOCHRONOLOGY AND TEPHROSTRATIGRAPHY

by
Christopher J. Harpel

Submitted in Partial Fulfillment of the Requirements
for the Degree of Master of Science in Geology
November, 2000

Department of Earth and Environmental Science
New Mexico Institute of Mining and Technology
Socorro, New Mexico

ABSTRACT

Mount Erebus has been active throughout the last 109 ky. During this time period extensive volcanic activity, in the form of both effusive and explosive eruptions, has taken place. The $^{40}\text{Ar}/^{39}\text{Ar}$ dating method has been applied to lava flows in the summit region of Mount Erebus to obtain ages for the flows and also to constrain the ages of two caldera-collapse events. Pre-caldera lavas from the north and east sides of the summit region range in age from 109 ± 11 ka to 78 ± 6 ka. Another group of pre-caldera flows on the southwest side of the caldera, is much younger with ages of 26 ± 3 ka and 21 ± 3 ka. The oldest caldera-collapse event is constrained between the ages of these pre-caldera flows and occurred between 23 ka and 84 ka. Post-caldera flows range in age from 16 ± 7 ka to 0 ka (at 2σ error). The youngest caldera-collapse event is bracketed in age between the southwestern and post-caldera flows and occurred between 24 ka and 11 ka.

Explosive eruptive activity has produced multiple englacial tephra layers found in the area surrounding Mount Erebus. Two distal tephra are found in blue ice areas up to 210 km away from the volcano. These tephra layers were deposited from by large phreatomagmatic and plinian eruptions. The large plinian eruption has been dated at 39 ± 6 ka and might be related to formation of the older caldera. Many tephra layers occur exposed in blue ice on the Barne Glacier. Two of these tephra layers are dated at a maximum of 70 ± 4 ka and 15 ± 4 ka. However, the older of the two ages is likely too old due to xenocrystic contamination and must be regarded as a maximum age rather than an eruptions age for the tephra sample. The Barne Glacier provides a natural stratigraphic framework for the tephra. All of the tephra are phonolitic in composition

and show no major of trace element variations. The majority of explosive activity has been either strombolian or phreatomagmatic in nature. A trachytic tephra layer was found that is believed to result from a plinian eruption at The Pleiades in northern Victoria Land.

ACKNOWLEDGMENTS

Many people deserve my thanks for their help, both directly and indirectly, in the completion of this thesis. My committee members have been supportive of my work during this long process and have all provided help in their individual ways. Phil Kyle gave me the opportunity to work in Antarctica, by far one of the most beautiful and magical places on Earth, and has also provided guidance during the long process of my thesis work. Bill McIntosh has kept my writing concise and honest, while at the same time becoming a good friend. Nelia Dunbar throughout this entire process has served as the necessary voice of reason, has enthusiastically encouraged me in the microscopic exploration of my tephra, and was very patient with me during all of my “Nelia, come quick, black smoke is pouring out of the probe!” moments of humor. Also, both Pat Mills and Connie Apache have been helpful in dealing with the bureaucratic aspects of graduate school.

Field assistance in Antarctica was provided by Phil Kyle, Jean Wardell, Kurt Panter, and Al Eschenbacher. I owe Al a special thanks for both sharing his book and not trying to implant the “Scooby Doo” theme song in my head while we were tent-bound at Hooper’s Shoulder during Christmas 1997. Al was also a tremendous help when the weather finally cleared and we were able to sample tephra layers. GPS equipment was provided by UNAVCO during the 1997 field season and both Oivind Ruud and Bjorn Johns provided assistance with processing the GPS data. Without the pilots of Petroleum Helicopters Inc., who were responsible for our safe transportation around Mount Erebus,

this project would never have existed. Funding for this project was provided by a NSF Polar Programs grant to Phil Kyle.

Assistance during the $^{40}\text{Ar}/^{39}\text{Ar}$ dating process was provided by Rich Esser, Lisa “you used how much HF?!?” Peters, and Matt Heizler of the New Mexico Geochronology Research Laboratory. I owe them thanks for always keeping their cool even when I was flipping out. Rich deserves special thanks for sampling tephra in Antarctica for me and for his patience, guidance, and assistance in the lab.

Many times in acknowledgments sections people neglect to mention their friends. However, during graduate work there are always times when things get rough and your moral is low. During these times having someone around to go hiking with or even just to rant at that understands what you are going through makes life a lot easier. I feel lucky that I was able to establish some close friendships during my thesis work and without people like Geff Rawling, Jeff Winick, Peter Rinkleff, Erik Munroe, and Erwin Melis (and of course his the four-footed furry symbiot Suske!) I probably would have gone insane. Also, I need to thank Matt Tennis who has always stood by my side through thick and thin.

Finally, I am truly indebted to my family, especially my parents and both sets of grandparents, who have always encouraged me throughout my college career. Without their support I would never have gotten this far.

TABLE OF CONTENTS

	Page
ABSTRACT	ii
ACKNOWLEDGMENTS	iv
TABLE OF CONTENTS	vi
LIST OF TABLES	vii
LIST OF FIGURES	ix
INTRODUCTION	xii
SUMMARY	xiii
REFERENCES	xiv

SECTION A

Late Pleistocene and Holocene Eruptive History of Mount Erebus Using the $^{40}\text{Ar}/^{39}\text{Ar}$ Dating Method

ABSTRACT	A-1
INTRODUCTION	A-2
METHODS	A-8
Sample Preparation	A-8
Analytical Procedure	A-9
RESULTS	A-10
Furnace Step-Heating	A-10
Laser Step-Heating	A-18
DISCUSSION	A-18
Laser vs. Furnace Step-Heating	A-18
Geologic Implications – Summit Lavas	A-22

Geologic Implications – Caldera Collapse	A-25
Geologic Implications – Tephra	A-29
CONCLUSIONS	A-31
REFERENCES	A-33

SECTION B

Tephrostratigraphy of Mount Erebus, Ross Island, Antarctica

ABSTRACT	B-1
INTRODUCTION	B-2
TEPHRA	B-6
Tephra Characteristics	B-11
METHODS	B-12
Sampling	B-12
Electron Microprobe Analysis	B-12
Instrumental Neutron Activation Analysis	B-13
Geochemical Correlation	B-20
Scanning Electron Microscopy	B-20
RESULTS	B-21
Geochemistry	B-21
Scanning Electron Microscopy	B-26
DISCUSSION	B-40
Geochemistry	B-40
Geochemical Correlation	B-41

Eruption Mechanisms	B-42
Spherical and Budding Ash	B-48
Analcime	B-51
Trachytic Tephra	B-52
CONCLUSIONS	B-56
REFERENCES	B-57

SECTION C

APPENDICES

INTRODUCTION	C-1
References	C-3
APPENDIX 1 - $^{40}\text{Ar}/^{39}\text{Ar}$ furnace step-heating data	C-4
APPENDIX 2 - $^{40}\text{Ar}/^{39}\text{Ar}$ laser step-heating data	C-9
APPENDIX 3 - Glass geochemistry from electron microprobe analysis	C-11
APPENDIX 4 - Glass standard analysis from electron microprobe analysis	C-125
APPENDIX 5 - Feldspar geochemistry from electron microprobe analysis	C-134
APPENDIX 6 - Feldspar standard analysis from electron microprobe analysis	C-152
APPENDIX 7 – Matrix of geochemical similarity	C-161
APPENDIX 8 – Sample locations	C-167
APPENDIX 9 – Tephra sample stratigraphy and equivalence	C-168

LIST OF TABLES

	Page
Table A1 – Summary of plateau ages for the summit lava flows and tephra.	A-16

Table A2 – Summary of samples that yielded invalid plateau ages or where no plateau age was assigned.	A-17
Table B1 – Electron microprobe analyses of glass from phonolitic tephra.	B-14
Table B2 – Instrumental neutron activation analysis of phonolitic tephra samples.	B-18
Table B3 – Table of the tephra component abundances, grain size distribution, morphological features, and eruption type.	B-28
Table B4 – Major element composition of sample EBT-61 and trachytes from Mount Erebus and The Pleiades.	B-54

LIST OF FIGURES

	Page
Figure A1 – A map of Mount Erebus showing the age and location of flank sites mentioned in the text.	A-3
Figure A2 – Typical examples of anorthoclase crystals used for $^{40}\text{Ar}/^{39}\text{Ar}$ dating.	A-5
Figure A3 – Fresh flow features on Mount Erebus summit lava flows.	A-5
Figure A4 – Typical melt inclusions that host both the $^{38}\text{Ar}_{\text{Cl}}$ (a proxy for Cl) and $^{40}\text{Ar}_{\text{E}}$ detected during $^{40}\text{Ar}/^{39}\text{Ar}$ analysis.	A-7
Figure A5 – Age spectra yielding valid ages from $^{40}\text{Ar}/^{39}\text{Ar}$ furnace step-heating.	A-11
Figure A6 – Age spectra for furnace and laser step-heated samples that yielded invalid $^{40}\text{Ar}/^{39}\text{Ar}$ ages or where plateau ages were not assigned.	A-14

Figure A7 – Age spectra for laser step-heated samples that yielded valid $^{40}\text{Ar}/^{39}\text{Ar}$ ages.	A-19
Figure A8 – Geologic map of the summit plateau of Mount Erebus showing the lava flows, sample locations, ages (ka), and general features of the region.	A-23
Figure A9 – Age distribution and ideogram of eruptive events for the last 121 ky on Mount Erebus.	A-24
Figure A10 – A photo looking northeast at the upper slopes of Mount Erebus showing the break in slope interpreted to be a nested caldera.	A-27
Figure B1 – Map of Victoria Land and the Ross Sea region showing the locations of sites mentioned in the text.	B-3
Figure B2 – Map of Mount Erebus and the immediate vicinity showing the tephra sampling sites and features mentioned in the text.	B-4
Figure B3 – Photos of tephra features.	B-8
Figure B4 – A map of the Hooper’s Shoulder site showing sampling locations determined using GPS.	B-10
Figure B5 – Total alkali vs. silica plot.	B-22
Figure B6 – Harker variation diagrams showing that all of the tephra plot as a group except for sample EBT-61.	B-23
Figure B7 – OIB and chondrite normalized spider diagrams for the phonolitic tephra.	B-24
Figure B8 – Trace element variation diagrams vs. Th.	B-25
Figure B9 – Feldspar ternary diagram showing feldspar analyses from all of the phonolitic tephra samples.	B-27
Figure B10 – Typical crystal phases found in the tephra samples.	B-32
Figure B11 – Typical examples of strombolian and phreatomagmatic tephra samples.	B-33
Figure B12 – Typical features of phreatomagmatic tephra samples.	B-34
Figure B13 – Typical tephra morphologies indicative of strombolian eruptions.	B-36

Figure B14 – Typical rounded droplets and budding ash associated with strombolian activity.	B-37
Figure B15 – Typical analcime crystals that are a xenocrystic phase in some of the phonolitic tephra samples.	B-38
Figure B16 – The distal samples erupted from Mount Erbeus.	B-39
Figure B17 – A typical mixed phreatomagmatic and strombolian tephra sample.	B-44
Figure B18 – Typical features of the trachytic sample EBT-61.	B-53

POCKET

CD ROM – Scanning electron microprobe images of tephra samples used in this study.	In Pocket
--	-----------

INTRODUCTION

The eruptive history of Mount Erebus has only recently begun to be unraveled through both observations and isotopic dating methods. The volcano was discovered 27 January 1841 by James Ross, but between that time and the International Geophysical Year (1956) observations of the volcano were sporadic. Close observations of the volcano only begin in 1972 with the discovery of the lava lake and the initiation of yearly visits (Giggenbach *et al.*, 1973 ;Kyle *et al.*, 1982). Esser (1996) used the $^{40}\text{Ar}/^{39}\text{Ar}$ dating method to investigate the pre-historic eruptive history of the volcano. However, a large portion of the eruptive record from the mid-Pleistocene through the Holocene remained unknown. Numerous young lava flows were known to exist in the summit region of Mount Erebus and recent discoveries of englacial tephra were suspected to be “young” in age.

The purpose of this study is to explore the eruptive history of Mount Erebus from the mid-Pleistocene to the present day. Two distinct approaches are used to achieve this objective and this study has been broken into two sections accordingly. The first section explores the eruptive history of lava flows in the summit region of the volcano and was conducted using the $^{40}\text{Ar}/^{39}\text{Ar}$ dating method. These young lava flows are broken into pre-caldera flows that were truncated during caldera collapse and post-caldera flows that filled in the resulting caldera in the summit region of Mount Erebus. By dating these flows it is possible to not only determine the age of the flows themselves, but to bracket the ages of caldera-forming events by using the ages of truncated and non-truncated flows.

The second portion of this work uses englacial tephra layers to investigate the pre-historic explosive eruptive history for Mount Erebus. Previously, the explosive eruptive record for Mount Erebus has been limited to the observed strombolian eruptions and a single phreatic eruption episode in 1993. Englacial tephra layers are found in patches of blue ice on the flanks of Mount Erebus and in the surrounding area of Ross Island. Two distal tephra layers from Mount Erebus are also found in blue ice localities in the Transantarctic Mountains, Victoria Land. The $^{40}\text{Ar}/^{39}\text{Ar}$ dating method was used to date two of the tephra units on the Barne Glacier and one of the distal tephra samples. Through using scanning electron microscopy (SEM) it is also possible to determine the type of eruption that produced the tephra. The eruptive record for Mount Erebus has been expanded using the $^{40}\text{Ar}/^{39}\text{Ar}$ ages to constrain the timing of explosive activity. Also, it is possible to investigate geochemical progressions exposed within the tephra.

SUMMARY

Mount Erebus has been active throughout the last 109 ky and has produced both lava flows and tephra fall deposits. The lava flows are broken into old-pre-, young-pre-, and post-caldera flows with two caldera-collapse events bracketed by the three groups of flows. The old pre-caldera flows are anorthoclase-tephriphonolite in composition and range in age from 109 ± 11 ka to 78 ± 6 ka. Following this period of summit activity volcanism appears to have shifted to the flanks of the volcano. Also during this time period there may have been a caldera-collapse event between 84 ka and 7 ka, but most likely occurring before 23 ka.

At around 33 ka a new pulse of magmatism occurred that heralded the onset of both anorthoclase phonolite volcanism and the reinitiation of summit activity. At around 25 ka the Three Sister's Cones and the two young-pre-caldera flows (21 ± 4 ka and 26 ± 4 ka) were erupted reinitiating summit activity. Eruption of the young pre-caldera flows was followed by the young-caldera-collapse event bracketed between 29 ka and 2 ka, and most likely occurring before 11 ka. Extrusion of the post-caldera lava flows followed the young-caldera-collapse event. These flows range in age from 16 ± 7 ka to within 2σ error of zero age.

Eruptive activity also took the form of explosive, tephra-producing eruptions. Numerous englacial tephra layers have been found on the flanks of Mount Erebus and in the surrounding regions on Ross Island. Two distal tephra layers have also been found in the Transantarctic Mountains to the northwest of Mount Erebus. All of the tephra, with the one exception, are phonolitic in composition and are derived from Mount Erebus. Both the major and the trace element geochemistry are homogeneous for the phonolitic tephra. The proximal tephra layers show evidence of both strombolian and phreatomagmatic eruptive activity at Mount Erebus. The two distal layers are derived from large-phreatomagmatic and plinian eruptions indicating that the volcano is capable of large-scale explosive eruptive activity. A single trachytic tephra from blue ice near the summit of Mount Terra Nova is derived from a plinian eruption at The Pleiades in northern Victoria Land.

REFERENCES

- Esser, R.P., 1996, $^{40}\text{Ar}/^{39}\text{Ar}$ dating of Mount Erebus volcano, Antarctica: Socorro, NM, New Mexico Institute of Mining and Technology, Master's, 183 p.

Giggenbach, W.F., Kyle, P.R., and Lyon, G.L., 1973, Present volcanic activity on Mount Erebus, Ross Island, Antarctica: *Geology*, v. 1, p. 135-136.

Kyle, P.R., Dibble, R.R., Giggenbach, W.F., and Keys, J., 1982, Volcanic activity associated with the anorthoclase phonolite lava lake, Mount Erebus, Antarctica, *in* Craddock, C., ed., *Antarctic Geoscience*: Madison, Wisconsin, University of Wisconsin Press, p. 735-745.

Late Pleistocene and Holocene Eruptive History of Mount Erebus Using the $^{40}\text{Ar}/^{39}\text{Ar}$ Dating Method

ABSTRACT

Furnace and laser step-heating $^{40}\text{Ar}/^{39}\text{Ar}$ ages have been determined for 15 lava flows in the summit region of Mount Erebus and three Erebus derived-englacial tephra layers. Mount Erebus is located on Ross Island, Antarctica, is currently the most active volcano in Antarctica. The summit region is composed of at least one caldera and possibly two superimposed calderas that have been filled by post-caldera lava flows ranging in age from 16 ± 7 ka to 2 ± 7 ka. Pre-caldera summit flows display two age populations at 109 ± 11 ka to 78 ± 6 ka and 26 ± 3 ka to 21 ± 3 ka that are tephriphonolitic and phonolitic in composition, respectively. Caldera-collapse occurred between 29 ka and 2 ka, and was likely before 11 ka. An older caldera-collapse event might have occurred between 84 ka and 7 ka, and potentially before 23 ka. Two tephra layers from the flanks of Mount Erebus have been dated at 70 ± 4 ka and 15 ± 4 ka. These ages have been used to bracket the ages for other undated-englacial tephra layers. The single distal-plinian-fall tephra sample has an age of 39 ± 6 ka and is one of the first true phonolites produced at Mount Erebus. The summit region of Mount Erebus has been active for the last 109 ky and has experienced at least one plinian eruption, likely two caldera-forming events, and multiple lava flows and small explosive eruptions.

INTRODUCTION

Mount Erebus, located on Ross Island, is currently the most active volcano on the Antarctic plate (Fig. A1). Current activity is in the form of frequent strombolian eruptions from a convecting anorthoclase-phonolite lava lake in the main crater of the summit cone (Kyle *et al.*, 1982). Surrounding the summit cone is a broad circular plateau (~4.5 km diameter) previously interpreted as a caldera that has been filled by post-collapse lava flows and pyroclastic deposits (Moore and Kyle, 1987). The summit plateau region has been geologically mapped and divided into ten individual post-caldera flow units and pre-caldera flows truncated during caldera collapse (Caldwell, 1989). The composition of the post-caldera lava flows is phonolitic whereas the pre-caldera flows range from phonolitic to tephriphonolitic (Moore and Kyle, 1987; Caldwell, 1989). Both the pre- and post-caldera lava flows contain abundant (up to 30% by volume) anorthoclase feldspar megacrysts as large as 10 cm in length (Fig. A2a) (Kyle, 1977; Dunbar *et al.*, 1994). The lava flows exhibit abundant features characteristic of young lava flows (Fig. A3), such as pahoehoe ropes, glassy rinds, and tumuli, and have been considered some of the youngest eruptive features on the volcano. Englacial tephra layers derived from Mount Erebus have been recognized in blue ice areas exposed along the Transantarctic Mountains at Mt. DeWitt and Manhaul Bay, Allen Hills and at numerous places on Mount Erebus and adjacent areas of Ross Island. These tephra layers provide evidence for previously undocumented explosive eruptive activity of Mount Erebus.

The eruptive history of Mount Erebus has only recently begun to be understood through both observation and isotopic dating. The historic record for Mount Erebus

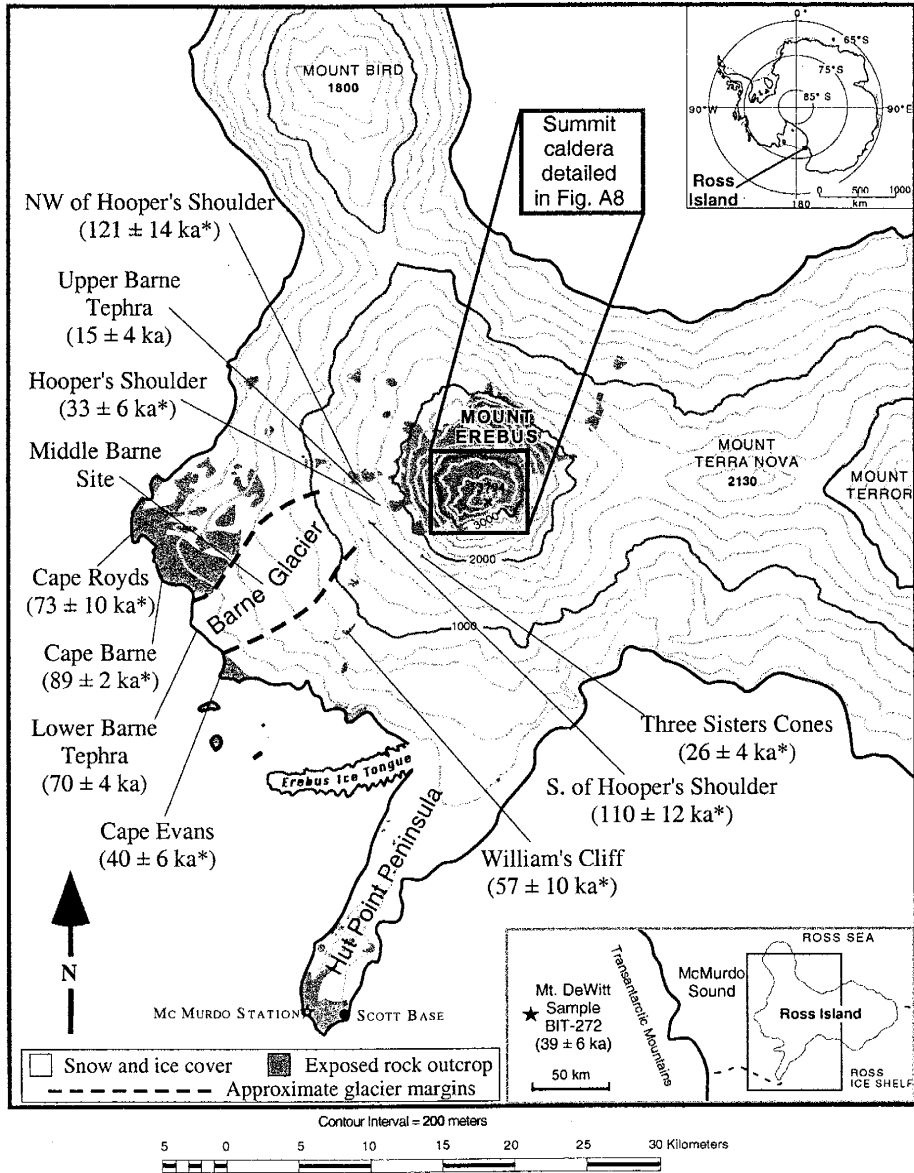


Figure A1-A map of Mount Erebus showing the age and location of flank sites mentioned in the text (modified from Esser, 1996). Ages marked with an * are from Esser (1996). The tephra collection sites and ages are also marked along with the location of the distal tephra in the inset box.

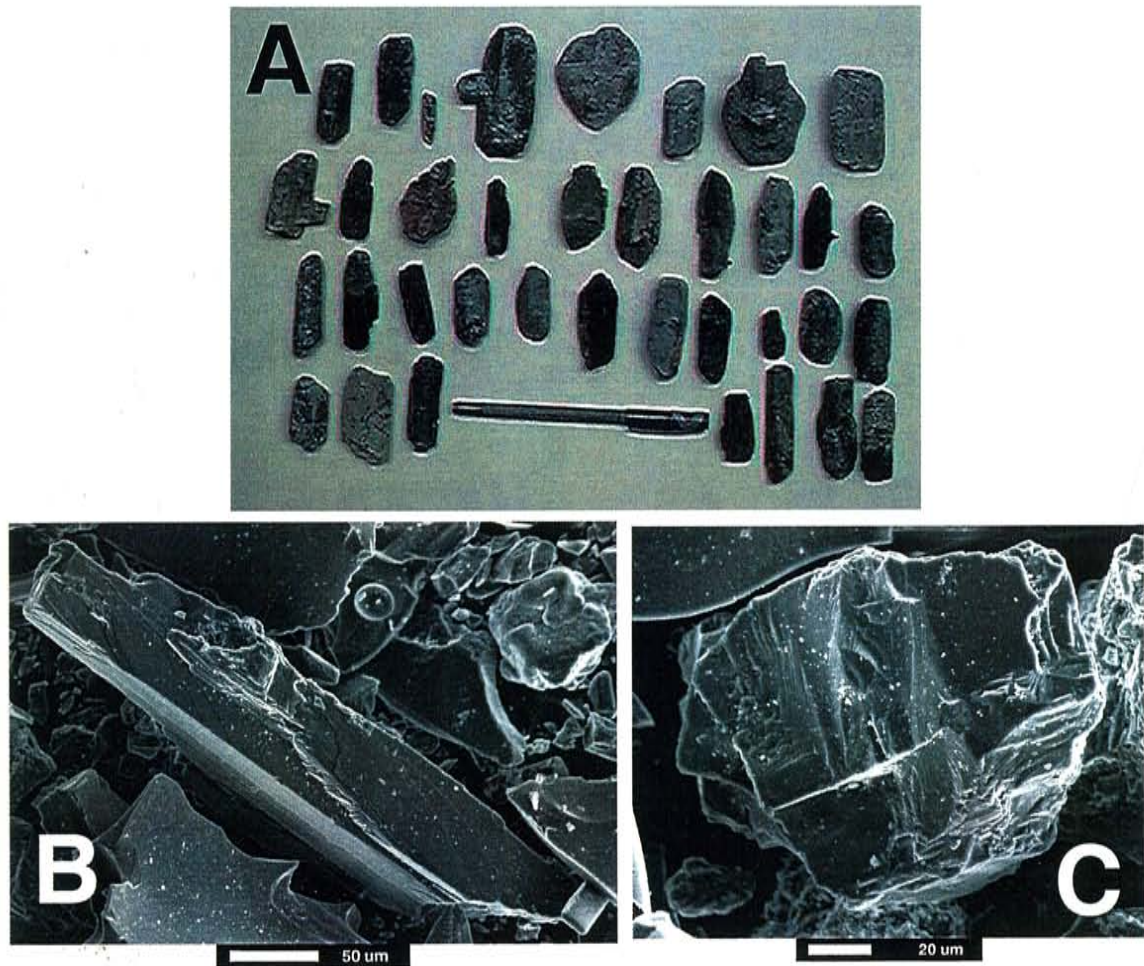


Figure A2-Typical examples of anorthoclase crystals used for $^{40}\text{Ar}/^{39}\text{Ar}$ dating. **A:** Anorthoclase crystals similar to those in the summit lava flows. These crystals are up to 10 cm in length and generally have abundant adhering glass. Pen for scale is around 15 cm long. **B and C:** Typical anorthoclase from the tephra layers. This anorthoclase is an independent crystal phase within the tephra samples and generally has little adhering glass.

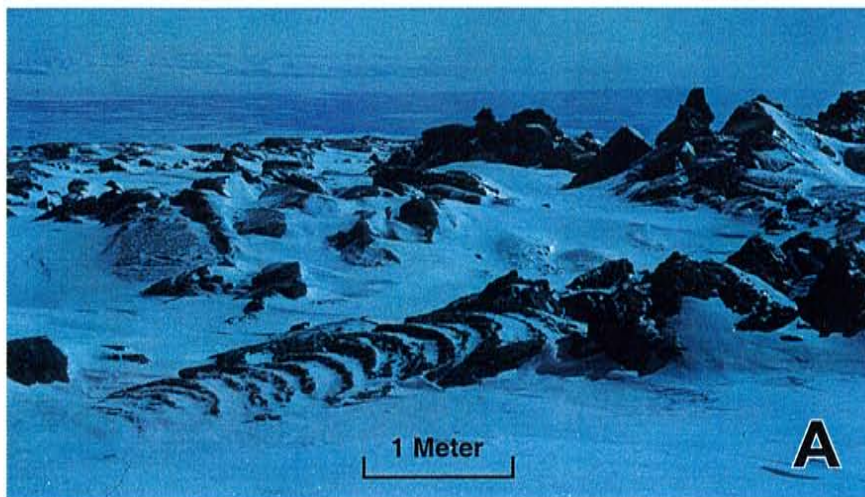


Figure A3-Fresh flow features of Mount Erebus summit lava flows. **A:** Ropy pahoehoe on the Lower Hut flow. **B:** Ropy pahoehoe on the Nausea Knob flow. Note the circled ice axe for scale. **C:** A tumuli in the Lower Hut flow with large pahoehoe ropes on the sides. Note the person for scale.

extends back to the discovery of the volcano in 1841. However, detailed eruptive records only exist since 1972 (Kyle *et al.*, 1982, Kyle, 1994). Initial ages for prehistoric eruptive activity were limited to a few conventional K/Ar ages (Treves, 1968; Armstrong, 1978; Moore and Kyle, 1987). Esser *et al.* (1997) obtained apparent ages up to 700 ka for historically erupted anorthoclase feldspar and concluded that significant excess argon ($^{40}\text{Ar}_E$; as defined by Dalrymple and Lanphere, 1969) is present within the anorthoclase. Conventional K/Ar dating calculates an age based on the total amount of ^{40}Ar released from a sample. Because all of the released gas is used in K/Ar age calculations, the effect of $^{40}\text{Ar}_E$ can not be ascertained. Therefore the original K/Ar ages for Mount Erebus are now considered unreliable. Esser *et al.* (1997) used the $^{40}\text{Ar}/^{39}\text{Ar}$ dating method to determine that $^{40}\text{Ar}_E$ is hosted in melt inclusions (Fig. A4) within the anorthoclase feldspar and is positively correlated with the Cl/K ratio. Esser *et al.* (1997) also developed a sample preparation method capable of removing the melt inclusions. Esser (1996) examined the eruptive record for Mount Erebus between 1131 ± 16 ka (all error values are reported at 2σ) and 11 ± 8 ka. However, Esser (1996) concentrated on dating lavas on the flanks of Mount Erebus and most of the summit plateau lava flows remained of unknown age. The recently discovered englacial tephra were also of unknown age.

Advances in the $^{40}\text{Ar}/^{39}\text{Ar}$ dating method during the late 1980's and 1990's have facilitated the dating of rocks under 1 Ma in age. The predominant analytical method used in these studies is single crystal laser fusion of high potassium phases such as sanidine (van den Bogaard *et al.*, 1989; Deino and Potts, 1990; Chesner *et al.*, 1991; Deino and Potts, 1992; Turbeville, 1992; Izett and Obradovich, 1994; Hu *et al.*, 1994; van den Bogaard, 1995; Chen *et al.*, 1996). The furnace step-heating method has been

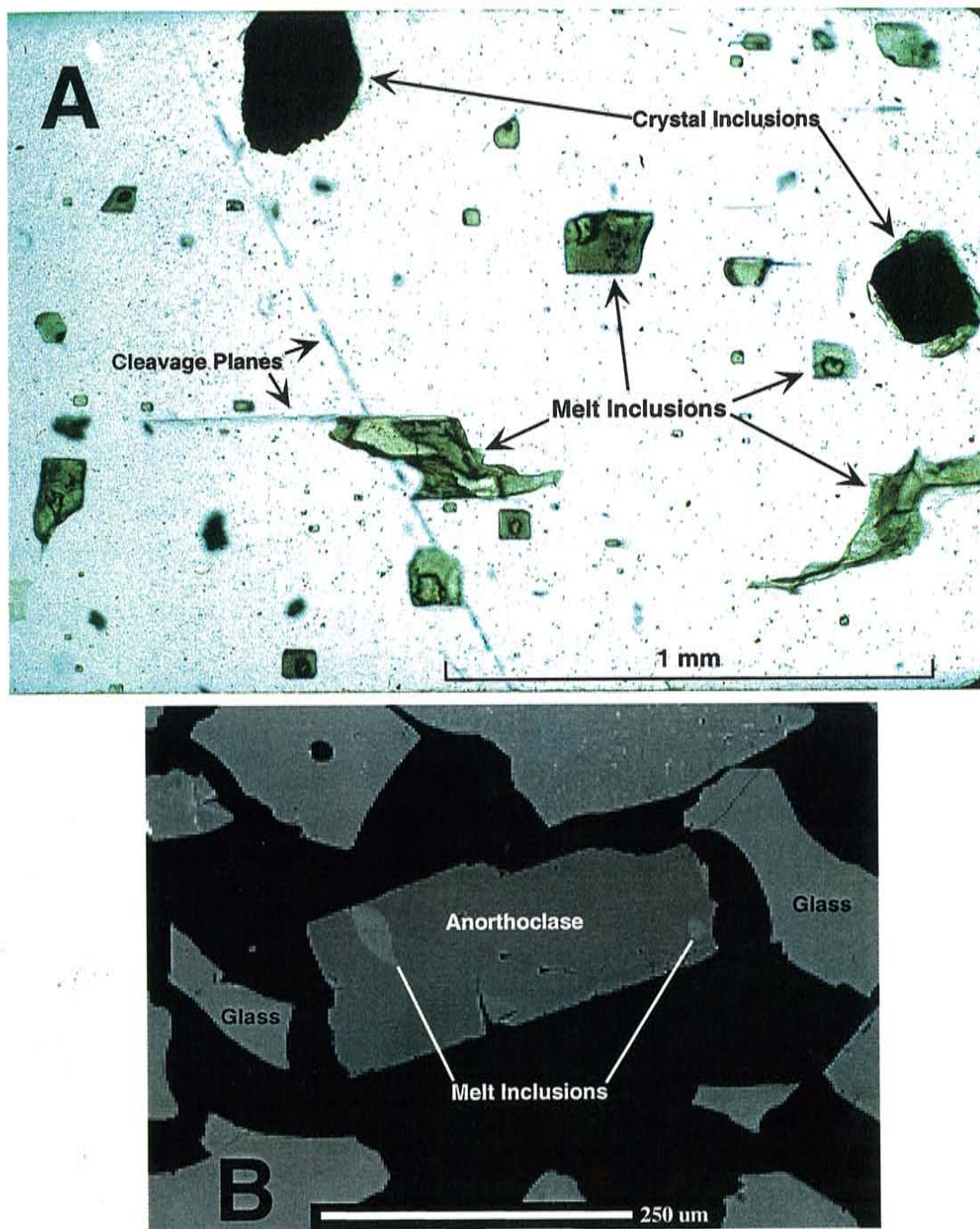


Figure A4-Typical melt inclusions that host both the $^{38}\text{Ar}_{\text{Cl}}$ (a proxy for Cl) and $^{40}\text{Ar}_{\text{E}}$ detected during $^{40}\text{Ar}/^{39}\text{Ar}$ analysis. **A:** A photomicrograph of melt inclusions within an anorthoclase crystal typical of the summit lava flows (photo N.W. Dunbar). **B:** A backscattered electron image of an anorthoclase crystal with melt inclusions from a tephra sample.

successfully used in several studies to date sanidine (McDougall, 1985; Lippolt *et al.*, 1990; Heizler *et al.*, 1999; Rose *et al.*, 1999), anorthoclase (Esser, 1996; Wilch *et al.*, 1999), plagioclase (Pringle *et al.*, 1992; Singer and Pringle, 1996), and whole rock or groundmass samples (Baksi *et al.*, 1992; Duncan and Hogan, 1994; Singer and Pringle, 1996; Esser and Kyle, 1999; Heizler *et al.*, 1999; Wilch *et al.*, 1999). Laser step-heating has also yielded accurate results for young sanidine phenocrysts (Pringle *et al.*, 1992; Renne *et al.*, 1997). Most of these studies have yielded ages in the hundreds of thousands of years range but several have yielded Holocene ages (*e.g.* Chen *et al.*, 1996; Renne *et al.*, 1997; Esser and Kyle, 1999). In this study the $^{40}\text{Ar}/^{39}\text{Ar}$ method has been used to investigate the young eruptive history of the Mount Erebus. Specific emphasis has been placed on constraining the timing of caldera collapse, summit lava flow activity, and explosive, tephra-producing eruptions.

METHODS

Sample Preparation

To obtain accurate $^{40}\text{Ar}/^{39}\text{Ar}$ ages for Mount Erebus anorthoclase it is crucial to mitigate the effect of $^{40}\text{Ar}_E$ by removing melt inclusions (Fig. A4). Sample preparation generally followed Esser *et al.* (1997). Anorthoclase phenocrysts were hand-picked from coarsely crushed lava flow samples, and further crushed and sieved to 125-250 μm to expose melt inclusions. The tephra samples are fine-grained and were not sieved. The tephra samples and fine phenocryst fractions were magnetically separated using a Frantz Isodynamic separator to remove the relatively magnetic glass and phenocrysts (such as olivine). The low-magnetic portions were leached for an initial 30 to 75 minutes in 15%

hydrofluoric acid in an ultrasonic bath to remove melt inclusions and adhering glass. Magnetic separation and hydrofluoric acid leaching was repeated progressively until the samples were nearly pure anorthoclase. The crystal concentrates were finally hand-picked to remove remaining impurities.

Analytical Procedure

Irradiation procedures were identical for samples analyzed with both the furnace and laser step-heating methods. All of the samples were split into ~100 mg aliquots, wrapped in copper foil, and placed into evacuated glass tubes for irradiation. Packets of Fish Canyon Tuff sanidine crystals were interspersed between sample packets as neutron flux monitors and were analyzed by single-crystal fusion with a CO₂ laser (Deino and Potts, 1990). An age of 27.84 Ma was used for the Fish Canyon Tuff sanidine monitor (Deino and Potts, 1990) based on an age of 520.4 Ma for MMhb-1 (Samson and Alexander, 1987).

Furnace step-heating was the primary method of analysis in this study. Approximately 300 mg to 400 mg of anorthoclase was used for each analysis. Samples were heated in a double-vacuum resistance furnace capable of 1750° C and fitted with a molybdenum crucible and liner. A new liner was installed into the furnace prior to analyzing each batch of samples to avoid contamination from previously run older samples. An initial low-temperature step was used to remove atmospheric argon and heating progressed incrementally to ~1700° C.

Laser step-heating was used to analyze five samples. Aliquots of ~200 mg of anorthoclase were used for laser step-heating, except for sample 62 (b) where only ~60

mg was used. Samples were laser step-heated using a 50 W CO₂ laser fitted with a beam integrator that distributes power evenly over a 6 mm by 6 mm square profile. Laser step-heating began at 1 W and progressively increased to 45 W. The initial steps between 1 W and 3 W were run in duplicate for samples 30 (b) and 85 to determine if samples were degassing completely during each step.

All ages are calculated as plateau ages. However, the traditional definition of a plateau as defined by Fleck *et al.* (1977) is not used. In this study a plateau is defined as the relatively flat contiguous steps that have a mean sum weighted deviate (MSWD) that meets or approaches the 95% confidence level using the criteria of Mahon (1996). Error is calculated using the Taylor (1982) method if the MSWD value of the plateau defining steps is within the 95% confidence level defined by Mahon (1996). If the steps are outside the 95% confidence level the Taylor (1982) error is multiplied by the square root of the MSWD to obtain a revised error value.

RESULTS

Furnace Step-heating

Anorthoclase from 20 summit lava flow and tephra samples were analyzed using furnace step-heating and the results can be divided into 17 concordant (Fig. A5) and five discordant age spectra (Fig. A6). The 17 concordant age spectra have plateaus as defined in this study. These plateaus are all composed of at least two contiguous steps and generally include three or more steps. The low-temperature steps have large uncertainties and contain the majority of atmospheric argon and only a small amount of the total ³⁹Ar released. Plateau ages were generally calculated using the steps between 800° C and

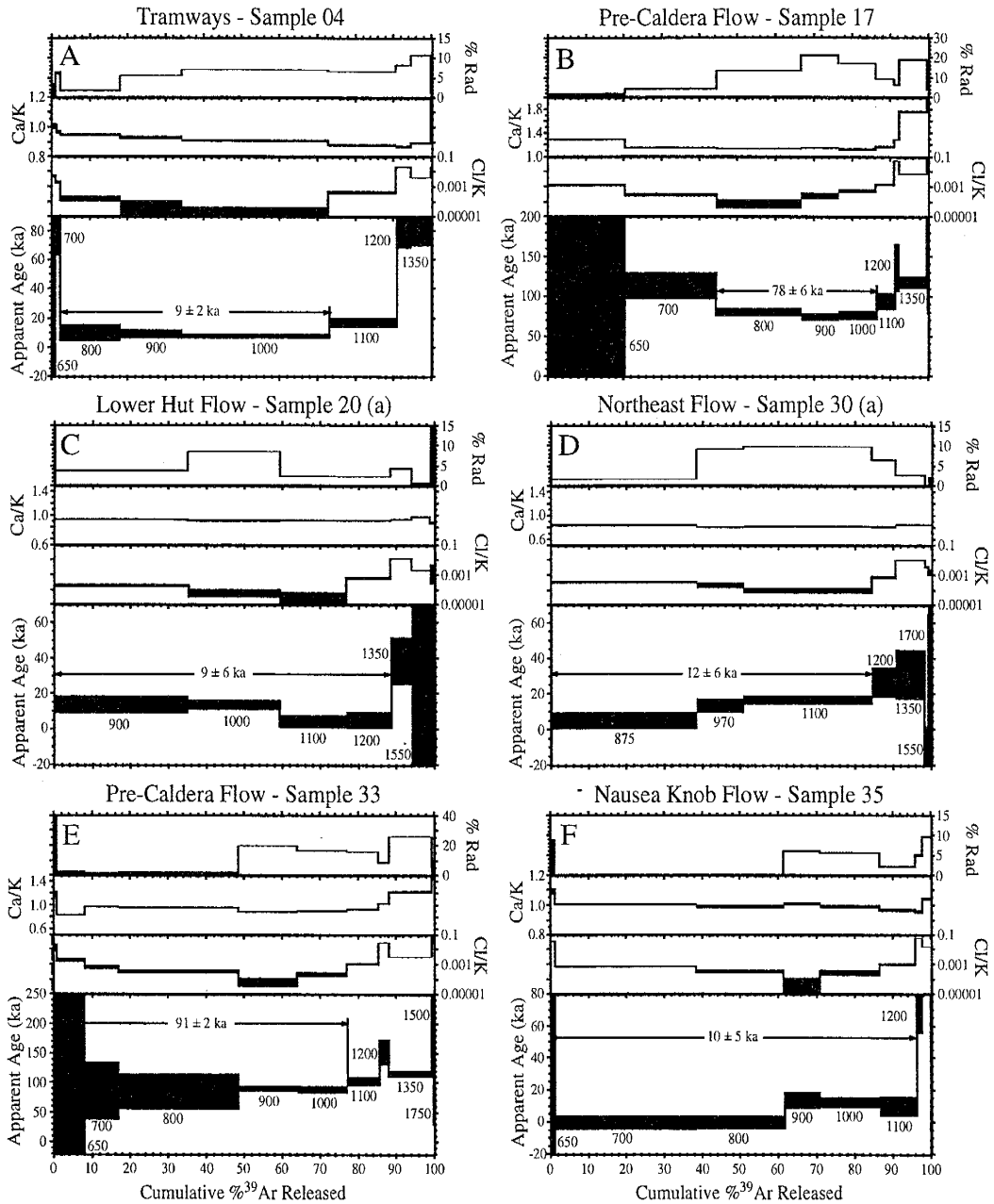


Figure A5-Age spectra yielding valid ages from $^{40}\text{Ar}/^{39}\text{Ar}$ furnace step-heating. Note that the scales on the Y-axis vary between the age spectra, but are the same for all of the samples on the X-axis. Each spectrum shows the radiogenic yield, Cl/K ratio, Ca/K ratio, and apparent age plotted against the cumulative percent ^{39}Ar released. Temperature ($^{\circ}\text{C}$) for each step is indicated below the step and error on each step is shown at 2σ . Note the pervasive increase in apparent age, Cl/K ratio, and radiogenic yield that occurs at around 1200°C in all of the age spectra indicating melting of the anorthoclase and release of trapped gas within melt inclusions. Age spectra A through Q are referred to in the text and Table A1.

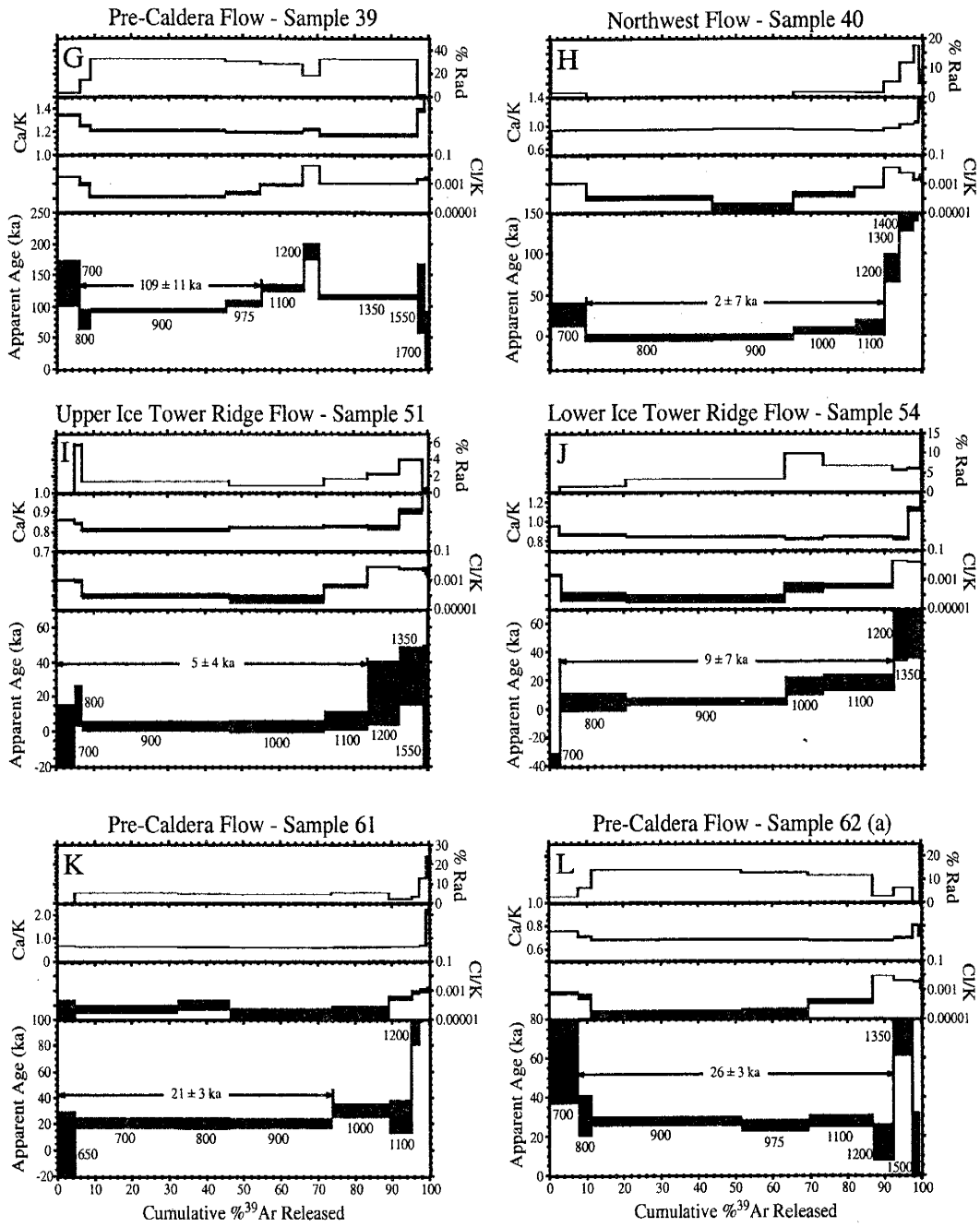


Figure A5 continued

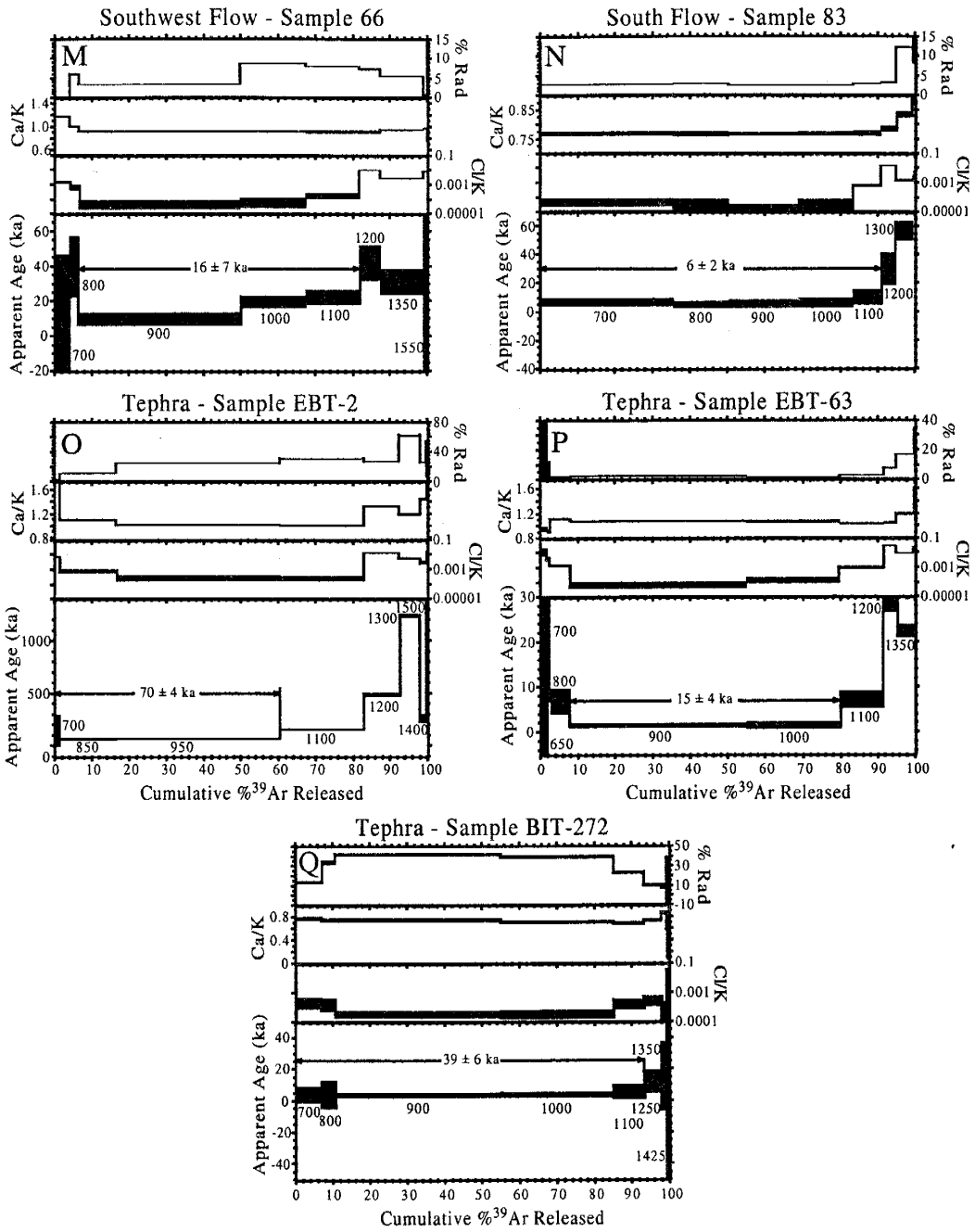


Figure A5 continued

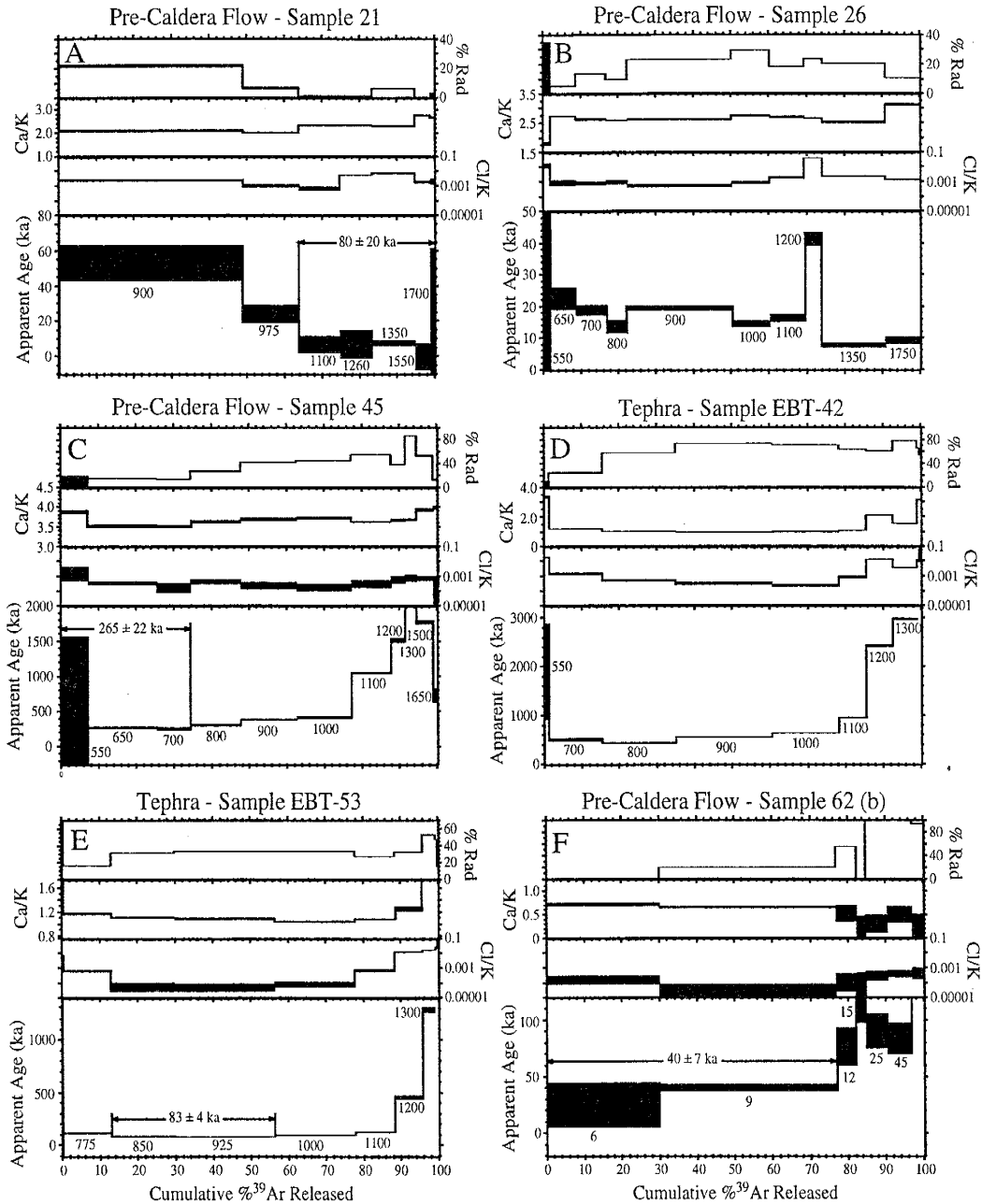


Figure A6-Age spectra for furnace and laser step-heated samples that yielded invalid $^{40}\text{Ar}/^{39}\text{Ar}$ ages or where plateau ages were not assigned. Note that the scale on the Y-axes varies between age spectra, but is the same on the X-axes. Each spectrum shows the radiogenic yield, Cl/k ratio, Ca/K ratio, and apparent age plotted against the cumulative percent ^{39}Ar released. Temperature ($^{\circ}\text{C}$) or power (Watts; for sample 62 (b)) for each step is indicated below the step and error on each step is shown at 2σ . Age spectra A through F are referred to in the text and Table A2.

1100° C, but steps as low as 550° C and as high as 1200° C were used when the apparent ages were isochronous with the main plateau forming steps and have low Cl/K ratios. K/Ca ratios are stable for plateau-forming steps and generally range from 0.9 to 1.1. All plateau-forming steps have low Cl/K ratios indicating that the influence of $^{40}\text{Ar}_E$ on the apparent age of the step is minimal (Esser *et al.*, 1997). Anorthoclase begins to melt at 1200° C causing characteristic increases in apparent age, Cl/K ratio, and radiogenic yield due to the release of $^{40}\text{Ar}_E$ and $^{38}\text{Ar}_{Cl}$ from small melt inclusions (Fig. A5) (Esser *et al.*, 1997). Plateau ages from concordant age spectra are interpreted to represent accurate eruption ages (Table A1).

The discordant age spectra do not yield geologically significant ages (Fig. A6) (Table A2). The first sample, 45, has an age spectrum (Fig. A6c) that is flat for the initial three heating steps with an apparent age of 265 ± 22 ka. The low temperature steps are strongly contaminated with atmospheric argon and the Cl/K ratio is relatively high indicating that $^{40}\text{Ar}_E$ is being released from the glass making the apparent age too old. Sample 21 has an age spectrum (Fig. A6a) with the minimum apparent ages between 1100° C and 1500° C. However, because $^{40}\text{Ar}_E$ is typically released from trapped melt inclusions at 1200° C the apparent age is considered meaningless. An age of 83 ± 4 ka is calculated for sample EBT-53, but sample EBT-63 (Fig. A5p) is from the same tephra layer and has an age of 15 ± 4 ka. The age for sample EBT-53 is too old likely due to the influence of $^{40}\text{Ar}_E$. The age spectra for samples 26 (Fig. A6b) and EBT-42 (Fig. A6d) do not have any steps that are considered to define plateaus. No age was calculated for these samples.

Table A1–Summary of plateau ages for the summit lava flows and tephra.

Sample #	Figure	Flow	L #*	Method	Steps [†]	# Steps	Age	Error ($\pm 2\sigma$)
39	6g	Pre-Caldera	9864	Furnace	800-975	3	109	11
33	6e	Pre-Caldera	50615	Furnace	700-1000	4	91	2
E93013 [‡]	-	Pre-Caldera	2646	Furnace	-	-	87	14
17	6b	Pre-Caldera	50614	Furnace	800-1100	4	78	6
62 (a)	6l	Pre-Caldera	9870	Furnace	800-1200	5	26	3
61	6k	Pre-Caldera	50613	Furnace	650-900	4	21	3
66	6m	Southwest	9869	Furnace	900-1100	3	16	7
85	8d	Southeast	9874	Laser	2-6	5	13	3
30 (a)	6d	Northeast	9865	Furnace	900-1100	3	12	6
30 (b)	8b		9872	Laser	1-9	10	14	3
30 (c)	8c		9879	Laser	5-6	2	10	4
					<i>Weighted Mean</i>		13	2
20 (a)	6c	Lower Hut	9867	Furnace	900-1200	4	9	6
20 (b)	8a		9873	Laser	4-6	2	14	7
34 [‡]	-		842	Furnace	-	-	11	8
					<i>Weighted Mean</i>		11	4
35	6f	Nausea Knob	50612	Furnace	650-1100	6	10	5
04	6a	Tramways	50611	Furnace	800-1000	3	9	2
54	6j	Lower Ice Tower Ridge	8857	Furnace	800-1100	4	9	7
83	6n	South	8851	Furnace	700-1100	5	6	2
51	6i	Upper Ice Tower Ridge	8860	Furnace	700-1100	5	5	4
40	6h	Northwest	8855	Furnace	800-1100	4	2	7
EBT-2	6o	Tephra	8852	Furnace	700-960	3	70	4
BIT-272	6q	Tephra	8428	Furnace	700-1100	5	39	6
EBT-63	6p	Tephra	50618	Furnace	1000-1100	2	15	4

Notes: All sample numbers are prefixed by "E870" except for tephra samples and sample E93013. Samples were irradiated in four batches, NM-??, NM-85, NM-99, and NM-112, at the University of Michigan Ford Research Reactor for 30 minutes under a fast neutron flux of approximately 7.0×10^{-5} to 8.5×10^{-5} J hr⁻¹. All analyses were carried out at the New Mexico Geochronological Research Laboratory, New Mexico Institute of Mining and Technology on a Mass Analyzer Products 215-50 mass spectrometer. Ages are calculated using the decay constants of Steiger and Jäger (1977) and precision includes error accrued from background, isotope measurements, isotope correction factors, and J measurements. Error in J measurements based on analysis of four sanidine crystals per location generally did not exceed $\pm 0.1\%$ at 2σ . All ages have been corrected for blank.

Furnace blanks were 15.765 pA, 25.642 pA, 50.000 pA, and 42.866 pA for ⁴⁰Ar and 0.068 pA, 0.096 pA, 0.050 pA, and 0.113 pA for ³⁹Ar during the NM-78, NM-85, NM-99, and NM-112 batches respectively. Laser blanks were 12.253 pA and 0.068 pA for ⁴⁰Ar and ³⁹Ar respectively. Interfering reactor induced reactions were accounted for using the following correction factors: (³⁶Ar/³⁷Ar)Ca = 0.00026 \pm 0.00002, (³⁹Ar/³⁷Ar)Ca = 0.007 \pm 0.00005, (⁴⁰Ar/³⁹Ar)K = 0.0002 \pm 0.0003 (for NM-78), (⁴⁰Ar/³⁹Ar)K = 0.025 \pm 0.005 (for all other irradiations). Reactive gases during furnace heating were cleaned during furnace analysis for 600 seconds in the first stage and 420 seconds in the second stage. Argon was purified using three SAES GP-50 getters, two operated at $\sim 450^\circ\text{C}$ and the third at $\sim 20^\circ\text{C}$, and a tungsten filament operated at $\sim 2000^\circ\text{C}$. Reactive gases during laser heating were removed using two SAES GP-50 getters operated at $\sim 450^\circ\text{C}$ and $\sim 20^\circ\text{C}$, a $\sim 2000^\circ\text{C}$ tungsten filament, and a cold finger operated at -140°C to aid in H₂O removal. Sensitivity of the electron multiplier was 1×10^{-16} mol. pA⁻¹ during furnace step-heating and 7×10^{-17} mol. pA⁻¹ for laser step-heating analysis.

*Laboratory Number

[†]In $^\circ\text{C}$ for furnace step-heated samples and Watts for laser step-heated samples.

[‡]From Esser (1996)

Table A2—Summary of samples that yielded invalid plateau ages or where no plateau age was assigned.

Sample #	Figure	Flow	L #*	Method	Steps [†]	# Steps	Age	Error ($\pm 2\sigma$)
26	7b	Pre-Caldera	50617	Furnace	-	-	n.a.	n.a.
45	7c	Pre-Caldera	50616	Furnace	550-700	3	265	22
21	7a	Pre-Caldera	9866	Furnace	1100-1700	5	80	20
62 (b)	7f	Pre-Caldera	9878	Laser	6-9	2	40	7
EBT-42	7d	Tephra	8854	Furnace	-	-	n.a.	n.a.
EBT-53	7e	Tephra	8853	Furnace	850-925	2	83	4

Notes: For the analytical details see the notes in Table A1, "n.a." indicates that no plateau age was assigned to the sample.

*Laboratory Number

[†]In °C for furnace step-heated samples and Watts for laser step-heated samples.

Laser Step-heating

Laser step-heating was performed on four anorthoclase samples to evaluate the extraction method for dating young samples. Prior to laser step-heating, all of the samples, except for 85, were dated by furnace step-heating. Replicate analyses of sample 30 were laser step-heated to determine reproducibility. Plateau ages were usually calculated using steps between 3 W and 9 W (Fig. A7). The Cl/K ratios are generally negative with large uncertainties during the intermediate steps, and the radiogenic yield rises as power increases. Initial low power steps generally have high uncertainty due to the degassing of atmospheric argon.

DISCUSSION

Laser vs. Furnace Step-Heating

The effectiveness of laser step-heating can be evaluated by comparing the results with those of furnace step-heating. Laser step-heating analysis of sample 62 (b) (Fig. A6f) yields an inaccurate age of 40 ± 7 ka. The furnace step-heated sample 62 (a) (Fig. A5l), yields a robust plateau age of 26 ± 3 ka. Sample 30 yielded replicate laser step-heating ages, 14 ± 3 ka and 10 ± 4 ka, that agree with the furnace step-heating age of 12 ± 6 ka. The laser step-heating age for sample 20, 14 ± 7 ka, is also in agreement with both the furnace step-heating age of 9 ± 6 ka and an age of 11 ± 8 ka reported by Esser (1996) for a different sample from the same flow. The weighted mean of these ages is used as the eruption age of the Lower Hut and Northeast flows (Table A1).

The ages of samples 20 and 30 show that laser step-heating is capable of yielding accurate ages for young samples. The benefit of laser step-heating is the lower blank

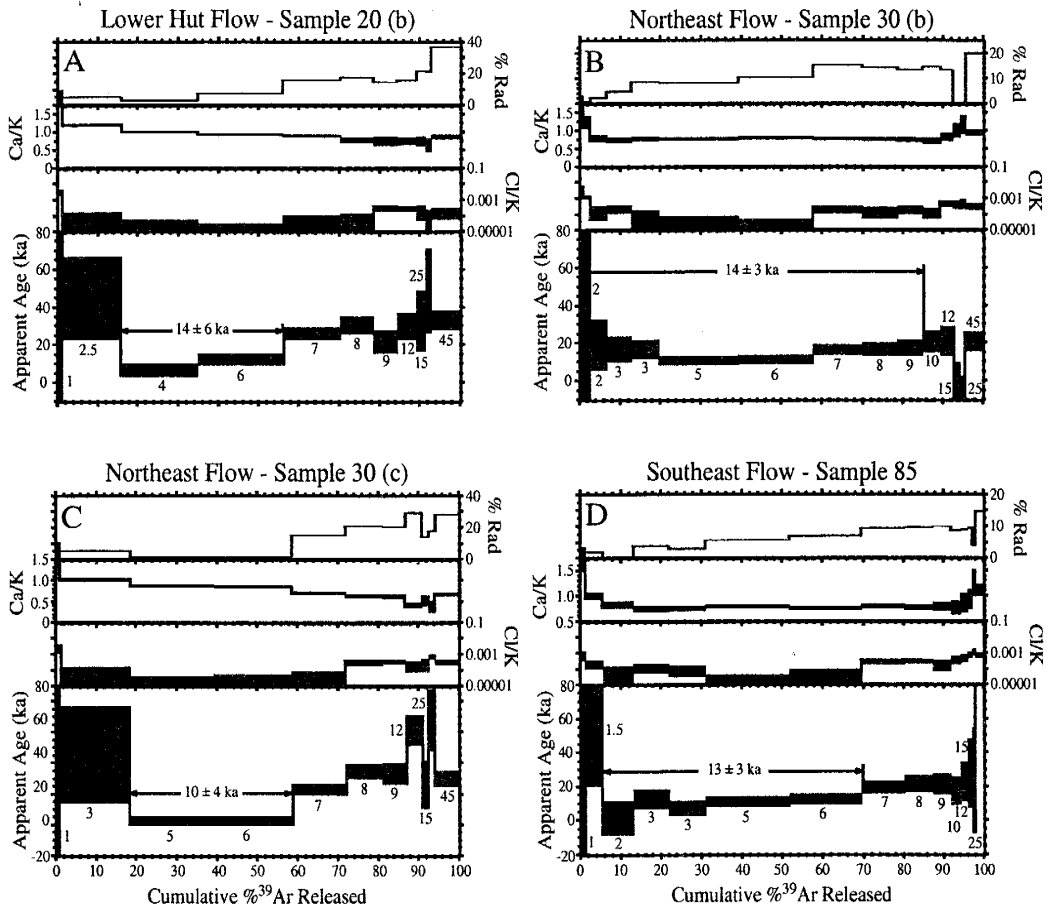


Figure A7-Age spectra for laser step-heated samples that yielded valid $^{40}\text{Ar}/^{39}\text{Ar}$ ages. Note that the scales on the Y-axes vary between the samples but are the same on the X-axes. Each spectrum shows the radiogenic yield, Cl/K ratio, Ca/K ratio, and apparent age plotted against the cumulative percent ^{39}Ar released. Power (Watts) for each step is indicated below the step and error on each step is shown at 2σ . Age spectra A through D are referred to in the text and Table A1.

compared to furnace step-heating (Table A1, notes). However, both inhomogeneous heating and coupling are problems with laser step-heating of young, fine-grained, low-potassium phases such as the Mount Erebus anorthoclase used in this study.

Inhomogeneous heating of the sample will result in gas, which might be released at a specific temperature in the furnace, being released over several power steps rather than in a single step during laser step-heating. For example, sample 30 (b) yields a plateau age that is older than, although within 2σ error of, the other two ages for the flow.

Inhomogeneous heating of the sample likely caused the apparent age for each power step to be slightly elevated which caused the slight discrepancy between the laser and furnace step-heating ages.

Inhomogeneous heating of a sample during laser step-heating can be caused by several processes. If a crystal is shielded from the laser by another crystal it will be heated differentially related to the overlying crystal. To mitigate this effect the sample should be in a single-crystal-thick layer during heating. This severely limits the volume of sample that can be analyzed and because of the fine grain size it is impractical, if not impossible, to meet this condition in such young samples.

Inhomogeneous heating can also occur when the individual grains move under the influence of the laser. This results in grains jumping out of the beam or landing on and shielding other crystals. To mitigate the effect of crystal movement the sample was contained in a series of 6 mm by 6 mm (the laser beam dimensions) sample holders during analysis.

The coupling systematics of the laser with anorthoclase and also melt inclusions is poorly understood at this time. If the laser couples better with the melt inclusions they

will act as heating foci. This could cause a melt inclusion near the surface of the crystal to differentially heat the surrounding anorthoclase or cause a grain with abundant melt inclusions to heat faster. Perhaps in extreme cases this differential heating could cause localized fusion of the anorthoclase, releasing a small amount of trapped $^{40}\text{Ar}_E$ and driving the apparent age of the step slightly up. Also, if rare exposed glass is present it might degass $^{40}\text{Ar}_E$ during the intermediate steps used to calculate plateau ages. For example, this effect likely caused sample 62 (b) to yield an apparent age that is too high (Fig. A6f). The 6 W step yields an apparent age ~ 25 ka that is the same as the furnace step-heating age of 26 ka (Fig. A5l) but the 9 W step is significantly older, more precise, and dominates the plateau age. During the 9 W step the laser was probably coupling with melt inclusions in the sample causing the release of $^{40}\text{Ar}_E$ and driving the apparent age up. In contrast, if small amounts of glass are exposed on a furnace step-heated sample the glass should be fully degassed by the 900°C step leaving the intermediate temperature steps free of $^{40}\text{Ar}_E$ (Esser *et al.*, 1997).

Laser step-heating is an effective method of dating young samples, such as sanidine from the 79 A.D. Vesuvius eruption, that are coarse-grained (up to 8 mm in diameter), have a high potassium content (13.7% to 15.7% K_2O), and contain only “sparse” melt inclusions (Cioni *et al.*, 1995; Renne *et al.*, 1997). Valid laser step-heating ages were also obtained in this study on the fine-grained low-potassium ($\sim 3\%$ K_2O) Erebus anorthoclase samples. However, the problems of inhomogeneous coupling and heating counteract the benefits of laser step-heating over furnace step-heating. Furnace step-heating is currently considered to be the superior method of $^{40}\text{Ar}/^{39}\text{Ar}$ dating young

fine-grained-melt inclusion-bearing samples, such as Mount Erebus anorthoclase, until these problems can be overcome.

Geologic Implications – Summit Lavas

A total of five pre-caldera summit lava flows were successfully dated in this study (Table A1). The samples were collected from the east, north, and southwestern edges of the caldera rim (Fig. A8). Samples 33 and 39, from the eastern side of the caldera, have ages of 91 ± 2 ka and 109 ± 11 ka, respectively. The northern pre-caldera flow sample, 17, has an age of 78 ± 6 ka. A pre-caldera flow, sample E93013, dated by Esser (1996) is also from the northern rim of the caldera and has an age of 87 ± 14 . Samples 61 and 62 are from the southwestern edge of the caldera rim and have ages of 21 ± 3 ka and 26 ± 3 ka, respectively. From the ages it is apparent that the eastern and northern pre-caldera flows are significantly older than the southwestern pre-caldera flows. During the time period between the two groups of pre-caldera flows extensive flank volcanism occurred possibly indicating a hiatus in summit activity (Fig. A9) (Esser, 1996). However, many undated pre-caldera flows are exposed immediately below the caldera rim. If these flows were dated they could possibly fill the apparent temporal gap between the southwestern pre-caldera flows and the north and eastern pre-caldera flows. Three pre-caldera samples (21, 26, and 45) collected from the southeastern and western caldera edges did not yield accurate ages. These ages might be erroneous because the samples were not completely cleaned of adhering glass and melt inclusions. This would cause $^{40}\text{Ar}_\text{E}$ to be released during steps generally used to calculate plateau ages.

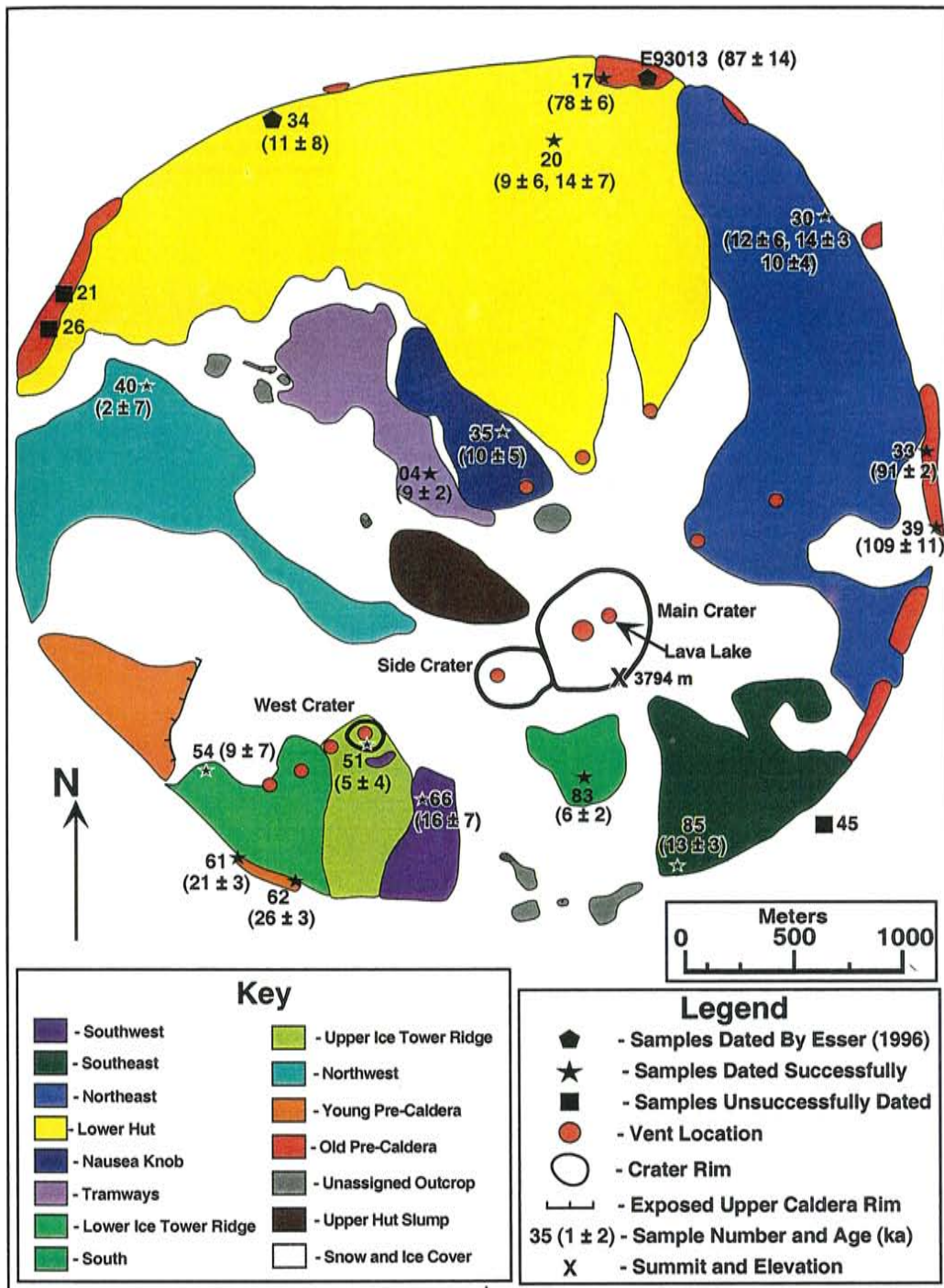


Figure A8-Geologic map of the summit plateau of Mount Erebus showing the lava flows, sample locations, ages (ka), and general features of the region (modified from Caldwell, 1989). The edges of the map approximately follow the caldera rim.

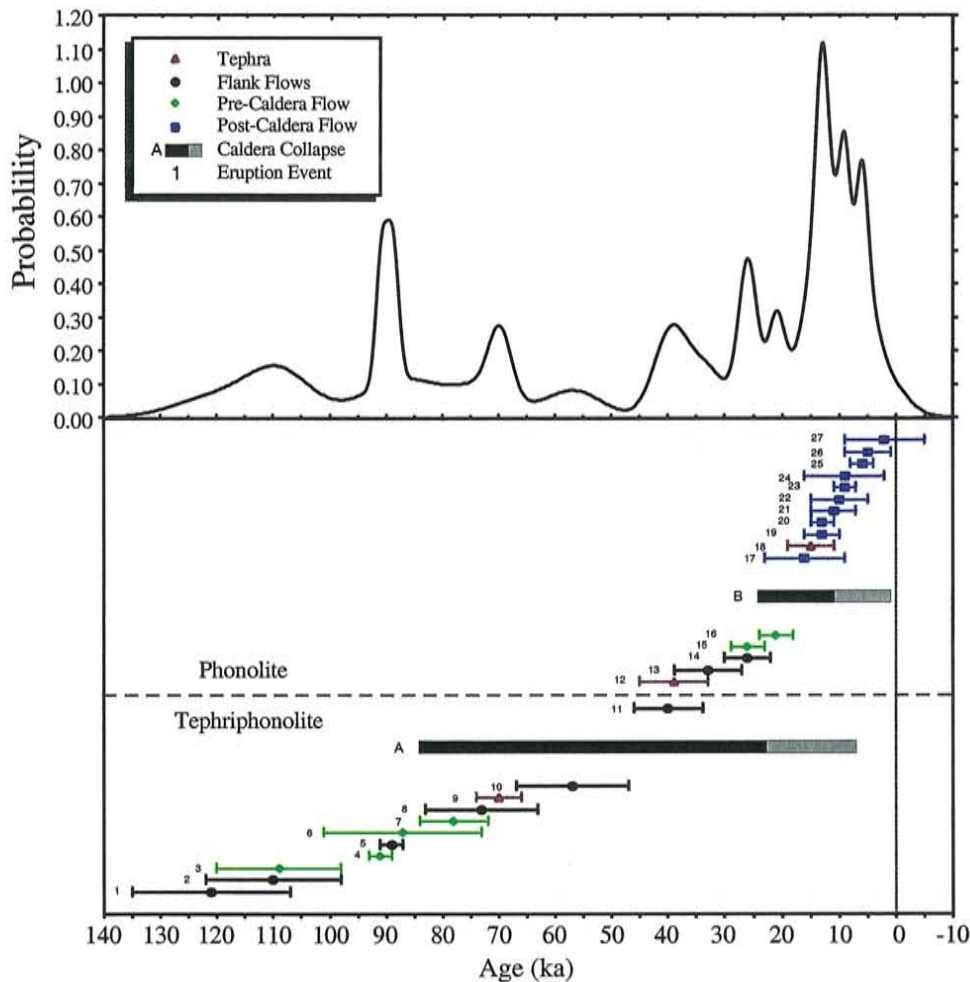


Figure A9—Age distribution and ideogram of eruptive events for the last 121 ky on Mount Erebus. Ages are shown with error bars at 2σ . The timing of caldera-collapse events are also shown, with the complete bar representing bracketing ages defined from overlapping relationships and the black portion representing the most likely timing considering other indirect field evidence. Caldera-collapse A is inferred from indirect evidence, whereas the timing of caldera-collapse B is defined by direct field evidence. The eruptive events are: (1) NW of Hooper's Shoulder*, (2) S of Hooper's Shoulder*, (3) Pre-caldera flow, (4) Pre-caldera flow, (5) Cape Barne*, (6) Pre-caldera flow*, (7) Pre-caldera flow, (8) Cape Royds*, (9) Tephra EBT-2, (10) William's Cliff*, (11) Cape Evans*, (12) Tephra BIT-272, (13) Hooper's Shoulder*, (14) Three Sister's Cones*, (15) Pre-caldera flow, (16) Pre-caldera flow, (17) Southwest flow, (18) Tephra EBT-63, (19) Southeast flow, (20) Northeast flow, (21) Lower Hut flow, (22) Nausea Knob flow, (23) Tramways flow, (24) Lower Ice Tower Ridge flow, (25) South flow, (26) Upper Ice Tower Ridge flow, (27) Northwest flow. Events marked with an * are from Esser (1996). The timing of the geochemical shift from tephriphonolite to phonolite is also indicated.

Extensive post-caldera volcanism has occurred in the summit area. The $^{40}\text{Ar}/^{39}\text{Ar}$ ages of the post-caldera flows confirm the field relations proposed by Caldwell (1989) for five of the flows infilling the summit caldera. On the basis of field relationships, the Lower Hut flow (11 ± 4 ka) appears to have been diverted by the Northeast flow (13 ± 2 ka). Similarly the Nausea Knob flow (10 ± 5 ka) is thought to have ponded against the Lower Hut flow. On the south side of the summit plateau a small section of the Southwestern flow (16 ± 7 ka) is exposed as a kipuka in the Upper Ice Tower Ridge flow (5 ± 4 ka) indicating that the Southwestern flow is older (Caldwell, 1989).

Esser (1996) also determined $^{40}\text{Ar}/^{39}\text{Ar}$ apparent ages for three post-caldera lavas. These apparent ages for the Lower Hut, Nausea Knob, and Northeast flows are 11 ± 8 ka, 46 ± 18 ka, and 76 ± 10 ka, respectively. The Lower Hut Flow age, as mentioned previously, agrees with the two ages obtained in this study and is considered reliable. However, the ages reported for the Nausea Knob and Northeast flows are inconsistent with the results of this study. For example, the same sample, 35, from the Nausea Knob flow was used in both studies, but an age of 10 ± 4 ka was obtained in this study. The sample preparation procedures used by Esser (1996) were less rigorous than those used in this study likely resulting in melt inclusion glass being incompletely removed from the samples. Because of the presence of glass the apparent ages of the Nausea Knob and Northeast flows are too old due to contamination by $^{40}\text{Ar}_E$.

Geologic Implications – Caldera Collapse

Formation of the summit caldera is one of the most important events in the late Pleistocene and Holocene eruptive history of Mount Erebus. The timing of caldera

collapse can be constrained using the ages of the pre- and post-caldera flows. However, overlapping relationships between the dated pre- and post-caldera flows are only exposed in the Lower Hut and Lower Ice Tower Ridge flows (Fig. A8), where caldera formation can be bracketed between 84 ka and 7 ka, and 29 ka and 2 ka, respectively. These ages can be interpreted to represent either multiple caldera-forming events or a single caldera collapse that truncated all of the pre-caldera flows. In both situations a caldera-forming event must have occurred between 29 ka and 2 ka, after the youngest pre-caldera flow was erupted. The young bracketing age of this caldera-collapse is likely conservative and may be older if other non-overlapping post-caldera flows are considered. For example, the Northeastern flow does not overlap the southwestern pre-caldera flows, but could push the young bracketing age to 11 ka.

Several indirect observations support the multiple caldera theory. A significant break in slope on the southwestern side of the summit plateau (Figs. A8, A10) might represent two juxtaposed caldera rims. To explain this Caldwell (1989) suggested that a nested caldera is present within the southwestern side of the main summit plateau caldera. This nested caldera would incorporate the young pre-caldera flows, samples 61 and 62, and would represent the caldera formed between 29 ka and 2 ka. No age control exists for the specific portion of the lower caldera rim where stratigraphic relationships are exposed. However, the lower caldera rim can be followed from where the two caldera rims are exposed to where the older pre-caldera flows were sampled. Caldwell (1989) also concluded on the basis of trace element compositions that the northeastern and eastern sections of caldera rim, where the old pre-caldera samples were sampled, are geochemically identical to the western portion of the lower caldera rim exposed beneath

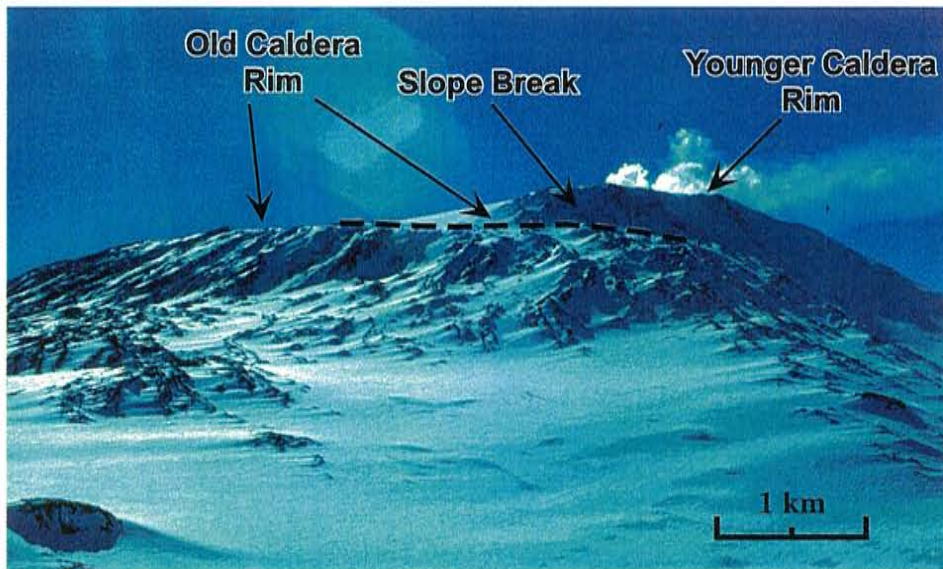


Figure A10-A photo looking to the northeast at the upper slopes of Mount Erebus showing the break in slope interpreted by Caldwell (1989) to be a nested caldera. The rim of the older caldera composes the northern edge of the summit plateau and can be traced at around the same elevation (dashed line on the figure) beneath the flanks of the young caldera. The young caldera composes the southern edge of the summit plateau.

the upper caldera rim. The major element geochemistry of the caldera rims is also distinct. The pre-caldera flows of the younger, upper caldera rim is phonolitic, whereas the older, lower caldera rim is composed of tephriphonolitic lavas. Both the topographic and geochemical arguments lead to the assumption that the portion of caldera rim where the old pre-caldera flows were sampled is part of the lower caldera rim. By this assumption it is possible to bracket a second caldera-forming event between 84 ka and 11 ka by using the age of the northern pre-caldera sample 17 and the overlapping Lower Hut flow. However, because this caldera-collapse event formed the lower caldera rim it should be younger than the upper caldera-collapse event. Therefore, the young age of the old caldera collapse is bracketed at 23 ka by the oldest pre-caldera flow of the nested caldera. It is also possible that the lower caldera was formed during more than one caldera collapse event rather than just during a single event.

Many methods of caldera formation have been recognized (Lipman, 2000). For Mount Erebus the important distinction is whether caldera formation occurred as a result of passive gravitational collapse or during explosive activity. Calderas formed by passive gravitational collapse tend to form incrementally and contain abundant step-faulting within the caldera. It is also common for gravitationally formed calderas to contain nested calderas (Lipman, 2000). In the summit region of Mount Erebus any evidence of step-faulting within the caldera has been covered under post-caldera flows and snow, but there might be a nested caldera. Tephra sample BIT-272 is from a plinian eruption (Section B, this study) that occurred at 39 ± 6 ka. This tephra is within the age bracket for the possible older caldera-collapse and leads to the speculation that the two events are related indicating an explosive origin for at least one of the calderas in the summit region.

However, the connection between these two events is tenuous and a gravitational genesis is still possible.

Geologic Implications – Tephra

Three of the tephra samples, EBT-2, EBT-63, and BIT-272 (Table A1), dated in this study yielded valid ages, while the remaining two samples, EBT-42 and EBT-53, yielded spurious results. Sample EBT-2, from the nose of the Barne Glacier on the west flank of Mount Erebus, has an apparent age of 70 ± 4 ka. However, the feldspar compositions indicate that some contaminating feldspar is present in the sample (Section B, this study) making the $^{40}\text{Ar}/^{39}\text{Ar}$ apparent age a maximum age. Assuming that the age of the tephra is identical to the age of the surrounding glacial ice, the glacial movement rate was calculated and can be compared to other glaciers in the region. The source for the ice in the Barne Glacier is not well known, but is between 10 km and 15 km from the nose. Assuming the tephra was entrained at the head of the glacier, the minimum movement rate is calculated to be between 0.14 m a^{-1} and 0.20 m a^{-1} . The only glaciological studies carried out on Mount Erebus are on the Erebus Glacier Tongue (Fig. A1) where movement rates are as high as 100 m a^{-1} to 158 m a^{-1} (Holdsworth, 1974; Holdsworth, 1982; Jacobs, 1987). However, the dynamics of the Erebus Glacier Tongue are too different from the Barne Glacier to make this a relevant comparison. Slower movement rates are recorded at glaciers across McMurdo Sound in the Dry Valleys region of southern Victoria Land. For example, the Sykes Glacier has a movement rate between 0.1 m a^{-1} to 0.5 m a^{-1} (Chinn, 1988). The calculated movement rate for the Barne Glacier is reasonable to the local region, but still must be regarded only as a

minimum movement rate because the apparent age of sample EBT-2 is considered a maximum age.

A blue ice site in the central portion of the Barne Glacier, the Middle Barne site, contains five tephra layers. Because the Middle Barne site is upstream of the terminus of the Barne site, the ages of these five layers are older than the age of tephra sample EBT-2 (70 ± 4 ka).

Tephra sample EBT-63, from the Upper Barne site, has an age of 15 ± 4 ka (Fig. A1) (detailed in Section B as the Hooper's Shoulder site). This site is located approximately 1 km northwest of the Hooper's Shoulder flow. The Upper Barne site contains 29 tephra layers with 19 upslope from sample EBT-63 and nine downslope from EBT-63. No deformation in the ice or tephra layers is observed that would indicate the tephra are not in stratigraphic order. Therefore, 19 tephra layers are interpreted as younger than 15 ka and nine are older than 15 ka.

The higher tephra layers in the Upper Barne sequence have been uniformly deformed around the Hooper's Shoulder flow by glacial movement. The catchment for the glacial ice begins ≤ 1 km upslope from where sample EBT-63 was collected and a local maximum movement rate of 0.09 m a^{-1} can be calculated for the glacier. This extremely slow rate indicates that the ice is nearly stagnant which is consistent with the presence of blue ice. Also, because the tephra layers are deformed around the Hooper's Shoulder flow the age of the tephra samples below EBT-63 can be bracketed in age between 15 ka and the 33 ka eruption age of Hooper's Shoulder.

The single distal sample, BIT-272, is 39 ± 6 ka (Fig. A1). This sample is unique because it was deposited in the Mt. DeWitt area, 180 km from vent, and was formed

during the only known plinian eruption of Mount Erebus (Section B, this study). The timing of this plinian eruption falls within the bracketed time of the older caldera-forming event. This gives credibility to the possibility that caldera formation resulted from the plinian eruption rather than gravitational collapse as previously thought (*e.g.* Esser, 1996). However, a gravitational genesis for the older caldera still can not be ruled out.

CONCLUSIONS

An eruptive history for Mount Erebus throughout the last 109 ky is developed using the $^{40}\text{Ar}/^{39}\text{Ar}$ dating method. Mount Erebus has produced both lava flows and explosive eruptions during this time period. Three tephra samples have been dated along with 15 lava flows in the summit region of the volcano. The lava flows are categorized as both pre- and post-caldera flows. The pre-caldera flows are exposed along the rim of the summit caldera and have been truncated during at least one caldera-forming event and possibly a minimum of two events. These flows occupy two distinct groups of ages with the older pre-caldera flows being between 109 ± 11 ka and 78 ± 6 ka in age and the younger pre-caldera flows being between 26 ± 3 and 21 ± 3 ka in age. Between these two groups of pre-caldera flows it is speculated that there was at least one caldera-collapse event bracketed in age between 84 ka and 7 ka, but likely occurring prior to 23 ka.

Sample EBT-2 has an apparent age of 70 ± 4 ka, but is likely contaminated and the eruption age must be considered $<70 \pm 4$ ka. Sample BIT-272 was derived from a plinian eruption at 39 ± 6 ka and is from the Mt. DeWitt area, 180 km distal. A geochemical transition from tephriphonolite to phonolite occurs with the eruption of BIT-

272 and the Hooper's Shoulder flank flow (33 ± 6 ka; Esser, 1996). Phonolitic magmatism continued at around 25 ka with the eruption of the Three Sister's Cones flank flow (26 ± 4 ka; Esser, 1996) and the young pre-caldera flows at 26 ± 3 ka and 21 ± 3 ka. A caldera-forming event occurred between 29 ka and 2 ka, and probably before 11 ka. Post-caldera volcanism has occurred throughout the late Pleistocene and Holocene with flows ranging in age from 16 ± 7 ka to 2 ± 7 ka.

The youngest tephra layer, EBT-63, from the Upper Barne blue ice site is 15 ± 4 ka in age. The Upper Barne blue ice site is a location of nearly stagnant ice with a maximum glacial movement rate of 0.09 m a^{-1} . At the Upper Barne site 19 tephra layers are exposed upslope from EBT-63 that are therefore younger than 15 ka. Another nine tephra layers are older than EBT-63 and are likely younger than the Hooper's Shoulder flow, bracketing their age between 15 ± 4 ka and 33 ± 6 ka. Six tephra layers from the middle Barne area are bracketed in age between 15 ± 4 ka and 70 ± 4 ka, the ages of EBT-63 and EBT-2, respectively. Also, the age of sample EBT-2, from the terminus of the Barne Glacier, indicates a minimum glacial movement rate of between 0.14 m a^{-1} to 0.20 m a^{-1} for the Barne Glacier.

The ages of the tephra layers and 15 lava flows from Mount Erebus indicate that the volcano has been active throughout the last 109 ky. Within this time period the volcano has experienced not only small explosive eruptions and lava flows, but at least one, and possibly a minimum of two caldera-forming events. Also, at least one plinian eruption occurred at Mount Erebus that may have been at least partially responsible for caldera formation.

REFERENCES

- Armstrong, R.L., 1978, K-Ar dating: Late Cenozoic McMurdo Volcanic Group and dry valley glacial history, Victoria Land, Antarctica: *New Zealand Journal of Geology and Geophysics*, v. 21, no. 6, p. 685-698.
- Baksi, A.K., Hsu, V., McWilliams, M.O., and Farrar, E., 1992, $^{40}\text{Ar}/^{39}\text{Ar}$ dating of the Brunhes-Matuyama geomagnetic field reversal: *Science*, v. 256, p. 356-357.
- Caldwell, D.A., 1989, Physical and geochemical properties of summit flows and recent volcanic ejecta from Mount Erebus, Ross Island, Antarctica: Socorro, NM, New Mexico Institute of Mining and Technology, Master's Independent Study, 113 p.
- Chen, Y., Smith, P.E., Evensen, N.M., York, D., and Lajoie, R., 1996, The edge of time: Dating of young volcanic ash layers with the ^{40}Ar - ^{39}Ar laser probe: *Science*, v. 274, p. 1176-1178.
- Chesner, C.A., Rose, W.I., Deino, A., Drake, R., and Westgate, J.A., 1991, Eruptive history of the Earth's largest Quaternary caldera (Toba, Indonesia) clarified: *Geology*, v. 19, p. 200-203.
- Chinn, T.J., 1988, The 'Dry Valleys' of Victoria Land, in Swithinbank, C., ed., *Satellite image atlas of the World: Antarctica*, U.S. Geological Survey Professional Paper 1386-B, p. 39-41.
- Cioni, R., Civetta, L., Marianelli, P., Metrich, N., Santacroce, R., and Sbrana, A., 1995, Compositional layering and syn-eruptive mixing of a periodically refilled shallow magma chamber: the AD 79 plinian eruption of Vesuvius: *Journal of Petrology*, v. 36, no. 3, p. 739-776.
- Dalrymple, G.B., and Lanphere, M.A., 1969, *Potassium-argon dating*: San Francisco, Freeman.
- Deino, A., and Potts, R., 1990, Single Crystal $^{40}\text{Ar}/^{39}\text{Ar}$ dating of the Olorgesailie Formation, southern Kenya Rift: *Journal of Geophysical Research*, v. 95, no. B6, p. 8453-8470.
- Deino, A., and Potts, R., 1992, Age-probability spectra for examination of single-crystal $^{40}\text{Ar}/^{39}\text{Ar}$ dating results: Examples from Olorgesailie, southern Kenya Rift: *Quaternary International*, v. 13/14, p. 47-53.
- Duncan, R.A., and Hogan, L.G., 1994, Radiometric dating of young MORB using the ^{40}Ar - ^{39}Ar incremental heating method: *Geophysical Research Letters*, v. 21, no. 18, p. 1927-1930.

- Dunbar, N.W., Cashman, K.V., and Dupré, R., 1994, Crystallization processes of anorthoclase phenocrysts in the Mount Erebus magmatic system: Evidence from crystal composition, crystal size distributions, and volatile contents of melt inclusions, *in* Kyle, P.R., ed., *Volcanological and Environmental Studies of Mount Erebus, Antarctica*, Antarctic Research Series, V. 66, p. 129-146.
- Esser, R.P., 1996, $^{40}\text{Ar}/^{39}\text{Ar}$ dating of Mount Erebus volcano, Antarctica: Socorro, NM, New Mexico Institute of Mining and Technology, unpublished Master's Thesis, 183 p.
- Esser, R.P., and Kyle, P.R., 1999, $^{40}\text{Ar}/^{39}\text{Ar}$ chronology of The Pleiades Volcanic Centre, northern Victoria Land, Antarctica: a potential source of Late-Pleistocene englacial tephra layers [abs]: 8th Symposium on Antarctic Earth Sciences, Wellington, New Zealand, p. 100.
- Esser, R.P., McIntosh, W.C., Heizler, M.T., and Kyle, P.R., 1997, Excess argon in melt inclusions in zero-age anorthoclase feldspar from Mount Erebus, Antarctica, as revealed by the $^{40}\text{Ar}/^{39}\text{Ar}$ method: *Geochimica et Cosmochimica Acta*, v. 61, no. 18, p. 3789-3801.
- Fleck, R.J., Sutter, J.F., and Elliot, D.H., 1977, Interpretation of discordant $^{40}\text{Ar}/^{39}\text{Ar}$ age spectra of Mesozoic tholeiites from Antarctica: *Geochimica et Cosmochimica Acta*, v. 41, p. 15-32.
- Heizler, M.T., Perry, F.V., Crowe, B.M., Peters, L., and Appelt, R., 1999, The age of Lathrop Wells volcanic center: An $^{40}\text{Ar}/^{39}\text{Ar}$ dating investigation: *Journal of Geophysical Research*, v. 104, no. B1, p. 767-804.
- Holdsworth, G., 1974, Erebus Glacier Tongue, McMurdo Sound, Antarctica: *Journal of Glaciology*, v. 13, no. 67, p. 27-35.
- Holdsworth, G., 1982, Dynamics of Erebus Glacier Tongue: *Annals of Glaciology*, v. 3, p. 131-137.
- Hu, Q., Smith, P.E., Evensen, N.M., and York, D., 1994, Lasing in the Holocene: extending the $^{40}\text{Ar}/^{39}\text{Ar}$ laser probe method into the ^{14}C range: *Earth and Planetary Science Letters*, v. 123, p. 331-336.
- Izett, G.A., and Obradovich, J.D., 1994, $^{40}\text{Ar}/^{39}\text{Ar}$ age constraints for the Jaramillo Normal Subchron and the Matuyama-Brunhes geomagnetic boundary: *Journal of Geophysical Research*, v. 99, no. B2, p. 2925-2934.
- Jacobs, S.S., 1987, Ice fronts and icebergs in the Ross and Weddell seas: *Antarctic Journal of the United States*, p. 91-94.

- Kyle, P.R., 1977, Mineralogy and glass chemistry of recent volcanic ejecta from Mt. Erebus, Ross Island, Antarctica: *New Zealand Journal of Geology and Geophysics*, v. 20, no. 6, p. 1123-1146.
- Kyle, P.R., 1994, Volcanological and environmental studies of Mount Erebus, Antarctica, American Geophysical Union, Antarctic Research Series, v. 66, 162 p.
- Kyle, P.R., Dibble, R.R., Giggenbach, W.F., and Keys, J., 1982, Volcanic activity associated with the anorthoclase phonolite lava lake, Mount Erebus, Antarctica, *in* Craddock, C., ed., *Antarctic Geoscience: Madison, Wisconsin, University of Wisconsin Press*, p. 735-745.
- Lipman, P.W., 2000, Calderas, *in* Sigurdsson, H., Houghton, B.F., McNutt, S.R., Rymer, H., and Stix, J., eds., *Encyclopedia of volcanoes*, Academic Press, p. 643-662.
- Lippolt, H.J., Troesch, M., and Hess, J.C., 1990, Excess argon and dating of the Quaternary Eifel volcanism, IV. Common argon with high and lower-than-atmospheric $^{40}\text{Ar}/^{36}\text{Ar}$ ratios in phonolitic rocks, East Eifel, F.R.G.: *Earth and Planetary Science Letters*, v. 101, p. 19-33.
- McDougall, I., 1985, K-Ar and ^{40}Ar - ^{39}Ar dating of the hominid-bearing Pliocene-Pleistocene sequence at Koobi Fora, Lake Turkana, northern Kenya: *Geological Society of America Bulletin*, v. 96, p. 159-175.
- Mahon, K.I., 1996, The new "York" regression: Application of an improved statistical method to geochemistry: *International Geology Review*, v. 38, p. 293-303.
- Moore, J.A., and Kyle, P.R., 1987, Volcanic geology of Mount Erebus, Ross Island, Antarctica: *Proceedings of the NIPR symposium on Antarctic geosciences*, Tokyo, Japan, v. 1, p. 48-65.
- Pringle, M.S., McWilliams, M., Houghton, B.F., Lanphere, M.A., and Wilson, C.J.N., 1992, $^{40}\text{Ar}/^{39}\text{Ar}$ dating of Quaternary feldspar: Examples from the Taupo Volcanic Zone, New Zealand: *Geology*, v. 20, p. 531-534.
- Renne, P.R., Sharp, W.D., Deino, A.L., Orsi, G., and Civetta, L., 1997, $^{40}\text{Ar}/^{39}\text{Ar}$ dating into the historical realm: Calibration against Pliny the Younger: *Science*, v. 277, p. 1279-1280.
- Rose, W.I., Conway, F.M., Pullinger, C.R., Deino, A., and McIntosh, W.C., 1999, An improved age framework for late Quaternary silicic eruptions in northern Central America: *Bulletin of Volcanology*, v. 61, p. 106-120.
- Samson, S.D., and Alexander, E.C., Jr., 1987, Calibration of the interlaboratory $^{40}\text{Ar}/^{39}\text{Ar}$ dating standard, MMhb-1: *Chemical Geology*, v. 66, p. 27-34.

- Singer, B.S., and Pringle, M.S., 1996, Age calibration of the Matuyama-Brunhes geomagnetic polarity reversal from $^{40}\text{Ar}/^{39}\text{Ar}$ incremental heating analyses of lavas: *Earth and Planetary Science Letters*, v. 139, p. 47-61.
- Steiger, R.H., and Jäger, E., 1977, Subcommittee on geochronology: Convention on the use of decay constants in geo- and cosmochemistry: *Earth and Planetary Science Letters*, v. 36, p. 359-362.
- Taylor, J.R., 1982, *An introduction to error analysis: The study of uncertainties in physical measurements*: Mill Valley, CA., University Science Books, 270 p.
- Treves, S.B., 1968, Volcanic rocks of the Ross Island area: *Antarctic Journal of the United States*, v. 3, no. 4, p. 108-109.
- Turbeville, B.N., 1992, $^{40}\text{Ar}/^{39}\text{Ar}$ ages and stratigraphy of the Latera caldera, Italy: *Bulletin of Volcanology*, v. 55, p. 110-118.
- van den Bogaard, P., 1995, $^{40}\text{Ar}/^{39}\text{Ar}$ ages of sanidine phenocrysts from Laacher See Tephra (12,900 yr BP): Chronostratigraphic and petrological significance: *Earth and Planetary Science Letters*, v. 133, p. 163-174.
- van den Bogaard, P., Hall, C.M., Schmincke, H.-U., and York, D., 1989, Precise single-grain $^{40}\text{Ar}/^{39}\text{Ar}$ dating of a cold to warm climate transition in central Europe: *Nature*, v. 342, p. 523-525.
- Wilch, T.I., McIntosh, W.C., and Dunbar, N.W., 1999, Late Quaternary volcanic activity in Marie Byrd Land: Potential $^{40}\text{Ar}/^{39}\text{Ar}$ -dated time horizons in West Antarctic ice and marine cores: *Geological Society of America Bulletin*, v. 111, no. 10, p. 1563-1580.

Tephrostratigraphy of Mount Erebus, Ross Island, Antarctica

ABSTRACT

Mount Erebus tephra samples from glacial ice, firn, and historical eruptions were sampled, characterized geochemically, and observed using scanning electron microscopy to determine eruption mode. All but one of the tephra samples are phonolitic in composition and are geochemically homogeneous with the exception of slight feldspar-controlled trace element variations. The phonolitic tephra, including two distal tephra samples, were all produced from eruptions at Mount Erebus including two distal tephra samples. The majority of the tephra-forming eruptions at Mount Erebus have been strombolian or phreatomagmatic. However, at least one plinian eruption has occurred as well as one large phreatomagmatic eruption. Tephra samples from Mount Erebus contain several unique features. Glass droplets and ash with budding morphology were derived from strombolian eruptions. The budding morphology has not been previously reported and is described as a parent melt bleb with quenched spheres in the process of pinching off. Clustered and rare single xenocrystic analcime crystals are also present in some phonolitic tephra samples. The analcime was likely entrained from a hydrothermal system present prior to eruption. A single tephra sample of trachytic composition was also found in blue ice near Mount Erebus. This tephra sample is not from Mount Erebus, but is from a plinian eruption from The Pleiades volcanic field in northern Victoria Land.

INTRODUCTION

Mount Erebus is an active intraplate alkaline volcano located on Ross Island, Antarctica (Figs. B1, B2). The volcano has been active since at least 1.3 Ma and has erupted lava compositions varying from basanite to phonolite (Kyle *et al.*, 1992; Esser, 1996). Late Pleistocene and Holocene activity has taken the form of both anorthoclase-phyric phonolitic lava flows and explosive eruptions (Section A, this study). The lavas fill a summit caldera and form a broad annular plateau region that slopes up to the summit crater (Moore and Kyle, 1987). Volcanic activity has been focused exclusively at the summit for around the last 25 ky, and two caldera-collapse events have occurred between 11 ka and 24 ka and between 23 ka and 84 ka (Section A, this study). Gravitational collapse has been proposed as the mechanism for caldera formation (Moore and Kyle, 1987, Esser, 1996). But the two distal tephra deposits indicate that Mount Erebus has definitely had large-scale explosive eruptions. An explosive origin for the young caldera must be considered because of these distal deposits.

The historic record for Mount Erebus is limited, with detailed records beginning only around 1972. The volcano currently contains a convecting anorthoclase-phonolite lava lake, located in a pit crater within the summit crater, that experiences frequent small strombolian eruptions (Giggenbach *et al.*, 1973; Kyle *et al.* 1982; Dibble *et al.* 1984). These eruptions are periodically powerful enough to deposit bombs beyond the crater rim area approximately 250 m above the lava lake. In the last 20 years enhanced anomalous explosive activity has only been observed twice. In 1984 a three month period of sustained strombolian eruptions hurled 10 m diameter bombs more than 1 km from the

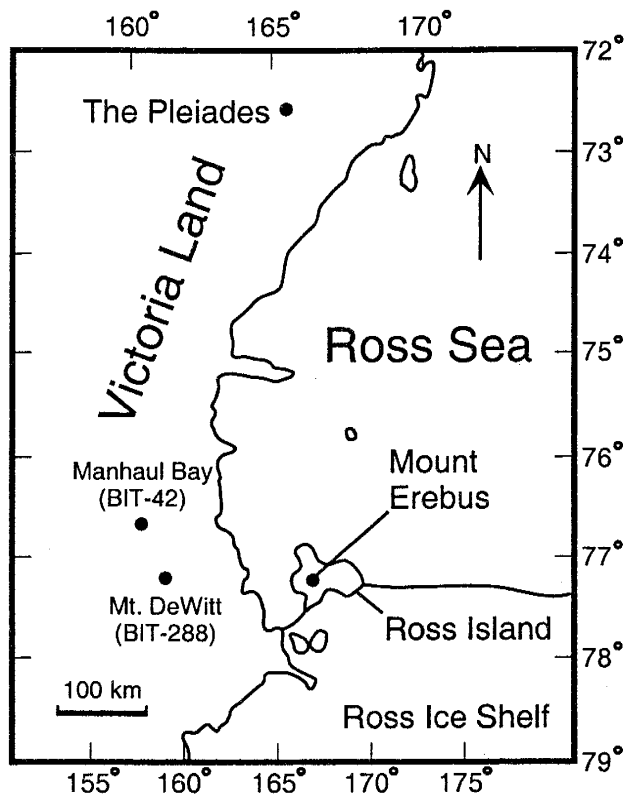


Figure B1-Map of Victoria Land and the Ross Sea region showing the locations of sites mentioned in the text.

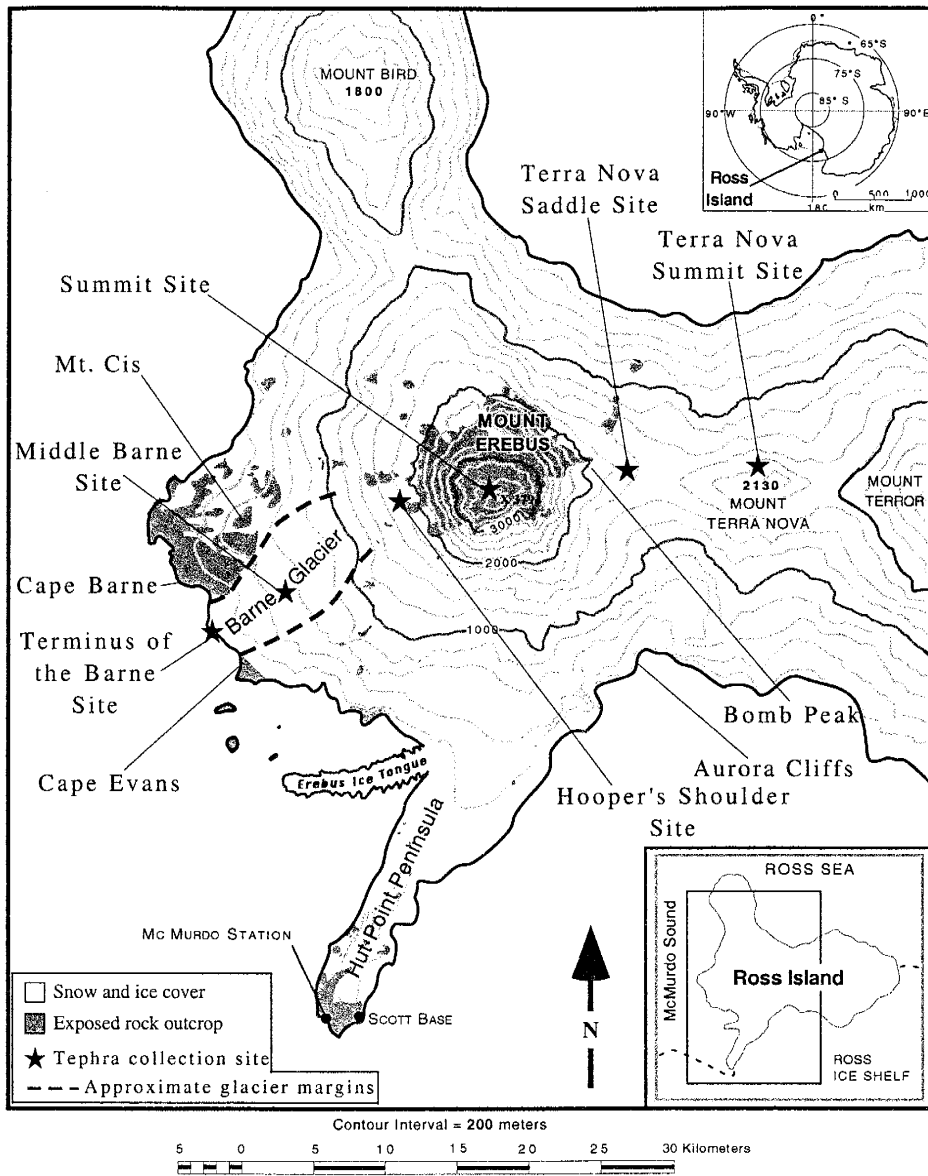


Figure B2-Map of Mount Erebus and the immediate vicinity showing the tephra sampling sites and features mentioned in the text.

vent and in 1993 two phreatic explosions excavated a small crater within the main summit crater (Caldwell and Kyle, 1994; Dibble *et al.*, 1994).

Evidence for pre-historic explosive activity is extremely limited due to both the extensive glacier cover on the flanks of Mount Erebus and the lack of dissection that would expose stratigraphic sections. The occurrence of pyroclastic deposits is limited to exposures in the main crater walls. Lyon and Giggenbach (1974) described volcanic ash in the walls of an ice cave near the summit of Mount Erebus and Keys *et al.* (1977) found ash in firn on the Fang Glacier, but these layers are no longer accessible. The ages of these tephra were estimated to range over hundreds of years (Keys *et al.*, 1977).

During investigations of englacial tephra from the Manhaul Bay area of the Allan Hills blue ice region, Victoria Land (Fig. B1), a single ash layer was geochemically correlated to Mount Erebus 210 km away (Dunbar *et al.*, 1995). Another Erebus tephra layer has been recognized at Mount DeWitt (Fig. B1) 180 km to the northwest of Mount Erebus (N.W. Dunbar, pers. commun., 2000). The Allan Hills tephra provided the first evidence of explosive eruptive activity besides the ongoing small strombolian eruptions at Mount Erebus. These discoveries provided the impetus to investigate several potential englacial tephra layers on the flanks of Mount Erebus. Initial investigation indicated that the layers were composed of volcanic ash and further study was necessary.

Tephra samples from each layer were characterized both geochemically and morphologically to further understand the pre-historic explosive eruptive history of Mount Erebus. The overall geochemistry of Mount Erebus is well known (Kyle *et al.*, 1992; Esser, 1996), but the only geochemical studies of explosive products from the volcano are limited to bombs erupted between 1972 and 1986. During this time period

no significant geochemical changes were observed (Kyle, 1977; Caldwell and Kyle, 1994), but 14 years is a short period of time relative to the life of the volcano and may not be representative of any long term trends that may exist. The englacial tephra samples span a significant amount of time (Section A, this study) and provide an opportunity to study geochemical trends in tephra samples over a longer period. Also, to better understand the eruptive history of Mount Erebus it is necessary to investigate the nature of the explosive behavior of the volcano. The morphology of ash in each tephra sample is characterized using scanning electron microscopy to determine the eruptive mechanism that formed the tephra layer (Sheridan and Marshall, 1983; Heiken and Wohletz, 1985).

TEPHRA

An extensive search for englacial tephra was carried out on the flanks of Mount Erebus and the surrounding region. Several areas of tephra-bearing blue ice were discovered and a detailed study was focussed on the Barne Glacier, located on the west side of Mount Erebus. Tephra samples were collected from three blue ice areas referred to as terminus of the Barne, middle Barne, and Hooper's Shoulder (Fig. B2). Assuming that the ice is younger progressing upstream in the glacier the three areas can be relatively dated with the oldest being terminus of the Barne and the youngest being Hooper's Shoulder. An important caveat to this is that the dynamics of the Barne Glacier are unknown and aberrant ice conditions could exist that would cause the relative dating to be unreliable. This is especially relevant to the Hooper's Shoulder blue ice site, which has a slow movement rate (Section A, this study), and could potentially contain tephra

that are older than the other blue ice areas. However, stratigraphic relationships between tephra layers within individual blue ice areas are considered to be reliable.

Eight samples were collected from four tephra layers at the terminus of the Barne Glacier between Cape Barne and Cape Evans along the sea ice interface (Fig. B1). The youngest of the four layers has a maximum age of 70 ± 4 ka (Section A, this study) and is exposed in a broad synclinal form at the glacial front (Fig. B3a).

The middle Barne site (Fig. B2) is stratigraphically above the terminus of the Barne site. Ten samples were collected from six tephra layers at the middle of the Barne site. The layers trend generally north to south, are not deformed, and dip east from nearly horizontal to $\sim 16^\circ$.

The Hooper's Shoulder site yielded a total of 29 tephra layers (Figs. B2, B4) and is likely the youngest blue ice site on the Barne Glacier. The layers dip from 10° to 38° east and are uniformly deformed in a broad flat S-shape around the Hooper's Shoulder dome to the southeast. This site contains the largest continuously exposed stratigraphic sequence of tephra layers on Mount Erebus. The tephra layers are concealed under snow to the south and are truncated by a small east-west trending moraine to the north.

Additional samples proximal to Mount Erebus were collected from the summit of the neighboring Mount Terra Nova and the saddle between Terra Nova and Erebus (Fig. B2). At the Terra Nova Saddle site four samples were obtained from a small area of ice containing very disseminated tephra. The Terra Nova Summit site is located in blue ice on the north side of the summit ice cap where an east to west trending tephra layer is exposed parallel to a distinct moraine downslope from the tephra layer. Sample EBT-62

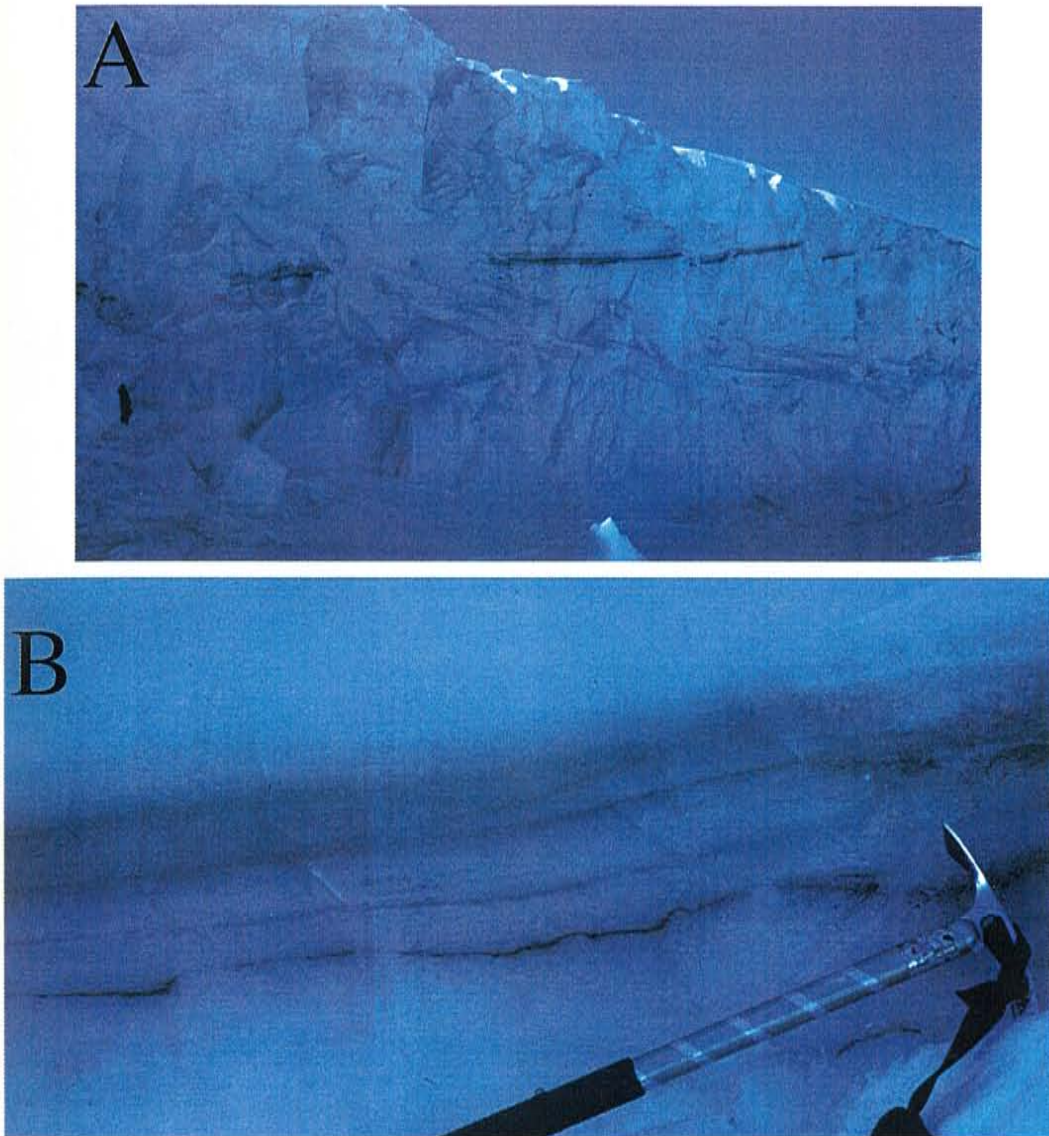


Figure B3-Photos of tephra features. **A:** A concentrated tephra layer at the terminus of the Barne Glacier. This tephra layer has a maximum age of 70 ± 4 ka (Section A, this study). Samples EBT-1, EBT-2, and EBT-56 are from this layer. Note the person in the lower left for scale. **B:** Close up of the tephra layer in photo A showing that more than one tephra deposit is present forming a composite layer. This is one of the most concentrated layers found. **C:** Typical surface exposure of a tephra layer (EBT-30). Snow has collected in the slight depression caused by enhanced ablation. Note the pen in the snow for scale. **D:** Close up of the layer in photo C showing melt pods that have formed by the concentration of ash beneath the ice surface during melting. Scale is the toe of a boot with crampons.



Figure B3 continued

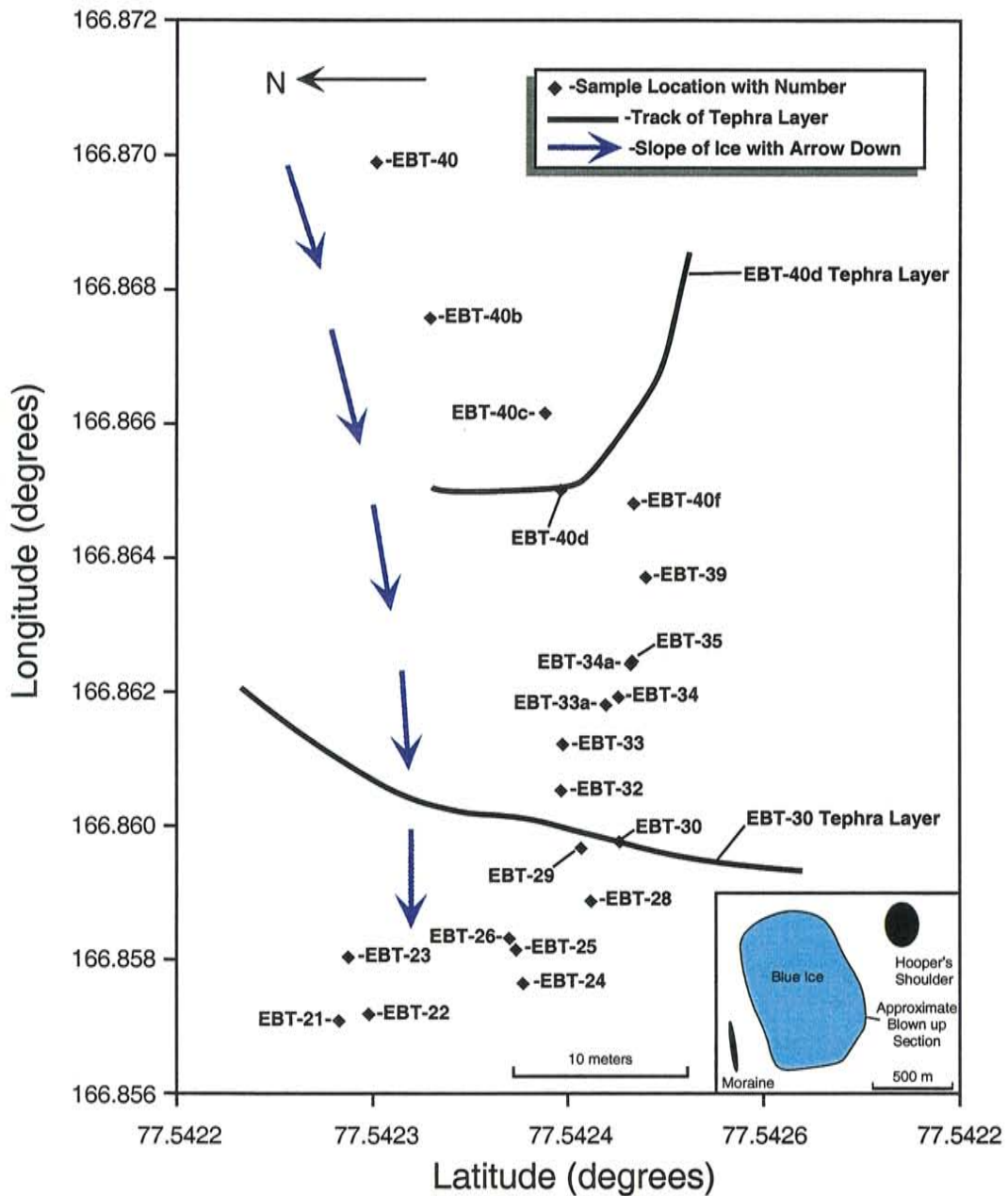


Figure B4-A map of the Hooper's Shoulder site showing sampling locations determined using GPS. Two of the tephra layers have been drawn using kinematic GPS. This site provides the most extensive stratigraphy of tephra layers with the samples younging upslope. The inset is a sketch map showing the location of the blue ice site relative to the Hooper's Shoulder dome.

underlies EBT-61. These tephra samples can not be placed in a relative stratigraphic context because they were not collected from the Barne Glacier.

Sample EBT-19 is from an eruption that occurred on 16 December 1997. This sample was collected from the surface of snow along the north rim of the main crater (Fig. B2).

Two distal tephra samples collected from the Transantarctic Mountains are also included in this study. BIT-42 was collected at Manhaul Bay, located approximately 210 km northwest of Mount Erebus (Fig. B1). The Manhaul Bay blue ice locality is an isolated region of blue ice positioned within a large U-shaped embayment into the Allan Hills Nunatak. BIT-288 was collected from a tephra layer at the Mt. DeWitt blue ice site located along the Transantarctic Mountains approximately 180 km west-northwest of Mount Erebus (Fig. B1).

Tephra Characteristics

The tephra layers are exposed as dark bands in the ice or firn. They range in both thickness and concentration from nearly clean ice up to ~30 cm of concentrated tephra (Fig. B3b). The dark colored tephra decreases the albedo of the glacial ice and absorbs the sunlight increasing ablation and causing the surface exposure of the tephra to be slightly depressed relative to the clean ice surface (Fig. B3c). For highly concentrated tephra layers, small pods of tephra (melt pods) may be present just below the surface of the ice (Fig. B3d). These melt pods are formed by the redistribution of the tephra in the ice during melting caused by solar heating

METHODS

Sampling

All samples were obtained from blue ice with the exceptions of samples EBT-41 through EBT-46 that were sampled from firn and samples EBT-19 and EBT-20 that were collected from the snow surface. During the initial exploration for tephra, small reconnaissance samples (~1-3 kg) were taken using an ice axe to chip ice from the surface exposure of a tephra layer. Later larger ice samples, ranging from ~25 kg to ~365 kg, were taken from selected layers using a chainsaw to cut blocks of tephra-bearing ice from the glacier. These ice blocks were melted in a large pot using a camping stove, the water was decanted, and the remaining tephra sample was air-dried.

Electron Microprobe Analysis

Geochemical analysis of major and some trace elements (Si, Ti, Al, Fe, Mn, Mg, Ca, Na, K, P, S, F, and Cl) was made on glass and feldspar using a Cameca SX-100 electron microprobe at the New Mexico Bureau of Mines and Mineral Resources. Glass shards were analyzed using a defocused 25 μm beam to mitigate Na_2O loss (Hunt and Hill, 1993). Sample EBT-61 is significantly finer grained than the other tephra, necessitating the use of a 10 μm beam to analyze the glass shards. Feldspar was analyzed in all of the samples using a 10 μm beam. Beam current was 10 nA for glass and 20 nA for feldspar. An accelerating potential of 15 kV was used throughout. Counts on peak were 20 seconds for all elements except Na, Cl, and F, which were counted at 40, 40, and 100 seconds, respectively. The Berkeley 310 Albite and Berkeley 374 Orthoclase feldspar standards and VG568 rhyolite, KN18, and KE12 glass standards were analyzed

during each analytical session to monitor the accuracy of microprobe calibration. Typical analytical precision for the microprobe is listed in the notes to Table B1.

Instrumental Neutron Activation Analysis

Instrumental neutron activation analysis (INAA) was used to measure trace element concentrations (As, Ba, Ce, Co, Cr, Cs, Eu, Hf, La, Lu, Nd, Rb, Sb, Sc, Sm, Ta, Tb, Th, U, Yb) and some major element concentrations (FeO and Na₂O). Whole tephra samples were split into ~100 mg portions, sealed into high purity quartz vials, and irradiated at the University of Missouri research reactor for 24 hours under an average neutron flux of $2.5 \times 10^{13} \text{ n cm}^{-2} \text{ s}^{-1}$. All analyses were counted at the New Mexico Institute of Mining and Technology (as detailed in Hallett and Kyle, 1993) using two coaxial p-type high purity Ge detectors with resolutions at 1.8 keV at 1332 keV and 0.6 keV at 122 keV. A total of 8192 channels of spectra data were collected using a Nuclear Data 9900 system and reduced by the TEABAGS (Trace Element Analysis By Automated Gamma-ray Spectrometry) program (Lindstrom and Korotev, 1982) using a Digital VAXstation 3100 computer. Samples were counted between 6 to 12 days and again at 30 to 45 days after irradiation. Analytical precision was determined using four aliquots of the intralaboratory Antarctic tephra standard BIT-110 and is listed in the notes of Table B2. Standard NIST SRM 1633a (coal fly ash) was used as a reference standard for all of the elements except Na₂O, where USGS Rock Standard G-2 was used.

Table B1-Electron microprobe analyses of glass from phonolitic tephra.

Sample	EBT-1	EBT-3	EBT-4	EBT-5	EBT-6	EBT-7	EBT-8	EBT-9	EBT-10	EBT-12	EBT-16	EBT-17	EBT-18	EBT-19	EBT-21	EBT-22	EBT-23a
# points	(n=9)	(n=7)	(n=9)	(n=8)	(n=4)	(n=8)	(n=10)	(n=10)	(n=10)	(n=10)	(n=7)	(n=8)	(n=10)	(n=10)	(n=6)	(n=7)	(n=9)
SiO ₂	55.01	55.08	55.29	54.99	55.86	55.16	55.05	54.96	54.91	54.46	54.95	55.53	55.14	55.59	54.23	54.49	54.44
sig. Si	0.19	0.16	0.19	0.62	1.29	0.26	0.12	0.17	0.15	0.28	0.27	0.29	0.16	0.32	0.26	0.37	0.21
TiO ₂	1.05	1.09	1.01	1.03	0.95	1.04	1.08	1.02	1.04	1.04	1.11	1.07	1.04	1.02	1.04	1.05	1.08
sig. Ti	0.05	0.04	0.03	0.09	0.19	0.06	0.04	0.02	0.05	0.06	0.04	0.05	0.05	0.03	0.05	0.03	0.05
Al ₂ O ₃	19.59	19.67	20.18	19.91	19.35	20.30	19.68	19.75	19.75	20.10	19.70	19.96	19.70	19.87	19.90	19.98	19.81
sig. Al	0.12	0.09	0.13	0.30	0.83	0.19	0.11	0.13	0.08	0.27	0.14	0.23	0.08	0.15	0.13	0.13	0.10
FeO	5.65	5.69	5.36	5.73	5.64	5.40	5.64	5.60	5.65	5.42	5.71	5.44	5.58	5.53	5.53	5.52	5.55
sig. Fe	0.08	0.09	0.08	0.24	0.20	0.16	0.14	0.13	0.09	0.08	0.12	0.10	0.12	0.09	0.08	0.12	0.09
MnO	0.25	0.25	0.24	0.24	0.21	0.24	0.23	0.24	0.25	0.25	0.23	0.25	0.28	0.26	0.28	0.26	0.21
sig. Mn	0.04	0.05	0.06	0.04	0.03	0.05	0.06	0.06	0.05	0.02	0.05	0.03	0.05	0.04	0.03	0.05	0.05
MgO	0.87	0.91	1.00	0.90	0.92	0.96	0.88	0.87	0.88	0.88	0.92	0.90	0.88	0.86	0.89	0.90	0.92
sig. Mg	0.03	0.02	0.24	0.09	0.29	0.05	0.02	0.03	0.03	0.03	0.06	0.01	0.02	0.03	0.01	0.03	0.03
CaO	1.84	1.89	1.86	2.05	1.89	1.86	1.87	1.86	1.87	2.05	2.03	1.90	1.87	1.82	2.07	2.01	2.08
sig. Ca	0.07	0.04	0.05	0.20	0.10	0.04	0.05	0.05	0.03	0.05	0.06	0.07	0.06	0.04	0.09	0.10	0.05
Na ₂ O	9.29	8.95	8.76	8.86	8.92	8.80	9.17	9.43	9.37	9.50	9.16	8.65	9.15	8.84	9.67	9.39	9.61
sig. Na	0.00	0.00	0.00	0.00	0.00	0.00	0.00	0.00	0.00	0.00	0.00	0.00	0.00	0.00	0.00	0.00	0.00
K ₂ O	5.67	5.70	5.51	5.56	5.56	5.52	5.61	5.55	5.59	5.63	5.46	5.49	5.63	5.51	5.61	5.63	5.53
sig. K	0.09	0.08	0.08	0.17	0.13	0.08	0.05	0.06	0.08	0.06	0.28	0.09	0.10	0.06	0.16	0.09	0.09
P ₂ O ₅	0.30	0.30	0.29	0.28	0.28	0.25	0.32	0.28	0.29	0.29	0.27	0.28	0.30	0.27	0.32	0.30	0.30
sig. P	0.04	0.05	0.03	0.06	0.08	0.03	0.04	0.06	0.03	0.05	0.04	0.08	0.05	0.05	0.06	0.04	0.02
F	2632	2348	2587	2428	2248	2434	2480	2124	2045	1802	2463	3556	2037	2156	2371	2338	2717
sig. F	452	628	941	673	669	993	978	816	584	931	733	2245	850	963	862	522	854
SO ₂	0.07	0.08	0.09	0.09	0.08	0.07	0.09	0.08	0.08	0.08	0.08	0.06	0.07	0.08	0.09	0.09	0.09
sig. S	0.02	0.02	0.03	0.03	0.04	0.02	0.01	0.01	0.02	0.02	0.01	0.01	0.01	0.02	0.01	0.01	0.01
Cl	1627	1721	1571	1442	1423	1440	1520	1578	1551	1507	1530	1581	1638	1645	1520	1619	1353
sig. Cl	187	155	154	201	104	76	107	181	153	133	115	129	146	170	210	160	103
Total	100.03	100.00	100.01	100.03	100.04	100.01	100.02	100.02	100.02	100.03	100.02	100.05	100.02	100.03	100.02	100.02	100.03

Notes: Oxides reported are as weight percent, F and Cl reported in ppm. Typical analytical precision for microprobe is represented by the standard deviation of

replicate analyses of standard VG568, KNI18, and KE12: SiO₂ (0.47wt%), TiO₂ (0.03wt%), Al₂O₃ (0.18wt%), FeO (0.06wt%), MnO (0.06wt%), MgO (0.07wt%),

CaO (0.02wt%), Na₂O (0.55wt%), K₂O (0.27wt%), P₂O₅ (0.02wt%), F (1910 ppm), SO₂ (0.01 wt%), Cl (67 ppm). MgO precision N.W. Dunbar, pers. Commun., 2000.

Table B1 continued-Electron microprobe analyses of glass from phonolitic tephra.

Sample # points	(n=10)	(n=10)	(n=5)	(n=5)	(n=6)	(n=10)	(n=10)	(n=9)	(n=8)	(n=7)	(n=8)	(n=8)	(n=7)	(n=7)	(n=7)	(n=7)	(n=7)	(n=7)	(n=10)	(n=10)
SiO ₂	54.16	54.61	55.07	55.10	55.46	55.43	55.44	55.10	54.79	54.97	55.73	55.71	55.24	55.27	55.09	54.26	55.16	55.16	55.16	55.16
sig. Si	0.36	0.35	0.26	0.18	0.54	0.17	0.30	0.31	0.33	0.28	0.40	0.16	0.36	0.37	0.51	0.22	0.29	0.29	0.29	0.29
TiO ₂	1.10	1.04	1.09	1.09	1.13	1.10	1.08	1.05	1.06	1.04	1.10	1.09	1.09	1.05	1.11	1.07	1.02	1.02	1.02	1.02
sig. Ti	0.04	0.05	0.04	0.05	0.08	0.07	0.06	0.05	0.07	0.07	0.06	0.06	0.05	0.04	0.06	0.03	0.06	0.06	0.06	0.06
Al ₂ O ₃	20.01	20.17	19.76	19.78	20.03	20.23	20.02	20.17	19.71	20.30	20.26	20.12	20.10	20.13	20.05	20.19	19.72	19.72	19.72	19.72
sig. Al	0.25	0.16	0.14	0.18	0.17	0.18	0.12	0.05	0.51	0.13	0.27	0.11	0.32	0.10	0.29	0.14	0.16	0.16	0.16	0.16
FeO	5.59	5.52	5.67	5.66	5.51	5.54	5.36	5.47	5.68	5.41	5.46	5.52	5.55	5.40	5.50	5.56	5.63	5.63	5.63	5.63
sig. Fe	0.09	0.07	0.19	0.11	0.05	0.07	0.12	0.13	0.40	0.12	0.15	0.08	0.06	0.09	0.18	0.09	0.11	0.11	0.11	0.11
MnO	0.24	0.22	0.23	0.24	0.27	0.21	0.20	0.25	0.28	0.22	0.24	0.28	0.26	0.21	0.25	0.25	0.25	0.25	0.25	0.25
sig. Mn	0.05	0.03	0.05	0.02	0.08	0.07	0.06	0.08	0.07	0.06	0.05	0.04	0.06	0.05	0.06	0.05	0.03	0.03	0.03	0.03
MgO	0.90	0.81	0.91	0.90	0.81	0.96	0.92	0.95	0.90	0.98	0.93	0.96	0.96	0.90	0.94	0.90	0.88	0.88	0.88	0.88
sig. Mg	0.04	0.26	0.03	0.02	0.35	0.01	0.02	0.08	0.02	0.16	0.04	0.02	0.05	0.01	0.02	0.04	0.03	0.03	0.03	0.03
CaO	2.11	2.07	2.00	2.00	2.01	1.98	2.00	1.98	2.01	1.97	1.98	2.02	2.06	1.94	2.00	2.09	1.86	1.86	1.86	1.86
sig. Ca	0.05	0.04	0.08	0.04	0.04	0.07	0.05	0.06	0.06	0.07	0.08	0.06	0.13	0.07	0.08	0.04	0.08	0.08	0.08	0.08
Na ₂ O	9.59	9.25	9.10	9.03	8.52	8.29	8.90	8.95	9.21	8.88	8.03	8.16	8.55	8.85	8.81	9.35	9.12	9.12	9.12	9.12
sig. Na	0.00	0.00	0.00	0.00	0.00	0.00	0.00	0.00	0.00	0.00	0.00	0.00	0.00	0.00	0.00	0.00	0.00	0.00	0.00	0.00
K ₂ O	5.55	5.62	5.47	5.49	5.43	5.40	5.40	5.42	5.64	5.54	5.51	5.40	5.48	5.47	5.45	5.61	5.59	5.59	5.59	5.59
sig. K	0.11	0.09	0.07	0.08	0.10	0.06	0.13	0.12	0.10	0.11	0.04	0.07	0.04	0.12	0.07	0.09	0.09	0.09	0.09	0.09
P ₂ O ₅	0.32	0.28	0.28	0.30	0.33	0.32	0.29	0.28	0.30	0.26	0.29	0.30	0.31	0.27	0.29	0.29	0.31	0.31	0.31	0.31
sig. P	0.04	0.04	0.03	0.03	0.02	0.05	0.04	0.03	0.02	0.04	0.05	0.03	0.03	0.05	0.03	0.04	0.03	0.03	0.03	0.03
F	2167	2140	2263	1965	2440	3007	1916	1869	2035	2126	1848	1977	1977	2716	2808	2126	2378	2378	2378	2378
sig. F	695	654	779	881	689	978	534	512	480	811	785	712	558	548	775	1020	914	914	914	914
SO ₂	0.10	0.08	0.08	0.08	0.09	0.08	0.08	0.08	0.08	0.08	0.08	0.09	0.08	0.09	0.08	0.09	0.07	0.07	0.07	0.07
sig. S	0.02	0.02	0.01	0.01	0.01	0.00	0.01	0.03	0.02	0.02	0.02	0.02	0.02	0.01	0.01	0.04	0.02	0.02	0.02	0.02
Cl	1536	1445	1537	1599	1902	1703	1631	1379	1435	1437	2078	1828	1674	1900	2163	1593	1563	1563	1563	1563
sig. Cl	140	127	102	206	203	160	1021	169	89	130	359	277	119	173	652	288	171	171	171	171
Total	100.03	100.01	100.03	100.03	100.03	100.03	100.04	100.02	100.02	100.02	100.01	100.02	100.05	100.03	100.05	100.03	100.01	100.01	100.03	100.01

Table B1 continued—Electron microprobe analyses of glass from phonolitic tephra.

Sample	EBT-40	EBT-40a	EBT-40b	EBT-40c	EBT-40d	EBT-41	EBT-43	EBT-44	EBT-45	EBT-47	EBT-48	EBT-49	EBT-50	EBT-51	EBT-52	EBT-53	EBT-54	
# points	(n=9)	(n=10)	(n=10)	(n=8)	(n=10)	(n=10)	(n=9)	(n=9)	(n=10)	(n=9)	(n=10)	(n=10)	(n=10)	(n=10)	(n=10)	(n=10)	(n=10)	
SiO ₂	54.56	54.59	54.50	54.31	54.62	54.65	55.35	55.06	55.39	54.84	54.36	54.49	54.51	54.64	54.42	54.32	54.42	
sig. Si	0.21	0.14	0.22	0.38	0.28	0.22	0.16	0.34	0.29	0.16	0.12	0.34	0.20	0.15	0.31	0.21	0.23	
TiO ₂	0.98	0.98	1.01	1.05	1.04	0.99	1.01	1.00	1.02	1.06	1.06	1.08	1.07	1.07	1.07	1.05	1.03	
sig. Ti	0.05	0.05	0.05	0.07	0.04	0.02	0.05	0.04	0.06	0.03	0.03	0.04	0.04	0.02	0.04	0.05	0.04	
Al ₂ O ₃	20.17	20.08	20.14	20.25	20.17	19.99	20.27	20.22	20.18	20.01	20.13	19.88	19.98	20.06	20.19	20.25	20.20	
sig. Al	0.08	0.08	0.12	0.08	0.19	0.13	0.13	0.20	0.15	0.07	0.13	0.35	0.15	0.08	0.14	0.20	0.10	
FeO	5.52	5.48	5.51	5.48	5.48	5.50	5.34	5.45	5.33	5.47	5.49	5.51	5.52	5.50	5.50	5.46	5.50	
sig. Fe	0.09	0.09	0.11	0.25	0.10	0.20	0.13	0.09	0.21	0.04	0.09	0.09	0.08	0.04	0.11	0.05	0.13	
MnO	0.24	0.22	0.26	0.20	0.25	0.26	0.23	0.25	0.26	0.24	0.28	0.22	0.25	0.21	0.23	0.24	0.22	
sig. Mn	0.07	0.04	0.06	0.04	0.04	0.06	0.06	0.03	0.05	0.04	0.06	0.06	0.05	0.03	0.06	0.08	0.07	
MgO	0.85	0.85	0.87	0.88	0.96	0.87	0.90	0.99	0.87	0.91	0.96	0.94	0.91	0.94	0.92	0.89	1.01	
sig. Mg	0.04	0.03	0.03	0.05	0.11	0.06	0.05	0.17	0.05	0.04	0.08	0.03	0.03	0.03	0.02	0.03	0.28	
CaO	1.93	1.91	1.97	1.97	1.99	1.91	1.82	1.70	1.87	2.01	2.02	2.09	2.08	2.02	2.05	2.05	2.02	
sig. Ca	0.07	0.07	0.06	0.13	0.06	0.05	0.03	0.48	0.04	0.08	0.05	0.07	0.12	0.05	0.07	0.06	0.07	
Na ₂ O	9.26	9.36	9.32	9.36	9.13	9.43	8.97	9.17	8.88	9.17	9.30	9.35	9.23	9.11	9.11	9.25	9.23	
sig. Na	0.00	0.00	0.00	0.00	0.00	0.00	0.00	0.00	0.00	0.00	0.00	0.00	0.00	0.00	0.00	0.00	0.00	
K ₂ O	5.70	5.70	5.70	5.72	5.65	5.65	5.46	5.49	5.53	5.65	5.68	5.69	5.70	5.69	5.74	5.72	5.63	
sig. K	0.13	0.13	0.10	0.11	0.05	0.08	0.07	0.26	0.15	0.09	0.09	0.09	0.11	0.08	0.09	0.06	0.09	
P ₂ O ₅	0.30	0.29	0.29	0.31	0.30	0.29	0.24	0.27	0.23	0.28	0.31	0.33	0.31	0.32	0.31	0.31	0.31	
sig. P	0.03	0.05	0.05	0.05	0.03	0.04	0.05	0.04	0.05	0.04	0.02	0.04	0.03	0.03	0.03	0.04	0.05	
F	2582	2728	2104	2366	1973	2445	1964	1921	2251	1453	1894	2109	2439	2122	2231	2384	2199	
sig. F	494	745	761	832	641	534	439	685	1182	1037	933	741	1516	449	632	740	569	
SO ₂	0.08	0.08	0.08	0.09	0.08	0.08	0.08	0.09	0.09	0.07	0.09	0.08	0.08	0.09	0.09	0.09	0.08	
sig. S	0.01	0.02	0.02	0.02	0.02	0.01	0.02	0.04	0.04	0.01	0.02	0.02	0.01	0.02	0.02	0.01	0.02	
Cl	1605	1658	1631	1597	1543	1585	1490	1377	1447	1574	1472	1593	1552	1551	1577	1563	1472	
sig. Cl	125	93	138	137	74	197	114	114	141	85	158	90	76	117	128	87	82	
Total	100.01	100.01	100.01	100.00	100.01	100.02	100.03	100.03	100.01	100.02	100.02	100.03	100.02	100.01	100.01	100.02	100.02	100.02

Table B1 continued-Electron microprobe analyses of glass from phonolitic tephra.

Sample	(n=4)	(n=7)	(n=10)	(n=10)	(n=10)
# points					
SiO ₂	55.09	55.18	55.04	55.66	55.70
sig. Si	0.21	0.29	0.23	0.27	0.23
TiO ₂	1.02	0.98	1.00	0.95	0.95
sig. Ti	0.04	0.05	0.04	0.04	0.04
Al ₂ O ₃	19.75	19.93	19.92	19.56	19.56
sig. Al	0.08	0.24	0.14	0.07	0.09
FeO	5.66	5.55	5.58	5.92	5.87
sig. Fe	0.09	0.17	0.11	0.09	0.12
MnO	0.25	0.29	0.24	0.28	0.26
sig. Mn	0.08	0.07	0.05	0.05	0.04
MgO	0.89	0.86	0.84	0.80	0.81
sig. Mg	0.02	0.05	0.04	0.01	0.03
CaO	1.91	1.89	1.98	1.92	1.93
sig. Ca	0.05	0.05	0.10	0.04	0.04
Na ₂ O	9.09	9.27	9.05	8.76	8.72
sig. Na	0.00	0.00	0.00	0.00	0.00
K ₂ O	5.61	5.32	5.62	5.53	5.53
sig. K	0.07	0.44	0.21	0.15	0.06
P ₂ O ₅	0.30	0.28	0.26	0.24	0.27
sig. P	0.03	0.06	0.04	0.04	0.04
F	2108	2137	2332	1812	1969
sig. F	80	1077	751	807	854
SO ₂	0.06	0.07	0.08	0.08	0.09
sig. S	0.01	0.02	0.03	0.02	0.03
Cl	1618	2249	1572	1349	1388
sig. Cl	108	905	131	137	200
Total	100.01	100.05	100.02	100.01	100.02

Table B2-Instrumental neutron activation analysis of phonolitic tephra samples.

Sample	EBT-1	EBT-8	EBT-17	EBT-18	EBT-19	EBT-35A	EBT-36	EBT-37	EBT-38	EBT-40	EBT-40B	EBT-40D	EBT-41
Na ₂ O	8.61	8.42	8.31	8.07	7.85	8.65	8.73	8.73	8.53	8.17	8.66	8.67	8.99
Sc	2.79	2.75	3.17	2.91	2.69	2.88	2.73	2.86	2.87	2.85	2.92	2.84	2.86
FeO	5.23	5.26	6.13	5.65	5.13	5.58	5.21	5.60	5.63	5.55	5.84	5.39	5.42
Co	2.43	2.88	3.67	2.57	2.25	2.57	2.39	2.93	3.16	2.55	2.93	2.34	2.13
Zn	154	137	170	166	157	150	152	166	172	155	172	159	158
As	5.0	2.6	3.3	9.4	10.3	5.7	4.1	3.5	6.4	6.7	4.5	7.8	3.1
Br	3.9	3.3	3.4	4.7	4.9	4.8	4.8	4.3	3.8	4.3	4.1	4.3	4.2
Rb	136	112	128	123	132	136	140	138	134	129	133	144	145
Sr	427	785	476	471	258	302	381	333	343	454	402	337	234
Sb	0.32	0.34	0.70	0.67	0.47	0.52	0.40	0.43	0.56	0.41	0.34	0.48	0.44
Cs	1.80	1.45	1.59	1.84	1.86	1.86	1.80	1.84	1.81	1.86	1.68	1.88	1.87
Ba	621	836	628	688	473	574	639	546	510	660	626	493	535
La	148.0	136.4	149.0	148.7	149.0	155.7	150.2	152.9	153.3	152.1	153.7	156.0	160.7
Ce	284.7	261.6	287.0	287.4	287.4	306.0	288.3	299.3	293.9	289.4	297.9	300.0	309.0
Nd	107.6	87.3	98.9	100.9	97.5	101.9	102.0	97.0	101.3	104.0	105.4	107.0	113.3
Sm	17.54	15.67	17.55	17.64	17.31	18.39	17.29	17.60	17.89	17.74	17.75	18.17	18.97
Eu	3.88	4.44	4.03	4.13	3.59	3.84	3.80	3.76	3.73	4.11	4.08	3.74	3.75
Th	2.08	1.88	2.12	2.13	2.07	2.20	2.08	2.18	2.09	2.14	2.17	2.23	2.23
Yb	6.78	6.00	6.62	6.69	6.45	7.10	6.85	6.96	7.02	6.50	6.93	6.92	7.50
Lu	0.997	0.803	0.963	0.912	0.981	0.966	0.965	0.984	1.023	0.922	0.963	1.052	1.032
Hf	27.15	23.28	26.16	26.11	27.92	28.78	27.70	28.70	28.50	26.64	26.99	29.10	29.77
Ta	20.03	17.67	19.20	20.14	24.50	21.72	20.50	21.32	21.10	20.00	20.03	22.06	22.10
Th	25.88	22.05	24.23	25.10	26.33	27.53	25.92	27.26	26.60	25.02	25.60	27.82	28.37
U	6.61	7.59	8.25	6.74	6.90	8.07	8.02	7.83	9.20	7.14	8.50	8.06	8.83

Notes: Oxides reported as weight percent, all other elements in ppm

Table B2 continued-Instrumental neutron activation analysis of phonolitic tephra samples.

Sample	EBT-47	EBT-48	EBT-49	EBT-50	EBT-51	EBT-52	EBT-53	EBT-54	EBT-56	BIT-42	BIT-288	Precision*
Na ₂ O	8.21	8.57	8.52	8.27	8.58	8.51	8.41	8.56	8.33	8.18	8.41	0.01
Sc	3.20	2.85	2.85	3.06	2.86	2.93	2.64	2.90	3.00	2.30	2.79	0.06
FeO	5.65	5.57	5.51	5.51	5.50	5.44	5.30	5.64	5.40	4.73	4.78	0.03
Co	3.29	2.91	2.87	3.97	2.70	3.26	2.76	2.68	3.16	2.35	2.27	0.15
Zn	309	174	166	315	197	224	153	164	162	133	135	2
As	9.2	6.8	5.3	8.1	6.2	5.6	4.5	7.7	4.8	4.4	3.7	0.2
Br	4.3	4.8	4.4	5.1	4.3	3.9	4.0	3.9	3.8	2.5	3.5	0.2
Rb	125	135	136	137	140	130	124	138	130	102	114	2
Sr	426	314	477	356	334	488	542	293	456	836	722	54
Sb	3.57	1.90	3.14	2.12	0.66	6.72	0.55	1.79	0.53	0.67	1.50	0.04
Cs	1.76	1.88	1.79	1.80	1.78	-	1.64	1.97	1.80	1.43	1.37	0.04
Ba	659	537	603	587	567	712	716	533	581	1199	1038	13
La	151.3	153.9	155.2	150.8	155.3	147.5	146.7	155.8	145.7	139.0	138.4	0.2
Ce	285.8	298.3	298.8	293.5	299.2	283.1	280.0	304.0	276.8	271.0	270.3	0.9
Nd	105.2	100.0	104.7	101.0	105.2	95.3	101.6	100.0	95.0	99.0	102.0	2.0
Sm	17.98	18.06	18.11	17.35	18.24	17.32	16.86	18.13	17.22	16.58	17.12	0.13
Eu	3.90	3.80	3.93	3.72	3.75	4.08	4.12	3.79	3.75	5.28	5.01	0.02
Tb	2.10	2.20	2.19	2.13	2.16	2.09	2.01	2.23	2.07	1.96	2.00	0.03
Yb	6.70	6.68	7.22	6.88	7.08	6.49	6.52	7.01	6.46	5.65	5.97	0.05
Lu	0.969	1.025	0.974	0.977	1.023	0.918	0.913	0.962	0.914	0.804	0.815	0.009
Hf	27.41	28.60	27.81	28.00	29.00	26.18	25.64	28.50	26.50	21.00	22.50	0.20
Ta	20.30	21.82	20.45	21.13	21.30	19.71	18.88	21.67	19.15	15.33	16.00	0.01
Th	26.10	27.47	26.31	26.57	26.94	24.96	24.16	27.34	24.91	19.34	20.35	0.10
U	7.83	7.51	9.00	8.24	8.06	7.59	7.18	7.63	6.92	5.80	6.70	0.10

Notes: Oxides reported as weight percent, all other elements in ppm

*Precision determined from intralaboratory standard BIT-110.

Geochemical Correlation

The electron microprobe geochemistry of each sample is compared to all other samples using the Euclidean distance (D) as measured in units of standard deviation (Perkins *et al.*, 1995). D is defined as:

$$D^2 = \sum_{k=1}^n \left[\frac{(x_{k1} - x_{k2})^2}{2\sigma_k^2} \right]$$

where x_{k1} is the amount of element k in the first sample, x_{k2} is the amount of element k in the second sample, and σ_k is the analytical precision for element k . A D value of zero indicates perfect correlation between two samples with similarity diverging as D increases. However, because analytical precision is factored into the equation, D values up to 5.1 are considered to be geochemically indistinguishable. Analytical precision was determined using the Berkeley Albite 310 for SiO₂ (0.78%), Al₂O₃ (0.16%), Na₂O (0.38%), and K₂O (0.01%) to avoid problems due to Na₂O loss during microprobe analysis. Precision for all other elements was determined using the VG568 rhyolite glass standard (Table B1, notes).

Scanning Electron Microscopy

Scanning electron microscopy images were collected using the electron microprobe described above. Tephra samples were sprinkled onto double-sided carbon tape adhering to a glass slide then evaporatively coated with carbon. An accelerating potential of 15 kV and a beam current ranging from 0.05 to 1 nA was used for imaging.

RESULTS

Geochemistry

All of the tephra, except one, are phonolitic with an average of ~55% SiO₂ and 11% to 14.5% total alkalis (Na₂O + K₂O) (Table B1; Fig. B5). Sample EBT-61 is a trachyte (Fig. B5) with lower SiO₂, Al₂O₃, TiO₂, CaO, MgO, and alkalis, and higher FeO (Fig. B6) than the phonolites. No significant elemental variations are observed in the major element geochemistry of the phonolites (Fig. B6). Subtle differences are present in the Na₂O and K₂O concentrations, but are generally within analytical precision for both elements. Na₂O loss during microprobe analysis (Hunt and Hill, 1993) is not considered a problem because the values obtained from microprobe analysis are consistently higher than the concentrations measured using INAA of whole tephra samples (Table B2). If Na₂O loss had occurred concentrations measured with the electron microprobe should be lower than INAA because no Na₂O loss occurs during INAA analysis.

Only phonolitic samples were analyzed using INAA (Table B2). The OIB normalized trace element pattern (Fig. B7) shows a slight enrichment in LREE but no significant systematic variations among samples. Characteristically the proximal samples are depleted in Ba and Sr and have very slight negative Eu anomaly in the chondrite normalized trace element pattern (Fig. B7). However, sample EBT-8 does not have a Eu anomaly. Also, the distal tephra samples have slight positive Eu anomalies and are less depleted in Ba and Sr than the proximal tephra samples.

Trace element variation diagrams show trends related to the proportion of feldspar within the sample (*i.e.* feldspar control lines) (Fig. B8). The incompatible elements (Rb, Br, Ce, La, Cs, Hf, Ta, Lu, Yb, Tb, Nd, and Sm) have a strong positive relationship to the

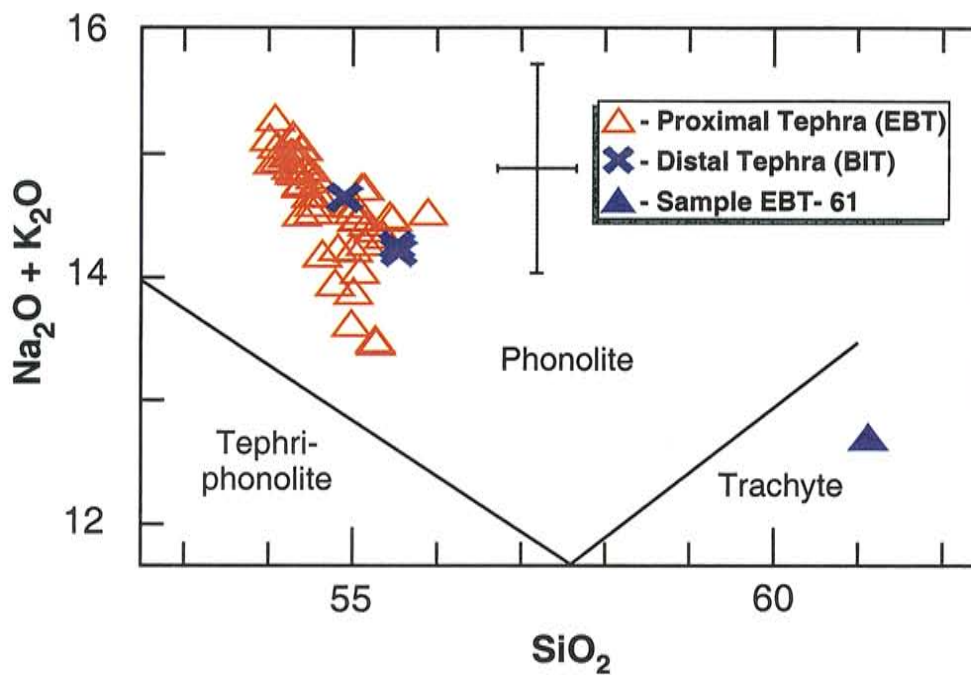


Figure B5-Total alkali vs. silica plot using the chemical classifications of Le Bas *et al.* (1986). Notice the single outlying trachytic tephra, EBT-61, and that all of the other tephra plot as phonolite, including the distal samples. Error bars showing typical analytical error are located next to the legend.

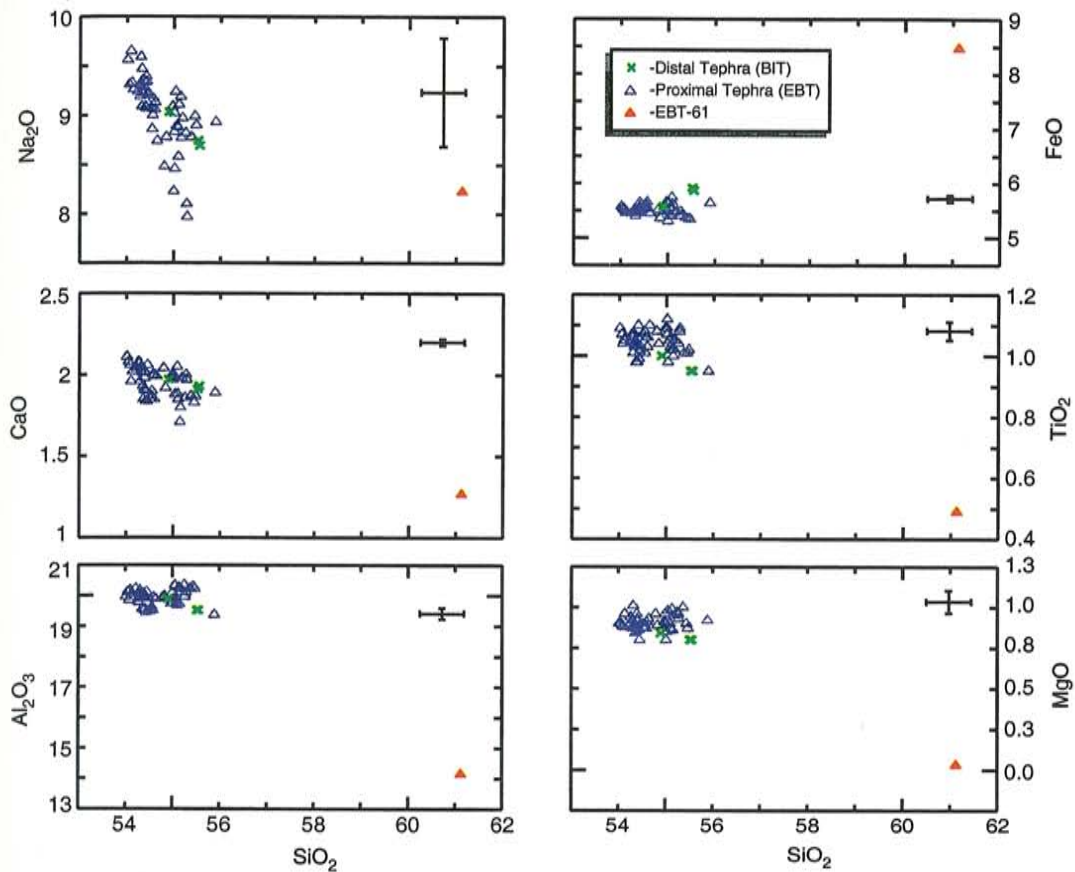


Figure B6-Harker variation diagrams showing that all of the tephra plot as a group except for sample EBT-61. The slight scatter in the Na_2O concentration is an analytical relict. Error bars located in the corners of each diagram indicate typical analytical error.

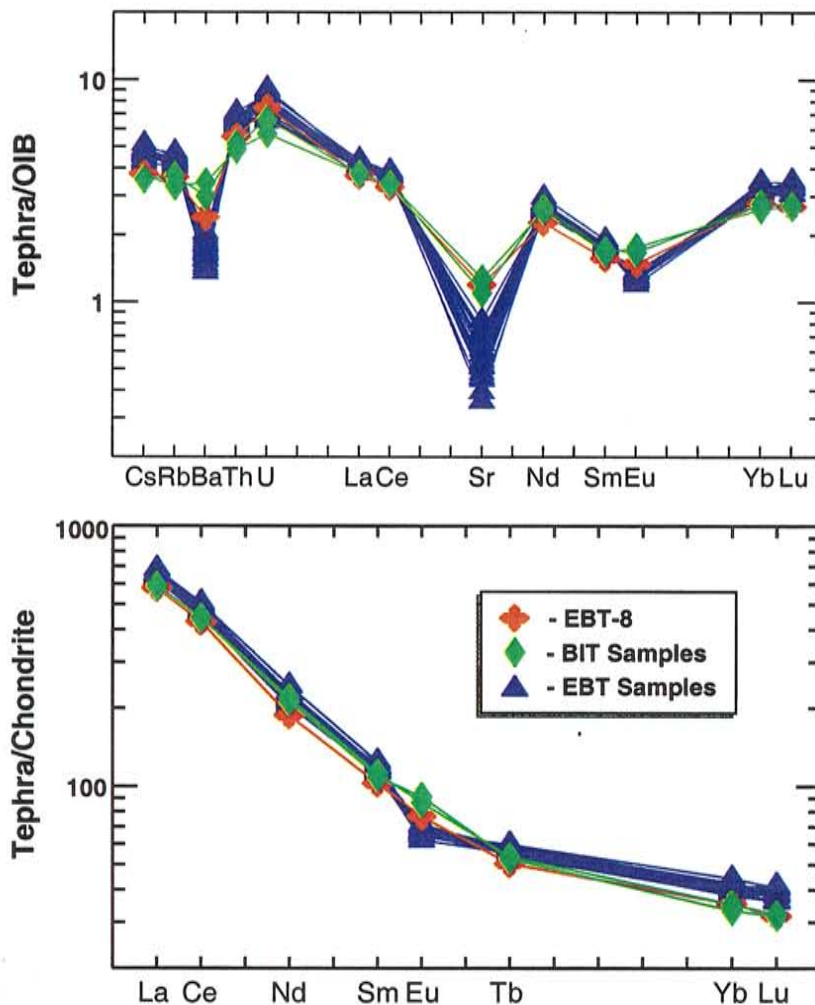


Figure B7-OIB and chondrite normalized (Sun and McDonough, 1989) spider diagrams for the phonolitic tephra samples. Only slight variations exist in the trace element compositions of Ba and Sr in the OIB normalized diagram, which is a result of varying feldspar content of the sample. Notice that sample EBT-8 and the distal BIT tephra samples have the highest concentrations of Ba and Sr indicating high feldspar contents. A high feldspar content for these samples is also indicated by the positive Eu anomalies of the BIT samples and the very slight negative, if any, Eu anomaly for sample EBT-8 on the chondrite normalized spider diagram.

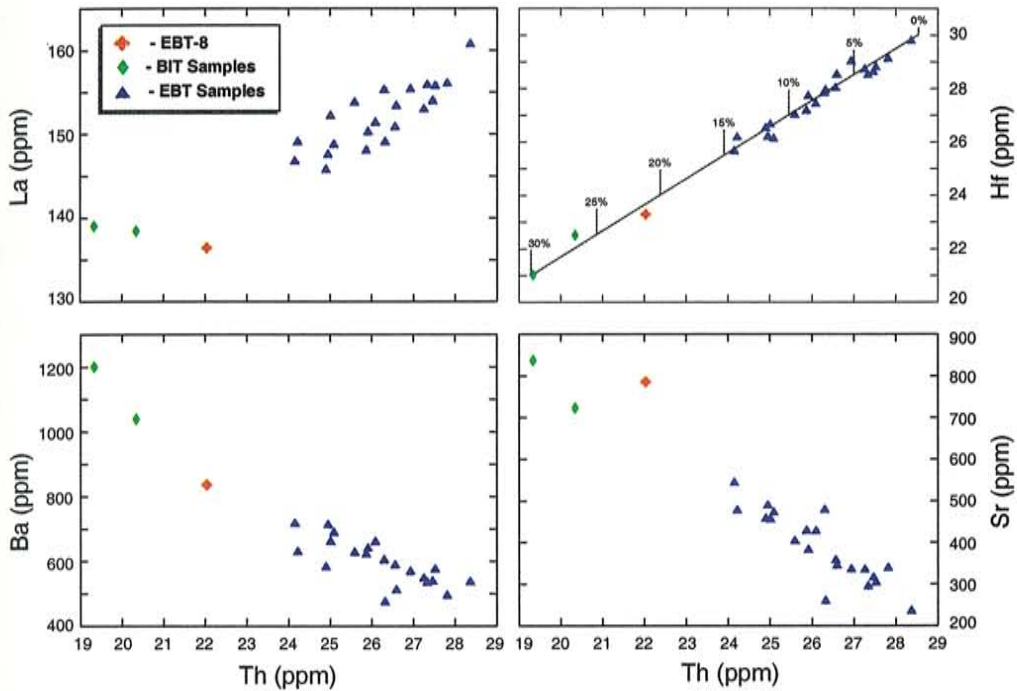


Figure B8-Trace element variation diagrams vs. Th. The trends observed in the trace element geochemistry are feldspar control lines. This is demonstrated in the Hf vs. Th plot where the feldspar content has been modeled. The glass contains approximately 30 ppm Hf and 28.5 ppm Th (Caldwell and Kyle, 1994), whereas the feldspar does not contain either of these trace elements. The feldspar content of the tephra can be calculated simply through dilution of the original trace element concentrations of the glass. The BIT tephra samples and sample EBT-8 all contain an abundance of feldspar, whereas the other phonolitic tephra samples contain at most 15% feldspar.

Th concentration and the compatible element (Sr, Ba, and Eu) concentrations all show well-defined negative control lines relative to Th. The concentrations of U, Sb, As, Sc, and Zn have no clear relationship to the Th concentration. Beside the feldspar controlled concentration differences, no significant geochemical variations exist among the samples.

Both juvenile and xenocrystic feldspar are present in the phonolitic tephra samples (Fig. B9). The juvenile feldspar is anorthoclase ranging in composition from $An_{22}Or_{13}$ – $An_{13}Or_{22}$ while xenocrystic feldspar ranges in composition from $An_{1.5}Or_{49.2}$ – $An_{57.8}Or_{2.8}$.

Scanning Electron Microscopy

Each tephra sample was examined and the relative abundance of key shard morphologies (*i.e.* blocky, pumice, etc.), and grain size and distribution recorded (Table B3). Also, the sorting and relative abundances of glass, crystals, and lithics in the tephra were estimated from SEM and backscattered electron images (Table B3). The main crystal phase observed in the phonolitic tephra is anorthoclase feldspar with subsidiary apatite and rare olivine and Fe oxide and sulfide phases (Fig. B10). Lithic fragments are present in varying degrees and have rough surface morphology (Fig. B10).

The majority of the tephra samples have shard morphologies that can be split into two end member groups (Fig. B11). The first group is composed of blocky and platy shards (Fig. B12) formed by mechanical fragmentation rather than gas driven fragmentation. Mossy shards (Fig. B12c) (Heiken and Wohletz, 1985) are also relatively common with hydration rinds, sublimate coatings, and dust filled cavities occurring less frequently (Fig. B12). The second group of tephra is characterized by a high degree of

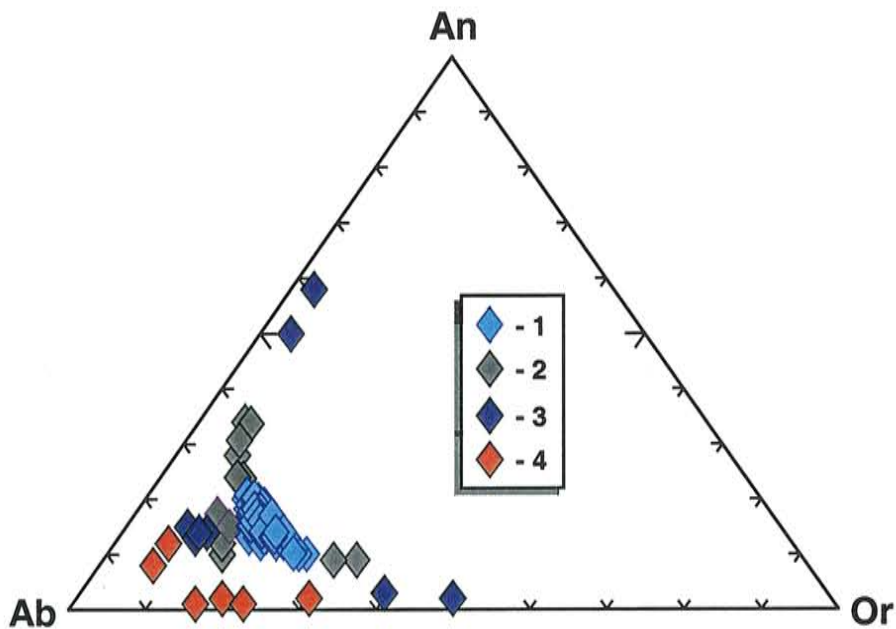


Figure B9-Feldspar ternary diagram showing feldspar analyses from all of the phonolitic tephra samples. The majority of the feldspar is juvenile, however, some xenocrystic feldspar is also present. For example, the two feldspar analyses from group 2 that have purple outlines are xenocrysts from sample EBT-2. **1:** Juvenile feldspar with compositions identical to modern anorthoclase (Kyle, 1977). **2:** Xenocrystic feldspar from a local source with compositions typical of the Erebus Lineage (Kyle *et al.*, 1992). **3:** Xenocrystic feldspar with compositions that suggest a likely local Erebus Lineage origin (Kyle *et al.*, 1992). **4:** Xenocrystic feldspar from distal sources.

Table B3-Table of the tephra component abundances, grain size distribution, morphological features, and eruption type.

Sample	1	2	3	6	7	8	9	10	12	16	17	18	19	21	22	23a	23b
Location	T	T	T	T	T	T	T	M	M	M	M	M	E	H	H	H	H
Glass	P	P	P	S	P	P	F	P	P	F	P	F	P	F	P	P	P
Crystal	S	F	F	S	F	F	S	S	S	F	S	F	S	F	S	S	S
Lithic	S		P	P	S	S	F	F	S	F	S	F	S	F	S	S	S
Vesicularity	high	mod.	low	low	mod.	low	mod.	high	mod.	low	mod.	high	high	low	mod.	mod.	low
Sorting	mod.	poor	well	well	mod.	poor	mod.	mod.	mod.	poor	mod.	poor	poor	poor	mod.	mod.	mod.
Maximum	500	460	280	270	270	400	300	280	660	580	460	115	465	510	370	525	460
Average	200	170	170	90	90	60	175	120	360	135	170	140	150	150	115	140	115
Minimum	30	10	57	30	45	25	30	30	165	30	25	20	45	15	30	30	55
Blocky	O	C	A	A	A	A	A	C	A	C	A	C	C	C	A	C	A
Platy	O		R		O	O	O	C	O	C	A	A	C	C	C	C	C
Mossy	R						O	O		A	O				A	O	R
Dust Aggregate								R									
Hydration Rind				X					X	X			X				
Lattice	O	O	R	O			C	O		C		C					R
Torn	A	A						O	R		R		O			R	
Pumice	C	C	R			R	O	C		R		O	R				
Fluidal	O	O	R			O	O	R		O		O	O			O	O
Droplets					R	O	O	R		R							
Welded Droplets						X	X	X		X						X	
Pele's Hair	R								R				O		R		
Analtime	X	X					X	X	X?	X?		?	X				
Adhering Dust	X	X	X	X	X	X	X	X	X	X	X	X	X	X	X	X	X
Eruption Mode	S	S	Pm	Pm	Pm	Pm	S	S	S	Pm	Pm	Pm	Pm	Pm	Pm	Pm	Pm
					S		Pm	Pm	Pm	S	S	S	S	S	S	S	S

Notes: All sample numbers preceded by "E11-". Sample locations are: T = Terminus of the Barne, M = Middle of the Barne, H = Hooper's Shoulder, E = Erebus Summit, N = Terra Nova Summit, S = Terra Nova Saddle, D = Distal. Modal abundances are represented as: P = Provalent (51-100%), F = Frequent (21-50%), and S = Scarce (1-20%). Relative abundances: A = Abundant, C = Common, O = Occasional, R = Rare, X = Present, but abundance not estimated. Eruption type: Pm = Phreatomagmatic, Pl = Plinian, S = Strombolian.

Table B3 continued-Table of the tephra component abundances, grain size distribution, morphological features, and eruption type.

Sample	30	32	32a	33	33a	34	34a	34b	34c	35	35a	35b	36	37	38	39	40
Modal Distribution																	
Location	H	H	H	H	H	H	H	H	H	H	H	H	H	H	H	H	H
Glass	P	P	P	P	P	P	P	F	P	P	P	P	P	P	P	P	P
Crystal	S	S	S	S	S	S	F	F	S	F	S	S	S	S	S	S	S
Lithic	S	S	S	S	S	S	S	S	S	S	S	S	S	S	S	S	S
Vesicularity	mod. mod.	mod. mod.	mod. mod.	mod. mod.	low mod.	low mod.	low mod.	low well	mod. mod.	mod. mod.	mod. mod.	mod. mod.	low mod.	low mod.	low mod.	low well	low mod.
Sorting	mod. mod.	mod. mod.	mod. mod.	mod. mod.	well mod.	low mod.	low well	well poor	mod. mod.	mod. mod.	mod. mod.	mod. mod.	poor mod.	poor mod.	poor mod.	poor well	poor mod.
Grain Size (um)	430	750	430	490	430	790	675	290	680	590	525	775	580	550	435	500	600
Maximum	120	230	200	150	160	235	135	140	130	200	180	240	180	90	120	130	110
Average	47	115	85	60	50	120	55	85	90	90	70	40	55	30	40	75	10
Minimum																	
Phreatomagmatic Textures																	
Blocky	C	A	C	A	A	O	A	A	A	C	C	C	A	C	A	A	C
Platy	C	C	C	C	O	A	C	C	C	C	C	C	A	A	A	C	C
Mossy	R	O			O		R	R								R	O
Dust Aggregate Hydration Rind																	
Lattice	O		X?	X	X		X	X	X						X		O
Torn	O	O	O	O		R	O	O	O	R	R	O	O	O	O	O	C
Pumice	O	R	O	R	R	C	C	C	O	C	O	R	O	O	O	O	O
Fluidal	O	O	C	C	R	C	R	O	O	O	C	O	O	O	O	R	O
Droplets	R																R
Welded Droplets																	R
Pele's Hair	R						X	X	X	X	X	X	R	R	X	X	R
Other																	
Analcime													R	R	R	R	X
Adhering Dust	X	X	X	X	X	X	X	X	X	X	X	X	X	X	X	X	X
Eruption Mode	S	S	Pm	S	Pm	S	Pm	Pm	Pm	S	S	S	Pm	S	Pm	Pm	S
	Pm	Pm	S	S	S	Pm	Pm	Pm	Pm	Pm	Pm	Pm	Pm	S	Pm	Pm	Pm

Table B3 continued-Table of the tephra component abundances, grain size distribution, morphological features, and eruption type.

Sample	40a	40b	40c	40d	40f	41	43	44	45	46	47	48	49	50	51	52	53
Modal Distribution	Location	H	H	H	H	H	S	S	S	S	H	H	H	H	H	H	H
	Glass	P	P	P	P	P	P	P	P	P	P	P	P	P	P	P	P
	Crystal	S	S	S	S	S	S	S	S	S	S	S	S	S	S	S	S
	Lithic	S	S	S	S	S	S	S	S	S	S	S	S	S	S	S	S
Vesicularity		low mod.	mod.	high	high	mod.	mod.	mod.	mod.	low mod.	mod.	mod.	high mod.	mod.	high mod.	high	low poor
Sorting		mod.	mod.	mod.	well	mod.	mod.	mod.	mod.	mod.	mod.	mod.	poor	mod.	well	well	poor
Grain Size (um)	Maximum	460	610	650	1110	430	1210	285	440	575	630	620	435	385	360	335	690
	Average	110	110	165	110	175	260	90	90	120	90	140	160	170	125	140	135
	Minimum	40	35	85	20	40	100	20	15	30	45	30	20	40	30	20	10
Phreatomagmatic Textures	Blocky	C	A	A	O	A	C	C	A	C	A	C	C	C	C	A	A
	Platy	C	C	C	C	C	O	O	A	A	C	C	A	C	C	O	C
	Mossy																
Dust Aggregate																	
Hydration Rind	X?			X	X?	X	X	X	X	X	X	X	X	X	X	X	X
Srombolian Textures	Lattice	R	O	O	O	R	C	O	O	O	O	R	R	R	O	O	O
	Torn	O	R	O	C	C	A	O	O	R	R	O	R	R	O	O	O
	Pumice	R	R	O	O	C		R	R	R	R	O	R	O	O	O	O
	Fluidal	R		C	C	O	C	R	R	R	R	O	R	R	R	R	R
	Droplets	O	R		R	R	O	R	R	R	R	R	R	R	O	O	C
	Welded Droplets	X	X	X	X	X	X	X	X	X	X	X	X	X	X	X	X
	Pele's Hair	R	R	O	O			R	R	R	R	R	R	R	R	R	R
Other	Analcime			X						X	X	X	X	X	X	X	X
	Adhering Dust	X	X	X	X	X	X	X	X	X	X	X	X	X	X	X	X
Eruption Mode		Pm	Pm	Pm	S	Pm	S	Pm	Pm	Pm	S	S	S	S	S	Pm	Pm
		S	S	S	S	S	S	S	S	S	Pm	S	Pm	Pm	S	Pm	S

Table B3 continued-Table of the tephra component abundances, grain size distribution, morphological features, and eruption type.

Sample	54	56	61	62	42*	288*
Modal Distribution	H	T	N	N	D	D
Location	P	P	P	P	P	P
Glass	S	S	S	S	F	F
Crystal	S	S	S	S	S	S
Lithic	high mod.	low mod.	low	low	low	mod.
Vesicularity	poor	poor	well	mod.	poor	poor
Sorting	650	230	25	35	140	190
Grain Maximum	150	70	7	10	35	60
Grain Average	20	20	2	5	4	5
Grain Minimum (um)	C	A	C	A	A	C
Blocky	C	A	C	A	C	C
Platy	C	A	C	C	C	C
Mossy				C		
Dust Aggregate			C	C		
Hydration Kind	X					
Strombolian Textures	O	R				O
Lattice	C	C				
Torn	C	O				R
Pumice	C					
Fluidal	C	R		C	C	R
Droplets	X		X	X		X
Welded Droplets	O	R			X	R
Pele's Hair	?	X				
Analcime	X	X	X	X		X
Adhering Dust	S	S	Pl	Pm	Pm	Pl
Eruption Mode						
Other						

*Samples are prefixed by "BIT-" rather than "EBT-". Sample BIT-42 is from Mount DeWitt and sample BIT-288 is from Manhaul Bay.

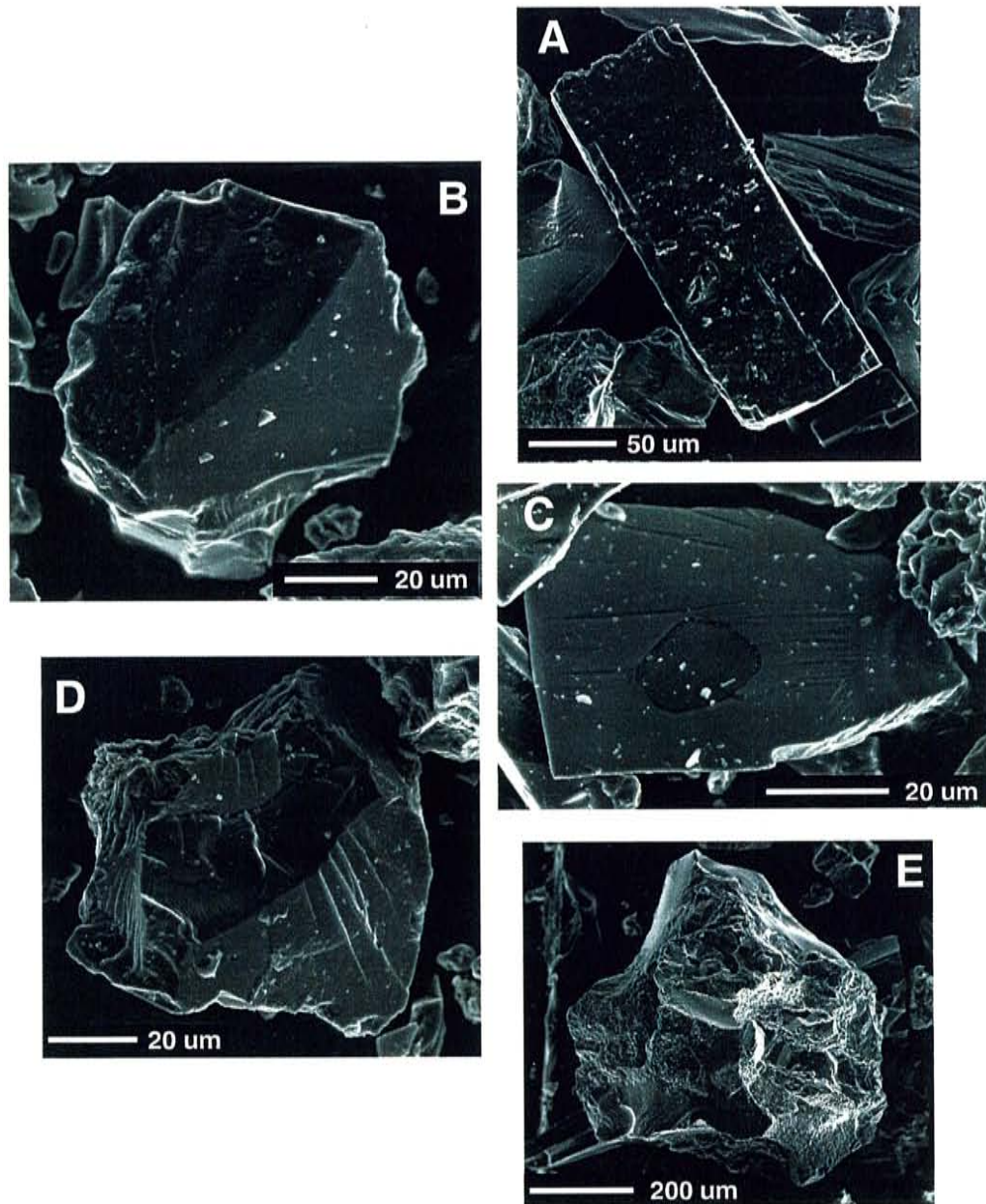


Figure B10-Typical crystal and lithic phases found in the tephra samples. **A:** Anorthoclase feldspar crystal (EBT-3). **B:** An apatite crystal (EBT-53). Apatite is the second most abundant mineral. **C:** An Fe oxide phase, probably magnetite (EBT-53). **D:** An olivine crystal (EBT-53). **E:** A lithic fragment (EBT-10) showing typical massive, blocky, and rough appearance.

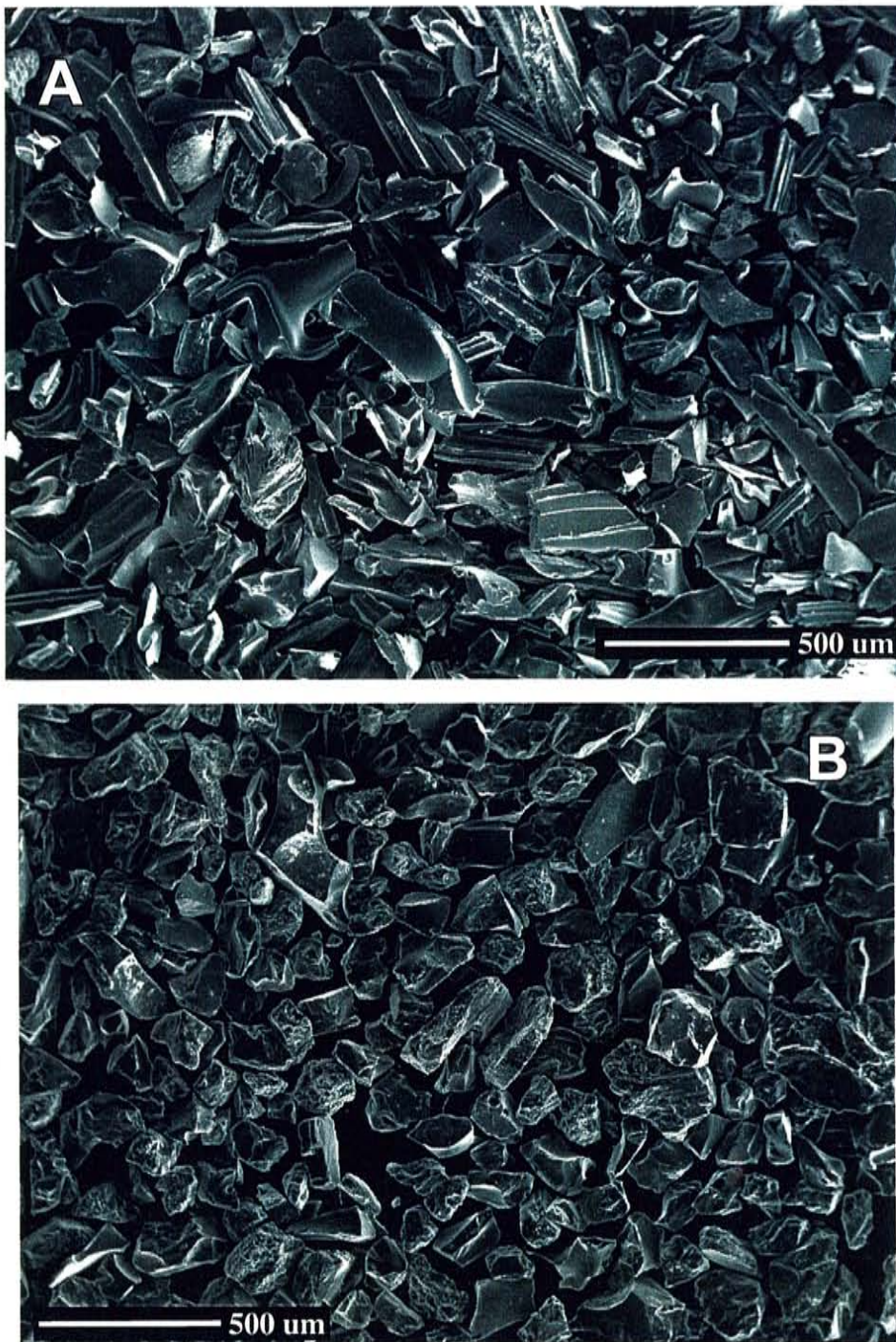


Figure B11-Typical examples of strombolian and phreatomagmatic tephra samples. **A:** Strombolian tephra sample (EBT-51) containing torn and fluidal shards and pumice. **B:** Phreatomagmatic tephra sample (EBT-39) composed of mainly non-vesicular blocky and platy shards.

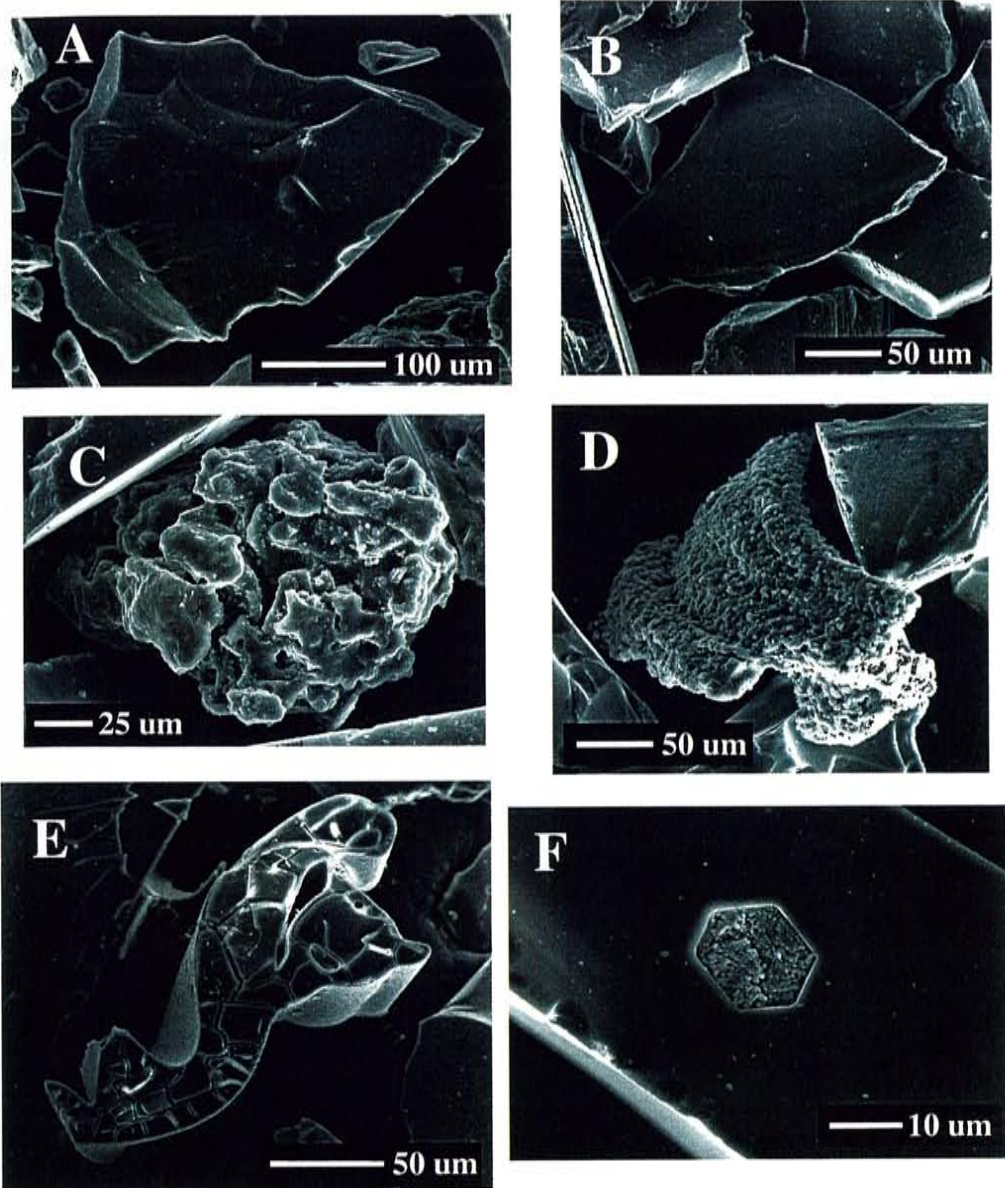


Figure B12-Typical features of phreatomagmatic tephra samples. **A:** Non-vesicular blocky shard (EBT-21). **B:** Platy shard (EBT-50). **C:** Mossy shard (EBT-39). **D:** Shard coated in sublimated material (EBT-36). **E:** Glassy shard with a hydration rind (EBT-19). **F:** Shard with an impression of a plucked crystal (apatite?) that has been filled with fine dust during a phreatomagmatic eruption (EBT-47).

vesiculation and the presence of fluidal shards, pumice, dictyotaxitic clasts, torn shards, and Pele's hair (Heiken, 1978; Heiken and Wohletz, 1985) (Fig. B13). Most of the tephra samples display some quantity of ash from both groups of shard morphologies and span the range of sorting and vesicularity.

Several unusual features are found in the phonolitic tephra. Droplets that range from spherical to subrounded and ash with "budding" morphology are found in some of the phonolitic tephra (Fig. B14). "Budding" morphology has not been previously reported and is described as a main bulbous melt bleb with covered with droplets in varying stages of disaggregation and coalescence. Also, in up to 15 of the tephra samples small clusters of hexagonal crystals were found along with rare individual crystals (Fig. B15). These crystals have been identified as analcime using qualitative elemental scans by electron microprobe. The crystals have excellent crystal form, are commonly twinned, and completely lack adhering glass.

The two distal tephra layers, BIT-42 and BIT-288, are both poorly sorted, contain abundant feldspar, and are distinct from the other tephra samples (Fig. B16). BIT-42 is poorly vesiculated and composed primarily of platy and blocky shards with occasional bubble wall shards. Glass shards in BIT-42 also commonly have chipped edges. BIT-288 is predominantly composed of bubble wall shards with subordinate platy shards and rare pumice. All of the glass shards in BIT-288 are pristine.

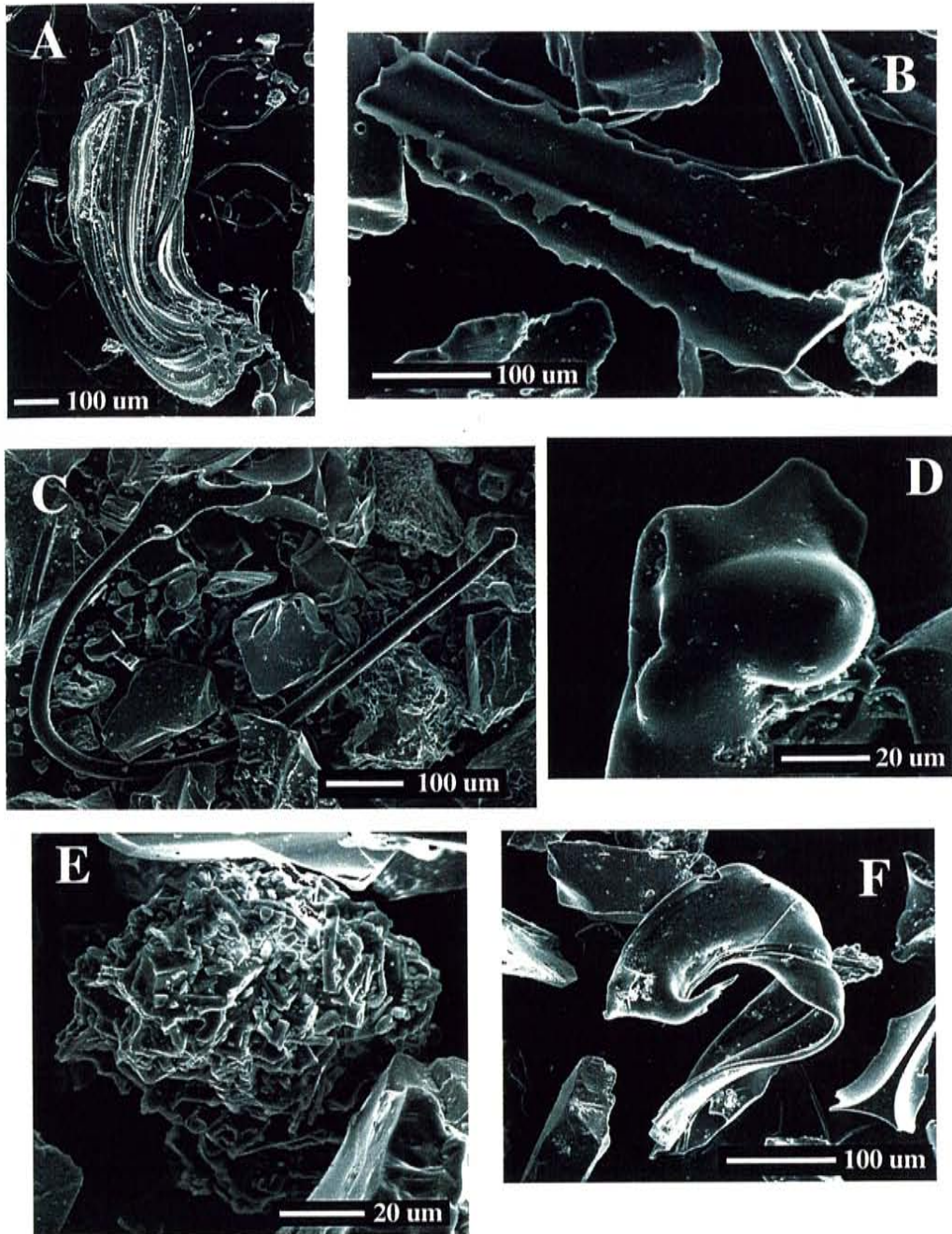


Figure B13-Typical tephra morphologies indicative of strombolian eruptions. **A:** Fluidal and twisted pumice shard (EBT-1). **B:** Torn shard (EBT-35). **C:** Pele's hair (EBT-53). **D:** Fluidal form (EBT-9). **E:** Dictyotaxitic shard (EBT-53). **F:** Fluidal shard (EBT-43).

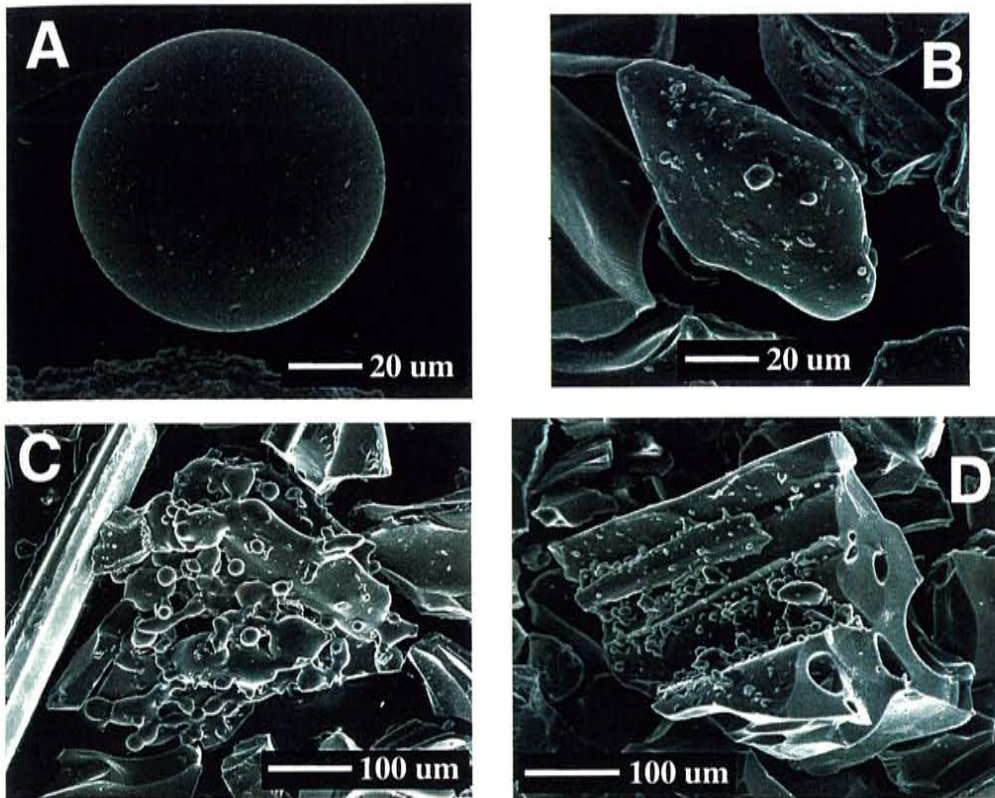


Figure B14-Typical rounded droplets and budding ash associated with strombolian activity. **A:** Spherical droplet (EBT-54). **B:** Sub rounded droplet with smaller droplets welded to the surface (EBT-8). **C:** Budding ash particle resulting from the quenching of a fine magmatic spray during strombolian eruptions (EBT-49). **D:** Shard with adhering fine droplets (EBT-38).

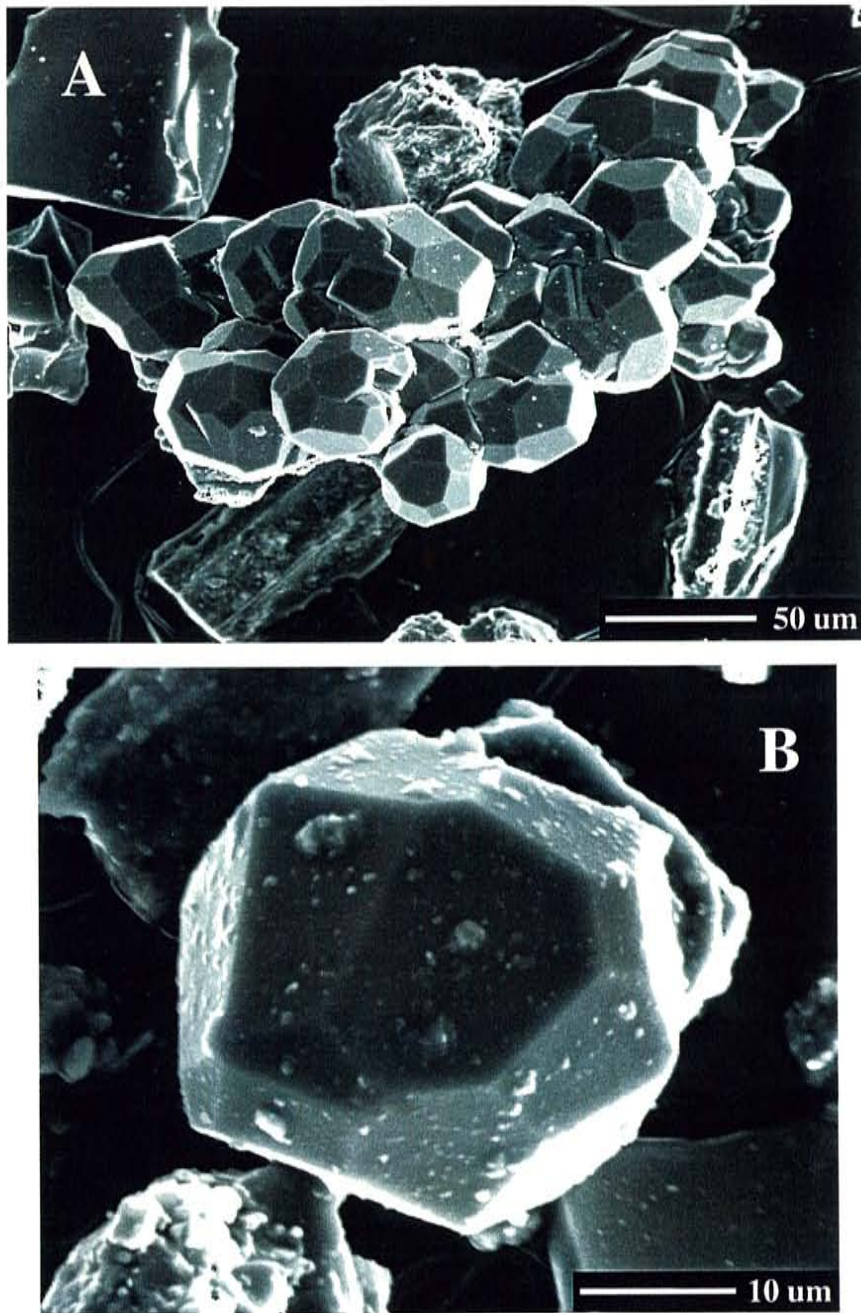


Figure B15-Typical analcime crystals that are a xenocrystic phase in some of the phonolitic tephra samples. Note the excellent crystal forms and lack of alteration, adhering glass, or other signs of contact with the pre-eruption magma. **A:** A typical cluster of analcime crystals (EBT-10). **B:** A rare individual analcime crystal (EBT-56).

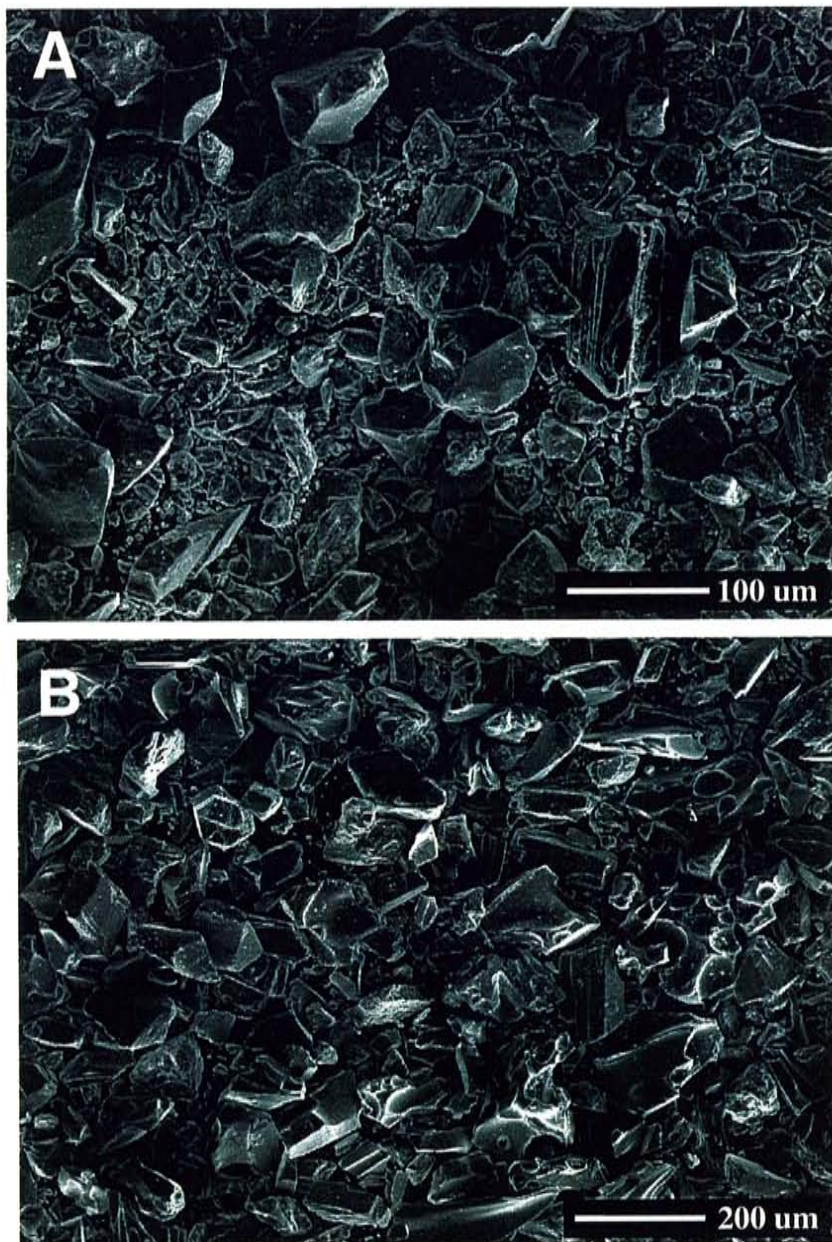


Figure B16-The distal samples erupted from Mount Erebus. Note that the BIT samples are similar in grain size to the other proximal tephra samples (Fig. B11). **A:** Sample BIT-42, from Manhaul Bay, is poorly sorted and has abundant fine ash. Note the chipped edges on the glass indicating wind transport. Also, note the abundant platy and blocky shards indicating phreatomagmatism. **B:** Sample BIT-288 from Mt. DeWitt. Note that the sample is composed of primarily bubble wall shards and is highly vesicular indicating a plinian origin, but has a distinct lack of pumice. Some platy shards are present, indicating that the eruption did have a minor phreatomagmatic component.

DISCUSSION

Geochemistry

The major (Fig. B5, B6) element geochemistry of the phonolitic tephra samples is indistinguishable within precision. The trace element compositions (Fig. B7) of the phonolitic tephra samples are also relatively homogeneous, except for feldspar content induced variations (Fig. B8). Generally, the chondrite normalized trace element diagrams for whole rock samples of Erebus lavas and bombs have small positive Eu anomalies representative of anorthoclase contents $\leq 30\%$ (Kyle *et al.*, 1992; Caldwell and Kyle, 1994). The slightly negative Eu anomaly of the proximal tephra geochemistry suggests that the samples are glass dominated. However, the variations in Ba, Sr, and Eu concentrations are directly proportional to the amount of feldspar in the samples. This is demonstrated in the elemental variation diagrams (Fig. B8). For example, sample EBT-8 and the distal samples contain $\sim 22\%$ and $\leq 30\%$ anorthoclase, respectively, and consistently plot away from the other tephra that contain $\leq 15\%$ feldspar. However, the trace element concentrations of all of the samples plot along the same feldspar control line. Feldspar control is also apparent in the chondrite normalized spider diagram (Fig. B7) where sample EBT-8 has the highest concentration of Eu in a proximal sample and does not have a Eu anomaly. Also, the distal tephra samples have small positive Eu anomalies that are consistent with high concentrations of anorthoclase.

The feldspar geochemistry of the phonolitic tephra samples demonstrates varying degrees of xenocrystic contamination among the juvenile components (Fig. B9). The juvenile feldspar is identical in composition to historically-erupted anorthoclase from Mount Erebus (Kyle, 1977). The majority of the xenocrysts plot within the

compositional range of feldspar from the Erebus Lineage (Kyle *et al.*, 1992) and are considered to be locally derived. These locally derived feldspar crystals were either incorporated during eruption or are aeolian in origin. In addition, several of the tephra samples have xenocrystic feldspar with compositions distinct from the local phenocryst compositions. These feldspar crystals are likely aeolian in origin and are from distal sources.

Geochemical Correlation

The method of geochemical correlation developed by Perkins *et al.* (1995) has been employed in this study to help highlight and quantify geochemical differences between the tephra that are not evident in the plots. By comparing the D values between the tephra layers over a stratigraphic sequence it is possible to determine if any subtle geochemical trends exist over time. This method is not used for the INAA data because the D value is too sensitive to aeolian contamination and variations in the feldspar and lithic content of the tephra samples.

The electron microprobe data (major element, F, SO₂, and Cl concentrations) show very little variation in D between any of the samples (see Appendix 7 for D values). D values generally range between five and seven for the phonolitic samples with the largest difference occurring between samples EBT-23b and EBT-44 (D = 15). The overwhelming majority of the phonolitic tephra have D values ≤ 10.2 (two times the statistically indistinguishable value) of each other indicating that no systematic variations are present. The phonolitic tephra, including the historically erupted samples (EBT-19 and EBT-20), are considered geochemically identical.

Because all of the phonolitic tephra samples are geochemically similar to the historically erupted tephra samples, the source for all of the tephra is considered to be Mount Erebus. It is unlikely that the tephra layers represent the deposits from only a few eruptions that have been exposed and sampled in multiple localities. The two tephra samples with reliable ages, EBT-2 (15 ± 4 ka) and BIT-272 (39 ± 6 ka), indicate that the tephra samples have been erupted over a significant period of time (Section A, this study). Also, at the Hooper's Shoulder blue ice site no overlapping relationships are observed and all of the tephra layers are exposed and dip relatively parallel to each other. This indicates that each tephra layer is an independent unit within the glacial ice and represents a discrete eruptive event.

Sample EBT-61, the trachytic sample, has D values between 65 and 75 when compared to the phonolitic tephra. This tephra sample is geochemically distinct from the phonolitic tephra samples, as is discussed in further detail later.

Eruption Mechanisms

The proximal phonolitic tephra layers were formed by both strombolian and phreatomagmatic eruptions. Morphologies such as blocky, platy, and mossy are indicative of phreatomagmatic eruptions (Wholes, 1983) and are common in the phonolitic tephra samples. Other common features such as hydration rinds, sublimate coatings, and filled vesicles are also associated with phreatomagmatic eruptions (Heiken and Wohletz, 1985). The tephra layers in which these morphologies are considered phreatomagmatic in origin and are similar to other comparable phreatomagmatic deposits (Fig. B12) (*e.g.* Wohletz, 1983; Heiken and Wohletz, 1985).

The strombolian tephra samples also display typical morphologies such as a fluidal and dictyotaxitic shards (Walker and Croasdale, 1971; Heiken, 1978). However, the strombolian tephra samples also contain Pele's hair, pumice, and torn shards (Fig B13), features that are uncommon for strombolian eruptions. Pele's hair is traditionally associated with hawaiian style eruptions (Duffield *et al.*, 1977). However, bombs erupted during modern strombolian eruptions at Mount Erebus commonly have thread-like stringers and often contain interior cavities crossed with abundant fine hairs that can be broken loose to form Pele's hair (Kyle, 1977). Morphologically similar Pele's hair is also formed by strombolian eruptions at Stromboli volcano (Rose, 1987). Pumice is generally associated with plinian eruptions (Heiken and Wohletz, 1985). However, modern strombolian bombs from Mount Erebus are highly vesiculated and often show signs of stretching and twisting similar to the pumice observed in the tephra samples (Fig. B13a) (Kyle, 1977). The torn shards are pumice wall shards that have been broken away from the pumice during fragmentation.

A significant number of the samples contain tephra shards typical of both strombolian and phreatomagmatic eruptions (Fig. B17). The combination of these two eruptive mechanisms is not unusual. It is common for eruptions that begin with phreatomagmatic activity to transition into strombolian activity as the water source is depleted. For example, this progression has been observed during the formation of Surtsey (Thorarinsson, 1966), Capelinhos (Walker and Croasdale, 1971), and the Ukinrek Maars (Self *et al.*, 1980). Closely related phreatomagmatic and strombolian activity has also been observed at White Island (Houghton and Nairn, 1991) and interpreted from the deposits of Rothenberg scoria cone (Houghton and Schmincke, 1989). Also, during the

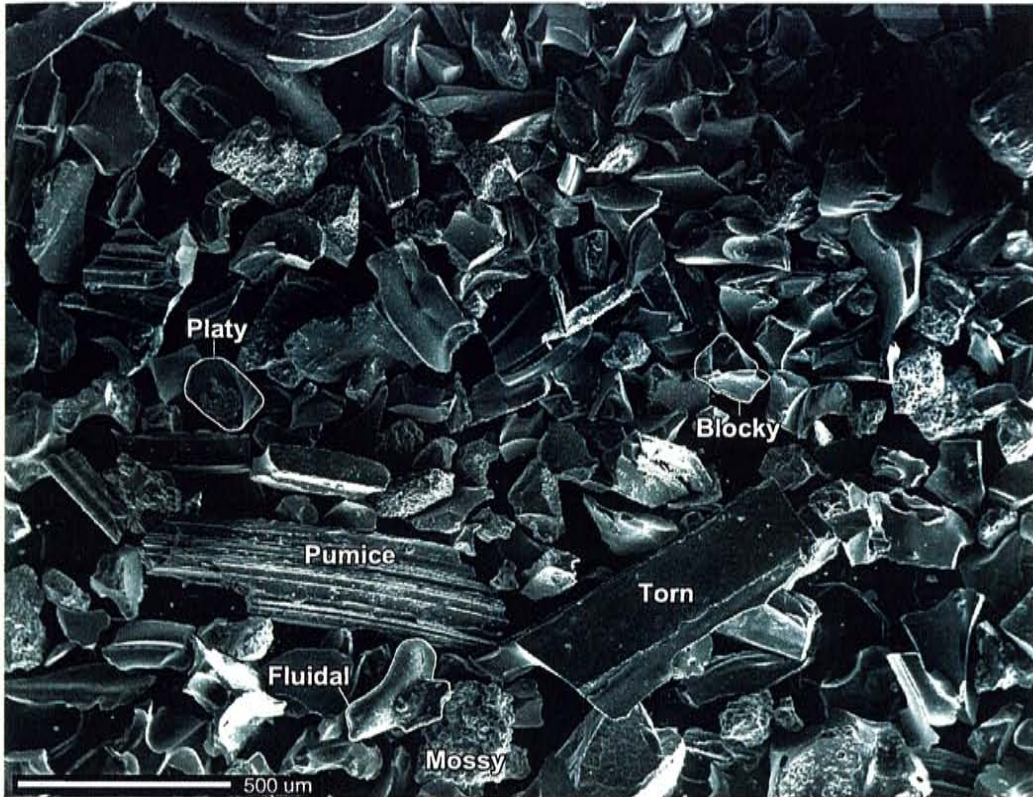


Figure B17-A typical mixed phreatomagmatic and strombolian tephra sample (EBT-50). Shard morphologies for each eruption mode are present within the sample and are indicated.

1971 eruption of Mount Etna, discrete phreatomagmatic bursts during an ongoing strombolian rift eruption were caused by melt-water from snow and ice interacting with the magma (Tanguy, 1971; as reported by Heiken and Wohletz, 1985). The presence of multiple eruption modes recorded in a single sample may also be explained by tephra from several eruptions combined to form a single tephra layer. For example, sample EBT-47 contains both phreatomagmatic and strombolian ash and was collected from a broad diffuse layer suspected in the field to contain two independent tephra units.

The distal tephra resulted from unique eruptive circumstances at Mount Erebus. Both of the samples, BIT-42 and BIT-288, have grain sizes that are only slightly finer (average $\sim 30 \mu\text{m}$ and $\sim 60 \mu\text{m}$ respectively) than the proximal tephra samples (average $\sim 90\text{-}260 \mu\text{m}$) (Figs. B10, B16). Also, both distal samples have anorthoclase contents that are significantly higher than the proximal tephra (Fig. B8). A plinian eruption column would generally be required to distribute tephra of this size and crystal content 180 km to 210 km from the vent (Walker, 1981). However, BIT-42 is composed of platy and subordinate blocky shards (Fig. B16). The presence of these shards indicates a phreatomagmatic rather than plinian origin. Self and Sparks (1978) have demonstrated that large-scale phreatomagmatic, termed phreatoplinian, eruptions can have magnitudes similar to plinian eruptions. However, the cases studied by Self and Sparks (1978) involved large rhyolitic eruptions through caldera lakes, conditions that are impossible at Mount Erebus. The summit area of Mount Erebus currently has extensive snow and ice cover and it is likely that conditions have been the same for an extended period of time. Begét *et al.* (1996) proposed that phreatomagmatic eruptions caused by magma interaction with ice are more explosive than from magma interaction with liquid water.

This is because only a thin layer of water is melted from the ice and interacts with the magma, resulting in a high magma to water ratio. Phreatomagmatic eruptions with high magma to water ratios are known to result in highly explosive eruption conditions (Wohletz, 1983). If the magma for the distal-tephra-producing eruptions interacted with snow, ice, or even melt water it would cause highly explosive phreatomagmatic activity. The eruption that produced sample BIT-42 was likely a large phreatomagmatic eruption at Mount Erebus caused by the interaction of magma with snow and ice. The glass shards in BIT-42 (Fig. 16A) also have abundant chipped edges indicating that the tephra has been subject to some wind transport after deposition.

Sample BIT-288 contains predominantly bubble wall shards with some platy shards and only very rare pumice. The bubble wall shards indicate that the main eruption mechanism was plinian, but the paucity of pumice fragments is enigmatic. Comparatively, a phonolitic tephra deposit from the 12.9 ka plinian eruption at Laacher See volcano collected at approximately the same distance from source has a similar grain size and is composed exclusively of pumice (van den Bogaard and Schmincke, 1985; Juvigné *et al.*, 1995). The platy shards in the tephra sample indicate that the eruption might have had a phreatomagmatic component. This phenomenon is not uncommon on snow and ice clad volcanoes or volcanoes with extensive hydrothermal systems. For example, three other notable plinian eruptions that have had strong phreatomagmatic components are the 13 August 1991 eruption of Hudson volcano and the 79 A.D. and 1631 eruptions of Mount Vesuvius (Cioni *et al.*, 1992; Rolandi *et al.*, 1993; Bitschene and Fernandez, 1995). The presence of a phreatomagmatic component can explain the dearth of pumice in the sample. Platy shards form when a vesiculated magma encounters

water and causes mechanical fracturing of the magma (Wohletz, 1983). This same mechanism might have fractured existing pumice into the abundant bubble wall shards. Sample BIT-288 was formed in a plinian eruption that had a phreatomagmatic component. The source of the water during this plinian eruption was probably snow and ice in the summit region. Also, the BIT-288 plinian eruption might be associated with formation of the older of the two calderas in the summit region of Mount Erebus (Section A, this study).

One question that remains in regards to the distal tephra samples is that there should be deposits of ash within the Dry Valleys region, which is directly between Mount Erebus and the distal-blue ice localities. Numerous tephra deposits have been described in the Dry Valleys (Marchant *et al.*, 1993; Marchant *et al.*, 1996). However, up to 75 tephra deposits have been reported in the Dry Valleys, 50 of which have been dated yielding ages in the millions to tens of millions of years range. Many of these tephra samples are phonolitic and contain abundant anorthoclase similar to Erebus tephra samples (Marchant *et al.*, 1993). It is possible that some of these undated tephra samples from the Dry Valleys are related to the distal Erebus tephra samples.

The eruptions that produced the majority of the proximal tephra layers are likely to have been small, producing only locally-deposited ash. However, in the last 20 years, including periods of enhanced eruptive activity, no eruptions have produced tephra in the volumes implied by the englacial tephra layers (Kyle *et al.*, 1982). Therefore, the eruptions that produced the englacial tephra were certainly large strombolian and phreatomagmatic events, but were small when considered on a regional level. The

observed activity at Mount Erebus also implies that many small eruptions could have occurred, but did not leave tephra deposits.

Spherical and Budding Ash

Droplets and budding ash have been found in many of the phonolitic tephra samples (Fig. B14). Multiple mechanisms have been proposed to form spherical ash particles including surface-tension effects and turbulent magma-water interaction. Also, microspheres can be formed either during eruptions or during periods of passive degassing. Man-made coal-fly ash can also occasionally contaminate volcanic ash causing spherical particles to be present (*e.g.* Rose and Hoffman, 1982). However, coal-fly ash contamination is not considered a possible source for the spheres in this study because of both the isolation of Antarctica from man-made pollutants and, more importantly, the pre-industrial age of the majority of tephra layers.

Spheres have been found in the plumes of passively degassing shallow (on the scale of meters) magma at St. Augustine volcano (Cadle and Mroz, 1978; Hobbs *et al.*, 1978), Mount Etna (Lefèvre *et al.*, 1986; Lefèvre *et al.*, 1991), and Kilauea (Lefèvre *et al.*, 1991; Meeker and Hinkley, 1993). These spheres are formed from a very fine magmatic mist caused by the bursting of bubbles during passive degassing. Generally the spheres are geochemically differentiated due to the leaching action of the entraining gases (Lefèvre *et al.*, 1986). Also, in the case of the spheres from Kilauea, chemical differentiation within the glass droplets is caused by the rapid crystallization of chromium oxide (likely spinel). This crystallization occurs when air mixes with the magmatic gases causing a rapid shift from reduced to oxidized conditions (Meeker and Hinkley, 1993).

Degassing of the Erebus lava lake should provide the appropriate conditions for the formation of glass spheres. However, in prior studies of the particulate composition of the Erebus plume no spheres have been found (Chuan *et al.*, 1983; Chuan, 1994). It is unknown if the droplets from the phonolitic tephra are geochemically differentiated or not. But because the spheres are found within tephra layers, it is likely they formed during an eruption rather than during passive degassing. Also, passive degassing tends to form discrete spheres and does not explain the presence of ash with budding morphology (Fig B14c).

The turbulent interaction of magma with water can also result in the formation of droplets (Wohletz, 1983). Generally these phreatomagmatic droplets are formed in low-viscosity basaltic or experimental settings (Heiken and Lofgren, 1971; Wohletz and McQueen, 1984; Zimanowski *et al.*, 1986). Zimanowski *et al.* (1986) suggest that in high SiO₂ melts viscosity will inhibit turbulent mixing between the melt and water and hence retard the production of droplets. The viscosity of an Erebus phonolite is approximately 6.3×10^4 Pa s (Pascal seconds) (Carmichael *et al.*, 1974) at a typical eruptive temperature of $\sim 1000^\circ$ C (the temperature of the lava lake; Kyle *et al.*, 1982). Comparatively, Hawaiian basalts can have viscosities as low as 50 Pa s to 100 Pa s during eruption (Shaw *et al.*, 1968; Moore, 1984). The Erebus phonolite is likely too viscous to allow the turbulent mixing of water and melt and therefore should not form phreatomagmatic droplets. This argument is further supported by the observation that typical phreatomagmatic tephra samples from Mount Erebus are characterized by blocky and platy shards, which are indicative of mechanical fracturing of the melt rather than turbulent mixing.

Surface-tension effects have formed spheres during fire fountaining at Kilauea (Baker, 1968; Heiken and Lofgren, 1971; Heiken, 1972; Lefèvre *et al.*, 1991), Etna (Lefèvre *et al.*, 1986; Lefèvre *et al.*, 1991), and also on the moon (Heiken and Lofgren, 1971; Heiken and Wohletz, 1985). The spheres in these situations are generally geochemically indistinguishable from other syneruptive products, distinguishing them from spheres formed during passive degassing. Also, spheres formed in this manner are generally formed from low-viscosity melts, such as Hawaiian basalts or even ultramafic melts in the case of the lunar specimens (Heiken and Wohletz, 1985). However, rare spheres have been reported in andesitic tephra samples which have viscosities of the same order of magnitude as Erebus phonolite (Carmichael *et al.*, 1974; King and Wagstaff, 1980; McBirney and Murase, 1984). The spherical ash particles found in the phonolitic tephra samples are proposed to form by surface tension effects acting on a melt spray during strombolian eruptions.

The relatively high viscosity of Erebus phonolite might also explain the formation of budding ash (Fig. B14c). To form spheres a bleb of melt needs to be pinched off from a parent portion of melt. The high viscosity might retard the pinching process enough to allow the parent melt to quench before all of the spheres have budded off. By the same reasoning, budding ash has not been found in basaltic tephra samples because the low viscosity allows pinching to occur prior to quenching. Partial coalescence of previously formed spheres may also play a part in the formation of budding ash. However, observed coagulation of droplets is rare even in low-viscosity melts (Heiken and Lofgren, 1971) and the high viscosity of Erebus phonolite will only act to further inhibit coalescence. Droplets are observed in the phonolitic tephra samples

that are welded to larger shards (Fig. B14d). However, these droplets appear to have been fully formed before being welded to the larger shards rather than truly coalescing.

Analcime

The analcime is likely a xenocrystic phase in the phonolitic tephra samples. Analcime has been previously observed in a tephra sample from Coliseum Diatreme in the Hopi Buttes volcanic field (Heiken and Wohletz, 1985) and nepheline (closely related to analcime) has been found in tephra samples from Ol Doniyo Lengai volcano (Heiken, 1972; Heiken, 1974; Heiken and Wohletz, 1985). However, in both locations the crystals are heavily covered in sublimate and or glass and have poor crystal form. The analcime crystals in this study generally have excellent crystal form with no adhering glass, embayment, resorption, or other signs of contact with the pre-eruption magma making it unlikely that they are a juvenile crystal phase. The crystals are also too large to have formed by vapor phase crystallization during the eruption. Morphologically identical analcime crystals are reported as a common phase in the hydrothermal system at Surtsey volcano (Jakobsson and Moore, 1986). However, the Erebus tephra samples were deposited almost instantaneously into a glacial environment and show no signs of post-depositional hydrothermal alteration. The analcime is most likely xenocrystic and was entrained from a hydrothermal system present in the volcano prior to the eruption.

Trachytic Tephra

The trachytic tephra, EBT-61, has an average grain size of around 7 μm and is well sorted (Fig. B18). The tephra sample is composed of bubble wall shards with rare lumpy rounded shards (Fig. B18). No lithic particles are present and crystals are uncommon. The fine grain size, trachytic composition, and well-sorted nature of the tephra suggest a distal source (Fisher, 1964). Also, the lack of lithics and low crystal content suggests a transport distance long enough for winnowing to have occurred (Fisher and Schmincke, 1984). Bubble wall shards are a typical morphology for pyroclasts formed during plinian eruptions. The small lumpy rounded shards that are present are unique but do not exclude a plinian origin.

To identify the source of EBT-61 it is necessary to compare the geochemistry of the tephra sample to known trachytes in the region (Table B4). Trachytic lavas appear on the flanks of Mount Erebus at Mt. Cis, Aurora Cliffs, and Bomb Peak (Fig. B2) (Moore and Kyle, 1987). Direct comparison between the geochemistry of the lavas and sample EBT-61 is inhibited because only whole rock analyses are available for the lavas, whereas only glass from the tephra samples was analyzed. However, a cursory comparison can be made that will illuminate any large differences between the samples. The Mt. Cis trachyte has ~59% SiO_2 and ~11% total alkalis (Smith, 1954) compared to sample EBT-61 which has 61% SiO_2 and ~12.5% total alkalis (Table B4). The Mt. Cis trachyte is also significantly enriched in TiO_2 (~1.35%) (Smith, 1954) compared to sample EBT-61 (~0.5%). These geochemical discrepancies are too large to be explained solely on the basis of different analytical methods. Thus, Mt. Cis is not the source for the sample EBT-61.

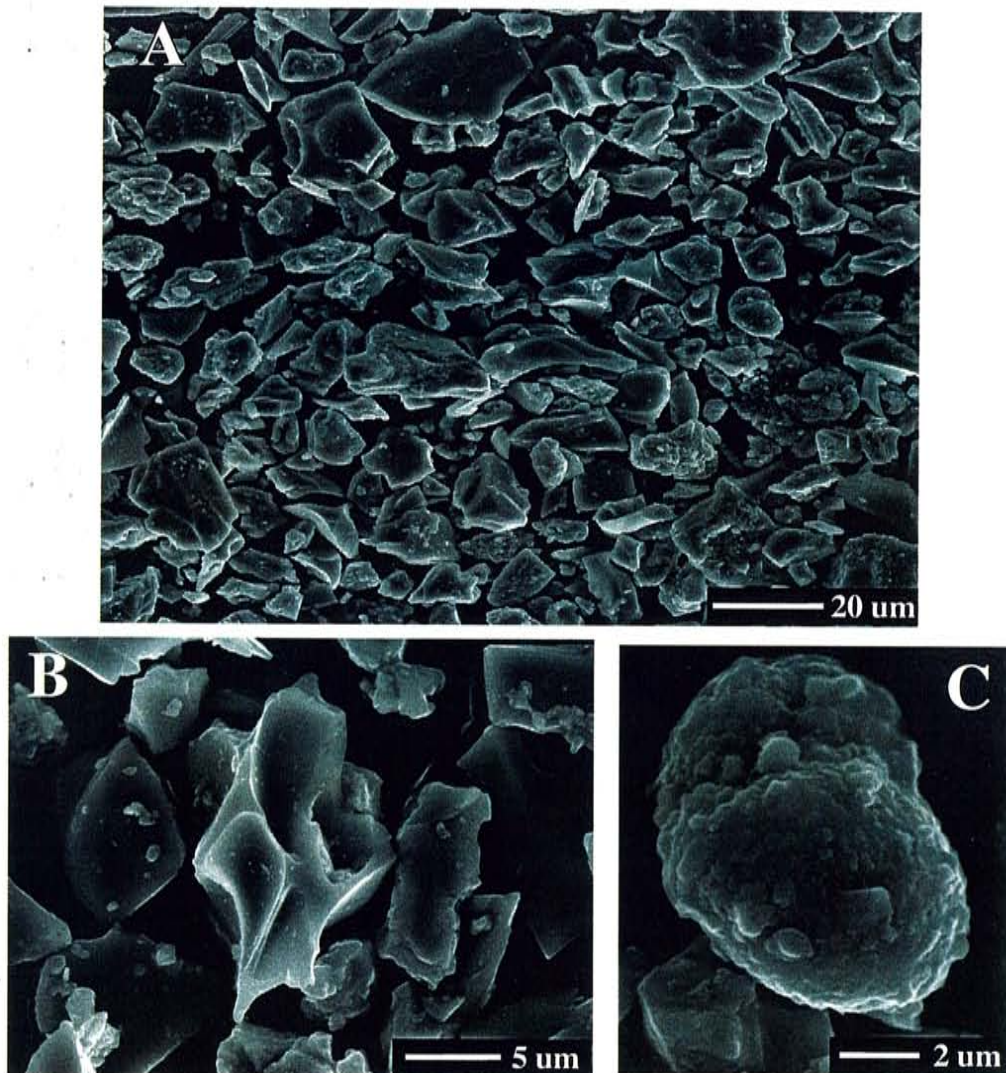


Figure B18-Typical features of the trachytic sample EBT-61. **A:** An image showing the general character of the tephra sample. Notice the well sorted nature and fine grain size relative to the other tephra samples. Also, note the abundance of bubble wall shards and the rare lumpy fragments. **B:** A typical pumice/bubble wall shard indicating a plinian origin. **C:** A rare lumpy rounded fragment.

Table B4—Major element composition of sample EBT-61 and trachytes from Mount Erebus and The Pleiades.

Sample	EBT-61	BIT-52*	Taylor*	Siple B*	BIT-11†	BIT-19†	BIT-65†	Mt. Cis [§]	Aurora	Bomb	Bomb
									Cliffs*	Peak-1*	Peak-2*
SiO ₂	61.13	63.39	62.12	60.90	62.10	62.41	64.27	58.9	60.59	62.92	63.51
TiO ₂	0.49	0.38	0.43	0.45	0.26	0.24	0.15	1.29	0.74	0.43	0.43
Al ₂ O ₃	14.16	15.92	16.52	16.55	17.01	17.21	17.50	16.24	15.85	15.12	15.33
Fe ₂ O ₃	n.a.	n.a.	n.a.	n.a.	n.a.	n.a.	n.a.	3.56	n.a.	n.a.	n.a.
FeO	8.46	6.18	6.41	6.51	5.80	5.76	3.81	4.43	6.79	6.11	6.15
MnO	0.25	0.23	0.24	0.26	0.18	0.20	0.15	0.18	0.22	0.21	0.21
MgO	0.03	0.08	0.15	0.15	0.01	0.01	0.05	0.77	0.56	0.17	0.14
CaO	1.27	1.06	1.19	1.19	1.42	1.51	0.85	2.27	1.94	1.43	1.44
Na ₂ O	8.23	7.18	7.05	8.18	7.22	6.95	7.51	5.6	6.38	7.31	6.56
K ₂ O	4.44	5.06	5.40	5.34	5.27	5.23	5.07	5.85	5.16	5.17	5.23
P ₂ O ₅	0.08	n.d.	0.05	0.08	0.04	n.a.	0.01	0.12	0.13	0.05	0.05
F	1859	2507	921	1961	3452	2436	2876	n.a.	n.a.	n.a.	n.a.
SO ₂	0.06	n.a.	0.06	0.03	n.a.	n.a.	n.a.	n.a.	n.a.	n.a.	n.a.
Cl	10477	2718	2945	2300	3467	2366	3368	n.a.	n.a.	n.a.	n.a.
LOI	n.a.	n.a.	n.a.	n.a.	n.a.	n.a.	n.a.	n.a.	0.07	0.39	0.18
Total	99.84	100	100.00	100.06	100	100	100	100.32	98.42	99.3	99.23

Oxides reported in weight % and trace elements in ppm. All data from electron microprobe analysis of glass except where noted. All Fe₂O₃ and FeO calculated as FeO in electron microprobe and XRF analyses.

*Correlative tephra, from 79.155 m in Taylor Dome ice core, 97.2-97.45 m in Siple B ice core, and Western #7 site, electron microprobe analyses N.W. Dunbar, unpub. data.

†Correlative tephra from the Allan Hills blue ice region, electron microprobe analyses N.W. Dunbar, unpub. data.

‡Proximal tephra from The Pleiades, electron microprobe analysis N.W. Dunbar, unpub. data.

§Whole rock wet chemical analysis from Smith (1954).

*Whole rock XRF analysis on samples 83454 (Aurora Cliffs), 83451 (Bomb Peak-1), and 82405 (Bomb Peak-1) from Moore (1987).

The geochemistry of Bomb Peak and Aurora Cliffs are depleted in MgO and K₂O and enriched in FeO and Na₂O (Table B4) relative to EBT-61. Bomb Peak is slightly closer in composition to EBT-61 than Aurora Cliffs (Moore, 1986) and is also the most proximal of the Erebus trachytes. However, the trachytes at Aurora Cliffs and Bomb Peak have been dated at 166 ± 10 ka (both at 2σ) and 157 ± 6 ka, respectively (Esser, 1996). Although the age of sample EBT-61 is unknown, the Bomb Peak and Aurora Cliffs trachytes are considered too old to be the source. For comparison, tephra from the terminus of the Barne Glacier has been dated at a maximum of 70 ± 4 ka and tephra from the Hooper's Shoulder site has been dated at 15 ± 4 ka (Section A, this work). However, these samples were collected from active glacial ice whereas sample EBT-61 was collected from the Terra Nova ice cap where the ice dynamics are unknown. Tephra from the Mount Moulton ice cap in Marie Byrd Land, West Antarctica has been dated at 492 ka demonstrating that old tephra can be preserved under unique circumstances (Wilch *et al.*, 1999; Dunbar *et al.*, 1999). Nonetheless, it is considered improbable that Bomb Peak or Aurora Cliffs is the source for sample EBT-61, although this can not be conclusively disproven.

Because of the fine grain size, unique composition, and sorting of sample EBT-61, a distal source for the tephra must be considered. The most likely candidate is The Pleiades volcanic field in northern Victoria Land (Fig. B1). Trachytic eruptive activity has been documented at The Pleiades throughout the last 100 ky (Esser and Kyle, 1999). Also, at least seven trachytic tephra layers tentatively correlated to four eruptions of The Pleiades have been found in ice cores and blue ice throughout Victoria Land and the Ross

Sea region (Perchiazzi *et al.*, 1999; N.W. Dunbar, 2000, unpub. data). One of these trachytic tephra, dated at 6 ± 6 ka, is exposed proximal to the Taygete Cone vent of The Pleiades and may have a regional distribution (Esser and Kyle, 1999). The geochemistry for these tephra layers is similar ($D \approx 25$) to the geochemistry of sample EBT-61 (Table B4) but the correlation is not perfect. Sample EBT-61 is higher in FeO and slightly lower in both Al_2O_3 and K_2O , making a direct correlation with any of the known tephra from The Pleiades impossible. However, the D values (Perkins *et al.*, 1995) between tephra samples from different eruptions from The Pleiades are also ~ 25 indicating that the geochemistry of EBT-61 is similar enough to have been erupted from the same volcano. Therefore, a plinian eruption from The Pleiades is considered to be the most likely source for tephra sample EBT-61.

Conclusions

Englacial tephra layers on the flanks of Mount Erebus record at least 47 explosive eruptions. The majority of these eruptions have been phreatomagmatic and strombolian in nature or combinations of the two eruption mechanisms. These eruptions deposited tephra onto the flanks of the volcano and in the local region. However, at least two large eruptions have occurred that deposited tephra as far as 200 km from source. One of these large eruptions was phreatomagmatic in nature and is likely the result of magma interaction with snow and ice. The second large eruption was plinian in nature but also had a small phreatomagmatic component.

All of the tephra samples analyzed in this study, except one, are phonolitic in composition. All of the phonolitic tephra are derived from Mount Erebus and have

homogeneous major element geochemistry. The trace element geochemistry is homogeneous with the exception of feldspar control on the concentrations of the compatible trace elements. No significant geochemical trends are apparent in either the major or trace element geochemistry.

Spherical glass droplets are present in some of the phonolitic tephra and were formed from a lava spray during strombolian eruptions. Ash with the previously unreported budding morphology represents the parent melt that has been quenched before these spheres could be pinched off. Small clusters of analcime crystals have also been found in the phonolitic tephra and are believed to have formed in a pre-eruption hydrothermal system. These analcime crystals were then incorporated as xenocrysts into the tephra during eruption.

A single trachytic tephra exposed in the Terra Nova ice cap was derived from a distal plinian eruption. The source of this tephra is proposed to be The Pleiades in northern Victoria Land.

References

- Baker, G., 1968, Micro-forms of hay-silica glass and volcanic glass: *Mineralogical Magazine*, v. 36, p. 1012-1023.
- Begét, J.E., Hopkins, D.M., and Charron, S.D., 1996, The largest known maars on Earth, Seward Peninsula, northwest Alaska: *Arctic*, v. 49, no. 1, p. 62-69.
- Bitschene, P.R., and Fernandez, M.I., 1995, Volcanology and petrology of fallout ashes from the August 1991 eruption of the Hudson volcano (Patagonian Andes), *in* Bitschene, P.R., and Mendia, J., eds., *The August 1991 eruption of the Hudson Volcano (Patagonian Andes): A thousand days after: Argentina, Comodoro Rivadavia*, p. 27-54.
- Cadle, R.D., and Mroz, E.J., 1978, Particles in the eruption cloud from St. Augustine volcano: *Science*, v. 199, p. 455-456.

- Caldwell, D.A., and Kyle, P.R., 1994, Mineralogy and geochemistry of ejecta erupted from Mount Erebus, Antarctica, between 1972 and 1986, *in* Kyle, P.R., ed., Volcanological and Environmental Studies of Mount Erebus, Antarctica, Antarctic Research Series, V. 66, p. 147-162.
- Carmichael, I.S.E., Turner, F.J., and Verhoogen, J., 1974, Igneous petrology: New York, McGraw-Hill International Series in the Earth and Planetary Sciences, 739 p.
- Chuan, R.L., 1994, Dispersal of volcano-derived particles from Mount Erebus in the Antarctic atmosphere, *in* Kyle, P.R., ed., Volcanological and Environmental Studies of Mount Erebus, Antarctica, Antarctic Research Series, V. 66, p. 97-102.
- Chuan, R.L., Palais, J.M., Rose, W.I., and Kyle, P.R., 1986, Particle sizes and fluxes of the Mt. Erebus volcanic plume, December, 1983: *Journal of Atmospheric Chemistry*, v. 4, p. 467-477.
- Cioni, R., Sbrana, A., and Vecchi, R., 1992, Morphologic features of juvenile pyroclasts from magmatic and phreatomagmatic deposits of Vesuvius: *Journal of Volcanology and Geothermal Research*, v. 51, p. 61-78.
- Dibble, R.R., Kienle, J., Kyle, P.R., and Shibuya, K., 1984, Geophysical studies of Erebus volcano, Antarctica from 1974 December to 1982 January: *New Zealand Journal of Geology and Geophysics*, v. 27, p. 425-455.
- Dibble, R.R., Kyle, P.R., and Skov, M.J., 1994, Volcanic activity and seismicity of Mount Erebus 1986-1994: *Antarctic Journal of the United States*, v. 29, no. 5, p. 11-14.
- Duffield, W.A., Gibson, E.K., Jr., and Heiken, G., 1977, Some characteristics of Pele's hair: *Journal of Research of the U.S. Geological Survey*, v. 5, no. 1, p. 93-101.
- Dunbar, N.W., Kyle, P.R., McIntosh, W.C., and Esser, R.P., 1995, Geochemical composition and stratigraphy of tephra layers in Antarctic blue ice: Insights into glacial tephrochronology: VII International Symposium on Antarctic Earth Sciences, Sienna, Italy.
- Dunbar, N.W., McIntosh, W.C., Esser, R.P., Wilch, T.I., and Zielinski, G.A., 1999, Englacial tephrochronology in West Antarctica: Constraints on ice sheet history, and potential longer ice climate records [abs]: 8th Symposium on Antarctic Earth Sciences, Wellington, New Zealand, p. 95.
- Esser, R.P., 1996, $^{40}\text{Ar}/^{39}\text{Ar}$ dating of Mount Erebus volcano, Antarctica: Socorro, NM, New Mexico Institute of Mining and Technology, Master's, 183 p.

- Esser, R.P., and Kyle, P.R., 1999, $^{40}\text{Ar}/^{39}\text{Ar}$ chronology of The Pleiades Volcanic Centre, northern Victoria Land, Antarctica: a potential source of Late-Pleistocene englacial tephra layers [abs]: 8th Symposium on Antarctic Earth Sciences, Wellington, New Zealand, p. 100.
- Fisher, R.V., 1964, Maximum size, median diameter, and sorting of tephra: *Journal of Geophysics*, v. 69, no. 2, p. 341-355.
- Fisher, R.V., and Schmincke, H.-U., 1984, *Pyroclastic rocks*, Springer-Verlag.
- Giggenbach, W.F., Kyle, P.R., and Lyon, G.L., 1973, Present volcanic activity on Mount Erebus, Ross Island, Antarctica: *Geology*, v. 1, p. 135-136.
- Hallett, R.B., and Kyle, P.R., 1993, XRF and INAA determinations of major and trace elements in Geological Survey of Japan igneous and sedimentary rock standards: *Geostandards Newsletter*, v. 17, no. 1, p. 127-133.
- Heiken, G., 1972, Morphology and Petrography of volcanic ashes: *Geological Society of America Bulletin*, v. 83, p. 1961-1988.
- Heiken, G., 1974, An atlas of volcanic ash, *Smithsonian Contributions to the Earth Sciences*, No. 12, 101 p.
- Heiken, G., 1978, Characteristics of tephra from Cinder Cone, Lassen Volcanic National Park, California: *Bulletin Volcanologique*, v. 41, no. 2, p. 119-130.
- Heiken, G., and Lofgren, G., 1971, Terrestrial glass spheres: *Geological Society of America Bulletin*, v. 82, p. 1045-1050.
- Heiken, G., and Wohletz, K., 1985, *Volcanic ash*: University of California Press, 246 p.
- Hobbs, P.V., Radke, L.F., and Stith, J.L., 1978, Response to "Particles in the eruption cloud from St. Augustine volcano" by Cadle and Mroz: *Science*, v. 199, p. 457-458.
- Houghton, B.F., and Nairn, I.A., 1991, The 1971-1982 strombolian and phreatomagmatic eruptions of White Island, New Zealand: eruptive and depositional mechanisms at a 'wet' volcano: *Bulletin of Volcanology*, v. 54, no. 25-59.
- Houghton, B.F., and Schmincke, H.-U., 1989, Rothenberg scoria cone, East Eifel: a complex strombolian and phreatomagmatic volcano: *Bulletin of Volcanology*, v. 52, p. 28-48.
- Hunt, J.B., and Hill, P.G., 1993, Tephra geochemistry: a discussion of some persistent analytical problems: *The Holocene*, v. 3, no. 3, p. 271-278.

- Jakobsson, S.P., and Moore, J.G., 1986, Hydrothermal minerals and alteration rates at Surtsey volcano, Iceland: Geological Society of America Bulletin, v. 97, p. 684-659.
- Juvigné, É., Kozarski, S., and Nowaczyk, B., 1995, The occurrence of Laacher See tephra in Pomerania, NW Poland: Boreas, v. 24, p. 226-231.
- Keys, J.R., Anderton, P.W., and Kyle, P.R., 1977, Tephra and debris layers in the Skelton Névé and Kempe Glacier, south Victoria Land, Antarctica: New Zealand Journal of Geology and Geophysics, v. 20, no. 5, p. 971-1002.
- King, E.A., and Wagstaff, J., 1980, Search for cometary dust in the Antarctic ice: Antarctic Journal of the United States, v. 15, no. 5, p. 78-79.
- Kyle, P.R., 1977, Mineralogy and glass chemistry of recent volcanic ejecta from Mt. Erebus, Ross Island, Antarctica: New Zealand Journal of Geology and Geophysics, v. 20, no. 6, p. 1123-1146.
- Kyle, P.R., Dibble, R.R., Giggenbach, W.F., and Keys, J., 1982, Volcanic activity associated with the anorthoclase phonolite lava lake, Mount Erebus, Antarctica, *in* Craddock, C., ed., Antarctic Geoscience: Madison, Wisconsin, University of Wisconsin Press, p. 735-745.
- Kyle, P.R., Moore, J.A., and Thirwall, M.F., 1992, Petrologic evolution of anorthoclase phonolite lavas at Mount Erebus, Ross Island, Antarctica: Journal of Petrology, v. 33, no. 4, p. 849-875.
- Le Bas, M.J., Le Maitre, R.W., Streckeisen, A., and Zanettin, B., 1986, A chemical classification of volcanic rocks based on the Total Alkali -Silica diagram: Journal of Petrology, v. 27, no. 3, p. 745-750.
- Lefèvre, R., Gaudichet, A., and Billon-Galland, M.A., 1986, Silicate microspherules intercepted in the plume of Etna volcano: Nature, v. 322, p. 817-820.
- Lefèvre, R., Gaudichet, A., and Leguern, F., 1991, Présence de microsphérules chimiquement variés dans les aérosols de certaines fontaines de lave d'Hawaii. Comparaison avec l'Etna: Comptes Rendus Academie des Sciences de Paris, v. 313, Serie II, p. 105-111.
- Lindstrom, D.J., and Korotev, R.L., 1982, TEABAGS: Computer program for instrumental neutron activation analysis: Journal of Radioanalytical Chemistry, v. 70, p. 439-458.
- Lyon, G.L., and Giggenbach, W.F., 1974, Geothermal activity in Victoria Land, Antarctica: New Zealand Journal of Geology and Geophysics, v. 17, no. 3, p. 511-521.

- Marchant, D.R., Denton, G.H., Swisher, C.C., III, and Potter, N.J., Jr., 1996, Late Cenozoic Antarctic paleoclimate reconstructed from volcanic ashes in the Dry Valleys region of southern Victoria Land: Geological Society of America, v. 108, p. 181-194.
- Marchant, D.R., Swisher, C.C., III, Lux, D.R., West, D.R., Jr., and Denton, G.H., 1993, Pliocene paleoclimate and East Antarctic ice-sheet history from surficial ash deposits: Science, v. 260, p. 667-670.
- Meeker, G.P., and Hinkley, T.K., 1993, The structure and composition of microspheres from the Kilauea volcano, Hawaii: American Mineralogist, v. 78, p. 873-876.
- McBirney, A.R., and Murase, T., 1984, Rheological properties of magmas: Annual Review of Earth and Planetary Sciences, v. 12, p. 337-357.
- Moore, H.J., 1987, Preliminary estimates of rheological properties of the 1984 Mauna Loa lava, *in* Decker, R.W., Wright, T.L., and Stauffer, P.H., eds., Hawaiian volcanism, U.S. Geological Survey Professional Paper 1350, p. 1569-1588.
- Moore, J.A., 1986, Mineralogy, geochemistry, and petrogenesis of the lavas of Mount Erebus, Antarctica, New Mexico Institute of Mining and Technology, Master's, 277 p.
- Moore, J.A., and Kyle, P.R., 1987, Volcanic geology of Mount Erebus, Ross Island, Antarctica: Proceedings of the NIPR symposium on Antarctic geosciences, Tokyo, Japan, v. 1, p. 48-65.
- Perchiazzi, N., Folco, L., and Mellini, M., 1999, Volcanic ash bands in the Frontier Mountain and Lichen Hills blue-ice fields, northern Victoria Land: Antarctic Science, v. 11, p. 353-361.
- Perkins, M.E., Nash, W.P., Brown, F.H., and Fleck, R.J., 1995, Fallout tuffs of Trapper Creek, Idaho - A record of Miocene explosive volcanism in the Snake River Plain volcanic province: Geological Society of America Bulletin, v. 107, no. 12, p. 1484-1506.
- Rolandi, G., Barrella, A.M., and Borrelli, A., 1993, The 1631 eruption of Vesuvius: Journal of Volcanology and Geothermal Research, v. 58, p. 183-201.
- Rose, W.I., 1987, Active pyroclast processes studied with scanning electron microscopy, *in* Marshall, J.R., ed., Clastic particles: Scanning electron microscopy and shape analysis of sedimentary and volcanic clasts, Van Nostrand Reinhold Company, p. 136-158.
- Rose, W.I., and Hoffman, M.F., 1982, The May 18, 1980 eruption of Mount St. Helens: The nature of the eruption, with an atmospheric perspective, *in* Deepak, A., ed.,

Atmospheric effects and potential climatic impact of the 1980 eruptions of Mount St. Helens: NASA Conference Publication 2240, p. 1-14.

- Shaw, H.R., Wright, T.L., Peck, D.L., and Okamura, R., 1968, The viscosity of basaltic magma: an analysis of field measurements in Makaopuhi lava lake, Hawaii: *American Journal of Science*, v. 266, p. 225-264.
- Self, S., Kienle, J., and Huot, J.-P., 1980, Ukinrek Maars, Alaska, II. Deposits and formation of the 1977 craters: *Journal of Volcanology and Geothermal Research*, v. 7, p. 39-65.
- Self, S., and Sparks, R.S.J., 1978, Characteristics of widespread pyroclastic deposits formed by the interaction of silicic magma and water: *Bulletin Volcanologique*, v. 41, no. 3, p. 196-212.
- Sheridan, M.F., and Marshall, J.R., 1983, Interpretation of pyroclast surface features using SEM images: *Journal of Volcanology and Geothermal Research*, v. 16, p. 153-159.
- Smith, W.C., 1954, The volcanic rocks of the Ross Archipelago: British Antarctic ("Terra Nova") Expedition, 1910, *Natural History Report*, v. 2, no. 1, p. 1-107.
- Sun, S.S., and McDonough, W.F., 1989, Chemical and isotopic systematics of oceanic basalts: implications for mantle composition and processes, *in* Saunders, A.D., and Norry, M.J., eds., *Magmatism in ocean basins*, Geological Society of London Special Publication No. 42, p. 313-345.
- Tanguy, J.C., 1971, Mt. Etna volcanic eruption, 5 April - 12 June 1971: Smithsonian Institute Center for Short-Lived Phenomenon, December, 5 p.
- Thorarinsson, S., 1966, Surtsey: The new island in the north Atlantic: Reykjavík, Almenna Bókafélagi, 54 p.
- van den Bogaard, P., and Schmincke, H.-U., 1985, Laacher See tephra: A widespread isochronous late Quaternary tephra layer in central and northern Europe: *Geological Society of America Bulletin*, v. 96, p. 1554-1571.
- Walker, G.P.L., 1981, Generation and dispersal of fine ash and dust by volcanic eruptions: *Journal of Volcanology and Geothermal Research*, v. 11, p. 81-92.
- Walker, G.P.L., and Croasdale, R., 1971, Characteristics of some basaltic pyroclasts: *Bulletin Volcanologique*, v. 35, p. 305-317.
- Wilch, T.I., McIntosh, W.C., and Dunbar, N.W., 1999, Late Quaternary volcanic activity in Marie Byrd Land: Potential $^{40}\text{Ar}/^{39}\text{Ar}$ -dated time horizons in West Antarctic ice

and marine cores: Geological Society of America Bulletin, v. 111, no. 10, p. 1563-1580.

Wohletz, K.H., 1983, Mechanisms of hydrovolcanic pyroclast formation: Grain-size, scanning electron microscopy, and experimental studies: Journal of Volcanology and Geothermal Research, v. 17, p. 31-63.

Wohletz, K.H., and McQueen, R.G., 1984, Volcanic and stratospheric dustlike particles produced by experimental water-melt interactions: Geology, v. 12, p. 591-594.

Zimanowski, B., Lorenz, V., and Frohlich, G., 1986, Experiments on phreatomagmatic explosions with silicate and carbonatitic melts: Journal of Volcanology and Geothermal Research, v. 30, p. 149-153.

APPENDICES

Introduction

These appendices have been added as supplementary data to support the previous two sections. The first two tables (C-1 and C-2) are the data from both the $^{40}\text{Ar}/^{39}\text{Ar}$ furnace and laser step-heating analyses. These data have been used to calculate $^{40}\text{Ar}/^{39}\text{Ar}$ plateau ages for each sample and are displayed graphically in Figures B6, B7, and B8.

Appendices C-1 through C-6 are the results of electron microprobe analyses of Mount Erebus tephra. The first appendix (C-1) is the glass geochemistry for each tephra sample. Generally ten points from each tephra sample were analyzed and four steps were used to obtain the final analysis. Tables C-3.X.1 show the raw microprobe data.

Analyses with totals of less than 98% are *italicized* indicating that they are not used to calculate the mean geochemical composition. Lower totals were allowed with sample EBT-61 due to the fine grain size. Tables C-3.X.2 show the data normalized to 100% totals. Fluorine can often give spurious results. Thus, if the fluorine value for an analysis is below 500 ppm it is corrected to the mean of other fluorine concentrations. The data is then normalized for sodium loss during analysis as reported in table C-3.X.3.

Normalization for sodium loss is calculated using a correction factor determined with the following equation:

$$C = \frac{100}{100 + (Na_{av} - Na_i)}$$

where C is the correction factor, Na_{av} is the mean of the two highest sodium concentrations normalized to 100% and Na_i is the initial measured sodium concentration

for the analysis being normalized. The final sodium value is considered to be Na_{Av} and each element is multiplied by the correction factor to obtain the final values for the analysis. The mean of all of the allowed analyses is considered to be the actual tephra geochemistry. Standard deviation is reported at one sigma. Appendices C-4 and C-6 give the measured values of glass and feldspar standards, respectively, from each day of microprobe use. As with the glass geochemistry any data that is *italicized* was not used due to low total values. Standards were analyzed at the beginning and end of each analytical session to monitor accuracy of probe calibration. For comparative purposes the accepted values of each standard have been included at the end of each table. Appendix C-5 contains the geochemical data from microprobe analyses of feldspar from the tephra samples. Where possible at least four feldspar crystals were analyzed for each tephra sample. Ternary end member values have been calculated for each feldspar crystal using 32 Oxygen atoms after the method of Deer *et al.* (1992).

Appendix C-7 contains the results of similarity calculations using the electron microprobe data from glass analyses for each tephra sample. Calculations were carried out using the methods of Perkins *et al.* (1995) explained in detail in Section B. The similarity values are expressed as D in the matrix.

Locations for the main tephra layers were determined using differential GPS and are listed in Appendix C-8. GPS locations were obtained by either a hand held GPS receiver, the GPS receiver from the helicopters, or differential GPS using a mobile receiver from UNAVCO and the McMurdo continuous base station. Differential GPS locations were processed at UNAVCO in Boulder, Colorado.

Appendix C-9 is a listing of all of the tephra samples and the general blue ice area (*i.e.* Hooper's Shoulder, or Terra Nova Summit) that they were collected from. Also, in many cases multiple samples were taken from the same tephra layer. In these cases, the equivalent samples are listed in the middle column of the table.

The CD-ROM in the pocket contains the SEM images used in this study along with the secondary electron backscatter images obtained during electron microprobe analysis. These images are in tif format and are organized in files according to the tephra sample number. The SEM images are named with the tephra sample number first, then the individual number of the image. For example, ebt34a-2, indicates that this is the second image of sample EBT-34a.

References

- Deer, W.A., Howie, R.A., and Zussman, J., 1992, An Introduction to the rock-forming minerals, Longman Scientific and Technical, 696 p.
- Perkins, M.E., Nash, W.P., Brown, F.H., and Fleck, R.J., 1995, Fallout tuffs of Trapper Creek, Idaho - A record of Miocene explosive volcanism in the Snake River Plain volcanic province: Geological Society of America Bulletin, v. 107, no. 12, p. 1484-1506.

Appendix 1

Table C1-40Ar/39Ar furnace step-heating data.

Temp (°C)	40Ar/39Ar	37Ar/39Ar	36Ar/39Ar (x10 ⁻³)	39Ar/K mol (x10 ⁻¹⁶)	K/Ca	Cl/K (x10 ⁻³)	40Ar* (%)	39Ar (%)	Age (ka)	Err (±2sigma)
E87004 (L#50611), 411.2 mg, J = 0.0000781, NM-112 irradiation										
550**	1456	0.34	4926	1.2	1.5	140	0.0	0.1	80	18046
650**	216	0.52	728	13	1.0	5.2	0.3	0.9	86	454
700**	11	0.50	36	18	1.0	1.8	4.3	2.2	68	32
800	3.8	0.49	13	233	1.1	0.13	1.3	18	7	5
900	1.2	0.47	3.9	237	1.1	n.d.	6.0	34	10	3
1000	0.8	0.46	2.5	566	1.1	n.d.	7.6	73	9	2
1100**	1.8	0.45	5.8	257	1.1	0.45	7.4	91	19	3
1200**	7.1	0.44	22	60	1.2	22	7.9	95	79	12
1350**	5.3	0.45	16	76	1.1	4.3	10.2	100	77	9
1500**	61	0.55	207	0.9	0.9	17	n.d.	100	-93	626
1750**	153	0.96	515	2.2	0.5	5.7	0.3	100	67	696
total gas age			n=11		1465	1.1			18	24
plateau	MSWD = 0.73		n=3		1037	1.1		71	9	2
E87017 (L#50614), 412.3 mg, J = 0.00007684, NM-112 irradiation										
650**	256	0.66	867	339	0.8	1.4	0.0	21	10	283
700**	18	0.59	58	398	0.9	0.3	4.6	45	114	17
800	4.4	0.58	13	363	0.9	0.1	13.2	66	80	4
900	2.5	0.58	6.80	162	0.9	0.25	21.1	76	74	4.6
1000	3.2	0.58	9.13	162	0.9	0.5	16.9	86	75	5.0
1100	7.1	0.60	22	82	0.9	1.4	9.3	91	91	10.2
1200**	15	0.66	48	23	0.8	51	6.5	92	135	30.0
1350**	4.5	0.89	12	119	0.6	7.6	18.9	100	118	7.0
1500**	73	4.37	240	2.1	0.1	97	4.1	100	414	392
1750**	129	16	436	4.2	0.0	173	0.9	100	170	374
total gas age			n=10		1655	0.8			77	66
plateau	MSWD = 3.76		n=4		769	0.9		47	78	6
E87020 (L#9867), 407.3 mg, J = 0.0000825, NM-99 irradiation										
550**	941	n.d.	3125	0.09	n.d.	113	1.9	n.d.	2614	26006
700**	1510	0.36	5047	2.6	1.4	81	1.2	0.18	2798	13594
800**	183	0.25	642	0.38	2.0	39	n.d.	0.21	-1034	3538
900	2.5	0.48	8.1	519	1.1	0.19	3.7	35	14	4
1000	1.1	0.47	3.4	368	1.1	0.06	8.2	59	13	2
1100	1.2	0.47	4.0	262	1.1	0.01	1.7	77	3	4
1200	1.4	0.47	4.8	172	1.1	0.60	2.7	88	6	4
1350**	5.9	0.48	19	85	1.1	13	4.5	94	40	14
1550**	82	0.50	276	71	1.0	2.1	n.d.	99	3	128
1700**	1268	0.45	4373	18	1.1	1.3	n.d.	100	-3553	4808
total gas age			n=10		1498	1.1			-27	98
plateau	MSWD = 9.72*		n=4		1320	1.1		88	9	6
E87021 (L#9866), 390.4 mg, J = 0.0000829, NM-99 irradiation										
550**	n.d.	n.d.	n.d.	0.01	n.d.	27	n.d.	0.01	7650	31956
700**	7180	1.8	24324	0.12	0.28	114	n.d.	0.13	-1132	144072
800**	298	1.8	1037	0.11	0.29	30	n.d.	0.24	-1223	2013
900**	16	1.1	43	47	0.47	2.6	22	49	533	101
975**	24	1.0	75	14	0.50	1.0	6.9	64	243	31956
1100	30	1.2	100	11	0.43	0.66	1.6	75	71	48
1200	47	1.2	158	8.0	0.43	5.5	1.0	83	68	78
1350	7.8	1.2	25	11	0.44	7.7	6.3	95	74	14
1550	43	1.4	146	3.9	0.36	2.0	n.d.	99	-15	73
1700**	234	1.4	792	1.2	0.37	2.5	0.20	100	79	484
total gas age			n=10		97	0.46			315	258
plateau	MSWD = 1.87		n=4		34	0.42		35	71	22
E87026 (L#50617), 399.8 mg, J = 0.0000750, NM-112 irradiation										
550**	915	0.92	3086	14	0.6	13	0.4	2.1	453	4730
650**	30	1.4	96	43	0.4	0.73	5.7	8.8	233	34
700**	10	1.3	30	53	0.4	0.72	14.1	17	194	16
800**	11	1.3	33	36	0.4	0.98	9.4	23	136	19
900**	6.3	1.3	17	181	0.4	0.55	23.1	51	196	6
1000**	3.7	1.4	9	63	0.4	0.91	28.2	60	143	9
1100**	6.8	1.4	19	57	0.4	2.0	17.5	69	161	12
1200**	13	1.4	36	31	0.4	42	22.3	74	406	22
1350**	2.8	1.3	7.9	109	0.4	2.4	20.4	91	79	6
1750**	6.4	1.6	20	60	0.3	1.4	10.9	100	94	11
total gas age			n=10		647	0.38			173	112
plateau			n=10		647	0.38		100	n.a.	n.a.

Table C1 continued-40Ar/39Ar furnace step-heating data.

Temp (°C)	40Ar/39Ar	37Ar/39Ar	³⁶ Ar/ ³⁹ Ar (x10 ⁻³)	³⁹ ArK mol (x10 ⁻¹⁶)	K/Ca	Cl/K (x10 ⁻³)	40Ar* (%)	39Ar (%)	Age (ka)	Err (±2sigma)
E87030 (L#9865), 410.8 mg, J = 0.0000817, NM-99 irradiation										
550**	1260	0.38	4290	1.3	1.3	159	n.d.	0.09	-1167	10921
700**	538	0.49	1831	2.2	1.0	56	n.d.	0.25	-451	2763
800**	n.d.	0.26	n.d.	0.05	2.0	13	n.d.	0.25	3741	8789
900	2.0	0.43	6.7	538	1.2	0.34	1.9	39	5.6	4
975	1.0	0.42	3.2	170	1.2	0.20	7.3	51	11	10921
1100	1.2	0.42	3.6	468	1.2	0.09	9.0	84	15	2
1200**	2.7	0.42	8.7	87	1.2	0.74	6.6	91	27	8
1350**	7.8	0.43	26	111	1.2	10	2.7	98	32	14
1550**	73	0.43	252	11	1.2	3.7	n.d.	99	-134	144
1700**	139	0.43	468	10	1.2	1.6	0.4	100	75	272
total gas age			n=10		1400	1.2			11	22
plateau	MSWD = 8.07*		n=3		1176	1.2		84	12	5
E87033 (L#50615), 410.0 mg, J = 0.00007496, NM-112 irradiation										
550**	1422	0.60	4770	14	0.9	15	0.9	0.9	1669	9844
650**	232	0.43	782	114	1.2	1.9	0.5	8.1	166	294
700	51	0.50	172	142	1.0	0.70	1.3	17	92	48
800	29	0.49	97	502	1.0	0.37	2.2	49	88	30
900	3.4	0.45	9	249	1.1	0.05	19.9	64	91	4
1000	3.9	0.46	11	206	1.1	0.20	17.1	77	91	5
1100**	5.0	0.48	14	131	1.1	1.0	16.2	86	109	7
1200**	13	0.53	39	45	1.0	29	8.8	88	151	22
1350**	3.3	0.63	8.4	177	0.8	3.3	25.6	99	114	5
1500**	104	1.76	333	1.9	0.3	34	5.7	100	808	480
1750**	86	13	288	7.1	0.0	115	1.7	100	200	190
total gas age			n=11		1589	1.0			117	128
plateau	MSWD = 0.02		n=4		1213	1.1		76	91	2
E87035 (L#50612), 406.6 mg, J = 0.0000762, NM-112 irradiation										
550**	n.d.	0.00	n.d.	0.07	n.d.	n.d.	n.d.	0.0	50825	101650
650	464	0.56	1566	14	0.92	36	0	1.3	191	382
700	4	0.51	13	389	0.99	0.71	0.6	38	3	7
800	3	0.51	9	193	1.0	0.32	1.9	56	7	14
900	2	0.51	5	113	0.99	n.d.	6.6	67	15	30
1000	1.5	0.51	5	192	1.0	0.27	6.7	85	14	28
1100	3	0.50	10	117	1.0	1.0	3.1	96	13	26
1200**	11	0.49	37	22	1.0	52	5.1	98	80	160
1350**	8.4	0.53	26	23	0.96	16	9.3	100	108	216
1500**	64	0.57	225	0	0.90	40	n.d.	100	-380	-760
1750**	236	0.81	822	0.46	0.63	21	n.d.	100	-937	-1874
total gas age			n=11		1065	1.0			17	30
plateau	MSWD = 4.08*		n=6		1019	1.0		96	10	4
E87039 (L#9864), 408.5 mg, J = 0.0000795, NM-99 irradiation										
550**	365	0.40	1256	0.245	1.3	261	n.d.	n.d.	-850	7061
700**	24	0.69	77	69.4	0.74	3.1	4.1	6.0	140	37
800	3.8	0.64	11	32.4	0.80	1.0	14	8.8	74	16
900	2.0	0.62	4.7	417.8	0.83	0.14	33	45	93	3
975	2.4	0.61	5.7	110.9	0.84	0.26	30	55	103	5
1100**	3.1	0.61	7.7	129.7	0.84	0.87	28	66	127	6
1200**	7.0	0.62	19	53.6	0.82	19	19	71	185	13
1350**	2.4	0.60	5.6	304.5	0.86	1.1	33	97	115	4
1550**	32	0.71	107	24.1	0.72	2.2	2.4	99	111	56
1700**	79	0.77	270	11.0	0.66	2.6	n.d.	100	-63	154
total gas age			n=10		1154	0.83			109	11
plateau	MSWD = 8.87*		n=3		561	0.83		49	95	8
E87040 (L#8855), 314.77 mg, J=0.00009, NM-85 irradiation										
550**	900	0.16	3034	4.5	3.3	26	0.40	0.36	600	11009
700**	9.7	0.48	33	118	1.1	1.1	1.4	9.9	21	15
800	2.6	0.48	8.8	419	1.1	0.11	n.d.	44	-1	4
900	2.3	0.48	7.9	264	1.1	n.d.	n.d.	65	-1	4
1000	2.5	0.48	8.4	200	1.1	0.21	1.7	81	7	5
1100	4.5	0.47	15	89	1.1	0.62	1.7	88	12	9
1200**	11	0.49	34	52	1.0	14	5.3	93	91	18
1300**	7.2	0.53	22	49	0.96	6.1	12	97	140	15
1400**	4.5	0.55	12	17	0.93	1.9	21	98	153	21
1500**	3.0	0.58	7.7	11	0.88	2.4	23	99	112	66
1600**	9.5	0.75	30	8.2	0.68	3.5	6.8	100	105	58
1700**	18	0.67	54	5.8	0.76	1.6	9.7	100	275	98
total gas age			n=12		1238	1.1			20	48
plateau	MSWD = 4.30*		n=4		973	1.1		79	2	5

Table C1 continued-40Ar/39Ar furnace step-heating data.

Temp (°C)	40Ar/39Ar	37Ar/39Ar	36Ar/39Ar (x10 ⁻³)	39ArK mol (x10 ⁻¹⁶)	K/Ca	Cl/K (x10 ⁻³)	40Ar* (%)	39Ar (%)	Age (ka)	Err (±2sigma)
E87045 (L#50616), 371.9 mg, J = 0.0000767, NM-112 irradiation										
550	1189	2.0	4056	6.0	0.26	1.9	n.d.	7.3	-1305	2874
650	13	1.8	38	15	0.28	0.41	15.0	26	276	14
700	13	1.8	38	7.3	0.28	0.33	14.0	35	250	16
800**	8.0	1.9	20	11	0.28	0.41	28.0	48	310	11
900**	6.7	1.9	13	12	0.27	0.23	43.0	63	397	7
1000**	6.8	1.9	13	12	0.27	0.18	45.0	78	426	7
1100**	14	1.9	21	8.5	0.28	0.28	56.0	88	1056	11
1200**	29	1.9	62	3.2	0.27	0.53	38.0	92	1546	30
1300**	79	1.9	36	2.5	0.27	0.72	87.0	95	9402	48
1500**	25	2.0	42	3.4	0.25	0.64	51.0	99	1770	24
1650**	45	2.0	135	0.77	0.25	n.d.	12.0	100	742	88
total gas age			n=11		82	0.27			680	222
plateau	MSWD = 3.45		n=3		28	0.28		35	265	22
E87051 (L#8860), 332.53 mg, J=0.00009, NM-85 irradiation										
550**	633	0.07	2127	0.39	7.2	43	0.70	0.04	744	10677
700	10	0.44	34.6	49	1.2	1.1	n.d.	4.7	-5	18
800	1.8	0.43	5.5	19	1.2	1.0	6.8	6.5	19	12
900	1.6	0.41	5.3	413	1.2	0.10	1.5	46	4	3
1000	2.1	0.42	7.1	263	1.2	0.05	1.2	71	4	4
1100	2.5	0.42	8.4	116	1.2	0.45	2.3	82	9	6
1200**	5.8	0.42	19	93	1.2	8.5	2.6	91	25	18
1350**	4.7	0.46	15	68	1.1	6.3	4.5	97	35	17
1550**	1.7	0.56	6	22	0.91	5.9	5.4	99	15	52
1700**	16	0.63	55	6.6	0.81	3.1	n.d.	100	-47	153
total gas age			n=10		1050	1.2			8	13
plateau	MSWD = 2.52		n=5		861	1.2		82	5	4
E87054 (L#8857), 416.07 mg, J = 0.00009, NM-85 irradiation										
550**	2118	0.56	7215	0.48	0.91	230	n.d.	0.04	-2299	41305
700**	29	0.49	102	37	1.0	2.4	n.d.	2.9	-107	73
800	1.9	0.44	6.4	227	1.2	0.08	1.6	21	5	7
900	0.99	0.43	3.3	551	1.2	0.05	3.3	64	5	2
1000	1.0	0.42	3.2	127	1.2	0.31	9.5	73	16	6
1100	1.7	0.43	5.3	240	1.2	0.42	6.8	92	18	6
1200**	6.8	0.42	22	53	1.2	21	5.5	96	61	30
1350**	6.2	0.58	20	45	0.88	17	5.9	100	59	27
1550**	10	1.6	30	2.9	0.32	18	12	100	187	152
1700**	134	3.2	459	0.94	0.16	30	n.d.	100	-221	1330
total gas age			n=10		1284	1.2			9	26
plateau	MSWD = 8.31*		n=4		1145	1.2		89	9	6
E87061 (L#50613), 368.3 mg, J=0.0000730, NM-112 irradiation										
550**	969	0.32	3376	0.87	1.6	n.d.	n.d.	0.10	-3806	9810
650	24	0.34	81	55	1.5	n.d.	0.1	4.2	3.9	28
700	3.9	0.33	12	301	1.6	0.05	4.2	27	21	4
800	3.1	0.32	10	201	1.6	0.10	5.2	42	21	4
900**	3.4	0.31	11	399	1.6	0.02	4.6	72	21	4
1000**	4.1	0.32	13	224	1.6	n.d.	5.7	88	31	5
1100**	8.5	0.32	28	89	1.6	0.32	2.4	95	27	13
1200**	23	0.33	76	31	1.6	0.82	3.8	97	119	36
1300**	12	0.35	36	25	1.5	1.0	13.4	99	217	30
1500**	9.1	1.1	23	9.4	0.47	1.2	24.4	100	294	62
1650**	75	1.1	250	2.4	0.45	n.d.	1.7	100	171	462
total gas age			n=11		1338	1.6			28	15
plateau	MSWD = 0.53		n=4		956	1.6		72	21	3
E87062 (L#9870), 407.9 mg, J = 0.0000836, NM-99 irradiation										
550**	1235	0.58	4258	0.69	0.88	72	n.d.	0.09	-3558	14916
700**	14	0.39	47	113	1.3	0.66	2.7	15	57	24
800	3.0	0.36	9.6	54	1.4	0.35	6.7	22	31	11
900	1.3	0.35	3.7	603	1.5	0.02	14	102	28	2
975	1.3	0.35	3.7	275	1.5	n.d.	12	138	24	3
1100	1.5	0.35	4.6	263	1.5	0.16	11	173	25	3
1200	n.d.	0.35	n.d.	n.d.	1.5	9.1	n.d.	129	16	11
1350**	n.d.	0.36	n.d.	n.d.	1.4	4.4	n.d.	106	75	19
1550**	n.d.	0.41	n.d.	n.d.	1.2	3.8	1.9	99	-50	84
1700**	932	0.37	3140	11	1.4	2.9	0.40	100	622	3533
total gas age			n=10		757	1.5			34	56
plateau	MSWD = 2.05		n=5		864	1.5		114	26	3

Table CI continued-40Ar/39Ar furnace step-heating data.

Temp (°C)	40Ar/39Ar	37Ar/39Ar	36Ar/39Ar (x10 ⁻³)	39Ar/K mol (x10 ⁻¹⁶)	K/Ca	Cl/K (x10 ⁻³)	40Ar* (%)	39Ar (%)	Age (ka)	Err (±2sigma)
E87066 (L#9869), 418.3 mg, J = 0.000835, NM-99 irradiation										
550**	1375	0.82	4692	0.93	0.62	104	n.d.	0.06	-1799	12875
700**	99	0.60	337	61	0.85	1.4	n.d.	4.1	-113	161
800**	4.4	0.51	14	34	0.99	0.71	5.0	6.4	33	18
900	1.9	0.47	6.4	648	1.1	0.05	3.2	50	9	12875
1000	1.5	0.47	4.7	268	1.1	0.07	8.0	67	18	3
1100	1.8	0.47	5.8	213	1.1	0.19	7.2	82	20	4
1200**	3.8	0.47	12	85	1.1	11	7.1	87	40	10
1350**	3.8	0.49	12	173	1.1	2.9	5.4	99	30	7
1550**	44	0.50	147	12	1.0	8.7	n.d.	100	-2	96
1700**	481	0.40	1607	5.2	1.3	8.3	1.2	100	886	2741
total gas age			n=10		1499	1.1			14	30
plateau	MSWD = 8.80*		n=3		1129	1.1		75	16	6.3
E87083 (L#8851), 348.84 mg, J = 0.00009, NM-85 irradiation										
550**	309	0.42	1055	4.2	1.2	38	n.d.	0.2	-380	1183
700	1.5	0.39	5.1	605	1.3	0.04	2.9	36	7.3	3
800	1.1	0.39	3.7	245	1.3	n.d.	2.7	50	4.9	2
900	1.4	0.39	4.8	319	1.3	n.d.	2.4	69	5.6	3
1000	1.6	0.39	5.4	249	1.3	n.d.	2.4	83	6.5	3
1100	2.2	0.39	7.2	128	1.3	0.71	2.8	91	9.9	5
1200**	5.7	0.40	19	74	1.3	16	3.2	95	29	11
1300**	2.8	0.43	8.5	75	1.2	1.5	12	99	57	6
1400**	1.8	0.45	4.9	4.7	1.1	2.2	21	100	61	38
1500**	7.0	0.55	21	1.9	0.92	3.5	13	100	151	102
1600**	8.3	0.68	26	2.3	0.75	5.6	8.7	100	117	86
1700**	25	0.66	79	1.9	0.77	1.7	7.3	100	299	148
total gas age			n=12		1710	1.3			10	7
plateau	MSWD = 1.01		n=5		1546	1.3		90	6	2
EBT-2 (L#8852), 136.79 mg, J = 0.00009, NM-85 irradiation										
550**	1213	0.84	4167	0.47	0.60	169	n.d.	0.1	-2903	24255
700	50	1.0	166	5.8	0.50	8.0	1.4	1.3	116	155
840	3.9	0.56	12	70	0.91	0.84	11	16	70	8
960	1.7	0.52	4.3	204	0.98	0.28	26	60	70	3
1100**	3.1	0.51	7.3	105	1.0	0.25	31	83	160	5
1200**	11	0.68	27	44	0.75	14	28	92	497	16
1300**	12	0.61	16	26	0.84	5.9	63	98	1254	17
1400**	5.6	0.74	13	8.1	0.69	3.1	30	99	273	33
1500**	8.8	1.2	n.d.	1.3	0.44	12	129	100	1844	342
1600**	48	1.0	134	0.69	0.50	4.0	18	100	1381	653
1700**	84	0.87	259	0.79	0.59	5.2	9.0	100	1224	815
total gas age			n=11		465	0.93			207	38
plateau	MSWD = 0.18		n=3		279	0.95		60	70	4
EBT-42 (L#8854), 322.31 mg, J = 0.00009, NM-85 irradiation										
550**	215	1.7	687	22	0.30	20	5.5	1.4	1908	980
700**	13	0.61	32	223	0.84	1.5	25	16	513	27
800**	4.7	0.52	6.7	308	0.99	0.54	58	35	447	7
900**	4.6	0.49	4.0	402	1.0	0.32	75	61	561	7
1000**	5.5	0.51	5.3	280	0.99	0.23	72	78	644	4
1100**	9.2	0.55	11	114	0.92	0.87	65	86	966	9
1200**	24	1.1	32	108	0.47	13	61	92	2416	18
1300**	23	0.78	16	103	0.66	3.8	79	99	2957	14
1400**	17	1.6	18	11	0.32	10	69	100	1858	33
1500**	60	7.8	84	2.5	0.07	61	60	100	5871	204
1600**	153	5.7	339	2.1	0.09	45	35	100	8632	552
1700**	118	3.8	272	1.3	0.13	31	32	100	6082	614
total gas age			n=12		1577	0.90			911	26
plateau			n=12		1577	0.90		100	n.a.	n.a.
EBT-53 (L#8853), 421.59 mg, J = 0.00009, NM-85 irradiation										
550**	928	1.6	3159	1.9	0.31	119	n.d.	0.1	-810	9639
625**	96	0.97	288	3.0	0.53	6.8	12	0.3	1842	380
700**	3.4	0.68	6.9	0.24	0.75	3.8	42	0.3	231	159
775**	4.5	0.60	13	194	0.85	0.68	16	13	118	6
850**	1.7	0.57	4.1	249	0.90	0.06	31	30	86	3
925**	1.5	0.56	3.6	401	0.91	0.06	33	56	82	2
1000**	1.8	0.53	4.2	322	0.96	0.09	33	77	97	3
1100**	2.9	0.56	7.2	159	0.92	0.71	28	88	131	4
1200**	8.5	0.64	19	115	0.80	13	34	96	464	17
1300**	15	1.6	23	53	0.32	19	54	99	1303	25
1400**	16	2.5	28	9.3	0.21	25	48	100	1219	65
1500**	45	36	115	1.6	0.01	325	30	100	2235	397
1600**	106	28	310	1.2	0.02	248	16	100	2783	1053
1700**	187	10	527	0.92	0.05	81	17	100	5201	1962
total gas age			n=14		1510	0.88			185	22
plateau			n=14		1510	0.88		100	n.a.	n.a.

Table C1 continued-40Ar/39Ar furnace step-heating data.

Temp (°C)	40Ar/39Ar	37Ar/39Ar	36Ar/39Ar (x10 ⁻³)	39Ar/K mol (x10 ⁻¹⁶)	K/Ca	Cl/K (x10 ⁻³)	40Ar* (%)	39Ar (%)	Age (ka)	Err (±2sigma)
EBT-63 (L#50618), 405.1 mg, J = 0.0000718, NM-112 irradiation										
550**	1960	0.28	6647	0.73	1.8	228	n.d.	0.1	-525	26332
650**	1675	0.49	5678	22	1.0	12	n.d.	1.8	-423	8186
700**	38	0.46	115	9.2	1.1	4.0	11.4	2.6	570	134
800**	27	0.57	89	64	0.89	1.5	2.0	7.8	69	28
900**	4.6	0.55	15	581	0.93	0.1	2.6	55	15	4
1000	7.1	0.55	24	305	0.93	0.2	1.6	80	15	7
1100	20	0.53	65	147	0.97	1.0	2.8	92	72	18
1200**	29	0.54	91	42	0.95	30	7.7	95	293	30
1350**	10	0.61	29	57	0.84	9.6	17.1	100	226	13
1750**	72	0.82	160	5.4	0.62	21	33.9	100	3144	166
total gas age			n=10		1232	0.93			54	170
plateau	MSWD = 0.01		n=2		886	0.93		72	15	4
BIT-272 (L#8428), 144.5 mg, J=0.0001200±0.10%, NM-78 irradiation										
700	1.4	0.40	4.2	2.4	1.3	0.46	14	6.8	43	0.041
800	0.59	0.38	1.4	1.3	1.3	0.40	34	11	44	0.081
900	0.41	0.38	0.89	16	1.3	0.19	43	55	38	0.007
1000	0.47	0.36	1.0	11	1.4	0.19	40	85	40	0.010
1100	1.1	0.35	3.0	2.9	1.4	0.41	24	93	57	0.036
1250**	5.4	0.38	16	1.6	1.3	0.54	11	98	123	0.065
1350**	7.7	0.44	24	0.48	1.2	0.20	9.3	99	156	0.21
1425**	35	0.36	107	0.01	1.4	0.05	9.2	99	690	6.3
1500**	16	0.05	52	0.10	11	-1.2	2.7	100	92	1.0
1750**	51	0.18	166	0.06	2.9	-0.86	4.7	100	525	1.7
1800**	36	0.04	118	0.10	13	1.2	3.4	100	266	1.0
total gas age			n=11		35	1.4			48	32
plateau	MSWD = 1.29		n=5		33	1.4		93	39	6

Isotopic ratios corrected for blank, radioactive decay, and mass discrimination, not corrected for interfering reactions.

Individual analyses show analytical error only; mean age errors also include error in J and irradiation parameters.

Correction factors:

$$(39\text{Ar}/37\text{Ar})\text{Ca} = 0.00070 \pm 0.00005$$

$$(36\text{Ar}/37\text{Ar})\text{Ca} = 0.00026 \pm 0.00002$$

$$(38\text{Ar}/39\text{Ar})\text{K} = 0.0119$$

$$(40\text{Ar}/39\text{Ar})\text{K} = 0.0250 \pm 0.0050 \text{ for NM-85, NM-99, and MN-112}$$

$$(40\text{Ar}/39\text{Ar})\text{K} = 0.0002 \pm 0.0003 \text{ for NM-78}$$

*Not within 95% tolerance (Mahon, 1996), error calculated using the square root of the MSWD multiplied by the Taylor (1982) error.

**Step not used to calculate plateau age.

Appendix 2

Table C2-40Ar/39Ar laser step-heating data.

Power (W)	40Ar/39Ar	37Ar/39Ar	36Ar/39Ar (x10 ⁻³)	39ArK mol (x10 ⁻¹⁶)	K/Ca	Cl/K (x10 ⁻³)	40Ar* (%)	39Ar (%)	Age (ka)	Err (±2sigma)
E87020 (L#9873), 101.86 mg, J = 0.0000847, NM-99 irradiation										
1**	110	2.0	355	19	0.25	3.1	4.2	1.3	712	827
2.5**	5.7	0.59	18	217	0.86	n.d.	5.5	16	48	22
4	1.4	0.50	4.6	287	1.0	n.d.	4.7	35	10	3
6	1.1	0.46	3.3	322	1.1	n.d.	10	57	16	3
7**	1.1	0.46	3.1	210	1.1	n.d.	16	71	27	3
8**	1.1	0.40	3.2	122	1.3	n.d.	18	79	31	5
9**	1.0	0.39	3.0	82	1.3	0.26	14	85	22	7
12**	1.3	0.39	3.8	67	1.3	0.24	15	89	29	8
15**	0.99	0.40	2.7	32	1.3	0.20	21	91	32	16
25**	1.5	0.36	4.1	23	1.4	0.19	20	93	45	20
45**	0.59	0.46	1.3	106	1.1	0.19	36	100	32	5
total gas age			n=11		1488	1.1			34	18
plateau	MSWD = 9.44*		n=2		608	1.1		41	14	6
E87030 (L#9872), 199.23 mg, J=0.0000849, NM-99 irradiation										
1	138	0.92	466	1.2	0.55	4.0	0.20	0.76	36	469
2	29	0.54	96	2.7	0.95	1.2	1.1	2.6	50	52
2	5.4	0.39	18	6.1	1.3	0.11	2.5	6.6	20	13
3	2.3	0.37	7.4	9.2	1.4	0.20	5.1	13	18	7
3	1.3	0.39	3.9	10	1.3	0.02	9.0	20	18	5
5	0.87	0.40	2.7	30	1.3	0.01	8.4	39	11	2
6	0.70	0.41	2.1	28	1.2	n.d.	11	58	12	2
7	0.70	0.40	2.0	18	1.3	0.19	15	70	16	3
8	0.77	0.39	2.3	13	1.3	0.11	14	79	16	3
9	0.84	0.39	2.5	9.5	1.3	0.16	12	85	16	4
10**	0.93	0.40	2.8	6.7	1.3	0.07	12	89	17	5
12**	1.0	0.46	3.1	4.8	1.1	0.38	9.3	92	14	7
15**	1.1	0.40	3.3	2.7	1.3	0.29	12	94	20	12
25**	1.9	0.40	6.0	2.0	1.3	0.30	8.0	96	24	17
45**	0.70	0.40	1.6	6.7	1.3	0.26	33	100	35	5
total gas age			n=15		151	1.3			17	9
plateau	MSWD = 2.66*		n=10		128	1.3		85	14	2
E87085 (L#9874), 196.19 mg, J=0.0000829, NM-99 irradiation										
1**	249	0.84	844	18	0.61	0.74	n.d.	1.3	-65	532
1.5**	20	0.46	65	61	1.1	0.21	1.8	5.6	53	33
2	4.9	0.41	16	106	1.2	0.01	0.6	13	4.3	10
3	2.2	0.38	7.1	125	1.3	0.10	4.6	22	15	5
3	1.6	0.39	5.2	128	1.3	0.06	4.1	31	9.9	4
5	1.3	0.41	4.1	293	1.2	n.d.	6.5	52	12	3
6	1.2	0.40	3.9	252	1.3	n.d.	7.9	69	15	3
7**	1.4	0.40	4.2	153	1.3	0.28	11	80	22	4
8**	1.5	0.38	4.5	102	1.3	0.28	11	87	24	5
9**	1.4	0.38	4.2	61	1.3	0.14	12	92	25	6
10**	1.4	0.36	4.1	36	1.4	0.32	11	94	23	9
12**	1.7	0.39	5.2	25	1.3	0.42	11	96	28	13
15**	2.0	0.36	5.5	16	1.4	0.66	18	97	52	20
25**	3.6	0.44	11	11	1.2	0.92	13	98	69	31
45**	4.6	0.48	13	29	1.1	0.64	18	100	122	18
total gas age			n=15		1417	1.3			19	14
plateau	MSWD = 1.89		n=5		904	1.3		64	13	3

Table C2-40Ar/39Ar laser step-heating data.

Power (W)	40Ar/39Ar	37Ar/39Ar	36Ar/39Ar (x10 ⁻³)	39ArK mol (x10 ⁻¹⁶)	K/Ca	Cl/K (x10 ⁻³)	40Ar* (%)	39Ar (%)	Age (ka)	Err (±2sigma)
E87062 (L#9878), 63.24 mg, J = 0.0000833, NM-99 irradiation										
1**	231	45	397	n.d.	0.01	32	51	n.d.	18094	51568
3**	213	15	391	n.d.	0.03	142	46	n.d.	14955	45094
6	12	0.37	39	15	1.4	0.17	1.4	30	25	19
9	1.3	0.34	3.6	24	1.5	n.d.	20	77	40	3
12**	0.92	0.27	1.4	2.8	1.9	0.10	55	82	76	17
15**	n.d.	0.00	n.d.	1.2	n.d.	n.d.	n.d.	85	133	36
25**	0.36	0.16	n.d.	3.0	3.2	0.27	168	90	91	15
45**	0.32	0.26	n.d.	3.4	2.0	0.40	172	97	84	14
45**	1.0	0.06	0.10	1.6	9.0	0.42	95	100	147	25
total gas age			n=9		52	1.8			47	6
plateau		MSWD = 2.39	n=2		40	1.5		77	40	7
E87030 (L#9879), 203.35 mg, J = 0.0000838, NM-99 irradiation										
1**	187	2.4	617	15	0.21	2.3	2.9	0.93	823	1209
3**	5.7	0.49	18	283	1.0	n.d.	5.8	18	50	31
5	1.2	0.41	3.7	341	1.2	n.d.	4.9	40	9	3
6	0.98	0.38	3.1	315	1.3	n.d.	7.8	59	12	3
7**	0.98	0.37	2.8	216	1.4	n.d.	15	72	23	4
8**	1.1	0.33	3.0	147	1.5	0.30	19	82	32	4
9**	1.1	0.35	3.1	90	1.5	0.33	16	87	26	6
12**	1.4	0.29	3.8	61	1.8	0.16	21	91	46	8
15**	1.2	0.29	3.5	30	1.8	0.18	17	93	31	15
25**	2.5	0.35	7.0	25	1.5	0.69	18	94	70	18
45**	0.72	0.42	1.8	93	1.2	0.31	27	100	29	4
total gas age			n=11		1615	1.3			33	21
plateau		MSWD = 2.19	n=2		656	1.3		41	10	4

Isotopic ratios corrected for blank, radioactive decay, and mass discrimination, not corrected for interfering reactions.

Individual analyses show analytical error only; mean age errors also include error in J and irradiation parameters.

Analyses in italics are excluded from mean age calculations.

Correction factors:

$$(39\text{Ar}/37\text{Ar})\text{Ca} = 0.00070 \pm 0.00005$$

$$(36\text{Ar}/37\text{Ar})\text{Ca} = 0.00026 \pm 0.00002$$

$$(38\text{Ar}/39\text{Ar})\text{K} = 0.0119$$

$$(40\text{Ar}/39\text{Ar})\text{K} = 0.0250 \pm 0.0050$$

*Not within 95% tolerance, Mahon (1996) error calculation method used

**Step not used to calculate plateau age.

Appendix 3

Table C3.1.1 Raw microprobe data for sample EBT-1

Analysis	1	2	3	4	5	6	7	8	9	10
SiO2	53.96	54.53	54.40	54.24	54.71	54.56	54.68	54.10	54.39	54.88
TiO2	0.98	0.95	1.04	1.08	1.08	1.04	1.01	1.05	0.99	1.12
Al2O3	19.50	19.30	19.20	19.48	19.49	19.51	19.58	19.56	19.25	19.33
FeO	5.68	5.52	5.57	5.54	5.63	5.47	5.71	5.59	5.72	5.64
MnO	0.23	0.32	0.28	0.26	0.24	0.21	0.22	0.20	0.28	0.25
MgO	0.87	0.90	0.85	0.84	0.87	0.88	0.89	0.89	0.81	0.82
CaO	1.87	1.84	1.85	1.94	1.79	1.76	1.85	1.89	1.72	1.82
Na2O	8.90	8.85	9.00	8.83	8.15	8.76	8.77	9.13	9.21	8.85
K2O	5.53	5.51	5.64	5.81	5.67	5.55	5.57	5.65	5.64	5.56
P2O5	0.17	0.27	0.24	0.32	0.36	0.35	0.27	0.30	0.28	0.33
F (ppm)	870	2020	2320	400	n.d.	2570	3390	2320	2340	3300
SO2	0.07	0.09	0.06	0.08	0.09	0.09	0.07	0.05	0.08	0.06
Cl (ppm)	1290	1590	1580	1650	1770	1700	1910	1450	1240	1620
Total	97.99	98.45	98.52	98.62	98.24	98.60	99.15	98.77	98.70	99.15

Table C3.1.2 Microprobe data for sample EBT-1 corrected to 100%

Analysis	1	2	3	4*	5*	6	7	8	9	10
SiO2	55.07	55.39	55.22	54.87	55.55	55.33	55.15	54.77	55.10	55.35
TiO2	1.00	0.96	1.05	1.09	1.09	1.05	1.02	1.06	1.00	1.13
Al2O3	19.90	19.60	19.49	19.71	19.78	19.79	19.74	19.80	19.50	19.50
FeO	5.80	5.61	5.65	5.61	5.72	5.55	5.76	5.66	5.79	5.69
MnO	0.24	0.33	0.28	0.27	0.25	0.21	0.22	0.20	0.29	0.25
MgO	0.89	0.91	0.86	0.85	0.88	0.89	0.90	0.90	0.82	0.82
CaO	1.91	1.86	1.88	1.96	1.81	1.79	1.87	1.91	1.74	1.83
Na2O	9.08	8.99	9.13	8.94	8.27	8.88	8.85	9.24	9.33	8.93
K2O	5.65	5.60	5.73	5.87	5.76	5.63	5.62	5.72	5.71	5.61
P2O5	0.18	0.28	0.24	0.32	0.36	0.36	0.27	0.30	0.28	0.34
F (ppm)	888	2052	2355	2641	2650	2607	3419	2349	2371	3328
SO2	0.08	0.10	0.06	0.08	0.09	0.09	0.07	0.05	0.08	0.06
Cl (ppm)	1317	1615	1604	1669	1797	1724	1926	1468	1256	1634
Total	100.00	100.00	100.00	100.00	100.00	100.00	100.00	100.00	100.00	100.00

*Fluorine corrected to an average of 2609 ppm

Table C3.1.3 Microprobe data for sample EBT-1 corrected for Sodium loss

Analysis	1	2	3	4	5	6	7	8	9	10	Mean	StdDev
Correction	0.99797	0.99708	0.99845	0.99653	0.98995	0.99597	0.99561	0.99957	1.00043	0.99642		
SiO2	54.96	55.23	55.14	54.68	54.99	55.11	54.91	54.75	55.13	55.15	55.01	0.19
TiO2	1.00	0.96	1.05	1.09	1.08	1.05	1.01	1.06	1.00	1.13	1.05	0.05
Al2O3	19.86	19.55	19.46	19.64	19.58	19.71	19.66	19.79	19.51	19.43	19.59	0.12
FeO	5.79	5.59	5.65	5.59	5.66	5.53	5.74	5.66	5.79	5.67	5.65	0.08
MnO	0.24	0.32	0.28	0.26	0.24	0.21	0.22	0.20	0.29	0.25	0.25	0.04
MgO	0.88	0.91	0.86	0.85	0.87	0.88	0.90	0.90	0.82	0.82	0.87	0.03
CaO	1.91	1.86	1.88	1.95	1.79	1.78	1.86	1.91	1.74	1.83	1.84	0.07
Na2O	9.29	9.29	9.29	9.29	9.29	9.29	9.29	9.29	9.29	9.29	9.29	0.00
K2O	5.64	5.58	5.72	5.85	5.70	5.60	5.59	5.72	5.71	5.59	5.67	0.09
P2O5	0.18	0.27	0.24	0.32	0.36	0.36	0.27	0.30	0.28	0.34	0.30	0.04
F (ppm)	886	2046	2351	2631	2623	2596	3404	2348	2372	3316	2632	452
SO2	0.08	0.10	0.06	0.08	0.09	0.09	0.07	0.05	0.08	0.06	0.07	0.02
Cl (ppm)	1314	1610	1601	1663	1779	1717	1918	1467	1257	1628	1627	187
Total	100.02	100.03	100.01	100.03	100.09	100.04	100.04	100.00	100.00	100.03	100.03	100.03

Table C3.2.1 Raw microprobe data for sample EBT-3

Analysis	1	2	3	4	5	6	7	8	9	10
SiO2	54.10	54.66	54.31	54.58	54.20	53.71	53.63	54.11	54.49	54.11
TiO2	1.01	1.11	1.11	1.06	1.12	1.07	0.94	1.06	1.10	1.03
Al2O3	19.34	19.40	19.65	19.28	19.40	19.53	19.46	19.35	19.45	19.29
FeO	5.62	5.51	5.78	5.54	5.57	5.47	5.65	5.62	5.64	5.43
MnO	0.18	0.26	0.23	0.20	0.29	0.15	0.33	0.32	0.27	0.21
MgO	0.92	0.87	0.89	0.91	0.93	0.91	0.89	0.88	0.88	0.84
CaO	1.79	1.82	1.89	1.86	1.90	1.88	1.86	1.87	1.91	1.86
Na2O	8.66	8.87	8.79	8.81	8.83	8.61	8.83	8.76	8.80	8.67
K2O	5.70	5.69	5.62	5.61	5.60	5.56	5.42	5.65	5.48	5.68
P2O5	0.33	0.26	0.26	0.25	0.34	0.34	0.33	0.29	0.38	0.26
F (ppm)	2120	n.d.	1600	3370	2350	1780	1900	1750	2870	1430
SO2	0.08	0.10	0.11	0.09	0.06	0.08	0.06	0.05	0.08	0.05
Cl (ppm)	1660	1770	1720	1960	1650	1510	1660	1680	1450	1520
Total	98.08	98.96	98.96	98.71	98.62	97.64	97.76	98.29	98.90	97.73

Table C3.2.2 Microprobe data for sample EBT-3 corrected to 100%

Analysis	1	2*	3	4	5	6	7	8	9	10
SiO2	55.15	55.25	54.88	55.29	54.96	55.01	54.86	55.05	55.09	55.37
TiO2	1.02	1.12	1.12	1.08	1.13	1.09	0.96	1.08	1.11	1.06
Al2O3	19.71	19.61	19.85	19.53	19.67	20.00	19.90	19.68	19.66	19.73
FeO	5.73	5.57	5.84	5.61	5.64	5.60	5.77	5.72	5.70	5.56
MnO	0.18	0.26	0.23	0.20	0.30	0.15	0.34	0.33	0.27	0.21
MgO	0.94	0.88	0.90	0.92	0.94	0.93	0.91	0.90	0.89	0.86
CaO	1.82	1.84	1.91	1.88	1.93	1.93	1.90	1.90	1.93	1.90
Na2O	8.83	8.97	8.88	8.93	8.95	8.82	9.03	8.91	8.90	8.87
K2O	5.81	5.76	5.68	5.68	5.68	5.70	5.55	5.75	5.54	5.81
P2O5	0.33	0.26	0.26	0.25	0.34	0.35	0.34	0.29	0.38	0.27
F (ppm)	2161	2183	1617	3414	2383	1823	1944	1780	2902	1463
SO2	0.08	0.10	0.11	0.09	0.06	0.08	0.06	0.05	0.08	0.05
Cl (ppm)	1692	1789	1738	1986	1673	1547	1698	1709	1466	1555
Total	100	100	100	100	100	100	100	100	100	100

*Fluorine corrected to an average of 2130 ppm

Table C3.2.3 Microprobe data for sample EBT-3 corrected for Sodium loss

Analysis	1	2	3	4	5	6	7	8	9	10	Mean	StdDev
Correction	0.99886	1.00021	0.99936	0.99980	1.00004	0.99874	1.00087	0.99966	0.99950	0.99929		
SiO2	55.09	55.27	54.85	55.28	54.96	54.94	54.91	55.03	55.07	55.33	55.08	0.16
TiO2	1.02	1.12	1.12	1.08	1.13	1.09	0.96	1.08	1.11	1.06	1.09	0.04
Al2O3	19.69	19.61	19.84	19.53	19.67	19.98	19.92	19.67	19.65	19.72	19.67	0.09
FeO	5.72	5.57	5.83	5.61	5.64	5.59	5.78	5.72	5.70	5.55	5.69	0.09
MnO	0.18	0.26	0.23	0.20	0.30	0.15	0.34	0.33	0.27	0.21	0.25	0.05
MgO	0.94	0.88	0.90	0.92	0.94	0.93	0.91	0.90	0.89	0.86	0.91	0.02
CaO	1.82	1.84	1.91	1.88	1.93	1.93	1.91	1.90	1.93	1.90	1.89	0.04
Na2O	8.95	8.95	8.95	8.95	8.95	8.95	8.95	8.95	8.95	8.95	8.95	0.00
K2O	5.80	5.76	5.68	5.68	5.68	5.69	5.55	5.75	5.54	5.81	5.70	0.08
P2O5	0.33	0.26	0.26	0.25	0.34	0.34	0.34	0.29	0.38	0.27	0.30	0.05
F (ppm)	2159	2184	1616	3413	2383	1821	1945	1780	2900	1462	2348	628
SO2	0.08	0.10	0.11	0.09	0.06	0.08	0.06	0.05	0.08	0.05	0.08	0.02
Cl (ppm)	1691	1790	1737	1985	1673	1545	1700	1709	1465	1554	1721	155
Total	100.01	100.00	100.01	100.00	100.00	100.01	99.99	100.00	100.00	100.01	100.00	100.00

Table C3.3.1 Raw microprobe data for sample EBT-4

Analysis	1	2	3	4	5	6	7	8	9	10
SiO ₂	55.48	55.96	55.50	55.74	55.19	55.63	56.31	56.07	56.13	55.77
TiO ₂	1.00	1.04	1.04	1.03	1.06	1.00	0.98	1.02	1.00	0.98
Al ₂ O ₃	20.72	20.29	20.35	20.40	20.34	20.49	20.35	20.20	20.57	20.39
FeO	5.23	5.48	5.47	5.53	5.21	5.41	5.40	5.47	5.43	5.32
MnO	0.30	0.28	0.27	0.24	0.18	0.24	0.28	0.30	0.12	0.30
MgO	3.04	0.89	0.96	1.00	0.95	0.92	0.88	0.95	1.67	0.91
CaO	1.93	1.90	1.84	1.94	1.84	1.88	1.89	1.96	1.88	1.80
Na ₂ O	8.60	8.62	8.75	8.59	8.64	8.84	8.72	8.81	8.66	8.82
K ₂ O	5.40	5.68	5.61	5.43	5.53	5.53	5.47	5.61	5.54	5.64
P ₂ O ₅	0.26	0.28	0.29	0.27	0.25	0.29	0.30	0.29	0.29	0.35
F (ppm)	3200	n.d.	3180	1210	3060	3460	1480	4060	1830	2610
SO ₂	0.10	0.05	0.13	0.14	0.12	0.08	0.07	0.08	0.10	0.08
Cl (ppm)	1210	1800	1470	1530	1740	1430	1790	1430	1490	1590
Total	102.48	100.64	100.68	100.57	99.79	100.79	100.97	101.32	101.72	100.78

Table C3.3.2 Microprobe data for sample EBT-4 corrected to 100%

Analysis	1	2*	3	4	5	6	7	8	9	10
SiO ₂	54.14	55.46	55.13	55.42	55.31	55.19	55.77	55.34	55.18	55.34
TiO ₂	0.98	1.03	1.03	1.02	1.06	1.00	0.97	1.01	0.98	0.97
Al ₂ O ₃	20.22	20.11	20.21	20.29	20.38	20.33	20.16	19.94	20.22	20.23
FeO	5.10	5.43	5.43	5.50	5.22	5.37	5.35	5.40	5.34	5.27
MnO	0.30	0.28	0.26	0.23	0.18	0.24	0.28	0.30	0.11	0.30
MgO	2.96	0.88	0.96	0.99	0.95	0.92	0.87	0.93	1.64	0.90
CaO	1.88	1.88	1.83	1.93	1.84	1.87	1.87	1.94	1.85	1.78
Na ₂ O	8.39	8.54	8.69	8.54	8.66	8.77	8.64	8.70	8.51	8.75
K ₂ O	5.26	5.62	5.57	5.40	5.54	5.49	5.42	5.54	5.45	5.60
P ₂ O ₅	0.25	0.28	0.29	0.27	0.25	0.28	0.30	0.29	0.29	0.34
F (ppm)	3123	2587	3158	1203	3067	3433	1466	4007	1799	2590
SO ₂	0.09	0.05	0.13	0.14	0.12	0.07	0.07	0.08	0.10	0.08
Cl (ppm)	1181	1784	1460	1521	1744	1419	1773	1411	1465	1578
Total	100.00	100.00	100.00	100.00	100.00	100.00	100.00	100.00	100.00	100.00

*Flourine corrected to an average of 2611 ppm

Table C3.3.3 Microprobe data for sample EBT-4 corrected for sodium loss

Analysis	1	2	3	4	5	6	7	8	9	10	Mean	StdDev
Correction	0.99632	0.9978019	0.99934	0.99781	0.99899	1.00005	0.99878	0.99935	0.99754	0.99994		
SiO2	53.94	55.34	55.09	55.30	55.25	55.20	55.70	55.31	55.04	55.34	55.29	0.19
TiO2	0.98	1.03	1.03	1.02	1.06	1.00	0.97	1.01	0.98	0.97	1.01	0.03
Al2O3	20.14	20.07	20.20	20.24	20.36	20.33	20.13	19.93	20.17	20.23	20.18	0.13
FeO	5.08	5.42	5.43	5.49	5.21	5.37	5.34	5.40	5.33	5.27	5.36	0.08
MnO	0.30	0.28	0.26	0.23	0.18	0.24	0.28	0.30	0.11	0.30	0.24	0.06
MgO	2.95	0.88	0.96	0.99	0.95	0.92	0.87	0.93	1.64	0.90	1.00	0.24
CaO	1.87	1.87	1.83	1.93	1.84	1.87	1.87	1.94	1.84	1.78	1.86	0.05
Na2O	8.76	8.76	8.76	8.76	8.76	8.76	8.76	8.76	8.76	8.76	8.76	0.00
K2O	5.25	5.61	5.57	5.39	5.54	5.49	5.41	5.53	5.43	5.60	5.51	0.08
P2O5	0.25	0.28	0.29	0.27	0.25	0.28	0.30	0.29	0.29	0.34	0.29	0.03
F (ppm)	3111	2581	3156	1201	3063	3433	1464	4005	1795	2590	2587	941
SO2	0.09	0.05	0.13	0.14	0.12	0.07	0.07	0.08	0.10	0.08	0.09	0.03
Cl (ppm)	1176	1780	1459	1518	1742	1419	1771	1410	1461	1578	1571	154
Total	100.03	100.02	100.01	100.02	100.01	100.00	100.01	100.01	100.02	100.00	100.01	0.01

Table C3.4.1 Raw microprobe data for sample EBT-5

Analysis	1	2	3	4	5	6	7	8	9	10
SiO2	53.74	46.40	42.67	55.75	53.57	54.93	56.29	55.33	55.19	56.34
TiO2	0.99	2.98	3.29	1.01	1.15	1.07	0.99	1.00	1.15	0.90
Al2O3	19.87	17.81	15.27	20.19	19.76	20.13	19.80	20.47	19.74	19.72
FeO	5.64	10.07	10.32	5.50	6.08	5.85	5.48	5.56	5.96	5.85
MnO	0.21	0.21	0.07	0.29	0.27	0.17	0.26	0.30	0.25	0.23
MgO	0.82	2.80	6.79	0.82	0.97	0.99	0.83	0.90	1.06	0.86
CaO	1.88	6.29	12.38	1.94	2.33	2.13	1.95	1.97	2.37	1.85
Na2O	8.95	6.08	3.59	8.69	8.49	8.56	8.51	8.55	8.18	8.43
K2O	5.77	3.46	1.40	5.74	5.51	5.65	5.45	5.55	5.34	5.56
P2O5	0.23	1.23	0.66	0.20	0.33	0.30	0.26	0.25	0.39	0.27
F (ppm)	1430	1780	3340	3540	2080	2910	180	1730	2940	300
SO2	0.05	0.24	0.13	0.08	0.10	0.11	0.10	0.09	0.06	0.16
Cl (ppm)	1350	1030	880	1940	1300	1310	1450	1460	1390	1370
Total	98.42	97.86	96.98	100.75	98.90	100.32	100.07	100.28	100.11	100.33

Table C3.4.2 Microprobe data for sample EBT-5 corrected to 100%

Analysis	1	2	3	4	5	6	7*	8	9	10*
SiO2	54.60	47.42	44.00	55.33	54.17	54.76	56.12	55.17	55.13	56.04
TiO2	1.01	3.05	3.39	1.00	1.16	1.07	0.98	0.99	1.15	0.89
Al2O3	20.19	18.20	15.74	20.04	19.98	20.06	19.74	20.41	19.71	19.61
FeO	5.73	10.29	10.64	5.46	6.15	5.83	5.46	5.55	5.95	5.82
MnO	0.21	0.21	0.07	0.28	0.27	0.17	0.26	0.30	0.25	0.23
MgO	0.83	2.86	7.00	0.81	0.98	0.99	0.82	0.90	1.06	0.85
CaO	1.91	6.43	12.77	1.92	2.35	2.12	1.95	1.97	2.36	1.84
Na2O	9.10	6.21	3.71	8.63	8.59	8.53	8.49	8.53	8.17	8.38
K2O	5.86	3.53	1.45	5.69	5.57	5.64	5.43	5.54	5.33	5.53
P2O5	0.23	1.26	0.68	0.20	0.33	0.30	0.26	0.25	0.39	0.27
F (ppm)	1453	1819	3444	3514	2103	2901	2433	1725	2937	2427
SO2	0.05	0.24	0.13	0.08	0.10	0.11	0.10	0.09	0.06	0.16
Cl (ppm)	1372	1053	907	1926	1314	1306	1446	1456	1388	1363
Total	100.00	100.00	100.00	100.00	100.00	100.00	100.00	100.00	100.00	100.00

*Flourine corrected to an average of 2438 ppm

Table C3.4.3 Microprobe data for sample EBT-5 corrected for sodium loss

Analysis	1	2	3	4	5	6	7	8	9	10	Mean	StdDev
Correction	1.002361	0.974182	0.95098	0.99766	0.99727	0.99674	0.99629	0.99671	0.99318	0.995249		
SiO2	54.73	46.19	41.84	55.20	54.02	54.58	55.91	54.99	54.75	55.77	54.99	0.62
TiO2	1.01	2.97	3.22	1.00	1.16	1.07	0.98	0.99	1.14	0.89	1.03	0.09
Al2O3	20.24	17.73	14.97	19.99	19.93	20.00	19.67	20.34	19.58	19.52	19.91	0.30
FeO	5.74	10.03	10.12	5.45	6.13	5.81	5.44	5.53	5.91	5.79	5.73	0.24
MnO	0.21	0.21	0.06	0.28	0.27	0.17	0.26	0.30	0.25	0.23	0.24	0.04
MgO	0.84	2.79	6.66	0.81	0.98	0.99	0.82	0.89	1.05	0.85	0.90	0.09
CaO	1.91	6.26	12.14	1.92	2.35	2.11	1.94	1.96	2.35	1.83	2.05	0.20
Na2O	8.86	8.86	8.86	8.86	8.86	8.86	8.86	8.86	8.86	8.86	8.86	0.00
K2O	5.87	3.44	1.38	5.68	5.56	5.62	5.41	5.52	5.29	5.51	5.56	0.17
P2O5	0.23	1.23	0.65	0.20	0.33	0.29	0.26	0.25	0.39	0.27	0.28	0.06
F (ppm)	1456	1772	3275	3505	2097	2891	2424	1720	2917	2415	2428	673
SO2	0.05	0.24	0.13	0.08	0.10	0.11	0.10	0.09	0.06	0.16	0.09	0.03
Cl (ppm)	1375	1025	863	1921	1311	1302	1440	1451	1379	1356	1442	201
Total	99.98	100.23	100.43	100.02	100.02	100.03	100.03	100.03	100.06	100.04	100.03	100.03

Table C3.5.1 Raw microprobe data for sample EBT-6

Analysis	5*	2	4	5
SiO2	54.10	54.83	55.30	58.99
TiO2	1.12	0.96	1.02	0.70
Al2O3	19.26	19.51	19.99	18.52
FeO	5.66	5.50	5.39	5.96
MnO	0.19	0.17	0.21	0.25
MgO	0.96	0.83	1.28	0.60
CaO	1.99	1.88	1.84	1.84
Na2O	8.79	8.79	8.90	7.27
K2O	5.64	5.46	5.43	5.67
P2O5	0.35	0.22	0.34	0.21
F (ppm)	n.d.	1300	2900	2550
SO2	0.09	0.12	0.09	0.03
Cl (ppm)	1300	1450	1360	1580
Total	98.29	98.55	100.21	100.47

*This analysis done on 10/14/99, all others done on 10/7/99

Table C3.5.2 Microprobe data for sample EBT-6 corrected to 100%

Analysis	5**	2	4	5
SiO2	54.92	55.64	55.18	58.72
TiO2	1.14	0.97	1.02	0.70
Al2O3	19.55	19.80	19.94	18.43
FeO	5.75	5.58	5.38	5.93
MnO	0.19	0.17	0.21	0.25
MgO	0.97	0.85	1.28	0.60
CaO	2.02	1.91	1.84	1.83
Na2O	8.92	8.92	8.88	7.24
K2O	5.73	5.54	5.42	5.65
P2O5	0.36	0.22	0.34	0.21
F (ppm)	2284	1319	2894	2538
SO2	0.09	0.12	0.09	0.03
Cl (ppm)	1320	1471	1357	1573
Total	99.99	100.00	100.00	100.00

**Flourine corrected to an average of 2250 ppm

Table C3.5.3 Microprobe data for sample EBT-6 corrected for sodium loss

Analysis	5	2	4	5	Mean	StdDev
Correction	1.000015	0.9999833	0.99956	0.98346		
SiO2	54.92	55.64	55.16	57.74	55.86	1.29
TiO2	1.14	0.97	1.02	0.69	0.95	0.19
Al2O3	19.55	19.80	19.93	18.13	19.35	0.83
FeO	5.75	5.58	5.38	5.84	5.64	0.20
MnO	0.19	0.17	0.21	0.25	0.21	0.03
MgO	0.97	0.85	1.28	0.59	0.92	0.29
CaO	2.02	1.91	1.84	1.80	1.89	0.10
Na2O	8.92	8.92	8.92	8.92	8.92	0.00
K2O	5.73	5.54	5.41	5.55	5.56	0.13
P2O5	0.36	0.22	0.34	0.21	0.28	0.08
F (ppm)	2284	1319	2893	2496	2248	669
SO2	0.09	0.12	0.09	0.03	0.08	0.04
Cl (ppm)	1320	1471	1356	1547	1423	104
Total	99.99	100.00	100.00	100.15	100.04	

Table C3.6.3 Microprobe data for sample EBT-7 corrected for sodium loss

Analysis	1	2	3	4	5	6	7	8	9	10	Mean	StdDev
Correction	0.9956	0.9973821	0.99876	0.99535	0.99912	0.99979	0.99762	0.99779	1.00021	0.99879		
SiO2	54.12	55.50	55.34	54.29	55.18	54.74	55.31	55.23	54.82	55.19	55.16	0.26
TiO2	0.99	1.01	1.12	1.00	0.96	0.99	1.11	1.02	1.12	1.01	1.04	0.06
Al2O3	19.72	20.25	20.16	20.09	20.69	20.43	20.09	20.27	20.19	20.35	20.30	0.19
FeO	5.33	5.35	5.38	5.46	5.08	5.55	5.39	5.42	5.61	5.44	5.40	0.16
MnO	0.18	0.22	0.27	0.35	0.24	0.28	0.20	0.20	0.20	0.35	0.24	0.05
MgO	3.20	0.90	1.01	2.03	0.90	0.99	0.96	1.02	1.02	0.92	0.96	0.05
CaO	1.71	1.83	1.82	1.74	1.90	1.83	1.92	1.89	1.80	1.85	1.86	0.04
Na2O	8.80	8.80	8.80	8.80	8.80	8.80	8.80	8.80	8.80	8.80	8.80	0.00
K2O	5.44	5.59	5.53	5.51	5.39	5.58	5.49	5.48	5.65	5.46	5.52	0.08
P2O5	0.35	0.24	0.23	0.32	0.26	0.26	0.20	0.32	0.27	0.25	0.25	0.03
F (ppm)	316	921	1625	1920	3577	3419	2955	1657	3251	2068	2434	993
SO2	0.05	0.08	0.04	0.09	0.10	0.06	0.10	0.06	0.07	0.06	0.07	0.02
Cl (ppm)	1274	1505	1427	1677	1465	1545	1433	1480	1321	1345	1440	76
Total	100.04	100.02	100.01	100.04	100.01	100.00	100.02	100.02	100.00	100.01	100.01	100.01

Table C3.7.3 Microprobe data for sample EBT-8 corrected for Sodium loss

Analysis	1	2	3	4	5	6	7	8	9	10	Mean	StdDev
Correction	0.99713	0.99847	0.99678	0.99915	0.99734	0.99729	0.99621	1.00084	0.99871	0.99879		
SiO2	54.90	55.11	54.94	55.05	54.98	55.24	55.23	54.92	55.07	55.08	55.05	0.12
TiO2	1.08	1.11	1.14	1.15	1.04	1.10	1.04	1.07	1.01	1.06	1.08	0.04
Al2O3	19.66	19.73	19.52	19.67	19.58	19.56	19.90	19.76	19.73	19.71	19.68	0.11
FeO	5.60	5.42	5.79	5.65	5.76	5.78	5.42	5.78	5.68	5.56	5.64	0.14
MnO	0.25	0.21	0.21	0.23	0.27	0.10	0.30	0.25	0.17	0.29	0.23	0.06
MgO	0.86	0.87	0.90	0.93	0.88	0.88	0.89	0.87	0.90	0.87	0.88	0.02
CaO	1.92	1.83	1.85	1.82	1.84	1.87	1.82	1.91	1.87	1.96	1.87	0.05
Na2O	9.17	9.17	9.17	9.17	9.17	9.17	9.17	9.17	9.17	9.17	9.17	0.00
K2O	5.70	5.61	5.61	5.57	5.60	5.50	5.57	5.61	5.65	5.62	5.61	0.05
P2O5	0.32	0.32	0.37	0.32	0.31	0.33	0.30	0.38	0.29	0.24	0.32	0.04
F (ppm)	3311	3895	2792	1910	3528	2761	1650	684	2410	1854	2480	978
SO2	0.08	0.10	0.10	0.10	0.08	0.08	0.08	0.07	0.07	0.11	0.09	0.01
Cl (ppm)	1555	1490	1421	1488	1545	1602	1539	1409	1754	1398	1520	107
Total	100.03	100.01	100.03	100.01	100.02	100.02	100.03	99.99	100.01	100.01	100.02	107

Table C3.8.3 Microprobe data for sample EBT-9 corrected for sodium loss

Analysis	1	2	3	4	5	6	7	8	9	10	Mean	StdDev
Correction	1.00003	0.99989	0.99744	0.99861	0.99606	0.99997	0.99560	0.99486	0.99740	0.99932		
SiO2	54.85	54.75	55.10	55.08	55.04	54.69	55.13	55.01	54.83	55.15	54.96	0.17
TiO2	1.01	1.00	1.03	0.99	1.01	1.06	1.06	1.04	0.99	1.02	1.02	0.02
Al2O3	19.86	19.73	19.50	19.73	19.86	19.89	19.64	19.74	19.90	19.67	19.75	0.13
FeO	5.62	5.66	5.67	5.51	5.36	5.57	5.67	5.64	5.83	5.51	5.60	0.13
MnO	0.19	0.32	0.30	0.20	0.27	0.20	0.24	0.30	0.16	0.26	0.24	0.06
MgO	0.92	0.92	0.88	0.88	0.86	0.84	0.89	0.84	0.83	0.88	0.87	0.03
CaO	1.93	1.84	1.79	1.89	1.88	1.90	1.82	1.84	1.79	1.91	1.86	0.05
Na2O	9.43	9.43	9.43	9.43	9.43	9.43	9.43	9.43	9.43	9.43	9.43	0.00
K2O	5.44	5.54	5.52	5.47	5.64	5.60	5.59	5.55	5.60	5.57	5.55	0.06
P2O5	0.25	0.39	0.26	0.34	0.25	0.21	0.19	0.28	0.32	0.26	0.28	0.06
F (ppm)	2605	2223	3028	2300	2135	3561	1664	1688	1008	1030	2124	816
SO2	0.08	0.05	0.09	0.08	0.08	0.10	0.07	0.08	0.06	0.07	0.08	0.01
Cl (ppm)	1628	1523	1348	1707	1654	1613	1674	1186	1774	1677	1578	181
Total	100.00	100.00	100.02	100.01	100.04	100.00	100.04	100.05	100.02	100.01	100.02	181

Table C3.9.1 Raw Microprobe data for sample EBT-10

Analysis	1	2	3	4	5	6	7	8	9	10
SiO2	54.57	54.94	53.71	54.27	53.89	54.36	53.90	54.11	54.81	54.56
TiO2	1.01	1.08	1.03	1.02	1.09	0.93	1.05	1.04	1.05	0.99
Al2O3	19.50	19.74	19.37	19.50	19.55	19.54	19.33	19.57	19.53	19.71
FeO	5.57	5.54	5.67	5.55	5.66	5.50	5.61	5.59	5.52	5.72
MnO	0.19	0.23	0.26	0.27	0.18	0.29	0.29	0.32	0.30	0.26
MgO	0.83	0.88	0.88	0.83	0.88	0.90	0.88	0.86	0.86	0.88
CaO	1.88	1.86	1.85	1.80	1.80	1.84	1.88	1.86	1.85	1.85
Na2O	8.94	8.78	9.20	9.26	8.94	9.03	9.08	9.01	9.08	8.89
K2O	5.54	5.47	5.55	5.59	5.40	5.48	5.57	5.62	5.47	5.55
P2O5	0.29	0.34	0.25	0.26	0.26	0.32	0.26	0.29	0.25	0.32
F (ppm)	2150	2370	2220	2000	2170	80	1770	1550	3040	800
SO2	0.08	0.09	0.08	0.05	0.07	0.08	0.11	0.06	0.07	0.08
Cl (ppm)	1560	1700	1620	1760	1600	1510	1360	1320	1570	1340
Total	98.76	99.37	98.23	98.77	98.11	98.33	98.28	98.61	99.25	99.03

Table C3.9.2 Microprobe data for sample EBT-10 corrected to 100%

Analysis	1	2	3	4	5	6*	7	8	9	10
SiO2	55.25	55.29	54.68	54.95	54.93	55.17	54.85	54.87	55.23	55.10
TiO2	1.03	1.09	1.05	1.03	1.12	0.95	1.07	1.05	1.05	1.00
Al2O3	19.75	19.87	19.72	19.74	19.93	19.83	19.67	19.84	19.68	19.90
FeO	5.63	5.58	5.77	5.62	5.77	5.58	5.71	5.67	5.56	5.78
MnO	0.19	0.23	0.27	0.28	0.18	0.20	0.29	0.32	0.30	0.26
MgO	0.84	0.88	0.90	0.84	0.90	0.91	0.90	0.87	0.87	0.89
CaO	1.90	1.87	1.88	1.82	1.84	1.86	1.92	1.89	1.86	1.87
Na2O	9.05	8.84	9.36	9.37	9.11	9.16	9.24	9.14	9.15	8.98
K2O	5.61	5.51	5.65	5.66	5.51	5.56	5.67	5.70	5.51	5.60
P2O5	0.29	0.34	0.25	0.26	0.26	0.33	0.27	0.29	0.25	0.32
F (ppm)	2177	2385	2260	2025	2212	2192	1801	1572	3063	808
SO2	0.09	0.09	0.08	0.05	0.07	0.09	0.11	0.06	0.07	0.08
Cl (ppm)	1580	1711	1649	1782	1631	1532	1384	1339	1582	1353
Total	100.00	100.00	100.00	100.00	100.00	100.00	100.00	100.00	100.00	100.00

*Fluorine corrected to an average of 2160 ppm

Table C3.9.3 Microprobe data for sample EBT-10 corrected for sodium loss

Analysis	1	2	3	4	5	6	7	8	9	10	Mean	StdDev
Correction	0.99681	0.99476	0.99996	1.00005	0.99748	0.99796	0.99874	0.99773	0.99780	0.99613		
SiO2	55.07	55.00	54.68	54.95	54.79	55.05	54.78	54.75	55.11	54.88	54.91	0.15
TiO2	1.02	1.08	1.05	1.03	1.11	0.94	1.07	1.05	1.05	0.99	1.04	0.05
Al2O3	19.68	19.77	19.72	19.74	19.88	19.79	19.65	19.80	19.63	19.83	19.75	0.08
FeO	5.62	5.55	5.77	5.62	5.75	5.57	5.70	5.66	5.55	5.76	5.65	0.09
MnO	0.19	0.23	0.27	0.28	0.18	0.20	0.29	0.32	0.30	0.26	0.25	0.05
MgO	0.84	0.88	0.90	0.84	0.90	0.91	0.89	0.87	0.87	0.89	0.88	0.03
CaO	1.90	1.86	1.88	1.82	1.83	1.86	1.91	1.88	1.86	1.86	1.87	0.03
Na2O	9.37	9.37	9.37	9.37	9.37	9.37	9.37	9.37	9.37	9.37	9.37	0.00
K2O	5.60	5.48	5.65	5.66	5.49	5.55	5.66	5.69	5.50	5.58	5.59	0.08
P2O5	0.29	0.34	0.25	0.26	0.26	0.33	0.27	0.29	0.25	0.32	0.29	0.03
F (ppm)	2170	2373	2260	2025	2206	2188	1799	1568	3056	805	2045	584
SO2	0.08	0.09	0.08	0.05	0.07	0.09	0.11	0.06	0.07	0.08	0.08	0.02
Cl (ppm)	1575	1702	1649	1782	1627	1529	1382	1336	1578	1348	1551	153
Total	100.03	100.05	100.00	100.00	100.02	100.02	100.01	100.02	100.02	100.04	100.02	100.02

Table C3.10.3 Microprobe data for sample EBT-12 corrected for sodium loss

Analysis	1	2	3	4	5	6	7	8	9	10	Mean	StdDev
Correction	0.99403	0.99360	0.99569	1.00777	0.99251	0.99628	0.99484	0.99323	1.00096	0.99904		
SiO2	54.94	54.69	54.42	54.26	54.87	54.34	54.27	54.08	54.33	54.38	54.46	0.28
TiO2	0.98	1.03	0.97	1.11	1.04	1.15	1.09	1.01	1.04	0.99	1.04	0.06
Al2O3	19.69	19.74	20.26	20.18	19.86	20.22	20.35	20.47	20.28	20.00	20.10	0.27
FeO	5.43	5.56	5.37	5.39	5.35	5.35	5.44	5.51	5.29	5.49	5.42	0.08
MnO	0.23	0.26	0.25	0.25	0.27	0.24	0.26	0.30	0.20	0.26	0.25	0.02
MgO	0.87	0.88	0.91	0.86	0.88	0.84	0.86	0.89	0.89	0.92	0.88	0.03
CaO	1.95	2.05	2.07	2.02	1.99	2.09	2.06	2.07	2.10	2.08	2.05	0.05
Na2O	9.50	9.50	9.50	9.50	9.50	9.50	9.50	9.50	9.50	9.50	9.50	0.00
K2O	5.58	5.59	5.71	5.69	5.63	5.60	5.54	5.71	5.65	5.62	5.63	0.06
P2O5	0.30	0.32	0.25	0.24	0.37	0.28	0.34	0.24	0.26	0.31	0.29	0.05
F (ppm)	3452	1965	938	2265	427	1883	1264	835	2510	2486	1802	931
SO2	0.11	0.10	0.10	0.05	0.10	0.07	0.06	0.07	0.07	0.07	0.08	0.02
Cl (ppm)	1495	1627	1411	1577	1569	1743	1545	1428	1285	1392	1507	133
Total	100.06	100.06	100.04	99.93	100.07	100.04	100.05	100.06	99.99	100.01	100.03	

Table C3.11.3 Microprobe data for sample EBT-16 corrected for Sodium loss

Analysis	1	2	3	4	5	6	7	8	9	10	Mean	StdDev
Correction	0.99672	0.99845	0.99691	0.99772	0.99833	1.00035	0.99917	0.96067	0.99769	0.99966		
SiO2	54.84	54.85	55.08	54.89	54.97	55.55	54.65	53.71	54.84	54.89	54.95	0.27
TiO2	1.06	1.08	1.14	1.18	1.11	1.12	1.13	1.04	1.09	1.05	1.11	0.04
Al2O3	19.46	19.76	19.59	19.81	19.87	19.80	19.58	19.01	19.88	19.75	19.70	0.14
Fe	5.76	5.68	5.65	5.60	5.67	5.69	5.98	5.46	5.60	5.71	5.71	0.12
MnO	0.20	0.25	0.26	0.10	0.22	0.26	0.26	0.14	0.23	0.26	0.23	0.05
MgO	0.88	0.93	0.82	0.90	0.91	1.00	0.95	0.88	0.95	0.90	0.92	0.06
CaO	2.04	1.98	2.02	2.03	2.01	1.97	2.15	1.84	2.07	2.02	2.03	0.06
Na2O	9.16	9.16	9.16	9.16	9.16	9.16	9.16	9.16	9.16	9.16	9.16	0.00
K2O	5.79	5.58	5.55	5.58	5.50	4.85	5.38	7.42	5.40	5.54	5.46	0.28
P2O5	0.23	0.30	0.25	0.28	0.31	0.22	0.34	0.29	0.27	0.29	0.27	0.04
F (ppm)	3814	2073	2569	2283	286	1633	1795	11823	3229	2312	2463	733
SO2	0.08	0.08	0.09	0.09	0.07	0.05	0.10	0.06	0.08	0.08	0.08	0.01
Cl (ppm)	1530	1597	1461	1684	1739	1623	1541	1590	1493	1307	1530	115
Total	100.03	100.01	100.03	100.02	100.02	100.00	100.01	100.36	100.02	100.00	100.02	100.02

Table C3.12.1 Raw microprobe data for sample EBT-17

Analysis	1	2	3	4	5	6	7	8	9	10
SiO2	56.21	55.97	56.72	55.36	57.36	57.89	57.47	56.42	56.96	55.54
TiO2	1.15	1.07	0.99	1.08	1.20	1.07	1.11	1.07	1.12	1.11
Al2O3	20.41	20.23	20.42	20.32	20.44	20.70	20.27	19.90	20.25	20.13
FeO	5.59	5.56	5.30	5.42	5.68	5.28	5.65	5.52	5.58	5.49
MnO	0.25	0.26	0.22	0.21	0.31	0.25	0.24	0.30	0.31	0.27
MgO	0.94	0.88	0.91	0.91	0.86	0.87	0.94	0.93	0.92	0.91
CaO	2.01	1.98	2.00	1.90	2.07	1.92	1.92	1.92	1.85	1.81
Na2O	8.47	7.69	8.42	7.90	8.42	9.10	7.68	8.57	8.66	7.94
K2O	5.49	5.65	5.65	5.51	5.52	5.64	5.72	5.50	5.45	5.54
P2O5	0.20	0.26	0.29	0.20	0.44	0.29	0.29	0.40	0.27	0.40
F (ppm)	560	1400	2180	3140	840	1370	n.d.	960	3110	8930
SO2	0.05	0.09	0.07	0.05	0.08	0.08	0.08	0.07	0.06	0.06
Cl (ppm)	1530	1750	1610	1670	1650	1610	1590	1610	1730	1340
Total	100.97	99.935	101.349	99.336	102.627	103.371	101.528	100.844	101.912	100.24

Table C3.12.2 Microprobe data for sample EBT-17 corrected to 100%

Analysis	1*	2	3	4	5	6	7*	8	9	10
SiO2	55.52	56.01	55.96	55.73	55.89	56.00	56.42	55.81	55.89	55.41
TiO2	1.13	1.07	0.97	1.09	1.17	1.03	1.09	1.06	1.10	1.11
Al2O3	20.16	20.24	20.14	20.46	19.91	20.03	19.90	19.69	19.87	20.08
FeO	5.52	5.56	5.23	5.46	5.53	5.11	5.55	5.46	5.48	5.48
MnO	0.25	0.26	0.22	0.21	0.31	0.24	0.24	0.30	0.31	0.27
MgO	0.92	0.88	0.89	0.91	0.84	0.84	0.92	0.92	0.90	0.91
CaO	1.99	1.98	1.98	1.91	2.02	1.86	1.88	1.90	1.82	1.80
Na2O	8.36	7.70	8.31	7.96	8.20	8.80	7.54	8.48	8.50	7.92
K2O	5.43	5.65	5.58	5.54	5.38	5.45	5.62	5.44	5.35	5.53
P2O5	0.20	0.26	0.29	0.20	0.43	0.28	0.29	0.40	0.26	0.40
F (ppm)	3319	1401	2151	3161	818	1325	3299	3324	3052	8909
SO2	0.05	0.09	0.07	0.05	0.08	0.07	0.07	0.07	0.05	0.06
Cl (ppm)	1511	1751	1589	1661	1608	1557	1561	1593	1698	1337
Total	100.00	100.00	100.00	100.00	100.00	100.00	100.00	100.00	100.00	100.00

*Flourine corrected to an average of 3355 ppm

Table C3.12.3 Microprobe data for sample EBT-17 corrected for Sodium loss

Analysis	1	2	3	4	5	6	7	8	9	10	Mean	StdDev
Correction	0.99712	0.99055	0.99659	0.99311	0.99555	1.00154	0.98901	0.99826	0.99847	0.99274		
SiO2	55.36	55.48	55.77	55.34	55.64	56.08	55.80	55.71	55.80	55.01	55.53	0.29
TiO2	1.13	1.06	0.97	1.08	1.16	1.04	1.08	1.06	1.10	1.10	1.07	0.05
Al2O3	20.10	20.05	20.08	20.32	19.82	20.06	19.68	19.65	19.84	19.94	19.96	0.23
FeO	5.50	5.51	5.21	5.42	5.51	5.12	5.49	5.45	5.47	5.44	5.44	0.10
MnO	0.25	0.25	0.21	0.21	0.30	0.24	0.23	0.30	0.30	0.26	0.25	0.03
MgO	0.92	0.87	0.89	0.91	0.83	0.84	0.91	0.91	0.90	0.90	0.90	0.01
CaO	1.98	1.97	1.97	1.90	2.01	1.86	1.86	1.90	1.81	1.79	1.90	0.07
Na2O	8.65	8.65	8.65	8.65	8.65	8.65	8.65	8.65	8.65	8.65	8.65	0.00
K2O	5.41	5.60	5.56	5.50	5.36	5.46	5.55	5.43	5.34	5.49	5.49	0.09
P2O5	0.20	0.25	0.28	0.19	0.43	0.28	0.28	0.40	0.26	0.40	0.28	0.08
F (ppm)	3309	1388	2144	3139	815	1327	3262	3318	3047	8844	3556	2245
SO2	0.05	0.09	0.07	0.05	0.08	0.07	0.07	0.07	0.05	0.06	0.06	0.01
Cl (ppm)	1507	1735	1583	1670	1601	1560	1544	1590	1695	1327	1581	129
Total	100.02	100.08	100.03	100.06	100.04	99.99	100.10	100.02	100.01	100.06	100.05	

Table C3.13.3 Microprobe data for sample EBT-18 corrected for sodium loss

Analysis	1	2	3	4	5	6	7	8	9	10	Mean	StdDev
Correction	0.99742	0.99878	0.99870	0.99578	0.99754	0.99975	1.00043	0.99956	0.99731	0.99744		
SiO2	55.26	55.13	55.30	55.05	55.06	54.94	55.02	55.48	55.02	55.12	55.14	0.16
TiO2	1.01	0.97	1.11	1.05	1.01	1.01	1.08	1.12	1.05	1.02	1.04	0.05
Al2O3	19.72	19.62	19.63	19.70	19.63	19.76	19.64	19.78	19.68	19.88	19.70	0.08
FeO	5.52	5.56	5.43	5.57	5.68	5.62	5.75	5.36	5.68	5.65	5.58	0.12
MnO	0.26	0.28	0.27	0.36	0.27	0.28	0.19	0.27	0.30	0.33	0.28	0.05
MgO	0.87	0.90	0.87	0.87	0.87	0.89	0.93	0.86	0.92	0.86	0.88	0.02
CaO	1.83	1.90	1.88	1.79	1.82	1.88	1.86	1.83	2.00	1.92	1.87	0.06
Na2O	9.15	9.15	9.15	9.15	9.15	9.15	9.15	9.15	9.15	9.15	9.15	0.00
K2O	5.68	5.66	5.69	5.68	5.71	5.69	5.67	5.56	5.59	5.37	5.63	0.10
P2O5	0.24	0.35	0.36	0.32	0.27	0.30	0.28	0.24	0.29	0.35	0.30	0.05
F (ppm)	2715	2634	786	2317	3339	2784	1912	1245	1080	1556	2037	850
SO2	0.06	0.07	0.08	0.08	0.06	0.06	0.08	0.08	0.08	0.09	0.07	0.01
Cl (ppm)	1518	1611	1723	1889	1549	1538	1700	1720	1751	1385	1638	146
Total	100.02	100.01	100.01	100.04	100.02	100.00	100.00	100.00	100.02	100.02	100.02	100.02

Table C3.14.3 Microprobe data for sample EBT-19 corrected for sodium loss

Analysis	1	2	3	4	5	6	7	8	9	10	Mean	StdDev
Correction	0.99612	1.0010396	0.99713	0.99010	0.99787	0.99228	0.99728	0.99320	0.99727	0.998962		
SiO2	55.43	56.14	55.23	55.98	55.74	55.08	55.63	55.51	55.67	55.50	55.59	0.32
TiO2	1.02	1.01	0.99	1.04	1.07	1.02	1.01	0.99	1.08	1.01	1.02	0.03
Al2O3	19.96	19.68	19.98	19.82	19.68	20.12	19.75	19.89	19.84	20.02	19.87	0.15
FeO	5.46	5.43	5.41	5.44	5.49	5.62	5.65	5.62	5.53	5.62	5.53	0.09
MnO	0.26	0.18	0.31	0.23	0.25	0.33	0.28	0.23	0.23	0.26	0.26	0.04
MgO	0.86	0.86	0.90	0.85	0.86	0.88	0.86	0.83	0.83	0.92	0.86	0.03
CaO	1.91	1.79	1.83	1.80	1.86	1.81	1.83	1.78	1.81	1.78	1.82	0.04
Na2O	8.84	8.84	8.84	8.84	8.84	8.84	8.84	8.84	8.84	8.84	8.84	0.00
K2O	5.50	5.47	5.62	5.48	5.59	5.57	5.45	5.53	5.47	5.46	5.51	0.06
P2O5	0.23	0.28	0.34	0.26	0.29	0.31	0.22	0.32	0.20	0.27	0.27	0.05
F (ppm)	3366	1094	3005	1168	1143	2298	2596	3233	2676	982	2156	963
SO2	0.08	0.07	0.09	0.06	0.06	0.11	0.07	0.06	0.07	0.09	0.08	0.02
Cl (ppm)	1481	1400	1696	1796	1754	1638	1852	1429	1843	1563	1645	170
Total	100.03	99.99	100.03	100.09	100.02	100.07	100.02	100.06	100.02	100.01	100.03	

Table C3.15.3 Microprobe data for sample EBT-21 corrected for sodium loss

Analysis	1	2	3	4	5	6	7	8	9	10	Mean	StdDev
Correction	1.00118	0.996569	0.9931595	0.9994985	0.997034	0.9951471	1.0053252	0.9981832	0.992999	1.001823		
SiO2	54.86	54.10	54.29	54.55	53.62	54.54	53.80	54.42	54.27	54.07	54.23	0.26
TiO2	1.08	1.05	1.05	1.10	1.13	1.05	1.11	1.05	0.99	0.98	1.04	0.05
Al2O3	19.83	19.89	19.83	19.06	20.37	19.71	20.00	19.98	20.05	19.81	19.90	0.13
FeO	5.51	5.61	5.40	5.78	5.64	5.65	5.52	5.54	5.49	5.56	5.53	0.08
MnO	0.17	0.23	0.34	0.19	0.15	0.30	0.26	0.24	0.29	0.28	0.28	0.03
MgO	0.83	0.96	0.89	0.96	0.91	0.90	0.89	0.89	0.89	0.91	0.89	0.01
CaO	1.70	2.09	2.14	2.08	1.99	2.01	1.98	2.09	1.98	2.19	2.07	0.09
Na2O	9.67	9.67	9.67	9.67	9.67	9.67	9.67	9.67	9.67	9.67	9.67	0.00
K2O	5.64	5.59	5.61	5.83	5.66	5.53	5.88	5.42	5.68	5.55	5.61	0.16
P2O5	0.28	0.33	0.29	0.36	0.32	0.28	0.25	0.34	0.35	0.40	0.32	0.06
F (ppm)	2401	2961	2371	1188	3694	1642	3595	1504	1900	3215	2371	862
SO2	0.03	0.07	0.11	0.11	0.05	0.10	0.08	0.07	0.08	0.09	0.09	0.01
Cl (ppm)	1420	1620	1939	1850	1510	1512	1422	1374	1423	1449	1520	210
Total	99.99	100.03	100.07	100.00	100.03	100.05	99.95	100.02	100.07	99.98	100.02	

Table C3.16.3 Microprobe data for sample EBT-22 corrected for sodium loss

Analysis	1	2	3	4	5	6	7	8	9	10	Mean	StdDev
Correction	1.02809	0.98210	0.99830	1.01119	0.99878	0.99579	0.99627	0.99854	1.07315	1.00122		
SiO2	54.94	54.66	54.54	53.76	54.79	54.22	54.85	54.36	53.19	54.49	54.49	0.37
TiO2	0.97	1.06	1.09	1.06	1.10	1.04	1.01	1.02	1.09	1.04	1.05	0.03
Al2O3	19.85	19.90	20.00	20.22	19.97	19.91	19.79	19.93	20.52	20.04	19.98	0.13
Fe	5.48	5.52	5.59	5.73	5.36	5.92	5.40	5.55	5.62	5.48	5.52	0.12
MnO	0.29	0.27	0.17	0.28	0.32	0.30	0.26	0.31	0.34	0.25	0.26	0.05
MgO	0.81	0.92	0.86	0.92	0.89	0.88	0.88	0.93	0.95	0.92	0.90	0.03
CaO	1.89	2.17	1.95	2.09	2.00	2.09	1.96	1.87	1.96	2.04	2.01	0.10
Na2O	9.39	9.39	9.39	9.39	9.39	9.39	9.39	9.39	9.39	9.39	9.39	0.00
K2O	5.50	5.58	5.66	5.66	5.51	5.46	5.61	5.79	5.59	5.58	5.63	0.09
P2O5	0.21	0.25	0.28	0.36	0.25	0.28	0.33	0.33	0.32	0.30	0.30	0.04
F (ppm)	1691	2253	2297	1931	1972	3582	3188	2913	1257	1814	2338	522
SO2	0.10	0.08	0.09	0.10	0.08	0.06	0.09	0.09	0.07	0.09	0.09	0.01
Cl (ppm)	1474	1512	1748	1441	1509	1394	1619	1601	1576	1904	1619	160
Total	99.74	100.17	100.02	99.89	100.01	100.04	100.03	100.01	99.31	99.99	100.02	

Table C3.17.3 Microprobe data for sample EBT-23a corrected for sodium loss

Analysis	1	2	3	4	5	6	7	8	9	10	Mean	StdDev
Correction	0.99387	1.00261	0.99495	0.99360	0.99741	0.99186	0.99461	0.99461	1.01058	0.99539		
SiO2	54.63	54.35	54.23	54.37	54.13	54.72	53.95	54.68	54.34	54.54	54.44	0.21
TiO2	0.99	1.11	1.08	1.13	1.10	1.09	1.11	1.00	1.07	1.11	1.08	0.05
Al2O3	19.75	19.82	19.82	19.83	19.97	19.61	20.30	19.88	19.73	19.86	19.81	0.10
FeO	5.64	5.43	5.68	5.64	5.52	5.55	5.58	5.43	5.52	5.52	5.55	0.09
MnO	0.14	0.27	0.30	0.20	0.22	0.20	0.18	0.22	0.19	0.14	0.21	0.05
MgO	0.92	0.92	0.88	0.91	0.95	0.96	0.87	0.90	0.96	0.86	0.92	0.03
CaO	2.09	2.13	2.05	2.03	2.07	2.08	2.02	2.02	2.17	2.06	2.08	0.05
Na2O	9.61	9.61	9.61	9.61	9.61	9.61	9.61	9.61	9.61	9.61	9.61	0.00
K2O	5.44	5.54	5.59	5.55	5.71	5.59	5.66	5.54	5.42	5.43	5.53	0.09
P2O5	0.32	0.34	0.27	0.29	0.32	0.29	0.29	0.31	0.33	0.27	0.30	0.02
F (ppm)	2859	2315	3018	2702	1959	1465	2368	2268	3582	4288	2717	854
SO2	0.11	0.08	0.11	0.09	0.08	0.08	0.09	0.08	0.07	0.09	0.09	0.01
Cl (ppm)	1221	1441	1225	1376	1350	1445	1474	1522	1314	1286	1353	103
Total	100.06	99.97	100.05	100.06	100.02	100.08	100.05	100.05	99.90	100.04	100.03	

Table C3.18.3 Microprobe data for sample EBT-23b corrected for sodium loss

Analysis	1	2	3	4	5	6	7	8	9	10	Mean	StdDev
Correction	0.997481	0.9958329	1.0025356	0.9970929	0.9956371	0.9934696	0.9960445	0.9975745	0.994725	0.9933313		
SiO2	54.21	54.53	53.98	53.70	54.49	54.60	53.69	53.75	54.28	54.39	54.16	0.36
TiO2	1.11	1.07	1.14	1.06	1.13	1.01	1.10	1.15	1.08	1.12	1.10	0.04
Al2O3	19.94	19.77	20.17	20.47	19.71	19.87	20.16	20.29	19.89	19.85	20.01	0.25
FeO	5.58	5.56	5.47	5.55	5.59	5.47	5.64	5.74	5.70	5.55	5.59	0.09
MnO	0.28	0.30	0.27	0.19	0.22	0.27	0.19	0.19	0.30	0.21	0.24	0.05
MgO	0.91	0.89	0.92	0.86	0.96	0.86	0.91	0.90	0.96	0.84	0.90	0.04
CaO	2.08	2.15	2.09	2.16	2.14	2.03	2.12	2.12	2.03	2.19	2.11	0.05
Na2O	9.59	9.59	9.59	9.59	9.59	9.59	9.59	9.59	9.59	9.59	9.59	0.00
K2O	5.57	5.53	5.49	5.54	5.56	5.45	5.84	5.55	5.44	5.52	5.55	0.11
P2O5	0.30	0.26	0.40	0.31	0.27	0.36	0.33	0.34	0.34	0.30	0.32	0.04
F (ppm)	2287	1562	1897	3274	1028	2708	2504	1347	2631	2437	2167	695
SO2	0.07	0.08	0.13	0.09	0.12	0.12	0.10	0.11	0.05	0.10	0.10	0.02
Cl (ppm)	1535	1502	1402	1733	1617	1690	1302	1570	1380	1625	1536	140
Total	100.02	100.04	99.98	100.03	100.04	100.06	100.04	100.02	100.05	100.06	100.03	

Table C3.19.1 Raw microprobe data for sample EBT-30

Analysis	1	2	3	4	5	6	7	8	9	10
SiO2	54.89	54.90	53.02	54.08	55.34	54.57	54.11	53.73	54.14	54.97
TiO2	1.02	1.08	0.98	0.98	1.06	1.07	0.96	1.04	1.09	1.06
Al2O3	20.17	19.95	20.08	19.78	20.40	19.98	20.45	19.97	19.80	20.30
FeO	5.46	5.43	5.53	5.43	5.49	5.48	5.59	5.50	5.46	5.56
MnO	0.20	0.21	0.24	0.19	0.26	0.20	0.27	0.18	0.22	0.23
MgO	0.86	0.87	0.86	0.91	0.93	0.85	0.92	0.85	0.08	0.91
CaO	2.00	2.10	2.05	2.05	2.04	2.07	2.08	2.02	2.07	2.10
Na2O	8.85	9.05	9.35	9.09	9.02	9.04	8.91	9.12	9.04	8.93
K2O	5.57	5.56	5.59	5.66	5.53	5.62	5.69	5.62	5.57	5.55
P2O5	0.27	0.30	0.26	0.22	0.24	0.29	0.22	0.29	0.31	0.35
F (ppm)	2010	2010	3120	1130	2460	130	2960	1360	2490	1640
SO2	0.07	0.10	0.08	0.10	0.12	0.05	0.08	0.07	0.06	0.08
Cl (ppm)	1190	1420	1380	1500	1440	1320	1650	1530	1490	1470
Total	99.67	99.89	98.48	98.76	100.81	99.38	99.73	98.67	98.23	100.33

Table C3.19.2 Microprobe data for sample EBT-30 corrected to 100%

Analysis	1	2	3	4	5	6*	7	8	9	10
SiO2	55.07	54.97	53.83	54.76	54.89	54.80	54.26	54.45	55.11	54.79
TiO2	1.03	1.08	0.99	0.99	1.05	1.08	0.96	1.05	1.11	1.05
Al2O3	20.24	19.97	20.39	20.03	20.24	20.07	20.50	20.24	20.15	20.23
FeO	5.48	5.44	5.62	5.50	5.45	5.51	5.61	5.57	5.55	5.54
MnO	0.20	0.21	0.24	0.19	0.25	0.20	0.27	0.18	0.23	0.23
MgO	0.87	0.87	0.87	0.92	0.92	0.86	0.92	0.86	0.08	0.91
CaO	2.01	2.10	2.08	2.08	2.02	2.08	2.08	2.05	2.11	2.09
Na2O	8.88	9.06	9.49	9.20	8.95	9.07	8.93	9.24	9.20	8.90
K2O	5.58	5.57	5.68	5.73	5.48	5.65	5.70	5.69	5.67	5.54
P2O5	0.27	0.30	0.27	0.22	0.24	0.29	0.22	0.29	0.32	0.35
F (ppm)	2017	2012	3168	1144	2440	2139	2968	1378	2535	1635
SO2	0.07	0.10	0.08	0.10	0.12	0.05	0.08	0.07	0.06	0.08
Cl (ppm)	1194	1422	1401	1519	1428	1326	1654	1551	1517	1465
Total	100.00	100.00	100.00	100.00	100.00	100.00	100.00	100.00	100.00	100.00

*Fluorine corrected to an average of 2130 ppm

Table C3.19.3 Microprobe data for sample EBT-30 corrected for sodium loss

Analysis	1	2	3	4	5	6	7	8	9	10	Mean	StdDev
Correction	0.99628	0.99810	1.00243	0.99950	0.99699	0.99823	0.99679	0.99888	0.99952	0.996455		
SiO2	54.87	54.86	53.96	54.73	54.73	54.70	54.08	54.44	55.08	54.59	54.61	0.35
TiO2	1.02	1.07	0.99	0.99	1.05	1.07	0.96	1.05	1.11	1.05	1.04	0.05
Al2O3	20.16	19.94	20.44	20.02	20.17	20.03	20.43	20.23	20.14	20.16	20.17	0.16
FeO	5.45	5.43	5.63	5.50	5.43	5.50	5.59	5.57	5.55	5.52	5.52	0.07
MnO	0.19	0.21	0.24	0.19	0.25	0.20	0.27	0.18	0.23	0.23	0.22	0.03
MgO	0.86	0.87	0.88	0.92	0.91	0.86	0.92	0.86	0.08	0.90	0.81	0.26
CaO	2.00	2.10	2.09	2.08	2.01	2.08	2.08	2.05	2.11	2.09	2.07	0.04
Na2O	9.25	9.25	9.25	9.25	9.25	9.25	9.25	9.25	9.25	9.25	9.25	0.00
K2O	5.56	5.55	5.69	5.73	5.47	5.64	5.68	5.69	5.67	5.52	5.62	0.09
P2O5	0.27	0.30	0.27	0.22	0.24	0.29	0.22	0.29	0.32	0.34	0.28	0.04
F (ppm)	2009	2008	3176	1144	2433	2135	2958	1378	2534	1629	2140	654
SO2	0.07	0.09	0.08	0.10	0.12	0.05	0.08	0.07	0.06	0.08	0.08	0.02
Cl (ppm)	1190	1419	1405	1518	1424	1323	1649	1550	1516	1460	1445	127
Total	100.03	100.02	99.98	100.00	100.03	100.02	100.03	100.00	100.00	100.03	100.01	

Table C3.20.3 Microprobe data for sample EBT-32 corrected for sodium loss

Analysis	1	2	3	4	5	6	7	8	9	10	Mean	StdDev
Correction	0.993492	0.9981797	0.99588	0.99523	0.99976	0.99371	0.99765	0.99577	1.00024	0.994669		
SiO2	55.30	55.18	54.75	55.26	55.04	54.87	55.13	55.54	54.78	54.82	55.07	0.26
TiO2	1.11	1.08	1.09	1.17	1.11	1.09	1.07	1.01	1.09	1.07	1.09	0.04
Al2O3	19.68	19.87	19.83	19.63	19.51	19.98	19.75	19.76	19.92	19.68	19.76	0.14
FeO	5.30	5.61	5.76	5.77	5.80	5.56	5.65	5.50	5.73	5.97	5.67	0.19
MnO	0.24	0.13	0.27	0.25	0.29	0.23	0.21	0.23	0.20	0.28	0.23	0.05
MgO	0.94	0.91	0.90	0.92	0.92	0.94	0.89	0.84	0.92	0.89	0.91	0.03
CaO	2.06	1.97	2.08	1.97	1.99	2.02	2.05	1.81	2.06	1.98	2.00	0.08
Na2O	9.10	9.10	9.10	9.10	9.10	9.10	9.10	9.10	9.10	9.10	9.10	0.00
K2O	5.49	5.48	5.62	5.39	5.46	5.47	5.44	5.54	5.44	5.37	5.47	0.07
P2O5	0.31	0.23	0.27	0.26	0.30	0.28	0.26	0.31	0.31	0.29	0.28	0.03
F (ppm)	2878	2256	1349	993	2779	2776	2641	1488	2056	3413	2263	779
SO2	0.08	0.09	0.08	0.08	0.08	0.10	0.06	0.07	0.08	0.08	0.08	0.01
Cl (ppm)	1615	1431	1459	1400	1474	1568	1485	1709	1593	1641	1537	102
Total	100.06	100.02	100.04	100.04	100.00	100.06	100.02	100.04	100.00	100.05	100.03	

Table C3.21.3 Microprobe data for sample EBT-32a corrected for sodium loss

Analysis	1	2	3	4	5	6	7	8	9	10	Mean	StdDev
Correction	0.994894	0.99582	0.99618	0.99470	0.99928	0.99785	1.00024	0.99686	0.99976	0.995421		
SiO2	55.26	55.17	55.07	54.98	55.13	55.18	54.66	55.30	55.21	55.09	55.10	0.18
TiO2	1.02	1.03	1.09	1.10	1.05	1.15	1.16	1.05	1.08	1.16	1.09	0.05
Al2O3	19.85	19.94	19.89	19.49	19.56	19.61	19.81	19.68	19.90	20.04	19.78	0.18
FeO	5.55	5.70	5.58	5.78	5.74	5.57	5.81	5.70	5.47	5.66	5.66	0.11
MnO	0.23	0.24	0.24	0.26	0.25	0.23	0.22	0.26	0.25	0.19	0.24	0.02
MgO	0.95	0.88	0.88	0.91	0.90	0.86	0.92	0.90	0.92	0.90	0.90	0.02
CaO	1.96	2.01	1.97	2.01	2.05	2.05	2.05	1.97	1.97	1.95	2.00	0.04
Na2O	9.03	9.03	9.03	9.03	9.03	9.03	9.03	9.03	9.03	9.03	9.03	0.00
K2O	5.46	5.44	5.52	5.51	5.55	5.62	5.53	5.49	5.49	5.32	5.49	0.08
P2O5	0.28	0.25	0.27	0.34	0.34	0.32	0.34	0.30	0.28	0.25	0.30	0.03
F (ppm)	1834	926	2572	4040	1696	1525	2208	1027	1850	1975	1965	881
SO2	0.07	0.08	0.09	0.07	0.10	0.09	0.10	0.10	0.07	0.07	0.08	0.01
Cl (ppm)	2022	1723	1425	1548	1387	1485	1532	1396	1658	1814	1599	206
Total	100.05	100.04	100.03	100.05	100.01	100.02	100.00	100.03	100.00	100.04	100.03	

Table C3.22.1 Raw microprobe data for sample EBT-33

Analysis	1	2	3	4	5	6	7	8	9	10
SiO2	57.22	55.69	56.99	57.25	56.88	57.19	57.30	55.83	57.70	56.37
TiO2	1.11	1.22	1.16	1.12	1.09	1.09	1.12	1.06	1.17	1.26
Al2O3	20.43	20.48	20.39	20.23	20.34	20.36	20.51	20.17	20.68	20.69
FeO	5.75	5.56	5.58	5.62	5.62	5.61	5.57	5.55	5.57	5.61
MnO	0.18	0.20	0.27	0.32	0.23	0.13	0.17	0.38	0.19	0.29
MgO	0.96	1.03	0.94	0.20	0.89	0.91	0.95	0.95	0.97	0.99
CaO	2.11	2.00	2.01	2.05	2.03	2.04	1.99	2.07	2.02	2.03
Na2O	7.86	8.30	9.11	7.88	8.98	8.42	8.55	8.95	7.97	8.27
K2O	5.49	5.67	5.15	5.53	5.66	5.57	5.66	5.43	5.49	5.52
P2O5	0.32	0.32	0.27	0.34	0.30	0.35	0.32	0.33	0.21	0.37
F (ppm)	1950	2880	1740	1700	3030	1440	2610	3400	2590	n.d.
SO2	0.08	0.09	0.09	0.10	0.05	0.09	0.09	0.09	0.09	0.08
Cl (ppm)	1800	1680	1670	2090	1820	1940	1920	2170	1960	1940
Total	101.87	100.99	102.31	100.99	102.54	102.11	102.67	101.37	102.50	101.67

Table C3.22.2 Microprobe data for sample EBT-33 corrected to 100%

Analysis	1	2	3	4	5	6	7	8	9	10*
SiO2	56.17	55.14	55.71	56.68	55.46	56.01	55.81	55.08	56.30	55.31
TiO2	1.09	1.21	1.13	1.11	1.07	1.07	1.09	1.04	1.14	1.24
Al2O3	20.05	20.28	19.93	20.03	19.83	19.94	19.97	19.89	20.18	20.30
FeO	5.65	5.50	5.46	5.56	5.48	5.49	5.42	5.47	5.43	5.50
MnO	0.17	0.19	0.26	0.31	0.22	0.13	0.16	0.38	0.19	0.28
MgO	0.94	1.02	0.92	0.19	0.86	0.89	0.93	0.94	0.94	0.97
CaO	2.07	1.98	1.97	2.03	1.98	2.00	1.94	2.04	1.97	1.99
Na2O	7.71	8.22	8.91	7.80	8.76	8.25	8.33	8.83	7.77	8.11
K2O	5.39	5.61	5.03	5.47	5.52	5.46	5.51	5.36	5.35	5.42
P2O5	0.31	0.32	0.26	0.34	0.29	0.34	0.31	0.32	0.20	0.36
F (ppm)	1914	2852	1701	1683	2955	1410	2542	3354	2527	2433
SO2	0.08	0.09	0.09	0.10	0.05	0.08	0.08	0.09	0.09	0.08
Cl (ppm)	1767	1663	1632	2070	1775	1900	1870	2141	1912	1904
Total	100.00	100.00	100.00	100.00	100.00	100.00	100.00	100.00	100.00	100.00

*Flourine corrected to an average of 2483 ppm

Table C3.22.3 Microprobe data for sample EBT-33 corrected for sodium loss

Analysis	1	2	3	4	5	6	7	8	9	10	Mean	StdDev
Correction	0.991941	0.99697	1.00386	0.99283	1.00239	0.99724	0.99808	1.00304	0.99254	0.995892		
SiO2	55.71	54.97	55.92	56.28	55.60	55.86	55.71	55.25	55.88	55.08	55.46	0.54
TiO2	1.08	1.20	1.13	1.10	1.07	1.07	1.09	1.04	1.13	1.24	1.13	0.08
Al2O3	19.89	20.22	20.01	19.88	19.88	19.89	19.94	19.96	20.03	20.22	20.03	0.17
FeO	5.60	5.48	5.48	5.52	5.50	5.48	5.41	5.49	5.39	5.48	5.51	0.05
MnO	0.17	0.19	0.26	0.31	0.22	0.13	0.16	0.38	0.19	0.28	0.27	0.08
MgO	0.93	1.01	0.92	0.19	0.87	0.89	0.92	0.94	0.94	0.96	0.81	0.35
CaO	2.05	1.97	1.98	2.02	1.98	1.99	1.93	2.05	1.95	1.98	2.01	0.04
Na2O	8.52	8.52	8.52	8.52	8.52	8.52	8.52	8.52	8.52	8.52	8.52	0.00
K2O	5.35	5.59	5.05	5.44	5.53	5.44	5.50	5.37	5.31	5.40	5.43	0.10
P2O5	0.31	0.32	0.26	0.34	0.29	0.34	0.31	0.33	0.20	0.36	0.33	0.02
F (ppm)	1899	2843	1707	1671	2962	1406	2537	3364	2508	2423	2440	689
SO2	0.08	0.09	0.09	0.09	0.05	0.08	0.08	0.09	0.09	0.08	0.09	0.01
Cl (ppm)	1753	1658	1639	2055	1779	1895	1866	2147	1898	1896	1902	203
Total	100.07	100.03	99.97	100.06	99.98	100.02	100.02	99.97	100.06	100.04	100.03	

Table C3.23.3 Microprobe data for sample EBT-34 corrected for sodium loss

Analysis	1	2	3	4	5	6	7	8	9	10	Mean	StdDev
Correction	0.99680	0.99756	1.00132	0.9930202	0.99584	1.00445	0.99505	0.99378	1.00246	1.00020		
SiO2	55.22	55.46	55.93	55.72	55.49	55.98	55.66	55.32	55.23	55.88	55.43	0.17
TiO2	1.04	1.04	1.07	1.11	1.16	1.05	1.17	1.04	1.07	1.18	1.10	0.07
Al2O3	20.70	20.10	20.10	19.98	20.06	19.74	20.16	20.39	20.46	19.87	20.23	0.18
FeO	5.28	5.63	5.34	5.47	5.48	5.46	5.48	5.51	5.59	5.63	5.54	0.07
MnO	0.26	0.28	0.35	0.30	0.26	0.29	0.12	0.17	0.20	0.31	0.21	0.07
MgO	0.91	0.96	0.89	0.95	0.97	0.97	0.96	0.96	0.97	0.94	0.96	0.01
CaO	2.04	2.05	1.90	2.06	2.04	2.01	2.01	1.92	1.90	1.93	1.98	0.07
Na2O	8.29	8.29	8.29	8.29	8.29	8.29	8.29	8.29	8.29	8.29	8.29	0.00
K2O	5.41	5.40	5.50	5.47	5.42	5.30	5.35	5.48	5.36	5.39	5.40	0.06
P2O5	0.23	0.35	0.32	0.33	0.30	0.31	0.33	0.24	0.35	0.23	0.32	0.05
F (ppm)	2274	2205	500	1313	2733	3258	2438	4676	2985	1013	3007	978
SO2	0.10	0.08	0.10	0.08	0.08	0.08	0.09	0.09	0.08	0.11	0.08	0.00
Cl (ppm)	3161	1464	1588	1605	1901	1458	1774	1684	1691	1461	1703	160
Total	100.03	100.02	99.99	100.06	100.03	99.96	100.04	100.05	99.98	100.00	100.03	

Table C3.24.1 Raw microprobe data for sample EBT-34a

Analysis	1	2	3	4	5	6	7	8	9	10
SiO ₂	56.58	55.74	56.90	57.27	57.44	57.27	56.67	55.97	57.72	56.61
TiO ₂	1.13	1.08	1.09	1.10	1.13	1.11	1.17	1.14	1.02	1.09
Al ₂ O ₃	20.46	20.40	20.32	20.45	20.49	20.48	20.43	20.39	20.83	22.45
FeO	5.60	5.35	5.58	5.54	5.65	5.55	5.69	5.36	5.41	5.63
MnO	0.29	0.20	0.36	0.27	0.21	0.18	0.15	0.15	0.30	0.18
MgO	0.89	0.96	0.93	0.94	0.93	0.93	0.96	0.90	0.97	0.96
CaO	1.98	2.06	2.05	2.01	2.00	2.11	2.09	2.03	2.00	2.01
Na ₂ O	8.96	8.88	8.29	7.90	8.01	7.86	8.50	9.16	7.61	8.72
K ₂ O	5.64	5.63	5.66	5.47	5.45	5.46	5.43	5.66	5.52	5.34
P ₂ O ₅	0.22	0.28	0.34	0.30	0.32	0.34	0.26	0.34	0.26	0.29
F (ppm)	2000	2750	1570	1980	2160	1830	1090	2150	n.d.	2470
SO ₂	0.07	0.06	0.08	0.10	0.06	0.09	0.09	0.11	0.08	0.09
Cl (ppm)	1570	1560	2780	1820	1780	2030	1400	3210	1570	1770
Total	102.18	101.07	102.04	101.70	102.08	101.76	101.68	101.73	101.86	103.78

Table C3.24.2 Microprobe data for sample EBT-34a corrected to 100%

Analysis	1	2	3	4	5	6	7	8	9*	10
SiO ₂	55.38	55.15	55.76	56.31	56.27	56.28	55.73	55.01	56.55	54.55
TiO ₂	1.10	1.07	1.07	1.08	1.11	1.09	1.15	1.12	1.00	1.05
Al ₂ O ₃	20.03	20.18	19.91	20.10	20.08	20.13	20.09	20.04	20.41	21.63
FeO	5.48	5.29	5.47	5.45	5.54	5.46	5.59	5.27	5.30	5.42
MnO	0.28	0.20	0.35	0.26	0.21	0.18	0.15	0.15	0.30	0.18
MgO	0.87	0.95	0.91	0.92	0.91	0.91	0.94	0.89	0.95	0.93
CaO	1.94	2.04	2.01	1.97	1.96	2.08	2.06	1.99	1.96	1.93
Na ₂ O	8.77	8.79	8.13	7.77	7.85	7.72	8.36	9.00	7.45	8.40
K ₂ O	5.52	5.57	5.54	5.37	5.34	5.36	5.34	5.56	5.41	5.14
P ₂ O ₅	0.22	0.28	0.34	0.29	0.31	0.33	0.25	0.33	0.25	0.27
F (ppm)	1957	2721	1539	1947	2116	1798	1072	2113	1920	2380
SO ₂	0.07	0.06	0.08	0.09	0.06	0.09	0.09	0.11	0.08	0.08
Cl (ppm)	1536	1543	2724	1790	1744	1995	1377	3155	1538	1706
Total	100.00	100.00	100.00	100.00	100.00	100.00	100.00	100.00	100.00	100.00

*Fluorine corrected to an average of 1960 ppm

Table C3.24.3 Microprobe data for sample EBT-34a corrected for sodium loss

Analysis	1	2	3	4	5	6	7	8	9	10	Mean	StdDev
Correction	0.99878	0.99890	0.99236	0.98883	0.99962	0.9883803	0.99465	1.00109	0.98580	0.99508		
SiO2	55.31	55.09	55.34	55.68	55.69	55.62	55.43	55.07	55.75	54.29	55.44	0.30
TiO2	1.10	1.06	1.06	1.07	1.10	1.08	1.14	1.12	0.99	1.04	1.08	0.06
Al2O3	20.00	20.16	19.76	19.88	19.87	19.89	19.99	20.06	20.12	21.53	20.02	0.12
FeO	5.47	5.29	5.43	5.39	5.48	5.39	5.56	5.27	5.23	5.39	5.36	0.12
MnO	0.28	0.20	0.35	0.26	0.20	0.18	0.15	0.15	0.29	0.18	0.20	0.06
MgO	0.87	0.95	0.91	0.91	0.90	0.90	0.94	0.89	0.94	0.92	0.92	0.02
CaO	1.93	2.04	1.99	1.95	1.94	2.05	2.05	2.00	1.93	1.92	2.00	0.05
Na2O	8.90	8.90	8.90	8.90	8.90	8.90	8.90	8.90	8.90	8.90	8.90	0.00
K2O	5.51	5.56	5.50	5.31	5.28	5.30	5.31	5.56	5.33	5.12	5.40	0.13
P2O5	0.22	0.28	0.33	0.29	0.31	0.33	0.25	0.33	0.25	0.27	0.29	0.04
F (ppm)	1955	2718	1527	1925	2094	1778	1066	2116	1893	2368	1916	534
SO2	0.07	0.06	0.08	0.09	0.06	0.08	0.09	0.11	0.08	0.08	0.08	0.01
Cl (ppm)	1535	0	2704	1770	1726	1972	1369	3159	1516	1697	1631	1021
Total	100.01	100.01	100.07	100.10	100.09	100.10	100.05	99.99	100.13	100.04	100.04	100.04

Table C3.25.1 Raw microprobe data for sample EBT-34b

Analysis	1	2	3	4	5	6	7	8	9	10
SiO2	55.90	55.75	56.15	56.05	54.23	55.84	55.18	55.77	55.44	55.00
TiO2	1.06	1.09	0.98	1.08	1.10	0.99	1.09	1.03	1.10	1.09
Al2O3	20.45	20.23	20.44	20.51	20.04	20.25	20.37	20.52	20.32	20.18
FeO	5.45	5.27	5.46	5.50	5.65	5.53	5.53	5.72	5.49	5.51
MnO	0.29	0.27	0.16	0.12	0.25	0.30	0.42	0.29	0.20	0.18
MgO	0.94	0.87	0.93	0.97	0.97	0.90	0.95	0.97	1.16	0.90
CaO	2.07	1.97	1.93	2.04	2.07	1.90	1.98	2.05	1.97	1.98
Na2O	8.55	8.81	8.45	8.55	8.99	8.93	8.92	8.71	8.77	8.86
K2O	5.44	5.60	5.58	5.49	5.58	5.35	5.49	5.29	5.37	5.42
P2O5	0.25	0.27	0.30	0.29	0.28	0.26	0.24	0.33	0.33	0.26
F (ppm)	2040	810	1360	2280	2680	n.d.	1810	2230	1860	430
SO2	0.05	0.04	0.11	0.06	0.11	0.12	0.06	0.10	0.07	0.06
Cl (ppm)	1480	1250	1260	1720	1450	1540	1310	1330	1450	1110
Total	100.79	100.38	100.74	101.07	99.68	100.52	100.53	101.13	100.55	99.60

Table C3.25.2 Microprobe data for sample EBT-34b corrected to 100%

Analysis	1	2	3	4	5	6*	7	8	9	10*
SiO2	55.46	55.54	55.74	55.46	54.41	55.45	54.89	55.15	55.14	55.14
TiO2	1.05	1.08	0.97	1.06	1.10	0.99	1.08	1.02	1.10	1.09
Al2O3	20.29	20.15	20.29	20.30	20.10	20.11	20.26	20.29	20.21	20.23
FeO	5.40	5.25	5.42	5.44	5.66	5.49	5.50	5.66	5.46	5.53
MnO	0.29	0.27	0.16	0.12	0.25	0.30	0.41	0.28	0.19	0.18
MgO	0.93	0.87	0.93	0.96	0.97	0.89	0.95	0.96	1.15	0.90
CaO	2.05	1.96	1.92	2.02	2.08	1.88	1.97	2.02	1.96	1.98
Na2O	8.48	8.78	8.38	8.46	9.02	8.86	8.87	8.61	8.72	8.89
K2O	5.40	5.58	5.53	5.43	5.60	5.31	5.46	5.23	5.34	5.43
P2O5	0.25	0.27	0.30	0.29	0.28	0.26	0.24	0.32	0.33	0.26
F (ppm)	2024	807	1350	2256	2689	1867	1801	2205	1850	1885
SO2	0.05	0.04	0.11	0.06	0.11	0.12	0.06	0.10	0.07	0.06
Cl (ppm)	1468	1245	1251	1702	1455	1529	1303	1315	1442	1113
Total	100.00	100.00	100.00	100.00	100.00	100.00	100.00	100.00	100.00	100.00

*Flourine corrected to an average of 1884 ppm

Table C3.25.3 Microprobe data for sample EBT-34b corrected for sodium loss

Analysis	1	2	3	4	5	6	7	8	9	10	Mean	StdDev
Correction	0.995291	0.9982413	0.99433	0.99512	1.00067	0.99910	0.99919	0.99656	0.99765	0.999331		
SiO2	55.20	55.44	55.42	55.19	54.44	55.40	54.84	54.96	55.01	55.11	55.10	0.31
TiO2	1.05	1.08	0.96	1.06	1.10	0.99	1.08	1.02	1.10	1.09	1.05	0.05
Al2O3	20.19	20.12	20.18	20.20	20.12	20.09	20.25	20.22	20.16	20.22	20.17	0.05
FeO	5.38	5.24	5.39	5.42	5.67	5.49	5.49	5.64	5.45	5.52	5.47	0.13
MnO	0.29	0.27	0.16	0.12	0.25	0.30	0.41	0.28	0.19	0.18	0.25	0.08
MgO	0.93	0.87	0.92	0.96	0.97	0.89	0.95	0.96	1.15	0.90	0.95	0.08
CaO	2.05	1.96	1.91	2.01	2.08	1.88	1.97	2.02	1.96	1.98	1.98	0.06
Na2O	8.95	8.95	8.95	8.95	8.95	8.95	8.95	8.95	8.95	8.95	8.95	0.00
K2O	5.37	5.57	5.50	5.40	5.60	5.30	5.46	5.21	5.33	5.43	5.42	0.12
P2O5	0.24	0.27	0.30	0.28	0.28	0.26	0.24	0.32	0.33	0.26	0.28	0.03
F (ppm)	2014	806	1342	2245	2690	1865	1799	2197	1845	1884	1869	512
SO2	0.05	0.04	0.10	0.06	0.11	0.12	0.06	0.10	0.07	0.06	0.08	0.03
Cl (ppm)	1461	1243	1244	1694	1456	1528	1302	1311	1439	1112	1379	169
Total	100.04	100.02	100.05	100.04	99.99	100.01	100.01	100.03	100.02	100.01	100.02	100.02

Table C3.26.1 Raw microprobe data for sample EBT-34d

Analysis	1	2	3	4	5	6	7	8	9	10
SiO2	55.21	54.63	55.49	55.72	55.37	54.63	55.54	54.95	54.97	55.45
TiO2	1.06	1.11	1.05	1.10	0.92	1.07	1.11	1.10	0.97	0.99
Al2O3	20.39	20.32	20.20	20.19	20.49	20.45	20.51	20.58	20.31	20.33
FeO	5.54	5.44	5.28	5.29	5.43	5.58	5.55	5.32	5.52	5.38
MnO	0.25	0.19	0.21	0.20	0.26	0.29	0.30	0.19	0.19	0.10
MgO	0.98	0.86	0.94	0.95	0.94	0.95	0.90	1.45	0.95	0.93
CaO	1.97	2.07	1.92	1.89	2.06	1.99	1.95	1.98	2.08	1.90
Na2O	8.94	8.78	8.88	8.70	8.65	8.48	8.54	8.68	8.81	8.84
K2O	5.39	5.55	5.71	5.77	5.65	5.47	5.51	5.50	5.64	5.48
P2O5	0.32	0.25	0.21	0.26	0.24	0.26	0.30	0.24	0.32	0.27
F (ppm)	1950	2210	1860	450	2960	2410	1560	600	3680	1980
SO2	0.04	0.08	0.10	0.09	0.07	0.10	0.06	0.08	0.07	0.11
Cl (ppm)	1220	1460	1360	1420	1600	1660	1430	1410	1540	1330
Total	100.42	99.64	100.30	100.35	100.54	99.67	100.58	100.25	100.34	100.11

Table C3.26.2 Microprobe data for sample EBT-34d corrected to 100%

Analysis	1	2	3	4*	5	6	7	8	9	10
SiO2	54.98	54.82	55.32	55.43	55.07	54.81	55.22	54.81	54.78	55.38
TiO2	1.06	1.11	1.05	1.10	0.92	1.07	1.10	1.10	0.96	0.99
Al2O3	20.30	20.40	20.14	20.09	20.38	20.52	20.40	20.53	20.24	20.31
FeO	5.52	5.46	5.26	5.26	5.40	5.60	5.52	5.30	5.50	5.37
MnO	0.25	0.19	0.21	0.19	0.26	0.29	0.30	0.19	0.19	0.10
MgO	0.98	0.87	0.94	0.94	0.94	0.96	0.89	1.44	0.95	0.93
CaO	1.96	2.08	1.92	1.88	2.05	2.00	1.94	1.97	2.08	1.90
Na2O	8.90	8.81	8.86	8.65	8.60	8.50	8.49	8.66	8.78	8.83
K2O	5.37	5.57	5.69	5.74	5.62	5.48	5.48	5.48	5.62	5.47
P2O5	0.32	0.25	0.20	0.26	0.24	0.26	0.30	0.24	0.31	0.27
F (ppm)	1942	2218	1854	2119	2944	2418	1551	598	3667	1978
SO2	0.04	0.08	0.09	0.09	0.07	0.10	0.06	0.08	0.07	0.11
Cl (ppm)	1215	1465	1356	1413	1591	1666	1422	1406	1535	1329
Total	100.00	100.00	100.00	100.00	100.00	100.00	100.00	100.00	100.00	100.00

*Fluorine corrected to an average of 2134 ppm

Table C3.26.3 Microprobe data for sample EBT-34d corrected for sodium loss

Analysis	1	2	3	4	5	6	7	8	9	10	Mean	StdDev
Correction	1.000213	0.9992893	0.99979	0.99777	0.99725	0.99627	0.99615	0.99779	0.99898	0.999553		
SiO2	54.99	54.78	55.31	55.31	54.92	54.61	55.01	54.69	54.73	55.36	54.97	0.28
TiO2	1.06	1.11	1.05	1.09	0.92	1.07	1.10	1.09	0.96	0.99	1.04	0.07
Al2O3	20.31	20.38	20.13	20.05	20.32	20.44	20.32	20.49	20.22	20.30	20.30	0.13
FeO	5.52	5.46	5.26	5.25	5.39	5.58	5.50	5.29	5.50	5.37	5.41	0.12
MnO	0.25	0.19	0.21	0.19	0.26	0.28	0.30	0.19	0.19	0.10	0.22	0.06
MgO	0.98	0.87	0.94	0.94	0.94	0.95	0.89	1.44	0.94	0.93	0.98	0.16
CaO	1.97	2.08	1.91	1.88	2.04	1.99	1.93	1.97	2.07	1.90	1.97	0.07
Na2O	8.88	8.88	8.88	8.88	8.88	8.88	8.88	8.88	8.88	8.88	8.88	0.00
K2O	5.37	5.57	5.69	5.72	5.60	5.46	5.46	5.47	5.62	5.47	5.54	0.11
P2O5	0.32	0.25	0.20	0.26	0.24	0.26	0.30	0.23	0.31	0.27	0.26	0.04
F (ppm)	1942	2216	1854	2114	2936	2409	1545	597	3664	1977	2126	811
SO2	0.04	0.08	0.09	0.09	0.07	0.10	0.06	0.08	0.07	0.11	0.08	0.02
Cl (ppm)	1215	1464	1356	1410	1587	1659	1416	1403	1533	1328	1437	130
Total	100.00	100.01	100.00	100.02	100.02	100.03	100.03	100.02	100.01	100.00	100.02	

Table C3.27.3 Microprobe data for sample EBT-34c corrected for sodium loss

Analysis	1	2	3	4	5	6	7	8	9	10	Mean	StdDev
Correction	1.000373	0.99937	0.99970	0.9975101	0.99706	0.99963	0.99892	0.99648	0.99573	0.998013		
SiO2	54.86	54.52	54.10	53.52	55.19	55.07	54.82	54.71	55.08	54.78	54.79	0.33
TiO2	1.03	1.11	1.09	1.10	0.97	0.98	0.99	1.07	1.15	1.16	1.06	0.07
Al2O3	19.32	19.94	20.29	19.85	19.02	18.99	20.16	20.14	19.43	20.06	19.71	0.51
FeO	6.02	5.53	5.50	5.47	6.28	6.23	5.37	5.32	5.73	5.19	5.68	0.40
MnO	0.37	0.23	0.37	0.19	0.19	0.29	0.32	0.21	0.27	0.31	0.28	0.07
MgO	0.91	0.91	0.94	2.48	0.88	0.93	0.87	0.88	0.91	0.89	0.90	0.02
CaO	1.97	2.05	2.04	2.10	1.89	2.03	1.96	2.00	2.08	2.07	2.01	0.06
Na2O	9.21	9.21	9.21	9.21	9.21	9.21	9.21	9.21	9.21	9.21	9.21	0.00
K2O	5.71	5.71	5.67	5.49	5.55	5.52	5.67	5.80	5.51	5.57	5.64	0.10
P2O5	0.26	0.30	0.31	0.35	0.35	0.29	0.28	0.29	0.30	0.29	0.30	0.02
F (ppm)	1165	2377	2557	428	2565	2251	1652	1773	1712	2261	2035	480
SO2	0.07	0.11	0.08	0.08	0.10	0.10	0.05	0.07	0.06	0.11	0.08	0.02
Cl (ppm)	1325	1525	1599	1380	1347	1408	1385	1438	1389	1494	1435	89
Total	100.00	100.01	100.00	100.02	100.03	100.00	100.01	100.03	100.04	100.02	100.02	

Table C3.28.3 Microprobe data for sample EBT-35 corrected for sodium loss

Analysis	1	2	3	4	5	6	7	8	9	10	Mean	StdDev
Correction	0.998651	0.99802	0.99628	0.99919	0.99776	0.99821	1.00082	0.99669	0.99639	1.00663		
SiO2	55.73	55.74	55.66	56.07	55.74	55.36	55.11	54.97	56.44	56.24	55.73	0.40
TiO2	1.15	1.14	1.16	1.15	1.00	1.13	1.04	1.05	1.03	1.10	1.10	0.06
Al2O3	20.06	20.31	20.05	20.11	20.49	20.51	20.66	21.32	19.91	20.07	20.26	0.27
FeO	5.51	5.44	5.57	5.33	5.26	5.66	5.57	5.45	5.31	5.38	5.46	0.15
MnO	0.16	0.21	0.32	0.20	0.26	0.24	0.27	0.21	0.29	0.27	0.24	0.05
MgO	0.96	0.96	0.92	0.86	0.95	0.94	0.99	0.94	0.88	0.90	0.93	0.04
CaO	2.11	1.96	1.97	1.89	2.04	1.96	2.03	1.90	1.89	2.00	1.98	0.08
Na2O	8.03	8.03	8.03	8.03	8.03	8.03	8.03	8.03	8.03	8.03	8.03	0.00
K2O	5.54	5.52	5.58	5.54	5.46	5.46	5.46	5.33	5.53	5.44	5.51	0.04
P2O5	0.38	0.30	0.36	0.26	0.27	0.24	0.24	0.37	0.29	0.27	0.29	0.05
F (ppm)	503	1527	1600	3104	1944	2267	2453	1413	1382	520	1848	785
SO2	0.09	0.08	0.07	0.05	0.09	0.09	0.08	0.12	0.09	0.05	0.08	0.02
Cl (ppm)	2464	1635	1865	2076	2311	1591	2542	1865	2143	1424	2078	359
Total	100.01	100.02	100.03	100.01	100.02	100.01	99.99	100.03	100.03	99.95	100.01	

Table C3.29.1 Raw microprobe data for sample EBT-35a

Analysis	1	2	3	4	5	6	7	8	9	10
SiO2	57.08	56.60	57.06	57.27	56.74	56.72	56.22	56.55	56.65	57.00
TiO2	1.06	1.10	1.09	1.17	1.02	1.11	1.06	1.09	1.22	1.14
Al2O3	20.32	20.37	20.29	20.72	20.57	20.35	20.41	20.57	20.53	20.37
FeO	5.71	5.64	5.82	5.64	5.45	5.70	5.60	5.56	5.63	5.70
MnO	0.27	0.26	0.24	0.18	0.32	0.27	0.30	0.31	0.30	0.21
MgO	0.97	0.97	0.96	0.92	0.99	0.96	0.95	0.99	0.97	1.02
CaO	1.99	1.97	1.99	2.00	2.05	2.15	2.12	2.07	2.03	1.98
Na2O	8.57	7.87	8.75	7.74	7.97	7.76	8.55	8.00	7.95	7.92
K2O	5.52	5.55	5.45	5.50	5.53	5.40	5.55	5.41	5.50	5.52
P2O5	0.28	0.29	0.34	0.35	0.29	0.34	0.33	0.32	0.29	0.26
F (ppm)	230	200	1720	2640	2640	3170	2100	1500	1500	1070
SO2	0.07	0.09	0.08	0.08	0.08	0.10	0.10	0.09	0.09	0.05
Cl (ppm)	2120	1510	1660	0.174	2100	2150	2050	1560	2030	1610
Total	102.08	100.88	102.41	102.02	101.47	101.38	101.59	101.26	101.51	101.46

Table C3.29.2 Microprobe data for sample EBT-35a corrected to 100%

Analysis	1	2*	3	4	5	6	7	8	9	10
SiO2	55.92	56.00	55.72	56.14	55.92	55.95	55.34	55.85	55.81	56.18
TiO2	1.04	1.09	1.07	1.15	1.00	1.09	1.04	1.08	1.20	1.13
Al2O3	19.90	20.15	19.81	20.31	20.27	20.07	20.09	20.31	20.22	20.08
FeO	5.59	5.58	5.68	5.53	5.37	5.62	5.52	5.49	5.54	5.62
MnO	0.27	0.26	0.24	0.18	0.32	0.27	0.29	0.30	0.29	0.21
MgO	0.95	0.96	0.94	0.90	0.97	0.95	0.94	0.98	0.96	1.01
CaO	1.95	1.95	1.94	1.96	2.02	2.12	2.08	2.04	2.00	1.95
Na2O	8.40	7.79	8.54	7.59	7.86	7.65	8.41	7.90	7.83	7.81
K2O	5.41	5.49	5.32	5.39	5.45	5.32	5.46	5.34	5.42	5.44
P2O5	0.27	0.29	0.33	0.34	0.28	0.34	0.32	0.31	0.28	0.26
F (ppm)	225	2068	1680	2588	2602	3127	2067	1481	1478	1055
SO2	0.07	0.09	0.08	0.08	0.08	0.10	0.10	0.09	0.09	0.05
Cl (ppm)	2077	1494	1621	1706	2070	2121	2018	1541	2000	1587
Total	100.00	100.00	100.00	100.00	100.00	100.00	100.00	100.00	100.00	100.00

*Flourine corrected to an average of 2089 ppm

Table C3.29.3 Microprobe data for sample EBT-35a corrected for sodium loss

Analysis	1	2	3	4	5	6	7	8	9	10	Mean	StdDev
Correction	1.00241	0.9962899	1.00387	0.99434	0.99698	0.99497	1.00256	0.99746	0.99669	0.996475		
SiO2	56.05	55.79	55.94	55.82	55.75	55.66	55.48	55.71	55.63	55.99	55.71	0.16
TiO2	1.04	1.08	1.07	1.14	1.00	1.09	1.05	1.08	1.20	1.12	1.09	0.06
Al2O3	19.95	20.08	19.89	20.20	20.21	19.97	20.14	20.26	20.15	20.00	20.12	0.11
FeO	5.60	5.56	5.71	5.50	5.36	5.59	5.53	5.47	5.52	5.60	5.52	0.08
MnO	0.27	0.26	0.24	0.18	0.32	0.27	0.29	0.30	0.29	0.21	0.28	0.04
MgO	0.95	0.96	0.94	0.89	0.97	0.95	0.94	0.97	0.95	1.01	0.96	0.02
CaO	1.96	1.94	1.95	1.95	2.02	2.11	2.09	2.04	2.00	1.95	2.02	0.06
Na2O	8.16	8.16	8.16	8.16	8.16	8.16	8.16	8.16	8.16	8.16	8.16	0.00
K2O	5.42	5.47	5.34	5.36	5.43	5.29	5.48	5.33	5.40	5.42	5.40	0.07
P2O5	0.27	0.29	0.33	0.34	0.28	0.34	0.32	0.31	0.28	0.26	0.30	0.03
F (ppm)	226	2060	1686	2573	2594	3111	2072	1478	1473	1051	1977	712
SO2	0.07	0.09	0.08	0.08	0.08	0.10	0.10	0.09	0.09	0.05	0.09	0.02
Cl (ppm)	2082	1488	1627	1696	2063	2110	2023	1537	1993	1581	1828	277
Total	99.98	100.03	99.97	100.05	100.02	100.04	99.98	100.02	100.03	100.03	100.02	

Table C3.30.1 Raw microprobe data for sample EBT-35b

Analysis	1	2	3	4	5	6	7	8	9	10
SiO2	57.97	57.16	55.85	56.79	55.73	56.45	55.74	57.51	56.40	56.05
TiO2	1.10	1.15	1.09	1.12	1.10	1.10	1.15	1.07	1.00	1.17
Al2O3	20.66	20.53	20.16	20.26	20.58	20.54	21.15	20.53	20.01	20.54
FeO	5.81	5.64	5.53	5.67	5.66	5.64	5.70	5.88	5.66	5.78
MnO	0.33	0.23	0.26	0.26	0.21	0.17	0.30	0.22	0.33	0.35
MgO	1.00	0.96	0.93	1.00	1.01	0.94	1.00	1.02	1.08	0.95
CaO	2.07	2.06	2.12	2.06	1.94	2.07	2.08	2.05	2.39	2.03
Na2O	7.97	7.62	8.73	7.80	7.77	8.08	7.84	7.89	8.60	8.60
K2O	5.52	5.68	5.55	5.63	5.59	5.54	5.63	5.64	5.56	5.51
P2O5	0.30	0.29	0.26	0.34	0.36	0.29	0.35	0.38	0.33	0.31
F (ppm)	2920	1450	280	2890	1570	1500	2810	2790	1700	n.d.
SO2	0.08	0.08	0.10	0.09	0.10	0.07	0.07	0.09	0.06	0.06
Cl (ppm)	1670	1840	1700	1530	1670	1850	1820	1910	1670	1560
Total	103.26	101.72	100.77	101.46	100.36	101.22	101.48	102.75	101.75	101.51

Table C3.30.2 Microprobe data for sample EBT-35b corrected to 100%

Analysis	1	2	3*	4	5	6	7	8	9	10*
SiO2	56.14	56.20	55.32	55.97	55.52	55.77	54.93	55.97	55.43	55.11
TiO2	1.07	1.13	1.08	1.11	1.10	1.08	1.14	1.04	0.98	1.15
Al2O3	20.01	20.18	19.97	19.97	20.51	20.29	20.84	19.98	19.67	20.19
FeO	5.63	5.54	5.48	5.58	5.64	5.58	5.61	5.72	5.56	5.68
MnO	0.32	0.23	0.26	0.25	0.21	0.17	0.30	0.22	0.32	0.35
MgO	0.97	0.94	0.92	0.99	1.00	0.93	0.99	1.00	1.06	0.93
CaO	2.00	2.03	2.10	2.03	1.94	2.04	2.05	2.00	2.35	2.00
Na2O	7.72	7.49	8.65	7.68	7.74	7.98	7.72	7.68	8.45	8.46
K2O	5.34	5.58	5.50	5.55	5.57	5.47	5.55	5.49	5.47	5.42
P2O5	0.29	0.28	0.26	0.34	0.36	0.28	0.34	0.37	0.32	0.31
F (ppm)	2828	1425	2080	2848	1564	1482	2769	2715	1671	2065
SO2	0.08	0.08	0.10	0.09	0.10	0.07	0.07	0.09	0.06	0.06
Cl (ppm)	1617	1809	1684	1508	1664	1828	1793	1859	1641	1534
Total	100.00	100.00	100.00	100.00	100.00	100.00	100.00	100.00	100.00	100.00

*Flourine corrected to an average of 2101 ppm

Table C3.30.3 Microprobe data for sample EBT-35b corrected for sodium loss

Analysis	1	2	3	4	5	6	7	8	9	10	Mean	StdDev
Correction	0.99172	0.98947	1.00096	0.99138	0.99193	0.99430	0.99177	0.99131	0.99903	0.99904		
SiO2	55.68	55.60	55.37	55.49	55.08	55.45	54.48	55.48	55.37	55.05	55.24	0.36
TiO2	1.06	1.12	1.08	1.10	1.09	1.08	1.13	1.03	0.98	1.15	1.09	0.05
Al2O3	19.84	19.97	19.99	19.80	20.34	20.18	20.67	19.80	19.65	20.17	20.10	0.32
FeO	5.58	5.49	5.48	5.54	5.59	5.54	5.57	5.67	5.55	5.67	5.55	0.06
MnO	0.32	0.22	0.26	0.25	0.21	0.17	0.30	0.21	0.32	0.34	0.26	0.06
MgO	0.96	0.93	0.92	0.98	1.00	0.92	0.98	0.99	1.06	0.93	0.96	0.05
CaO	1.98	2.01	2.10	2.01	1.92	2.03	2.04	1.98	2.35	2.00	2.06	0.13
Na2O	8.55	8.55	8.55	8.55	8.55	8.55	8.55	8.55	8.55	8.55	8.55	0.00
K2O	5.30	5.52	5.50	5.50	5.52	5.44	5.50	5.45	5.46	5.42	5.48	0.04
P2O5	0.29	0.28	0.26	0.34	0.35	0.28	0.34	0.37	0.32	0.31	0.31	0.03
F (ppm)	2805	1410	2082	2824	1552	1474	2746	2692	1669	2063	1977	558
SO2	0.08	0.08	0.10	0.09	0.10	0.07	0.07	0.09	0.06	0.06	0.08	0.02
Cl (ppm)	1604	1790	1686	1495	1651	1817	1779	1843	1640	1532	1674	119
Total	100.07	100.09	99.99	100.07	100.07	100.05	100.07	100.07	100.01	100.01	100.05	100.05

Table C3.31.3 Microprobe data for sample EBT-36 corrected for sodium loss

Analysis	1	2	3	4	5	6	7	8	9	10	Mean	StdDev
Correction	0.99941	1.00667	1.00182	0.99966	0.99660	0.99863	0.98861	0.99954	1.00034	0.991412		
SiO2	55.96	55.33	55.66	55.06	55.52	55.07	55.80	54.97	54.86	55.65	55.27	0.37
TiO2	1.00	1.19	1.04	1.03	1.10	1.00	1.02	1.08	1.08	1.06	1.05	0.04
Al2O3	19.75	20.23	20.79	20.27	20.06	20.25	20.03	20.08	20.12	20.10	20.13	0.10
FeO	5.25	5.76	5.68	5.44	5.33	5.42	5.28	5.50	5.51	5.32	5.40	0.09
MnO	0.35	0.24	0.25	0.22	0.13	0.24	0.21	0.24	0.16	0.25	0.21	0.05
MgO	0.89	<i>n.d.</i>	<i>n.d.</i>	0.90	0.89	0.91	0.89	0.91	0.91	0.88	0.90	0.01
CaO	1.82	1.99	1.95	1.86	2.02	1.96	1.83	1.99	1.95	1.95	1.94	0.07
Na2O	8.85	8.85	8.85	8.85	8.85	8.85	8.85	8.85	8.85	8.85	8.85	0.00
K2O	5.36	5.57	5.57	5.51	5.42	5.38	5.48	5.56	5.63	5.29	5.47	0.12
P2O5	0.28	0.30	0.33	0.29	0.19	0.34	0.24	0.25	0.30	0.26	0.27	0.05
F (ppm)	2514	2025	2391	3083	2877	3127	1815	2544	3343	2225	2716	548
SO2	0.09	0.10	0.07	0.08	0.07	0.08	0.11	0.10	0.09	0.07	0.09	0.01
Cl (ppm)	1618	1814	1604	1860	1679	1946	1805	2197	2026	1786	1900	173
Total	100.01	99.94	99.98	100.00	100.03	100.01	100.10	100.00	100.00	100.08	100.03	

Table C3.32.1 Raw microprobe data for sample EBT-37

Analysis	1	2	3	4	5	6	7	8	9	10
SiO2	55.4	57.0	54.6	56.5	57.0	56.3	56.9	57.0	55.6	57.4
TiO2	1.2	1.1	1.1	1.1	1.0	1.1	1.1	1.1	1.1	1.1
Al2O3	20.6	20.6	20.5	19.9	20.3	20.6	20.5	20.3	20.3	20.3
FeO	5.6	5.6	5.8	5.7	5.4	5.7	5.5	5.6	5.4	5.5
MnO	0.3	0.2	0.4	0.2	0.2	0.2	0.2	0.3	0.2	0.2
MgO	1.0	0.9	1.0	0.9	1.0	0.9	0.9	0.9	1.0	0.9
CaO	2.1	2.0	2.0	2.1	1.9	2.1	2.2	2.0	2.1	2.1
Na2O	9.0	7.8	8.0	9.0	7.8	8.3	9.0	8.7	8.2	8.8
K2O	5.6	5.6	5.4	5.5	5.6	5.6	5.5	5.4	5.6	5.6
P2O5	0.3	0.3	0.3	0.3	0.3	0.3	0.3	0.3	0.3	0.3
F (ppm)	3310	2560	2780	4330	n.d.	2280	1320	2280	1880	2050
SO2	0.10	0.09	0.09	0.09	0.10	0.06	0.08	0.08	0.09	0.10
Cl (ppm)	1960	1660	1250	2620	1990	3000	2880	2570	2930	1710
Total	101.64	101.54	99.64	101.91	100.83	101.55	102.46	102.01	100.42	102.66

Table C3.32.2 Microprobe data for sample EBT-37 corrected to 100%

Analysis	1	2	3	4	5*	6	7	8	9	10
SiO2	54.53	56.14	54.77	55.43	56.36	55.39	55.55	55.85	55.37	55.92
TiO2	1.20	1.08	1.12	1.10	1.03	1.12	1.03	1.06	1.14	1.05
Al2O3	20.26	20.25	20.62	19.57	20.08	20.26	19.96	19.90	20.18	19.78
FeO	5.49	5.48	5.85	5.57	5.32	5.61	5.33	5.48	5.39	5.32
MnO	0.26	0.25	0.39	0.20	0.21	0.22	0.21	0.26	0.23	0.22
MgO	0.94	0.93	0.96	0.91	0.97	0.92	0.90	0.85	0.97	0.89
CaO	2.06	1.94	2.04	2.03	1.89	2.03	2.10	1.99	2.11	2.09
Na2O	8.82	7.66	8.04	8.79	7.69	8.15	8.74	8.50	8.17	8.56
K2O	5.51	5.48	5.43	5.37	5.54	5.47	5.41	5.28	5.60	5.42
P2O5	0.31	0.31	0.30	0.26	0.33	0.25	0.29	0.28	0.27	0.28
F (ppm)	3257	2521	2790	4249	2828	2245	1288	2235	1872	1997
SO2	0.09	0.08	0.09	0.08	0.10	0.05	0.08	0.08	0.09	0.09
Cl (ppm)	1928	1635	1254	2571	1968	2954	2811	2519	2918	1666
Total	100.00	100.00	100.00	100.00	100.00	100.00	100.00	100.00	100.00	100.00

*Fluorine corrected to an average of 2857 ppm

Table C3.32.3 Microprobe data for sample EBT-37 corrected for sodium loss

Analysis	1	2	3	4	5	6	7	8	9	10	Mean	StdDev
Correction	1.000157	0.98864	0.99233	0.99984	0.98898	0.99350	0.99934	0.99689	0.99368	0.99751		
SiO2	54.54	55.50	54.35	55.42	55.74	55.03	55.51	55.68	55.02	55.78	55.09	0.51
TiO2	1.20	1.07	1.11	1.10	1.02	1.11	1.03	1.06	1.13	1.05	1.11	0.06
Al2O3	20.27	20.02	20.46	19.56	19.86	20.13	19.95	19.84	20.06	19.73	20.05	0.29
FeO	5.49	5.42	5.81	5.57	5.26	5.57	5.32	5.47	5.35	5.31	5.50	0.18
MnO	0.26	0.24	0.38	0.20	0.21	0.22	0.21	0.26	0.23	0.22	0.25	0.06
MgO	0.94	0.92	0.95	0.91	0.96	0.92	0.90	0.85	0.97	0.89	0.94	0.02
CaO	2.06	1.92	2.03	2.03	1.87	2.02	2.10	1.98	2.09	2.09	2.00	0.08
Na2O	8.81	8.81	8.81	8.81	8.81	8.81	8.81	8.81	8.81	8.81	8.81	0.00
K2O	5.51	5.41	5.39	5.37	5.47	5.43	5.40	5.27	5.56	5.41	5.45	0.07
P2O5	0.31	0.30	0.29	0.26	0.32	0.25	0.29	0.27	0.27	0.28	0.29	0.03
F (ppm)	3257	2492	2769	4248	2797	2231	1287	2228	1860	1992	2808	775
SO2	0.09	0.08	0.09	0.08	0.10	0.05	0.08	0.08	0.09	0.09	0.08	0.01
Cl (ppm)	1929	1616	1245	2970	1946	2935	2809	2512	2899	1662	2163	652
Total	100.00	100.10	100.07	100.00	100.10	100.06	100.01	100.03	100.06	100.02	100.05	

Table C3.33.3 Microprobe data for sample EBT-38 corrected for sodium loss

Analysis	1	2	3	4	5	6	7	8	9	10	Mean	StdDev
Correction	1.00050	0.99950	0.99491	0.99763	0.99640	0.99483	0.99614	0.99500	0.99683	0.998329		
SiO2	54.06	54.32	54.37	54.18	54.29	54.50	54.48	53.84	54.09	54.50	54.26	0.22
TiO2	1.09	1.04	1.01	1.06	1.08	1.05	1.10	1.08	1.07	1.11	1.07	0.03
Al2O3	20.38	20.07	20.17	20.12	20.29	20.24	20.02	20.41	20.23	19.99	20.19	0.14
FeO	5.49	5.43	5.54	5.56	5.64	5.52	5.56	5.74	5.65	5.51	5.56	0.09
MnO	0.21	0.31	0.28	0.27	0.26	0.19	0.32	0.23	0.24	0.16	0.25	0.05
MgO	0.89	0.89	0.93	0.90	0.86	0.90	0.90	0.99	0.91	0.86	0.90	0.04
CaO	2.10	2.15	2.06	2.11	2.11	2.03	2.10	2.04	2.04	2.11	2.09	0.04
Na2O	9.35	9.35	9.35	9.35	9.35	9.35	9.35	9.35	9.35	9.35	9.35	0.00
K2O	5.72	5.57	5.65	5.67	5.45	5.53	5.60	5.71	5.52	5.65	5.61	0.09
P2O5	0.29	0.31	0.36	0.28	0.27	0.21	0.30	0.31	0.30	0.24	0.29	0.04
F (ppm)	1848	1965	834	2207	2220	3254	834	1214	3862	3019	2126	1020
SO2	0.08	0.21	0.08	0.07	0.06	0.07	0.10	0.08	0.07	0.09	0.09	0.04
Cl (ppm)	1483	1656	1579	2317	1640	1468	1261	1405	1702	1414	1593	288
Total	100.00	100.00	100.05	100.02	100.03	100.05	100.04	100.05	100.03	100.02	100.03	100.03

Table C3.34.3 Microprobe data for sample EBT-39 corrected for sodium loss

Analysis	1	2	3	4	5	6	7	8	9	10	Mean	StdDev
Correction	0.997129	0.99982	0.99843	0.99890	1.00015	0.99948	0.99984	0.99839	0.99973	0.999154		
SiO2	55.30	55.03	55.28	54.85	55.21	55.06	55.64	55.39	54.58	55.24	55.16	0.29
TiO2	0.99	1.04	1.04	1.09	0.92	1.07	0.96	1.05	1.11	0.97	1.02	0.06
Al2O3	19.56	19.75	19.53	19.90	19.91	19.85	19.57	19.78	19.87	19.50	19.72	0.16
FeO	5.60	5.67	5.70	5.61	5.43	5.55	5.63	5.56	5.86	5.66	5.63	0.11
MnO	0.28	0.29	0.27	0.23	0.30	0.23	0.22	0.20	0.26	0.22	0.25	0.03
MgO	0.91	0.83	0.87	0.90	0.85	0.86	0.86	0.89	0.89	0.88	0.88	0.03
CaO	1.90	1.92	1.83	1.91	1.77	1.85	1.71	1.81	2.00	1.90	1.86	0.08
Na2O	9.12	9.12	9.12	9.12	9.12	9.12	9.12	9.12	9.12	9.12	9.12	0.00
K2O	5.58	5.65	5.40	5.63	5.55	5.60	5.70	5.52	5.59	5.67	5.59	0.09
P2O5	0.28	0.28	0.29	0.30	0.35	0.32	0.28	0.31	0.29	0.36	0.31	0.03
F (ppm)	2648	2321	4233	1937	3354	2197	804	1847	2135	2306	2378	914
SO2	0.06	0.04	0.10	0.07	0.09	0.10	0.07	0.06	0.08	0.08	0.07	0.02
Cl (ppm)	1775	1493	1561	1774	1525	1640	1669	1228	1370	1594	1563	171
Total	100.03	100.00	100.01	100.01	100.00	100.00	100.00	100.01	100.00	100.01	100.01	

Table C3.35.1 Raw microprobe data for sample EBT-40

Analysis	1	2	3	4	5	6	7	8	9	10
SiO2	52.58	53.98	54.88	54.72	53.49	54.81	55.06	54.09	54.68	54.80
TiO2	1.05	1.01	0.91	0.91	1.03	0.96	1.02	1.01	1.02	0.97
Al2O3	19.79	20.00	20.33	20.14	19.92	20.17	20.38	19.94	20.09	20.33
FeO	5.55	5.57	5.41	5.62	5.49	5.51	5.52	5.60	5.36	5.53
MnO	0.25	0.31	0.32	0.24	0.15	0.28	0.11	0.20	0.26	0.26
MgO	0.79	0.86	0.85	0.79	0.87	0.84	0.89	0.88	0.79	0.85
CaO	1.99	1.94	1.98	1.93	1.83	1.86	1.89	2.06	1.94	1.95
Na2O	9.19	9.14	9.04	9.01	9.00	9.09	8.98	9.27	9.18	9.19
K2O	5.66	5.67	5.55	5.75	5.90	5.75	5.64	5.66	5.62	5.72
P2O5	0.28	0.31	0.31	0.31	0.32	0.29	0.36	0.28	0.27	0.25
F (ppm)	1530	3210	2490	1760	2810	2580	2130	3280	2360	17910
SO2	0.08	0.09	0.08	0.07	0.07	0.10	0.08	0.09	0.08	0.06
Cl (ppm)	1740	1460	1610	1520	1380	1630	1800	1630	1740	1660
Total	97.55	99.35	100.07	99.82	98.49	100.08	100.32	99.55	99.70	101.87

Table C3.35.2 Microprobe data for sample EBT-40 corrected to 100%

Analysis	1	2	3	4	5	6	7	8	9	10*
SiO2	53.91	54.33	54.84	54.81	54.31	54.77	54.89	54.33	54.84	54.61
TiO2	1.08	1.01	0.91	0.91	1.05	0.96	1.01	1.01	1.02	0.97
Al2O3	20.29	20.13	20.32	20.18	20.22	20.16	20.32	20.03	20.15	20.27
FeO	5.69	5.61	5.41	5.63	5.57	5.50	5.50	5.62	5.38	5.51
MnO	0.26	0.31	0.32	0.24	0.15	0.28	0.10	0.20	0.26	0.26
MgO	0.81	0.87	0.85	0.79	0.89	0.84	0.88	0.88	0.79	0.85
CaO	2.03	1.95	1.98	1.94	1.86	1.86	1.89	2.06	1.95	1.94
Na2O	9.43	9.20	9.03	9.03	9.14	9.08	8.96	9.31	9.21	9.16
K2O	5.80	5.71	5.54	5.76	5.99	5.75	5.62	5.69	5.64	5.70
P2O5	0.29	0.32	0.31	0.31	0.33	0.29	0.36	0.28	0.27	0.25
F (ppm)	1569	3231	2488	1763	2853	2578	2123	3295	2367	2571
SO2	0.08	0.09	0.08	0.07	0.07	0.10	0.08	0.09	0.08	0.06
Cl (ppm)	1784	1470	1609	1523	1401	1629	1794	1637	1745	1654
Total	100.00	100.00	100.00	100.00	100.00	100.00	100.00	100.00	100.00	100.00

*Flourine corrected to an average of 2560 ppm

Table C3.35.3 Microprobe data for sample EBT-40 corrected for sodium loss

Analysis	1	2	3	4	5	6	7	8	9	10	Mean	StdDev
Correction	1.00168	0.99945	0.99774	0.99773	0.99882	0.9982305	0.99699	1.00053	0.99947	0.999011		
SiO2	54.00	54.30	54.72	54.69	54.25	54.67	54.72	54.36	54.82	54.56	54.56	0.21
TiO2	1.08	1.01	0.91	0.90	1.05	0.96	1.01	1.01	1.02	0.97	0.98	0.05
Al2O3	20.32	20.12	20.27	20.13	20.20	20.12	20.26	20.04	20.14	20.25	20.17	0.08
FeO	5.70	5.60	5.40	5.62	5.56	5.49	5.49	5.62	5.37	5.50	5.52	0.09
MnO	0.26	0.31	0.32	0.24	0.15	0.28	0.10	0.21	0.26	0.26	0.24	0.07
MgO	0.81	0.87	0.85	0.79	0.88	0.84	0.88	0.88	0.79	0.85	0.85	0.04
CaO	2.04	1.95	1.98	1.93	1.85	1.85	1.88	2.07	1.95	1.94	1.93	0.07
Na2O	9.26	9.26	9.26	9.26	9.26	9.26	9.26	9.26	9.26	9.26	9.26	0.00
K2O	5.81	5.70	5.53	5.75	5.98	5.74	5.61	5.69	5.64	5.70	5.70	0.13
P2O5	0.29	0.31	0.31	0.31	0.33	0.29	0.36	0.28	0.27	0.25	0.30	0.03
F (ppm)	1571	3229	2483	1759	2850	2573	2117	3297	2366	2569	2582	494
SO2	0.08	0.09	0.08	0.07	0.07	0.10	0.08	0.09	0.08	0.06	0.08	0.01
Cl (ppm)	1787	1469	1605	1519	1400	1626	1789	1638	1744	1653	1605	125
Total	99.98	100.01	100.02	100.02	100.01	100.02	100.03	100.00	100.00	100.01	100.01	

Table C3.36.1 Raw microprobe data for sample EBT-40a

Analysis	1	2	3	4	5	6	7	8	9	10
SiO2	54.31	54.36	54.73	54.50	54.74	53.71	54.13	54.13	54.48	54.55
TiO2	0.95	0.94	1.00	1.02	1.07	0.98	1.03	0.96	0.92	0.94
Al2O3	20.00	19.96	20.10	20.07	20.04	20.00	20.04	19.80	19.99	20.00
FeO	5.42	5.40	5.35	5.42	5.42	5.41	5.44	5.53	5.63	5.58
MnO	0.26	0.15	0.22	0.25	0.19	0.19	0.20	0.24	0.23	0.30
MgO	0.82	0.90	0.84	0.85	0.87	0.82	0.89	0.82	0.83	0.87
CaO	1.89	1.79	1.94	1.80	2.03	1.93	1.95	1.92	1.90	1.93
Na2O	9.04	9.34	9.33	9.39	9.10	9.14	9.17	8.94	9.28	9.18
K2O	5.55	5.89	5.52	5.86	5.60	5.75	5.59	5.59	5.72	5.74
P2O5	0.29	0.32	0.29	0.26	0.35	0.18	0.32	0.30	0.30	0.34
F (ppm)	3300	2370	2070	3460	1500	250	3960	2430	2220	3130
SO2	0.03	0.08	0.12	0.10	0.07	0.07	0.09	0.11	0.08	0.07
Cl (ppm)	1660	1730	1680	1710	1660	1780	1560	1680	1560	1490
Total	99.07	99.53	99.81	100.02	99.80	98.39	99.40	98.74	99.73	99.95

Table C3.36.2 Microprobe data for sample EBT-40a corrected to 100%

Analysis	1	2	3	4	5	6	7	8	9	10
SiO2	54.82	54.62	54.84	54.49	54.85	54.46	54.45	54.82	54.63	54.58
TiO2	0.96	0.94	1.00	1.02	1.07	0.99	1.04	0.98	0.92	0.94
Al2O3	20.19	20.06	20.14	20.07	20.08	20.28	20.16	20.06	20.05	20.00
FeO	5.48	5.42	5.36	5.42	5.43	5.48	5.48	5.60	5.64	5.58
MnO	0.26	0.15	0.22	0.25	0.19	0.19	0.20	0.25	0.23	0.30
MgO	0.83	0.90	0.84	0.85	0.88	0.84	0.89	0.83	0.83	0.87
CaO	1.91	1.79	1.94	1.80	2.03	1.96	1.96	1.94	1.90	1.93
Na2O	9.13	9.39	9.34	9.38	9.12	9.26	9.23	9.05	9.31	9.18
K2O	5.60	5.92	5.53	5.85	5.61	5.83	5.62	5.66	5.74	5.75
P2O5	0.29	0.32	0.29	0.25	0.35	0.18	0.32	0.30	0.30	0.34
F (ppm)	3331	2381	2074	3459	1503	2758	3984	2461	2226	3131
SO2	0.03	0.08	0.12	0.10	0.07	0.07	0.09	0.11	0.08	0.07
Cl (ppm)	1676	1738	1683	1710	1663	1805	1569	1701	1564	1491
Total	100.00	100.00	100.00	100.00	100.00	100.00	100.00	100.00	100.00	100.00

*Fluorine corrected to an average of 2720 ppm.

Table C3.36.3 Microprobe data for sample EBT-40a corrected for sodium loss

Analysis	1	2	3	4	5	6	7	8	9	10	Mean	StdDev
Correction	0.997656	1.0002102	0.9997904	1.00019	0.99758	0.99901	0.99865	0.99690	0.99941	0.99820		
SiO2	54.69	54.63	54.82	54.50	54.71	54.40	54.38	54.65	54.59	54.48	54.59	0.14
TiO2	0.96	0.94	1.00	1.02	1.07	0.99	1.04	0.97	0.92	0.94	0.98	0.05
Al2O3	20.14	20.06	20.13	20.07	20.04	20.26	20.13	19.99	20.04	19.97	20.08	0.08
FeO	5.46	5.42	5.36	5.42	5.42	5.48	5.47	5.58	5.64	5.57	5.48	0.09
MnO	0.26	0.15	0.22	0.25	0.19	0.19	0.20	0.25	0.23	0.30	0.22	0.04
MgO	0.83	0.90	0.84	0.85	0.87	0.83	0.89	0.82	0.83	0.87	0.85	0.03
CaO	1.90	1.79	1.94	1.80	2.03	1.95	1.96	1.93	1.90	1.93	1.91	0.07
Na2O	9.36	9.36	9.36	9.36	9.36	9.36	9.36	9.36	9.36	9.36	9.36	0.00
K2O	5.59	5.92	5.53	5.86	5.60	5.83	5.62	5.64	5.74	5.74	5.70	0.13
P2O5	0.29	0.32	0.29	0.26	0.35	0.18	0.32	0.30	0.30	0.34	0.29	0.05
F (ppm)	3323	2382	2074	3460	1499	2755	3979	2453	2225	3126	2728	745
SO2	0.03	0.08	0.12	0.10	0.07	0.07	0.09	0.11	0.08	0.07	0.08	0.02
Cl (ppm)	1672	1739	1683	1710	1659	1803	1567	1696	1563	1488	1658	93
Total	100.02	100.00	100.00	100.00	100.02	100.01	100.01	100.03	100.01	100.02	100.01	100.01

Table C3.37.1 Raw microprobe data for sample EBT-40b

Analysis	1	2	3	4	5	6	7	8	9	10
SiO2	54.63	54.64	54.87	54.36	54.86	53.89	53.96	53.25	54.70	54.80
TiO2	1.07	1.05	1.06	1.01	1.03	1.00	1.01	0.93	1.01	0.92
Al2O3	20.34	19.96	20.02	20.29	20.32	20.10	20.05	19.86	19.94	20.17
FeO	5.47	5.46	5.43	5.76	5.47	5.42	5.52	5.54	5.38	5.52
MnO	0.28	0.16	0.35	0.30	0.26	0.24	0.22	0.17	0.28	0.30
MgO	0.88	0.84	0.91	0.87	0.85	0.85	0.90	0.88	0.81	0.88
CaO	2.03	1.92	1.95	2.10	2.00	1.93	1.97	1.96	1.87	1.92
Na2O	9.12	9.18	9.02	9.25	9.12	9.30	9.00	9.18	9.25	9.03
K2O	5.62	5.67	5.77	5.57	5.71	5.83	5.54	5.62	5.82	5.73
P2O5	0.23	0.29	0.29	0.27	0.42	0.25	0.29	0.24	0.28	0.33
F (ppm)	2520	840	1600	2170	3890	1950	1750	430	430	740
SO2	0.08	0.07	0.06	0.08	0.07	0.07	0.11	0.06	0.09	0.11
Cl (ppm)	1960	1630	1660	1640	1760	1520	1460	1510	1520	1630
Total	100.19	99.48	100.06	100.22	100.68	99.24	98.87	97.88	99.60	99.95

Table C3.37.2 Microprobe data for sample EBT-40b corrected to 100%

Analysis	1	2	3	4	5	6	7	8*	9*	10
SiO2	54.52	54.93	54.83	54.24	54.49	54.31	54.57	54.31	54.83	54.75
TiO2	1.07	1.05	1.06	1.01	1.02	1.01	1.02	0.95	1.01	0.92
Al2O3	20.30	20.06	20.01	20.24	20.19	20.25	20.28	20.26	19.98	20.15
FeO	5.46	5.48	5.43	5.74	5.43	5.46	5.58	5.65	5.39	5.52
MnO	0.28	0.16	0.35	0.30	0.26	0.24	0.22	0.18	0.28	0.30
MgO	0.88	0.84	0.90	0.87	0.85	0.86	0.91	0.90	0.82	0.88
CaO	2.02	1.93	1.95	2.09	1.98	1.94	1.99	2.00	1.87	1.91
Na2O	9.10	9.23	9.02	9.23	9.06	9.37	9.11	9.36	9.27	9.02
K2O	5.61	5.70	5.77	5.55	5.67	5.87	5.60	5.73	5.83	5.73
P2O5	0.22	0.29	0.29	0.27	0.42	0.25	0.29	0.24	0.28	0.33
F (ppm)	2515	844	1599	2165	3864	1965	1770	2142	2105	2098
SO2	0.08	0.07	0.06	0.08	0.07	0.07	0.11	0.06	0.09	0.11
Cl (ppm)	1956	1638	1659	1636	1748	1532	1477	1540	1524	1629
Total	100.00	100.00	100.00	100.00	100.00	100.00	100.00	100.00	100.00	100.00

*Fluorine corrected to an average of 2100 ppm

Table C3.37.3 Microprobe data for sample EBT-40b corrected for sodium loss

Analysis	1	2	3	4	5	6	7	8	9	10	Mean	StdDev
Correction	0.997823	0.99911	0.9969597	0.99906	0.99742	1.00054	0.99787	1.00039	0.99947	0.99702		
SiO2	54.41	54.88	54.67	54.19	54.35	54.34	54.46	54.33	54.80	54.59	54.50	0.22
TiO2	1.07	1.05	1.05	1.01	1.02	1.01	1.02	0.95	1.01	0.92	1.01	0.05
Al2O3	20.26	20.04	19.95	20.23	20.14	20.26	20.23	20.27	19.97	20.09	20.14	0.12
FeO	5.45	5.48	5.41	5.74	5.42	5.47	5.57	5.65	5.38	5.50	5.51	0.11
MnO	0.28	0.16	0.35	0.30	0.26	0.24	0.22	0.18	0.28	0.30	0.26	0.06
MgO	0.87	0.84	0.90	0.87	0.84	0.86	0.91	0.90	0.82	0.88	0.87	0.03
CaO	2.02	1.92	1.94	2.09	1.98	1.94	1.99	2.00	1.87	1.91	1.97	0.06
Na2O	9.32	9.32	9.32	9.32	9.32	9.32	9.32	9.32	9.32	9.32	9.32	0.00
K2O	5.60	5.69	5.75	5.55	5.66	5.88	5.59	5.74	5.83	5.71	5.70	0.10
P2O5	0.22	0.29	0.29	0.27	0.42	0.25	0.29	0.24	0.28	0.33	0.29	0.05
F (ppm)	2510	844	1594	2163	3854	1966	1766	2143	2104	2092	2104	761
SO2	0.08	0.07	0.06	0.08	0.07	0.07	0.11	0.06	0.09	0.11	0.08	0.02
Cl (ppm)	1952	1637	1654	1635	1744	1533	1474	1541	1523	1624	1631	138
Total	100.02	100.01	100.03	100.01	100.02	99.99	100.02	100.00	100.00	100.03	100.01	

Table C3.38.3 Microprobe data for sample EBT-40c corrected for sodium loss

Analysis	1	2	3	4	5	6	7	8	9	10	Mean	StdDev
Correction	0.999049	0.99994	1.00004	0.99961	0.99962	0.99997	0.99856	1.0001698	1.000802	0.9992		
SiO2	54.41	54.06	54.06	54.39	54.36	53.74	55.03	53.83	54.00	54.41	54.31	0.38
TiO2	0.97	1.13	1.02	1.02	1.09	1.09	0.94	0.97	1.11	1.14	1.05	0.07
Al2O3	20.19	20.33	20.35	20.31	20.16	20.23	20.23	20.36	20.29	20.16	20.25	0.08
FeO	5.54	5.55	5.64	5.53	5.53	5.69	4.89	5.34	5.47	5.44	5.48	0.25
MnO	0.21	0.17	0.23	0.23	0.27	0.13	0.19	0.15	0.32	0.21	0.20	0.04
MgO	0.93	0.86	0.90	0.89	0.89	0.92	0.77	0.86	0.86	0.91	0.88	0.05
CaO	1.94	1.92	2.01	1.93	1.97	2.25	1.80	2.11	1.99	1.93	1.97	0.13
Na2O	9.36	9.36	9.36	9.36	9.36	9.36	9.36	9.36	9.36	9.36	9.36	0.00
K2O	5.76	5.73	5.67	5.66	5.60	5.77	5.95	5.73	5.89	5.62	5.72	0.11
P2O5	0.29	0.34	0.39	0.24	0.30	0.35	0.23	0.27	0.25	0.31	0.31	0.05
F (ppm)	1967	3044	1092	1618	2305	2412	3742	3631	2096	2750	2366	832
SO2	0.07	0.07	0.11	0.10	0.10	0.08	0.07	0.28	0.09	0.10	0.09	0.02
Cl (ppm)	1405	1683	1699	1819	1574	1445	1609	3662	1554	1538	1597	137
Total	100.01	100.00	100.00	100.00	100.00	100.00	100.01	100.00	99.99	100.01	100.00	

Table C3.39.1 Raw microprobe data for sample EBT-40d

Analysis	1	2	3	4	5	6	7	8	9	10
SiO2	55.61	54.46	54.56	54.24	55.78	55.78	54.85	55.94	54.66	55.63
TiO2	1.00	1.08	0.99	1.06	1.02	1.04	1.04	1.07	1.10	1.07
Al2O3	20.18	20.31	20.44	20.44	20.51	20.48	20.33	20.39	20.41	20.14
FeO	5.56	5.54	5.45	5.41	5.59	5.60	5.74	5.41	5.53	5.44
MnO	0.20	0.25	0.26	0.23	0.29	0.17	0.28	0.25	0.31	0.26
MgO	0.94	0.95	0.88	0.98	0.92	1.30	1.00	0.91	0.93	0.91
CaO	2.01	2.03	1.91	2.05	2.00	2.03	2.08	1.96	1.96	2.08
Na2O	8.91	9.04	9.00	9.18	9.07	9.14	9.02	9.07	9.00	9.17
K2O	5.70	5.68	5.73	5.67	5.67	5.81	5.63	5.73	5.68	5.71
P2O5	0.29	0.31	0.30	0.30	0.34	0.26	0.35	0.28	0.34	0.31
F (ppm)	1500	2480	2600	970	3050	n.d.	1410	2460	1480	2000
SO2	0.08	0.09	0.09	0.07	0.07	0.07	0.08	0.10	0.05	0.07
Cl (ppm)	1500	1550	1570	1440	1570	1690	1610	1460	1640	1550
Total	100.78	100.14	100.01	99.86	101.71	101.84	100.70	101.50	100.27	101.15

Table C3.39.2 Microprobe data for sample EBT-40d corrected to 100%

Analysis	1	2	3	4	5	6*	7	8	9	10
SiO2	55.18	54.39	54.55	54.31	54.84	54.67	54.47	55.11	54.51	55.00
TiO2	0.99	1.08	0.99	1.06	1.01	1.02	1.04	1.06	1.10	1.06
Al2O3	20.02	20.28	20.43	20.47	20.16	20.07	20.19	20.08	20.36	19.91
FeO	5.52	5.53	5.45	5.42	5.49	5.49	5.70	5.33	5.52	5.38
MnO	0.20	0.24	0.26	0.23	0.28	0.16	0.27	0.24	0.31	0.26
MgO	0.93	0.94	0.88	0.98	0.91	1.27	1.00	0.90	0.93	0.89
CaO	1.99	2.02	1.91	2.05	1.96	1.99	2.06	1.93	1.95	2.06
Na2O	8.84	9.03	8.99	9.20	8.91	8.95	8.96	8.94	8.98	9.07
K2O	5.66	5.68	5.73	5.68	5.57	5.70	5.59	5.64	5.66	5.65
P2O5	0.29	0.31	0.30	0.30	0.33	0.26	0.34	0.27	0.34	0.30
F (ppm)	1488	2477	2600	971	2999	1950	1400	2424	1476	1977
SO2	0.08	0.09	0.09	0.07	0.07	0.07	0.08	0.10	0.04	0.07
Cl (ppm)	1488	1548	1570	1442	1544	1656	1599	1438	1636	1532
Total	100.00	100.00	100.00	100.00	100.00	100.00	100.00	100.00	100.00	100.00

*Flourine corrected to an average of 1994 ppm

Table C3.39.3 Microprobe data for sample EBT-40d corrected for sodium loss

Analysis	1	2	3	4	5	6	7	8	9	10	Mean	StdDev
Correction	0.997121	0.99898	0.99863	1.00064	0.99782	0.99823	0.99825	0.99807	0.99845	0.999359		
SiO2	55.02	54.33	54.48	54.34	54.72	54.57	54.37	55.01	54.43	54.96	54.62	0.28
TiO2	0.99	1.08	0.98	1.06	1.00	1.02	1.03	1.05	1.09	1.06	1.04	0.04
Al2O3	19.96	20.26	20.41	20.48	20.12	20.03	20.15	20.04	20.33	19.89	20.17	0.19
FeO	5.50	5.52	5.44	5.42	5.48	5.48	5.69	5.32	5.51	5.38	5.48	0.10
MnO	0.20	0.24	0.26	0.23	0.28	0.16	0.27	0.24	0.31	0.26	0.25	0.04
MgO	0.93	0.94	0.88	0.98	0.90	1.27	1.00	0.90	0.93	0.89	0.96	0.11
CaO	1.98	2.02	1.90	2.05	1.96	1.98	2.06	1.93	1.95	2.06	1.99	0.06
Na2O	9.13	9.13	9.13	9.13	9.13	9.13	9.13	9.13	9.13	9.13	9.13	0.00
K2O	5.64	5.67	5.72	5.68	5.56	5.69	5.58	5.63	5.65	5.64	5.65	0.05
P2O5	0.29	0.31	0.30	0.30	0.33	0.26	0.34	0.27	0.33	0.30	0.30	0.03
F (ppm)	1484	2474	2596	972	2992	1947	1398	2419	1474	1976	1973	641
SO2	0.08	0.09	0.09	0.07	0.07	0.07	0.08	0.10	0.04	0.07	0.08	0.02
Cl (ppm)	1484	1546	1568	1443	1540	1653	1596	1436	1633	1531	1543	74
Total	100.03	100.01	100.01	99.99	100.02	100.02	100.02	100.02	100.01	100.01	100.01	100.01

Table C3.40.1 Raw microprobe data for sample EBT-41

Analysis	1	2	3	4	5	6	7	8	9	10
SiO2	54.68	55.74	55.85	55.60	54.40	55.14	54.43	55.57	55.66	55.78
TiO2	0.94	1.00	1.04	0.98	1.00	1.01	1.00	1.02	1.04	0.99
Al2O3	19.75	20.35	20.22	20.11	20.00	20.32	20.15	20.38	20.45	20.48
FeO	5.62	5.45	5.56	5.46	6.02	5.51	5.52	5.55	5.51	5.41
MnO	0.25	0.17	0.27	0.25	0.24	0.35	0.35	0.23	0.23	0.32
MgO	0.82	0.89	0.86	0.92	0.78	0.87	0.98	0.90	0.88	0.94
CaO	1.93	1.92	1.93	1.94	1.99	1.96	1.85	1.85	1.98	1.94
Na2O	9.35	9.34	9.41	9.18	9.53	9.20	9.27	9.19	9.34	9.10
K2O	5.66	5.86	5.63	5.77	5.76	5.55	5.60	5.73	5.79	5.78
P2O5	0.24	0.29	0.34	0.36	0.31	0.35	0.25	0.26	0.25	0.31
F (ppm)	3040	3070	130	2440	2290	2300	2960	1210	n.d.	690
SO2	0.09	0.07	0.10	0.10	0.08	0.05	0.08	0.07	0.10	0.08
Cl (ppm)	1830	1750	1330	1500	1230	1690	1560	1810	1650	1680
Total	99.83	101.55	101.34	101.06	100.45	100.70	99.94	101.04	101.39	101.36

Table C3.40.2 Microprobe data for sample EBT-41 corrected to 100%

Analysis	1	2	3	4	5	6	7	8	9*	10*
SiO2	54.78	54.89	54.99	55.01	54.16	54.76	54.46	54.99	54.77	54.94
TiO2	0.94	0.98	1.02	0.97	0.99	1.00	1.00	1.01	1.02	0.97
Al2O3	19.78	20.04	19.91	19.90	19.91	20.18	20.16	20.16	20.12	20.17
FeO	5.63	5.37	5.47	5.40	5.99	5.47	5.52	5.49	5.42	5.32
MnO	0.25	0.17	0.27	0.25	0.24	0.35	0.35	0.23	0.23	0.32
MgO	0.83	0.87	0.84	0.91	0.77	0.86	0.98	0.89	0.87	0.92
CaO	1.93	1.89	1.90	1.92	1.98	1.95	1.85	1.83	1.94	1.91
Na2O	9.37	9.20	9.26	9.08	9.49	9.14	9.28	9.09	9.19	8.96
K2O	5.67	5.77	5.54	5.71	5.73	5.51	5.60	5.67	5.70	5.69
P2O5	0.24	0.28	0.33	0.36	0.31	0.35	0.25	0.26	0.25	0.31
F (ppm)	3045	3023	2432	2414	2280	2284	2962	1198	2430	2433
SO2	0.09	0.07	0.10	0.10	0.07	0.05	0.08	0.07	0.09	0.08
Cl (ppm)	1833	1723	1309	1484	1225	1678	1561	1791	1623	1655
Total	100.00	100.00	100.00	100.00	100.00	100.00	100.00	100.00	100.00	100.00

*Flourine corrected to an average of 2473 ppm

Table C3.40.3 Microprobe data for sample EBT-41 corrected for sodium loss

Analysis	1	2	3	4	5	6	7	8	9	10	Mean	StdDev
Correction	0.999393	0.99768	0.99835	0.99656	1.00061	0.99708	0.99851	0.99665	0.99758	0.995352		
SiO2	54.74	54.77	54.90	54.82	54.19	54.60	54.38	54.81	54.63	54.68	54.65	0.22
TiO2	0.94	0.98	1.02	0.97	0.99	1.00	1.00	1.01	1.02	0.97	0.99	0.02
Al2O3	19.77	19.99	19.87	19.83	19.92	20.12	20.13	20.10	20.07	20.08	19.99	0.13
FeO	5.63	5.36	5.46	5.39	6.00	5.45	5.52	5.47	5.41	5.30	5.50	0.20
MnO	0.25	0.17	0.27	0.25	0.24	0.34	0.34	0.23	0.23	0.32	0.26	0.06
MgO	0.82	0.87	0.84	0.90	0.77	0.86	0.98	0.88	0.86	0.92	0.87	0.06
CaO	1.93	1.89	1.90	1.91	1.98	1.94	1.85	1.83	1.94	1.90	1.91	0.05
Na2O	9.43	9.43	9.43	9.43	9.43	9.43	9.43	9.43	9.43	9.43	9.43	0.00
K2O	5.67	5.76	5.53	5.69	5.73	5.49	5.60	5.65	5.68	5.66	5.65	0.08
P2O5	0.24	0.28	0.33	0.36	0.31	0.34	0.25	0.26	0.25	0.31	0.29	0.04
F (ppm)	3043	3016	2428	2406	2281	2277	2957	1194	2424	2421	2445	534
SO2	0.09	0.07	0.10	0.10	0.07	0.05	0.08	0.07	0.09	0.08	0.08	0.01
Cl (ppm)	1832	1719	1307	1479	1225	1673	1559	1785	1619	1647	1585	197
Total	100.01	100.02	100.02	100.03	99.99	100.03	100.01	100.03	100.02	100.04	100.02	

Table C3.41.3 Microprobe data for sample EBT-43 corrected for sodium loss

Analysis	1	2	3	4	5	6	7	8	9	10	Mean	StdDev
Correction	0.999732	0.9962601	0.99570	0.97523	0.99586	0.99602	0.99630	1.00027	0.99588	0.995566		
SiO2	55.45	55.15	55.31	53.94	55.31	55.17	55.48	55.22	55.51	55.58	55.35	0.16
TiO2	0.96	1.04	0.95	0.99	0.95	1.05	0.99	1.06	1.09	1.01	1.01	0.05
Al2O3	20.18	20.33	20.50	20.06	20.35	20.34	20.15	20.22	20.08	20.29	20.27	0.13
FeO	5.34	5.25	5.14	5.50	5.31	5.43	5.34	5.62	5.34	5.30	5.34	0.13
MnO	0.18	0.24	0.17	0.37	0.30	0.29	0.24	0.28	0.23	0.12	0.23	0.06
MgO	0.88	1.03	0.88	0.93	0.88	0.89	0.93	0.85	0.87	0.88	0.90	0.05
CaO	1.86	1.83	1.85	1.97	1.86	1.80	1.83	1.77	1.79	1.84	1.82	0.03
Na2O	8.97	8.97	8.97	8.97	8.97	8.97	8.97	8.97	8.97	8.97	8.97	0.00
K2O	5.43	5.53	5.60	5.72	5.41	5.42	5.50	5.46	5.44	5.38	5.46	0.07
P2O5	0.32	0.19	0.29	0.28	0.27	0.24	0.24	0.15	0.23	0.22	0.24	0.05
F (ppm)	2392	2341	1439	12875	2015	2214	1098	1802	2195	2179	1964	439
SO2	0.05	0.07	0.06	0.07	0.08	0.07	0.10	0.07	0.11	0.09	0.08	0.02
Cl (ppm)	1330	1617	1679	1522	1511	1393	1493	1512	1374	1503	1490	112
Total	100.00	100.03	100.04	100.22	100.04	100.04	100.03	100.00	100.04	100.04	100.03	100.03

Table C3.42.1 Raw microprobe data for sample EBT-44

Analysis	1	2	3	4	5	6	7	8	9	10
SiO2	55.72	54.80	56.62	57.39	54.44	55.96	56.27	56.51	54.61	55.15
TiO2	0.98	1.02	0.98	1.11	1.02	1.00	1.01	1.08	0.94	1.04
Al2O3	20.14	20.24	20.43	20.88	20.41	20.47	20.47	20.63	20.20	20.61
FeO	5.64	5.39	5.55	5.54	5.40	5.57	5.45	5.45	5.52	5.54
MnO	0.24	0.21	0.27	0.21	0.30	0.23	0.31	0.23	0.26	0.26
MgO	0.85	0.93	0.87	0.91	1.25	1.32	0.90	1.04	0.91	0.94
CaO	1.86	1.87	1.93	1.90	1.92	1.85	1.84	1.89	1.90	0.43
Na2O	9.04	8.99	8.79	9.51	9.08	8.82	9.02	8.78	9.23	7.79
K2O	5.45	5.55	5.33	5.72	5.58	5.39	5.46	5.52	5.45	6.10
P2O5	0.26	0.28	0.34	0.25	0.24	0.36	0.27	0.27	0.23	0.23
F (ppm)	3030	n.d.	1160	520	1580	1330	2340	1310	1850	2880
SO2	0.12	0.14	0.07	0.12	0.10	0.08	0.10	0.05	0.04	0.16
Cl (ppm)	1310	1510	1400	1280	1500	1520	1400	1210	1390	1260
Total	100.72	99.57	101.43	103.73	100.06	101.33	101.46	101.71	99.61	98.67

Table C3.42.2 Microprobe data for sample EBT-44 corrected to 100%

Analysis	1	2*	3	4	5	6	7	8	9	10
SiO2	55.32	54.93	55.82	55.33	54.41	55.22	55.46	55.56	54.82	55.89
TiO2	0.97	1.02	0.96	1.07	1.02	0.98	1.00	1.07	0.95	1.05
Al2O3	19.99	20.29	20.14	20.13	20.40	20.21	20.17	20.28	20.28	20.89
FeO	5.59	5.40	5.47	5.34	5.40	5.49	5.37	5.36	5.54	5.61
MnO	0.23	0.21	0.26	0.21	0.30	0.23	0.31	0.23	0.26	0.27
MgO	0.85	0.93	0.86	0.87	1.25	1.30	0.88	1.02	0.91	0.95
CaO	1.84	1.88	1.90	1.83	1.91	1.82	1.81	1.86	1.91	0.43
Na2O	8.98	9.01	8.66	9.17	9.08	8.71	8.89	8.63	9.27	7.89
K2O	5.41	5.57	5.26	5.52	5.58	5.32	5.38	5.43	5.47	6.19
P2O5	0.26	0.28	0.33	0.24	0.24	0.36	0.27	0.27	0.23	0.24
F (ppm)	3008	1945	1144	501	1579	1313	2306	1288	1857	2919
SO2	0.12	0.14	0.07	0.12	0.09	0.07	0.09	0.05	0.04	0.17
Cl (ppm)	1301	1514	1380	1234	1499	1500	1380	1190	1395	1277
Total	100.00	100.00	100.00	100.00	100.00	100.00	100.00	100.00	100.00	100.00

*Fluorine corrected to an average of 1935 ppm

Table C3.42.3 Microprobe data for sample EBT-44 corrected for sodium loss

Analysis	1	2	3	4	5	6	7	8	9	10	Mean	StdDev
Correction	0.998056	0.998378	0.99494	0.99993	0.99906	0.99534	0.99714	0.99461	1.00094	0.987374		
SiO2	55.21	54.84	55.54	55.33	54.36	54.97	55.30	55.26	54.87	55.19	55.06	0.34
TiO2	0.97	1.02	0.96	1.07	1.02	0.98	0.99	1.06	0.95	1.04	1.00	0.04
Al2O3	19.96	20.25	20.04	20.13	20.38	20.11	20.11	20.17	20.29	20.62	20.22	0.20
FeO	5.58	5.39	5.44	5.34	5.39	5.47	5.35	5.33	5.55	5.54	5.45	0.09
MnO	0.23	0.21	0.26	0.21	0.30	0.23	0.30	0.22	0.26	0.26	0.25	0.03
MgO	0.85	0.93	0.85	0.87	1.25	1.30	0.88	1.02	0.91	0.94	0.99	0.17
CaO	1.84	1.88	1.90	1.83	1.91	1.81	1.81	1.85	1.91	0.43	1.70	0.48
Na2O	9.17	9.17	9.17	9.17	9.17	9.17	9.17	9.17	9.17	9.17	9.17	0.00
K2O	5.40	5.56	5.23	5.52	5.57	5.30	5.37	5.40	5.48	6.11	5.49	0.26
P2O5	0.26	0.28	0.33	0.24	0.24	0.36	0.27	0.27	0.23	0.23	0.27	0.04
F (ppm)	3002	1941	1138	501	1578	1306	2300	1281	1859	2882	1921	685
SO2	0.12	0.14	0.07	0.12	0.09	0.07	0.09	0.05	0.04	0.16	0.09	0.04
Cl (ppm)	1298	1511	1373	1234	1498	1493	1376	1183	1397	1261	1377	114
Total	100.02	100.01	100.05	100.00	100.01	100.04	100.03	100.05	99.99	100.12	100.03	

Table C3.43.3 Microprobe data for sample EBT-45 corrected for sodium loss

Analysis	1	2	3	4	5	6	7	8	9	10	Mean	StdDev
Correction	0.995485	0.9996716	0.99693	0.99962	0.99615	1.00033	0.99870	0.99600	1.00156	0.999345		
SiO2	55.51	55.50	55.67	54.70	55.51	55.54	55.19	55.35	55.65	55.23	55.39	0.29
TiO2	0.95	0.97	1.04	1.06	1.02	1.05	0.96	0.97	1.09	1.10	1.02	0.06
Al2O3	20.20	20.03	20.21	20.47	20.21	20.03	19.98	20.21	20.13	20.32	20.18	0.15
FeO	5.36	5.50	5.28	5.34	4.79	5.38	5.61	5.38	5.31	5.32	5.33	0.21
MnO	0.24	0.18	0.30	0.34	0.23	0.26	0.33	0.26	0.23	0.23	0.26	0.05
MgO	0.87	0.87	0.88	0.98	0.77	0.85	0.86	0.86	0.86	0.90	0.87	0.05
CaO	1.88	1.85	1.84	1.92	1.82	1.82	1.93	1.88	1.87	1.84	1.87	0.04
Na2O	8.88	8.88	8.88	8.88	8.88	8.88	8.88	8.88	8.88	8.88	8.88	0.00
K2O	5.42	5.55	5.33	5.51	5.88	5.52	5.54	5.60	5.40	5.54	5.53	0.15
P2O5	0.17	0.25	0.20	0.30	0.21	0.22	0.29	0.25	0.26	0.15	0.23	0.05
F (ppm)	3042	1765	1915	1881	5098	1675	2599	1358	807	2366	2251	1182
SO2	0.12	0.10	0.08	0.14	0.07	0.13	0.01	0.12	0.08	0.09	0.09	0.04
Cl (ppm)	1309	1432	1313	1578	1322	1515	1564	1407	1315	1715	1447	141
Total	100.04	100.00	100.03	100.00	100.03	100.00	100.01	100.04	99.99	100.01	100.01	100.01

Table C3.44.3 Microprobe data for sample EBT-47 corrected for sodium loss

Analysis	1	2	3	4	5	6	7	8	9	10	Mean	StdDev
Correction	0.99721	0.99709	0.99643	0.99538	0.99960	0.99935	1.00039	0.99750	0.99632	0.99767		
SiO2	54.86	55.11	54.78	54.91	54.83	54.61	54.66	54.83	54.55	55.01	54.84	0.16
TiO2	1.00	1.04	1.08	1.08	1.06	1.09	1.08	1.09	0.96	1.05	1.06	0.03
Al2O3	20.11	19.96	20.02	20.05	20.02	20.13	19.95	19.92	19.93	19.94	20.01	0.07
FeO	5.43	5.45	5.51	5.46	5.56	5.46	5.47	5.41	5.33	5.46	5.47	0.04
MnO	0.20	0.26	0.21	0.20	0.28	0.27	0.23	0.31	0.23	0.18	0.24	0.04
MgO	0.94	0.91	0.87	0.93	0.93	0.95	0.84	0.96	1.49	0.88	0.91	0.04
CaO	2.08	1.96	2.03	2.10	1.93	2.09	1.85	2.02	1.98	2.06	2.01	0.08
Na2O	9.17	9.17	9.17	9.17	9.17	9.17	9.17	9.17	9.17	9.17	9.17	0.00
K2O	5.68	5.53	5.72	5.66	5.63	5.52	5.80	5.57	5.65	5.70	5.65	0.09
P2O5	0.26	0.24	0.33	0.22	0.27	0.33	0.33	0.26	0.26	0.30	0.28	0.04
F (ppm)	926	1648	925	456	916	1502	3628	2531	1973	541	1453	1037
SO2	0.08	0.06	0.05	0.08	0.07	0.08	0.09	0.07	0.11	0.08	0.07	0.01
Cl (ppm)	1399	1658	1595	1526	1652	1662	1592	1521	1709	1563	1574	85
Total	100.03	100.03	100.03	100.04	100.00	100.01	100.00	100.02	100.03	100.02	100.02	100.02

Table C3.45.1 Raw microprobe data for sample EBT-48

Analysis	1	2	3	4	5	6	7	8	9	10
SiO ₂	55.24	55.60	55.66	55.09	54.77	54.91	54.81	54.70	55.39	55.05
TiO ₂	1.06	1.13	1.05	1.06	1.09	1.06	1.13	1.02	1.09	1.09
Al ₂ O ₃	20.37	20.30	20.54	20.61	20.34	20.41	20.25	20.29	20.52	20.44
FeO	5.67	5.54	5.57	5.48	5.53	5.64	5.49	5.61	5.45	5.70
MnO	0.24	0.34	0.28	0.22	0.27	0.23	0.42	0.26	0.31	0.22
MgO	0.96	0.97	0.94	0.94	0.94	0.99	0.96	1.20	0.93	0.93
CaO	2.09	2.00	2.00	2.12	2.10	2.07	2.00	2.06	2.09	2.00
Na ₂ O	9.07	9.03	9.18	9.10	9.39	9.00	9.38	9.18	8.97	9.22
K ₂ O	5.61	5.99	5.73	5.70	5.68	5.79	5.79	5.72	5.77	5.82
P ₂ O ₅	0.31	0.32	0.32	0.31	0.33	0.31	0.34	0.32	0.34	0.25
F (ppm)	3970	3300	1830	1330	1330	1210	1780	1360	1200	470
SO ₂	0.08	0.10	0.07	0.06	0.11	0.11	0.09	0.08	0.08	0.10
Cl (ppm)	1460	1450	1410	1300	1360	1700	1760	1440	1670	1370
Total	101.23	101.79	101.67	100.96	100.82	100.81	101.01	100.73	101.22	101.01

Table C3.45.2 Microprobe data for sample EBT-48 corrected to 100%

Analysis	1	2	3	4	5	6	7	8	9	10*
SiO ₂	54.57	54.62	54.75	54.57	54.32	54.47	54.26	54.31	54.72	54.42
TiO ₂	1.04	1.11	1.04	1.05	1.08	1.05	1.12	1.02	1.08	1.08
Al ₂ O ₃	20.12	19.95	20.21	20.42	20.17	20.25	20.05	20.14	20.27	20.21
FeO	5.60	5.44	5.48	5.43	5.49	5.59	5.44	5.56	5.38	5.63
MnO	0.24	0.33	0.28	0.22	0.27	0.23	0.42	0.26	0.30	0.22
MgO	0.95	0.96	0.92	0.93	0.93	0.98	0.95	1.19	0.92	0.92
CaO	2.07	1.97	1.97	2.10	2.08	2.06	1.98	2.04	2.06	1.98
Na ₂ O	8.96	8.87	9.03	9.02	9.32	8.93	9.29	9.11	8.86	9.12
K ₂ O	5.54	5.88	5.63	5.65	5.63	5.74	5.73	5.68	5.70	5.75
P ₂ O ₅	0.30	0.32	0.31	0.31	0.33	0.31	0.33	0.32	0.34	0.25
F (ppm)	3922	3242	1800	1317	1319	1200	1762	1350	1185	1898
SO ₂	0.08	0.09	0.07	0.06	0.11	0.11	0.09	0.08	0.07	0.10
Cl (ppm)	1442	1425	1387	1288	1349	1686	1742	1430	1650	1354
Total	100.00	100.00	100.00	100.00	100.00	100.00	100.00	100.00	100.00	100.00

*Flourine corrected to an average of 1925 ppm

Table C3.45.3 Microprobe data for sample EBT-48 corrected for sodium loss

Analysis	1	2	3	4	5	6	7	8	9	10	Mean	StdDev
Correction	0.99655	0.99570	0.99730	0.99716	1.00013	0.99626	0.99986	0.99810	0.99559	0.99815		
SiO2	54.38	54.38	54.60	54.41	54.33	54.27	54.26	54.21	54.48	54.32	54.36	0.12
TiO2	1.04	1.10	1.03	1.05	1.08	1.05	1.12	1.01	1.07	1.07	1.06	0.03
Al2O3	20.05	19.86	20.15	20.36	20.18	20.17	20.04	20.10	20.18	20.17	20.13	0.13
FeO	5.58	5.41	5.46	5.42	5.49	5.57	5.44	5.55	5.36	5.62	5.49	0.09
MnO	0.24	0.33	0.27	0.22	0.27	0.23	0.42	0.26	0.30	0.22	0.28	0.06
MgO	0.94	0.95	0.92	0.93	0.93	0.98	0.95	1.19	0.92	0.92	0.96	0.08
CaO	2.06	1.96	1.96	2.09	2.08	2.05	1.98	2.04	2.05	1.98	2.02	0.05
Na2O	9.30	9.30	9.30	9.30	9.30	9.30	9.30	9.30	9.30	9.30	9.30	0.00
K2O	5.52	5.86	5.62	5.63	5.64	5.72	5.73	5.67	5.68	5.74	5.68	0.09
P2O5	0.30	0.31	0.31	0.31	0.33	0.31	0.33	0.32	0.34	0.25	0.31	0.02
F (ppm)	3908	3228	1795	1314	1319	1196	1762	1348	1180	1895	1894	933
SO2	0.08	0.09	0.07	0.06	0.11	0.10	0.09	0.08	0.07	0.10	0.09	0.02
Cl (ppm)	1437	1418	1383	1284	1349	1680	1742	1427	1643	1352	1472	158
Total	100.03	100.04	100.03	100.03	100.00	100.03	100.00	100.02	100.04	100.02	100.02	100.02

Table C3.46.1 Raw microprobe data for sample EBT-49

Analysis	1	2	3	4	5	6	7	8	9	10
SiO ₂	54.98	55.56	55.50	54.35	55.46	55.02	54.83	54.60	54.93	54.67
TiO ₂	1.06	1.14	1.14	1.08	1.02	1.11	1.09	1.05	1.06	1.13
Al ₂ O ₃	20.25	19.48	20.38	20.13	20.16	20.33	20.35	19.06	20.12	20.35
FeO	5.39	5.56	5.53	5.68	5.50	5.55	5.58	5.54	5.67	5.61
MnO	0.33	0.15	0.32	0.27	0.20	0.18	0.20	0.26	0.15	0.20
MgO	0.94	1.02	1.00	0.91	0.91	0.96	0.95	0.92	0.95	0.93
CaO	2.24	2.09	2.06	2.23	2.06	2.08	2.09	2.10	2.05	2.08
Na ₂ O	8.99	8.97	9.07	9.19	8.98	8.84	8.99	9.35	9.38	9.13
K ₂ O	5.90	5.70	5.69	5.82	5.60	5.75	5.70	5.75	5.74	5.72
P ₂ O ₅	0.32	0.27	0.29	0.35	0.39	0.40	0.36	0.33	0.30	0.32
F (ppm)	1310	2860	970	1550	2710	270	2110	0.274	3210	1670
SO ₂	0.09	0.08	0.07	0.12	0.05	0.09	0.06	0.09	0.08	0.08
Cl (ppm)	1570	1510	1520	1690	1510	1660	1770	1570	1690	1580
Total	100.77	100.45	101.30	100.45	100.75	100.50	100.58	99.47	100.92	100.55

Table C3.46.2 Microprobe data for sample EBT-49 corrected to 100%

Analysis	1	2	3	4	5	6*	7	8	9	10
SiO ₂	54.56	55.32	54.79	54.11	55.05	54.65	54.51	54.89	54.43	54.37
TiO ₂	1.06	1.13	1.13	1.07	1.01	1.10	1.08	1.05	1.05	1.13
Al ₂ O ₃	20.10	19.39	20.12	20.04	20.01	20.19	20.23	19.16	19.94	20.23
FeO	5.35	5.54	5.46	5.65	5.46	5.51	5.55	5.56	5.62	5.58
MnO	0.33	0.14	0.31	0.27	0.20	0.18	0.20	0.26	0.15	0.20
MgO	0.93	1.02	0.98	0.90	0.91	0.95	0.95	0.93	0.94	0.93
CaO	2.22	2.08	2.03	2.22	2.04	2.06	2.08	2.11	2.03	2.07
Na ₂ O	8.92	8.93	8.96	9.15	8.91	8.78	8.93	9.40	9.30	9.07
K ₂ O	5.85	5.67	5.62	5.80	5.56	5.71	5.67	5.78	5.69	5.69
P ₂ O ₅	0.32	0.27	0.29	0.34	0.39	0.40	0.36	0.34	0.30	0.31
F (ppm)	1300	2847	958	1543	2690	2116	2098	2755	3181	1661
SO ₂	0.08	0.07	0.07	0.12	0.05	0.09	0.06	0.09	0.08	0.08
Cl (ppm)	1558	1503	1500	1682	1499	1649	1760	1578	1675	1571
Total	100.00	100.00	100.00	100.00	100.00	100.00	100.00	100.00	100.00	100.00

*Fluorine corrected to an average of 2130 ppm

Table C3.46.3 Microprobe data for sample EBT-49 corrected for sodium loss

Analysis	1	2	3	4	5	6	7	8	9	10	Mean	StdDev
Correction	0.99571	0.9958399	0.9960695	0.9979545	0.9955987	0.9942853	0.9958564	1.0005267	0.999468	0.997258		
SiO2	54.33	55.09	54.57	54.00	54.81	54.34	54.29	54.91	54.40	54.22	54.49	0.34
TiO2	1.05	1.13	1.12	1.07	1.01	1.09	1.07	1.05	1.05	1.12	1.08	0.04
Al2O3	20.01	19.31	20.04	20.00	19.92	20.08	20.15	19.17	19.93	20.18	19.88	0.35
FeO	5.33	5.52	5.44	5.64	5.44	5.48	5.52	5.57	5.62	5.56	5.51	0.09
MnO	0.32	0.14	0.31	0.27	0.20	0.18	0.20	0.26	0.15	0.20	0.22	0.06
MgO	0.93	1.01	0.98	0.90	0.90	0.95	0.94	0.93	0.94	0.93	0.94	0.03
CaO	2.21	2.07	2.02	2.22	2.03	2.05	2.07	2.11	2.03	2.06	2.09	0.07
Na2O	9.35	9.35	9.35	9.35	9.35	9.35	9.35	9.35	9.35	9.35	9.35	0.00
K2O	5.82	5.65	5.59	5.78	5.54	5.68	5.64	5.78	5.69	5.68	5.69	0.09
P2O5	0.32	0.27	0.29	0.34	0.39	0.39	0.36	0.34	0.30	0.31	0.33	0.04
F (ppm)	1294	2835	954	1540	2678	2104	2089	2756	3179	1656	2109	741
SO2	0.08	0.07	0.07	0.12	0.05	0.09	0.06	0.09	0.08	0.08	0.08	0.02
Cl (ppm)	1551	1497	1495	1679	1492	1639	1752	1579	1674	1567	1593	90
Total	100.04	100.04	100.04	100.02	100.04	100.05	100.04	100.00	100.00	100.03	100.03	100.03

Table C3.47.1 Raw microprobe data for sample EBT-50

Analysis	1	2	3	4	5	6	7	8	9	10
SiO2	55.26	54.07	54.91	55.39	54.88	54.09	55.09	55.57	55.74	55.57
TiO2	1.14	1.05	1.07	1.07	0.98	1.10	1.08	1.13	1.11	1.05
Al2O3	20.14	19.60	20.30	20.39	20.43	19.95	20.18	20.18	20.22	20.42
FeO	5.53	5.66	5.46	5.52	5.64	5.52	5.58	5.63	5.62	5.59
MnO	0.29	0.29	0.22	0.27	0.19	0.30	0.33	0.16	0.25	0.25
MgO	0.88	0.88	0.90	0.94	0.95	0.95	0.90	0.93	0.90	0.95
CaO	2.02	2.04	2.10	2.00	2.03	2.08	2.43	2.09	2.09	2.10
Na2O	8.92	9.27	8.89	8.96	9.14	9.24	8.32	9.17	9.09	9.27
K2O	5.85	5.77	5.78	5.82	5.81	5.73	5.52	5.66	5.76	5.83
P2O5	0.33	0.28	0.34	0.33	0.29	0.30	0.37	0.31	0.30	0.33
F (ppm)	1430	2100	1230	2590	1970	2440	6480	2940	1010	440
SO2	0.08	0.08	0.10	0.06	0.08	0.08	0.09	0.08	0.07	0.09
Cl (ppm)	1590	1400	1600	1560	1580	1640	1510	1700	1540	1560
Total	100.75	99.34	100.36	101.16	100.77	99.75	100.69	101.37	101.41	101.65

Table C3.47.2 Microprobe data for sample EBT-50 corrected to 100%

Analysis	1	2	3	4	5	6	7	8	9	10*
SiO2	54.85	54.43	54.71	54.75	54.46	54.23	54.71	54.82	54.97	54.56
TiO2	1.13	1.05	1.07	1.05	0.98	1.10	1.08	1.11	1.09	1.03
Al2O3	19.99	19.73	20.23	20.15	20.27	20.00	20.05	19.90	19.94	20.05
FeO	5.49	5.70	5.44	5.46	5.60	5.53	5.54	5.55	5.54	5.49
MnO	0.29	0.29	0.22	0.26	0.19	0.30	0.33	0.16	0.25	0.25
MgO	0.87	0.89	0.90	0.93	0.94	0.96	0.89	0.92	0.89	0.93
CaO	2.01	2.05	2.10	1.98	2.02	2.09	2.41	2.06	2.06	2.06
Na2O	8.86	9.33	8.86	8.86	9.07	9.26	8.27	9.05	8.97	9.10
K2O	5.81	5.81	5.76	5.76	5.77	5.74	5.48	5.59	5.68	5.72
P2O5	0.33	0.29	0.34	0.33	0.28	0.30	0.36	0.31	0.30	0.33
F (ppm)	1419	2114	1226	2560	1955	2446	6436	2900	996	2425
SO2	0.08	0.08	0.10	0.06	0.08	0.08	0.09	0.07	0.07	0.09
Cl (ppm)	1578	1409	1594	1542	1568	1644	1500	1677	1519	1532
Total	100.00	100.00	100.00	100.00	100.00	100.00	100.00	100.00	100.00	100.00

*Flourine corrected to an average of 2470 ppm

Table C3.47.3 Microprobe data for sample EBT-50 corrected for sodium loss

Analysis	1	2	3	4	5	6	7	8	9	10	Mean	StdDev
Correction	0.996333	1.0010469	0.9963733	0.9963244	0.998453	1.0003416	0.9905031	0.998203	0.997416	0.998764		
SiO2	54.65	54.48	54.51	54.55	54.38	54.25	54.19	54.72	54.83	54.49	54.51	0.20
TiO2	1.12	1.06	1.06	1.05	0.97	1.10	1.07	1.11	1.09	1.03	1.07	0.04
Al2O3	19.91	19.75	20.16	20.08	20.24	20.01	19.85	19.87	19.89	20.03	19.98	0.15
FeO	5.47	5.71	5.42	5.44	5.59	5.54	5.49	5.54	5.52	5.48	5.52	0.08
MnO	0.29	0.29	0.22	0.26	0.19	0.30	0.33	0.16	0.24	0.25	0.25	0.05
MgO	0.87	0.89	0.89	0.93	0.94	0.96	0.88	0.92	0.88	0.93	0.91	0.03
CaO	2.00	2.06	2.09	1.97	2.01	2.09	2.39	2.06	2.06	2.06	2.08	0.12
Na2O	9.23	9.23	9.23	9.23	9.23	9.23	9.23	9.23	9.23	9.23	9.23	0.00
K2O	5.78	5.81	5.73	5.74	5.76	5.74	5.43	5.58	5.67	5.72	5.70	0.11
P2O5	0.33	0.29	0.33	0.33	0.28	0.30	0.36	0.31	0.30	0.33	0.31	0.03
F (ppm)	1414	2116	1221	2551	1952	2447	6375	2895	993	2422	2439	1516
SO2	0.08	0.08	0.10	0.06	0.08	0.08	0.09	0.07	0.07	0.09	0.08	0.01
Cl (ppm)	1572	1411	1588	1536	1565	1645	1485	1674	1515	1530	1552	76
Total	100.03	99.99	100.03	100.03	100.01	100.00	100.09	100.02	100.02	100.01	100.02	

Table C3.48.3 Microprobe data for sample EBT-51 corrected for sodium loss

Analysis	1	2	3	4	5	6	7	8	9	10	Mean	StdDev
Correction	0.999637	1.00036	0.99874	1.00038	0.99829	0.99662	0.99895	0.99815	0.99882	0.998467		
SiO2	54.65	54.38	54.45	54.50	54.67	54.83	54.75	54.74	54.77	54.68	54.64	0.15
TiO2	1.07	1.10	1.07	1.08	1.07	1.02	1.09	1.05	1.08	1.07	1.07	0.02
Al2O3	20.09	20.18	20.11	19.95	20.14	20.00	20.05	19.93	20.03	20.14	20.06	0.08
FeO	5.48	5.53	5.56	5.50	5.44	5.46	5.56	5.51	5.46	5.47	5.50	0.04
MnO	0.14	0.21	0.22	0.27	0.21	0.22	0.23	0.20	0.20	0.22	0.21	0.03
MgO	0.92	0.93	0.95	0.90	0.94	0.97	0.92	0.92	1.00	0.90	0.94	0.03
CaO	2.05	2.06	2.07	2.03	2.04	2.08	1.97	2.01	2.02	1.92	2.02	0.05
Na2O	9.11	9.11	9.11	9.11	9.11	9.11	9.11	9.11	9.11	9.11	9.11	0.00
K2O	5.64	5.73	5.75	5.78	5.72	5.65	5.70	5.64	5.50	5.75	5.69	0.08
P2O5	0.35	0.28	0.29	0.38	0.26	0.31	0.29	0.40	0.33	0.30	0.32	0.05
F (ppm)	2469	2229	1742	2187	1750	1564	1524	2537	2812	2408	2122	449
SO2	0.10	0.12	0.09	0.11	0.09	0.09	0.04	0.10	0.09	0.06	0.09	0.02
Cl (ppm)	1606	1509	1683	1732	1495	1348	1514	1524	1445	1658	1551	117
Total	100.00	100.00	100.01	100.00	100.02	100.03	100.01	100.02	100.01	100.01	100.01	100.01

Table C3.49.1 Raw microprobe data for sample EBT-52

Analysis	1	2	3	4	5	6	7	8	9	10
SiO2	54.16	53.27	54.67	55.06	55.22	54.60	54.41	55.20	54.60	54.97
TiO2	1.07	1.00	1.13	1.05	1.03	1.07	1.12	1.08	1.05	1.11
Al2O3	20.42	20.15	20.14	20.24	20.48	20.33	20.21	20.16	20.31	20.18
FeO	5.51	5.67	5.34	5.43	5.48	5.59	5.55	5.48	5.60	5.50
MnO	0.26	0.28	0.22	0.29	0.26	0.17	0.15	0.18	0.31	0.17
MgO	0.91	0.96	0.95	0.91	0.91	0.94	0.91	0.93	0.89	0.93
CaO	2.00	2.07	1.96	2.11	1.98	2.02	2.13	2.13	2.08	2.14
Na2O	9.01	9.19	9.00	9.01	8.96	8.97	9.18	9.07	9.32	9.02
K2O	5.75	5.91	5.69	5.70	5.76	5.82	5.68	5.71	5.74	5.79
P2O5	0.28	0.32	0.36	0.30	0.32	0.31	0.28	0.30	0.31	0.37
F (ppm)	710	2550	1720	3480	1630	240	2770	2020	1380	2720
SO2	0.07	0.12	0.06	0.10	0.10	0.10	0.06	0.09	0.10	0.13
Cl (ppm)	1500	1850	1560	1690	1480	1640	1510	1530	1430	1630
Total	99.66	99.38	99.86	100.71	100.82	100.12	100.10	100.66	100.59	100.75

Table C3.49.2 Microprobe data for sample EBT-52 corrected to 100%

Analysis	1	2	3	4	5	6*	7	8	9	10
SiO2	54.27	53.61	54.74	54.67	54.77	54.44	54.36	54.83	54.27	54.56
TiO2	1.07	1.01	1.13	1.04	1.02	1.06	1.12	1.07	1.05	1.11
Al2O3	20.46	20.28	20.17	20.10	20.31	20.27	20.19	20.03	20.19	20.03
FeO	5.52	5.70	5.35	5.39	5.44	5.58	5.55	5.44	5.57	5.46
MnO	0.26	0.28	0.22	0.28	0.26	0.17	0.15	0.18	0.31	0.17
MgO	0.91	0.97	0.96	0.90	0.91	0.93	0.91	0.92	0.89	0.92
CaO	2.00	2.08	1.96	2.10	1.96	2.02	2.13	2.11	2.07	2.12
Na2O	9.03	9.24	9.02	8.94	8.88	8.94	9.17	9.01	9.27	8.96
K2O	5.76	5.95	5.70	5.66	5.72	5.81	5.67	5.67	5.71	5.75
P2O5	0.28	0.32	0.36	0.30	0.32	0.31	0.28	0.30	0.31	0.37
F (ppm)	2064	2566	1722	3455	1617	2054	2767	2007	1372	2700
SO2	0.07	0.12	0.06	0.10	0.10	0.10	0.06	0.09	0.10	0.13
Cl (ppm)	1503	1862	1562	1678	1468	1635	1508	1520	1422	1618
Total	100.00	100.00	100.00	100.00	100.00	100.00	100.00	100.00	100.00	100.00

*Flourine corrected to an average of 2060 ppm

Table C3.49.3 Microprobe data for sample EBT-52 corrected for sodium loss

Analysis	1	2	3	4	5	6	7	8	9	10	Mean	StdDev
Correction	0.999182	1.0013367	0.9990644	0.9983369	0.997753	0.9983345	1.0006387	0.9989783	1.001562	0.998468		
SiO2	54.22	53.68	54.69	54.58	54.65	54.35	54.39	54.78	54.36	54.48	54.42	0.31
TiO2	1.07	1.01	1.13	1.04	1.02	1.06	1.12	1.07	1.05	1.10	1.07	0.04
Al2O3	20.45	20.31	20.15	20.07	20.27	20.24	20.20	20.01	20.22	19.99	20.19	0.14
FeO	5.52	5.71	5.34	5.38	5.42	5.57	5.55	5.43	5.58	5.45	5.50	0.11
MnO	0.26	0.28	0.22	0.28	0.26	0.17	0.15	0.18	0.31	0.17	0.23	0.06
MgO	0.91	0.97	0.95	0.90	0.90	0.93	0.91	0.92	0.89	0.92	0.92	0.02
CaO	2.00	2.08	1.96	2.09	1.96	2.01	2.13	2.11	2.07	2.12	2.05	0.07
Na2O	9.11	9.11	9.11	9.11	9.11	9.11	9.11	9.11	9.11	9.11	9.11	0.00
K2O	5.76	5.95	5.69	5.65	5.70	5.80	5.67	5.66	5.72	5.74	5.74	0.09
P2O5	0.28	0.32	0.36	0.30	0.32	0.31	0.28	0.30	0.31	0.37	0.31	0.03
F (ppm)	2062	2569	1721	3450	1613	2050	2769	2005	1374	2696	2231	632
SO2	0.07	0.12	0.06	0.10	0.10	0.10	0.06	0.09	0.10	0.13	0.09	0.02
Cl (ppm)	1502	1864	1561	1675	1465	1632	1509	1518	1424	1615	1577	128
Total	100.01	99.99	100.01	100.02	100.02	100.02	99.99	100.01	99.99	100.01	100.01	100.01

Table C3.50.1 Raw microprobe data for sample EBT-53

Analysis	1	2	3	4	5	6	7	8	9	10
SiO ₂	53.85	54.21	55.02	54.34	54.89	54.15	55.27	54.81	54.16	54.27
TiO ₂	1.10	1.04	1.07	1.04	1.10	1.09	0.98	1.04	0.96	1.06
Al ₂ O ₃	19.99	20.18	20.28	20.23	20.31	20.58	20.30	20.28	20.35	20.67
FeO	5.40	5.50	5.50	5.39	5.50	5.43	5.63	5.46	5.45	5.48
MnO	0.21	0.26	0.26	0.30	0.35	0.15	0.27	0.14	0.13	0.32
MgO	0.83	0.95	0.86	0.88	0.90	0.92	0.93	0.87	0.87	0.92
CaO	2.13	2.10	2.03	2.10	2.03	2.09	2.03	1.95	1.98	2.09
Na ₂ O	9.10	9.14	9.12	9.11	8.88	9.04	9.01	9.34	9.03	9.03
K ₂ O	5.71	5.76	5.92	5.77	5.75	5.66	5.73	5.65	5.70	5.74
P ₂ O ₅	0.36	0.30	0.40	0.28	0.27	0.32	0.30	0.26	0.33	0.31
F (ppm)	290	3990	n.d.	250	2320	1480	1730	3150	2400	1670
SO ₂	0.08	0.09	0.12	0.10	0.09	0.08	0.08	0.09	0.06	0.09
Cl (ppm)	1530	1580	1610	1580	1720	1490	1410	1580	1510	1670
Total	98.94	100.07	100.74	99.71	100.48	99.81	100.84	100.36	99.41	100.31

Table C3.50.2 Microprobe data for sample EBT-53 corrected to 100%

Analysis	1*	2	3*	4	5	6	7	8	9	10
SiO ₂	54.31	54.17	54.49	54.38	54.63	54.26	54.80	54.61	54.48	54.10
TiO ₂	1.11	1.04	1.06	1.04	1.10	1.10	0.97	1.04	0.97	1.05
Al ₂ O ₃	20.16	20.16	20.08	20.25	20.21	20.62	20.13	20.20	20.47	20.60
FeO	5.44	5.50	5.45	5.39	5.47	5.44	5.59	5.44	5.48	5.47
MnO	0.21	0.26	0.26	0.30	0.34	0.15	0.27	0.14	0.13	0.32
MgO	0.84	0.95	0.85	0.88	0.89	0.92	0.92	0.87	0.87	0.92
CaO	2.15	2.09	2.01	2.10	2.02	2.09	2.02	1.94	1.99	2.08
Na ₂ O	9.18	9.13	9.03	9.11	8.84	9.06	8.93	9.31	9.09	9.00
K ₂ O	5.76	5.76	5.86	5.77	5.72	5.67	5.69	5.62	5.73	5.72
P ₂ O ₅	0.36	0.30	0.40	0.28	0.27	0.32	0.29	0.26	0.33	0.31
F (ppm)	2410	3987	2367	2392	2309	1483	1716	3139	2414	1665
SO ₂	0.08	0.09	0.11	0.10	0.09	0.08	0.08	0.09	0.06	0.09
Cl (ppm)	1543	1579	1594	1581	1712	1493	1398	1574	1519	1665
Total	100.00	100.00	100.00	100.00	100.00	100.00	100.00	100.00	100.00	100.00

*Flourine corrected to an avege of 2388 ppm

Table C3.50.3 Microprobe data for sample EBT-53 corrected for sodium loss

Analysis	1	2	3	4	5	6	7	8	9	10	Mean	StdDev
Correction	0.999249	0.9987812	0.997798	0.9986284	0.9958755	0.9980468	0.9968064	1.0005624	0.998357	0.997524		
SiO2	54.27	54.11	54.37	54.31	54.41	54.15	54.63	54.64	54.39	53.97	54.32	0.21
TiO2	1.11	1.04	1.06	1.04	1.09	1.09	0.97	1.04	0.97	1.05	1.05	0.05
Al2O3	20.14	20.14	20.03	20.22	20.13	20.58	20.07	20.22	20.43	20.55	20.25	0.20
FeO	5.44	5.49	5.44	5.38	5.45	5.43	5.57	5.44	5.48	5.45	5.46	0.05
MnO	0.21	0.26	0.26	0.30	0.34	0.15	0.27	0.14	0.13	0.32	0.24	0.08
MgO	0.84	0.94	0.85	0.88	0.89	0.92	0.91	0.87	0.87	0.91	0.89	0.03
CaO	2.15	2.09	2.01	2.10	2.01	2.08	2.01	1.95	1.99	2.08	2.05	0.06
Na2O	9.25	9.25	9.25	9.25	9.25	9.25	9.25	9.25	9.25	9.25	9.25	0.00
K2O	5.76	5.75	5.85	5.76	5.70	5.66	5.67	5.63	5.73	5.70	5.72	0.06
P2O5	0.36	0.30	0.39	0.28	0.27	0.32	0.29	0.26	0.33	0.31	0.31	0.04
F (ppm)	2409	3983	2362	2388	2299	1480	1710	3140	2410	1661	2384	740
SO2	0.08	0.09	0.11	0.10	0.09	0.08	0.08	0.09	0.06	0.09	0.09	0.01
Cl (ppm)	1542	1577	1591	1579	1705	1490	1394	1575	1516	1661	1563	87
Total	100.01	100.01	100.02	100.01	100.04	100.02	100.03	99.99	100.02	100.02	100.02	

Table C3.51.1 Raw microprobe data for sample EBT-54

Analysis	1	2	3	4	5	6	7	8	9	10
SiO2	54.27	54.54	54.70	55.06	55.08	55.26	55.30	53.97	54.71	53.98
TiO2	0.99	0.99	1.04	1.07	1.02	1.08	1.01	1.04	1.03	1.09
Al2O3	20.05	20.33	20.46	20.14	20.67	20.52	20.45	19.98	20.27	20.18
FeO	5.46	5.45	5.66	5.67	5.43	5.51	5.35	5.63	5.52	5.58
MnO	0.22	0.29	0.28	0.26	0.21	0.22	0.22	0.19	0.31	0.05
MgO	0.96	0.98	0.90	0.96	1.84	0.90	0.93	0.92	0.91	0.86
CaO	2.07	2.14	2.04	1.94	1.98	1.97	2.08	2.06	2.01	2.07
Na2O	8.90	9.19	9.06	9.03	8.95	9.03	8.91	9.15	9.21	9.21
K2O	5.68	5.71	5.65	5.62	5.77	5.62	5.52	5.68	5.65	5.72
P2O5	0.32	0.31	0.25	0.32	0.22	0.27	0.28	0.36	0.37	0.38
F (ppm)	690	2760	3190	1860	1350	2090	80	1700	2870	1860
SO2	0.07	0.11	0.06	0.09	0.07	0.11	0.10	0.05	0.06	0.06
Cl (ppm)	1400	1340	1460	1540	1420	1570	1590	1540	1510	1420
Total	99.19	100.45	100.58	100.48	101.51	100.85	100.31	99.34	100.48	99.51

Table C3.51.2 Microprobe data for sample EBT-54 corrected to 100%

Analysis	1*	2	3	4	5	6	7*	8	9	10
SiO2	54.63	54.29	54.39	54.80	54.27	54.80	55.01	54.33	54.45	54.25
TiO2	1.00	0.99	1.04	1.06	1.00	1.07	1.01	1.04	1.03	1.10
Al2O3	20.18	20.24	20.34	20.04	20.36	20.35	20.34	20.11	20.18	20.28
FeO	5.49	5.42	5.62	5.64	5.35	5.46	5.32	5.67	5.50	5.61
MnO	0.23	0.29	0.28	0.25	0.20	0.22	0.22	0.19	0.31	0.05
MgO	0.97	0.97	0.89	0.95	1.81	0.90	0.92	0.92	0.90	0.86
CaO	2.08	2.13	2.03	1.93	1.95	1.95	2.07	2.07	2.00	2.08
Na2O	8.96	9.15	9.01	8.99	8.81	8.96	8.86	9.21	9.16	9.26
K2O	5.71	5.69	5.62	5.59	5.69	5.57	5.49	5.72	5.62	5.75
P2O5	0.32	0.31	0.25	0.32	0.22	0.27	0.28	0.36	0.36	0.38
F (ppm)	2225	2748	3172	1851	1330	2072	2198	1711	2856	1869
SO2	0.07	0.11	0.06	0.09	0.07	0.10	0.09	0.05	0.06	0.06
Cl (ppm)	1409	1334	1452	1533	1399	1557	1582	1550	1503	1427
Total	100.00	100.00	100.00	100.00	100.00	100.00	100.00	100.00	100.00	100.00

*Flourine corrected to an average of 2210 ppm

Table C3.51.3 Microprobe data for sample EBT-54 corrected for sodium loss

Analysis	1	2	3	4	5	6	7	8	9	10	Mean	StdDev
Correction	0.99730	0.99922	0.99779	0.99755	0.99585	0.99728	0.99631	0.99975	0.99933	1.00026		
SiO2	54.48	54.25	54.27	54.66	54.04	54.65	54.81	54.31	54.41	54.27	54.42	0.23
TiO2	0.99	0.98	1.03	1.06	1.00	1.07	1.00	1.04	1.03	1.10	1.03	0.04
Al2O3	20.13	20.23	20.30	19.99	20.28	20.29	20.27	20.10	20.16	20.28	20.20	0.10
FeO	5.48	5.42	5.61	5.63	5.32	5.45	5.30	5.67	5.49	5.61	5.50	0.13
MnO	0.22	0.29	0.28	0.25	0.20	0.22	0.22	0.19	0.31	0.05	0.22	0.07
MgO	0.96	0.97	0.89	0.95	1.80	0.89	0.92	0.92	0.90	0.86	1.01	0.28
CaO	2.08	2.13	2.03	1.93	1.94	1.95	2.06	2.07	2.00	2.08	2.02	0.07
Na2O	9.23	9.23	9.23	9.23	9.23	9.23	9.23	9.23	9.23	9.23	9.23	0.00
K2O	5.70	5.68	5.61	5.58	5.66	5.56	5.47	5.72	5.61	5.75	5.63	0.09
P2O5	0.32	0.31	0.25	0.32	0.22	0.27	0.28	0.36	0.36	0.38	0.31	0.05
F (ppm)	2219	2745	3165	1847	1324	2067	2190	1711	2855	1870	2199	569
SO2	0.07	0.11	0.06	0.09	0.07	0.10	0.09	0.05	0.06	0.06	0.08	0.02
Cl (ppm)	1406	1333	1448	1529	1393	1553	1576	1550	1502	1427	1472	82
Total	100.02	100.01	100.02	100.02	100.04	100.03	100.03	100.00	100.01	100.00	100.02	

Table C3.52.1 Raw microprobe data for sample EBT-56

Analysis	1	2	3	4
SiO2	54.58	54.78	54.64	54.17
TiO2	1.06	1.04	0.99	0.96
Al2O3	19.66	19.56	19.42	19.57
FeO	5.68	5.49	5.67	5.57
MnO	0.27	0.19	0.19	0.35
MgO	0.86	0.86	0.90	0.89
CaO	1.85	1.90	1.87	1.96
Na2O	9.03	8.84	8.99	8.77
K2O	5.66	5.57	5.45	5.56
P2O5	0.31	0.30	0.32	0.26
F (ppm)	530	800	1990	2180
SO2	0.05	0.07	0.05	0.07
Cl (ppm)	1690	1700	1550	1470
Total	99.25	98.85	98.84	98.49

Table C3.52.2 Microprobe data for sample EBT-56 corrected to 100%

Analysis	1*	2*	3	4
SiO2	54.91	55.35	55.28	55.00
TiO2	1.07	1.05	1.00	0.98
Al2O3	19.78	19.77	19.65	19.87
FeO	5.72	5.54	5.74	5.65
MnO	0.27	0.19	0.19	0.36
MgO	0.86	0.87	0.91	0.90
CaO	1.86	1.92	1.89	1.99
Na2O	9.09	8.93	9.09	8.90
K2O	5.70	5.62	5.52	5.64
P2O5	0.31	0.30	0.32	0.26
F (ppm)	2103	2112	2013	2213
SO2	0.05	0.07	0.05	0.08
Cl (ppm)	1700	1718	1568	1492
Total	100.00	100.00	100.00	100.00

*Flourine corrected to an average of 2080 ppm

Table C3.52.3 Microprobe data for sample EBT-56 corrected for Sodium loss

Analysis	1	2	3	4	Mean	StdDev
Correction	0.99996	0.99844	1.00003	0.99815		
SiO2	54.91	55.26	55.28	54.90	55.09	0.21
TiO2	1.07	1.05	1.00	0.97	1.02	0.04
Al2O3	19.78	19.73	19.65	19.83	19.75	0.08
FeO	5.72	5.53	5.74	5.64	5.66	0.09
MnO	0.27	0.19	0.19	0.36	0.25	0.08
MgO	0.86	0.87	0.91	0.90	0.89	0.02
CaO	1.86	1.92	1.89	1.98	1.91	0.05
Na2O	9.09	9.09	9.09	9.09	9.09	0.00
K2O	5.69	5.61	5.52	5.63	5.61	0.07
P2O5	0.31	0.30	0.32	0.26	0.30	0.03
F (ppm)	2102	2108	2013	2209	2108	80
SO2	0.05	0.07	0.05	0.07	0.06	0.01
Cl (ppm)	1700	1715	1568	1490	1618	108
Total	100.00	100.01	100.00	100.02	100.01	

Table C3.53.1 Raw microprobe data for sample EBT-61

Analysis	2	3	4	5	6	7	8	10
SiO2	46.47	46.74	44.78	45.40	49.37	40.20	38.59	44.30
TiO2	0.46	0.33	0.30	0.41	0.35	0.29	0.23	0.51
Al2O3	11.62	10.55	10.30	10.86	10.93	8.91	8.80	10.50
FeO	6.52	6.59	6.36	5.84	7.88	5.49	4.55	6.29
MnO	0.19	0.15	0.18	0.22	0.14	0.14	0.11	0.21
MgO	0.06	0.01	n.d.	0.07	0.01	n.d.	n.d.	0.05
CaO	1.46	0.67	0.70	1.04	0.81	0.72	0.72	1.31
Na2O	4.77	5.76	5.67	3.76	7.05	4.73	4.38	4.69
K2O	3.46	3.34	3.36	3.39	3.60	2.89	2.68	3.14
P2O5	0.11	0.04	0.02	0.05	0.06	0.05	0.02	0.11
F (ppm)	2300	3000	1800	n.d.	400	400	400	n.d.
SO2	0.06	0.03	0.04	0.01	0.08	0.02	0.05	0.08
Cl (ppm)	5700	7500	7000	6900	6700	9400	9600	7000
Total	75.99	75.24	72.59	71.75	81.13	64.44	61.13	71.88

Table C3.53.2 Microprobe data for sample EBT-61 corrected to 100%

Analysis	2	3	4	5*	6	7	8	10*
SiO2	61.15	62.12	61.69	63.15	60.85	62.38	63.13	61.51
TiO2	0.61	0.44	0.41	0.57	0.43	0.45	0.38	0.71
Al2O3	15.29	14.02	14.19	15.11	13.47	13.83	14.40	14.58
FeO	8.58	8.76	8.76	8.12	9.71	8.52	7.44	8.73
MnO	0.25	0.20	0.25	0.31	0.35	0.22	0.18	0.29
MgO	0.08	0.01	n.d.	0.10	0.01	n.d.	n.d.	0.07
CaO	1.92	0.89	0.96	1.45	1.00	1.12	1.18	1.82
Na2O	6.28	7.66	7.81	5.23	8.69	7.34	7.17	6.51
K2O	4.55	4.44	4.63	4.72	4.44	4.48	4.38	4.36
P2O5	0.14	0.05	0.03	0.07	0.07	0.08	0.03	0.15
F (ppm)	3027	3987	2480	1920	493	621	654	1916
SO2	0.08	0.04	0.06	0.01	0.10	0.03	0.08	0.11
Cl (ppm)	7501	9968	9643	9598	8258	14587	15704	9720
Total	99.99	100.03	100.00	99.99	100.00	99.97	100.00	100.01

*Fluorine corrected to an average of 1383 ppm

Table C3.53.3 Microprobe data for sample EBT-61 corrected for sodium loss

Analysis	2	3	4	5	6	7	8	10	Mean	StdDev
Correction	0.980653	0.9940902	0.99563	0.97069	1.00442	0.99098	0.98927	0.98292		
SiO2	59.97	61.75	61.42	61.30	61.12	61.82	62.45	60.46	61.29	0.79
TiO2	0.59	0.44	0.41	0.55	0.43	0.45	0.37	0.70	0.49	0.11
Al2O3	15.00	13.94	14.13	14.66	13.53	13.70	14.24	14.33	14.19	0.48
FeO	8.41	8.71	8.72	7.89	9.76	8.44	7.36	8.58	8.48	0.69
MnO	0.25	0.20	0.25	0.30	0.35	0.22	0.18	0.29	0.25	0.06
MgO	0.08	0.01	n.d.	0.09	0.01	n.d.	n.d.	0.07	0.03	0.04
CaO	1.88	0.89	0.96	1.40	1.00	1.11	1.17	1.79	1.27	0.38
Na2O	8.25	8.25	8.25	8.25	8.25	8.25	8.25	8.25	8.25	0.00
K2O	4.47	4.41	4.61	4.58	4.46	4.44	4.34	4.29	4.45	0.11
P2O5	0.14	0.05	0.03	0.07	0.07	0.08	0.03	0.15	0.08	0.05
F (ppm)	2968	3964	2469	1863	495	615	647	1883	1863	1248
SO2	0.08	0.04	0.05	0.01	0.10	0.03	0.08	0.11	0.06	0.03
Cl (ppm)	7356	9909	9601	9317	8295	14456	15536	9554	10503	2908
Total	100.15	100.08	100.04	100.23	99.96	100.04	100.09	100.15	100.09	100.09

Table C3.54.1 Raw microprobe data for sample EBT-62

Analysis	1	2	3	4	5	6	7	8	9	10
SiO2	55.75	54.66	54.99	48.77	53.42	55.91	48.31	54.00	52.02	44.37
TiO2	1.00	1.03	1.03	0.85	0.93	0.93	0.89	0.90	0.95	0.83
Al2O3	19.95	19.78	20.23	17.89	19.05	20.53	17.75	19.18	18.85	15.96
FeO	5.66	5.60	5.47	4.54	5.56	5.68	4.68	5.08	5.26	4.57
MnO	0.37	0.30	0.32	0.19	0.32	0.35	0.28	0.16	0.20	0.12
MgO	0.90	0.86	0.79	0.75	0.86	0.89	0.73	0.77	0.83	0.73
CaO	1.87	1.84	1.84	1.67	1.88	1.98	1.75	1.80	1.81	1.57
Na2O	8.96	8.52	8.58	8.09	8.86	9.46	7.49	8.18	7.75	7.01
K2O	5.61	5.43	5.68	4.38	4.82	4.49	4.95	5.44	5.23	4.20
P2O5	0.18	0.25	0.35	0.28	0.26	0.25	0.18	0.29	0.32	0.29
F (ppm)	1700	1900	2800	5100	3600	2400	1300	2200	200	1400
SO2	0.03	0.07	0.07	0.07	0.06	0.08	0.10	0.09	0.08	0.07
Cl (ppm)	1700	1900	1300	3700	3400	1600	2600	2200	3300	5300
Total	100.60	98.71	99.76	88.36	96.71	100.94	87.52	96.34	93.66	80.39

Table C3.54.2 Microprobe data for sample EBT-62 corrected to 100%

Analysis	1	2	3	4	5	6	7	8	9	10
SiO2	55.42	55.37	55.12	55.19	55.24	55.39	55.20	56.05	55.54	55.19
TiO2	0.99	1.04	1.03	0.96	0.96	0.92	1.02	0.93	1.01	1.03
Al2O3	19.83	20.04	20.28	20.25	19.70	20.34	20.28	19.91	20.13	19.85
FeO	5.63	5.67	5.48	5.14	5.75	5.63	5.35	5.27	5.62	5.68
MnO	0.37	0.30	0.32	0.22	0.33	0.35	0.32	0.17	0.21	0.15
MgO	0.89	0.87	0.79	0.85	0.89	0.88	0.83	0.80	0.89	0.91
CaO	1.86	1.86	1.84	1.89	1.94	1.96	2.00	1.87	1.93	1.95
Na2O	8.91	8.63	8.60	9.16	9.16	9.37	8.56	8.49	8.27	8.72
K2O	5.58	5.50	5.69	4.96	4.98	4.45	5.66	5.65	5.58	5.22
P2O5	0.18	0.25	0.35	0.32	0.27	0.25	0.21	0.30	0.34	0.36
F (ppm)	1690	1925	2807	5772	3722	2378	1485	2284	214	1742
SO2	0.03	0.07	0.07	0.08	0.06	0.08	0.11	0.09	0.09	0.09
Cl (ppm)	1690	1925	1303	4187	3516	1585	2971	2284	3523	6593
Total	100.02	100.01	100.00	100.00	100.01	100.01	99.98	99.99	99.99	100.00

Table C3.54.3 Microprobe data for sample EBT-62 corrected for sodium loss

Analysis	1	2	3	4	5	6	7	8	9	10	Mean	StdDev
Correction	0.996409	0.9936836	0.99338	0.99889	0.99895	1.00105	0.99296	0.99230	0.99017	0.99456		
SiO2	55.22	55.02	54.76	55.13	55.18	55.45	54.81	55.62	55.00	54.89	55.18	0.29
TiO2	0.99	1.04	1.03	0.96	0.96	0.92	1.01	0.93	1.00	1.03	0.98	0.05
Al2O3	19.76	19.91	20.14	20.22	19.68	20.36	20.14	19.76	19.93	19.75	19.93	0.24
FeO	5.61	5.64	5.45	5.13	5.74	5.63	5.31	5.23	5.56	5.65	5.55	0.17
MnO	0.37	0.30	0.32	0.21	0.33	0.35	0.32	0.16	0.21	0.15	0.29	0.07
MgO	0.89	0.87	0.79	0.85	0.89	0.88	0.83	0.79	0.88	0.90	0.86	0.05
CaO	1.85	1.85	1.83	1.89	1.94	1.96	1.99	1.85	1.91	1.94	1.89	0.05
Na2O	9.27	9.27	9.27	9.27	9.27	9.27	9.27	9.27	9.27	9.27	9.27	0.00
K2O	5.56	5.47	5.66	4.95	4.98	4.45	5.62	5.60	5.53	5.20	5.32	0.44
P2O5	0.18	0.25	0.35	0.32	0.27	0.25	0.20	0.30	0.34	0.36	0.28	0.06
F (ppm)	1684	1913	2788	5765	3719	2380	1475	2266	211	1732	2137	1077
SO2	0.03	0.07	0.07	0.08	0.06	0.08	0.11	0.09	0.08	0.09	0.07	0.02
Cl (ppm)	1684	1913	1295	4183	3512	1587	2950	2266	3489	6557	2249	905
Total	100.05	100.07	100.06	100.01	100.02	100.00	100.04	100.06	100.08	100.05	100.05	

Table C3.55.1 Raw microprobe data for sample BIT-42

Analysis	1	2	3	4	5	6	7	8	9	10
SiO2	54.99	55.73	54.51	54.91	55.73	54.64	55.84	55.63	55.52	55.85
TiO2	1.01	0.94	1.03	0.94	1.04	0.99	1.01	1.04	1.00	1.05
Al2O3	20.01	20.00	19.84	20.05	20.03	20.20	20.05	20.13	20.00	19.99
FeO	5.79	5.62	5.66	5.64	5.60	5.57	5.59	5.68	5.54	5.43
MnO	0.23	0.18	0.31	0.21	0.33	0.24	0.23	0.23	0.19	0.28
MgO	0.86	0.80	0.88	0.78	0.82	0.82	0.90	0.89	0.87	0.86
CaO	2.20	2.11	2.02	1.84	1.97	1.98	2.02	1.94	1.92	1.90
Na2O	8.94	7.95	9.00	9.10	8.99	8.97	8.93	8.92	8.86	8.80
K2O	5.42	6.27	5.58	5.59	5.53	5.56	5.58	5.65	5.74	5.62
P2O5	0.22	0.18	0.26	0.25	0.27	0.32	0.23	0.29	0.28	0.28
F (ppm)	1700	2800	2200	2800	3400	2600	700	n.d.	2900	2000
SO2	0.05	0.06	0.10	0.08	0.08	0.08	0.10	0.14	0.03	0.08
Cl (ppm)	1700	1500	1600	1600	1400	1500	1700	1800	1600	1400
Total	100.08	100.26	99.56	99.83	100.87	99.79	100.73	100.74	100.40	100.48

Table C3.55.2 Microprobe data for sample BIT-42 corrected to 100%

Analysis	1	2	3	4	5	6	7	8*	9	10
SiO2	54.95	55.59	54.75	55.00	55.25	54.75	55.44	55.09	55.30	55.58
TiO2	1.01	0.94	1.03	0.94	1.03	0.99	1.00	1.03	1.00	1.04
Al2O3	19.99	19.95	19.93	20.08	19.86	20.24	19.90	19.94	19.92	19.89
FeO	5.79	5.61	5.69	5.65	5.55	5.58	5.55	5.63	5.52	5.40
MnO	0.23	0.18	0.31	0.21	0.33	0.24	0.23	0.23	0.19	0.28
MgO	0.86	0.80	0.88	0.78	0.81	0.82	0.89	0.88	0.87	0.86
CaO	2.20	2.10	2.03	1.84	1.95	1.98	2.01	1.92	1.91	1.89
Na2O	8.93	7.93	9.04	9.12	8.91	8.99	8.87	8.83	8.82	8.76
K2O	5.42	6.25	5.60	5.60	5.48	5.57	5.54	5.60	5.72	5.59
P2O5	0.22	0.18	0.26	0.25	0.27	0.32	0.23	0.29	0.28	0.28
F (ppm)	1699	2793	2210	2805	3371	2605	695	2317	2888	1990
SO2	0.05	0.06	0.10	0.08	0.08	0.08	0.10	0.14	0.03	0.08
Cl (ppm)	1699	1496	1607	1603	1388	1503	1688	1783	1594	1393
Total	99.98	100.01	100.01	100.00	100.00	99.99	99.99	99.98	100.00	100.00

*Flourine corrected to an average of 2344 ppm

Table C3.55.3 Microprobe data for sample BIT-42 corrected for sodium loss

Analysis	1	2	3	4	5	6	7	8	9	10	Mean	StdDev
Correction	0.99881	0.9888985	0.99988	1.00064	0.99861	0.99937	0.99814	0.99782	0.99773	0.997068		
SiO2	54.88	54.97	54.74	55.04	55.17	54.72	55.33	54.97	55.17	55.42	55.04	0.23
TiO2	1.01	0.93	1.03	0.94	1.03	0.99	1.00	1.03	0.99	1.04	1.00	0.04
Al2O3	19.97	19.73	19.93	20.10	19.83	20.23	19.87	19.89	19.88	19.84	19.92	0.14
FeO	5.78	5.54	5.68	5.65	5.54	5.58	5.54	5.61	5.51	5.39	5.58	0.11
MnO	0.23	0.18	0.31	0.21	0.33	0.24	0.23	0.23	0.19	0.28	0.24	0.05
MgO	0.86	0.79	0.88	0.78	0.81	0.82	0.89	0.88	0.86	0.85	0.84	0.04
CaO	2.20	2.08	2.03	1.84	1.95	1.98	2.00	1.92	1.91	1.89	1.98	0.10
Na2O	9.05	9.05	9.05	9.05	9.05	9.05	9.05	9.05	9.05	9.05	9.05	0.00
K2O	5.41	6.18	5.60	5.60	5.47	5.57	5.53	5.58	5.70	5.58	5.62	0.21
P2O5	0.22	0.18	0.26	0.25	0.27	0.32	0.23	0.29	0.28	0.28	0.26	0.04
F (ppm)	1697	2762	2209	2807	3366	2604	694	2312	2882	1985	2332	751
SO2	0.05	0.06	0.10	0.08	0.08	0.08	0.10	0.14	0.03	0.08	0.08	0.03
Cl (ppm)	1697	1480	1607	1604	1386	1502	1685	1779	1590	1389	1572	131
Total	99.99	100.11	100.01	99.99	100.01	100.00	100.01	100.00	100.02	100.03	100.02	100.02

Table C3.56.1 Raw microprobe data for sample BIT-272

Analysis	1	2	3	4	5	6	7	8	9	10
SiO2	55.25	55.16	53.90	55.62	55.54	55.69	55.52	55.44	55.61	55.39
TiO2	0.96	0.97	0.98	0.95	0.92	0.97	0.87	0.94	0.91	1.00
Al2O3	19.32	19.45	19.29	19.53	19.52	19.43	19.34	19.58	19.55	19.31
FeO	5.99	5.94	5.81	5.79	5.80	5.87	5.96	6.01	5.79	5.89
MnO	0.28	0.21	0.26	0.34	0.32	0.24	0.27	0.33	0.22	0.31
MgO	0.80	0.79	0.76	0.80	0.80	0.81	0.81	0.82	0.80	0.80
CaO	1.86	1.90	1.94	1.83	1.87	1.93	1.93	1.93	1.91	1.93
Na2O	8.40	8.46	8.70	8.58	8.38	8.58	8.47	8.48	8.51	8.57
K2O	5.51	5.40	5.78	5.47	5.53	5.35	5.37	5.51	5.57	5.41
P2O5	0.28	0.22	0.22	0.18	0.25	0.22	0.21	0.29	0.31	0.19
F (ppm)	800	2500	2600	1800	2900	700	900	1800	2400	1600
SO2	0.09	0.06	0.05	0.07	0.07	0.11	0.09	0.09	0.10	0.06
Cl (ppm)	1400	1400	1400	1300	1400	1500	1400	1100	1400	1100
Total	98.95	98.96	98.10	99.47	99.43	99.43	99.07	99.72	99.67	99.13

Table C3.56.2 Microprobe data for sample BIT-272 corrected to 100%

Analysis	1	2	3	4	5	6	7	8	9	10
SiO2	55.84	55.74	54.94	55.92	55.86	56.01	56.04	55.60	55.79	55.88
TiO2	0.97	0.98	1.00	0.96	0.93	0.98	0.88	0.94	0.91	1.01
Al2O3	19.53	19.65	19.66	19.63	19.63	19.54	19.52	19.63	19.61	19.48
FeO	6.05	6.00	5.92	5.82	5.83	5.90	6.02	6.03	5.81	5.94
MnO	0.28	0.21	0.27	0.34	0.32	0.24	0.27	0.33	0.22	0.31
MgO	0.81	0.80	0.77	0.80	0.80	0.81	0.82	0.82	0.80	0.81
CaO	1.88	1.92	1.98	1.84	1.88	1.94	1.95	1.94	1.92	1.95
Na2O	8.49	8.55	8.87	8.63	8.43	8.63	8.55	8.50	8.54	8.65
K2O	5.57	5.46	5.89	5.50	5.56	5.38	5.42	5.53	5.59	5.46
P2O5	0.28	0.22	0.22	0.18	0.25	0.22	0.21	0.29	0.31	0.19
F (ppm)	808	2526	2650	1810	2917	704	908	1805	2408	1614
SO2	0.09	0.06	0.05	0.07	0.07	0.11	0.09	0.09	0.10	0.06
Cl (ppm)	1415	1415	1427	1307	1408	1509	1413	1103	1405	1110
Total	100.01	99.99	99.99	100.00	100.00	99.99	100.00	99.99	99.99	100.00

Table C3.56.3 Microprobe data for sample BIT-272 corrected for sodium loss

Analysis	1	2	3	4	5	6	7	8	9	10	Mean	StdDev
Correction	0.997329	0.9979234	1.00112	0.99869	0.99672	0.99872	0.99793	0.99747	0.99782	0.998883		
SiO2	55.69	55.62	55.01	55.84	55.68	55.94	55.93	55.46	55.67	55.81	55.66	0.27
TiO2	0.97	0.98	1.00	0.95	0.92	0.97	0.88	0.94	0.91	1.01	0.95	0.04
Al2O3	19.47	19.61	19.69	19.61	19.57	19.52	19.48	19.59	19.57	19.46	19.56	0.07
FeO	6.04	5.99	5.93	5.81	5.81	5.90	6.00	6.01	5.80	5.94	5.92	0.09
MnO	0.28	0.21	0.27	0.34	0.32	0.24	0.27	0.33	0.22	0.31	0.28	0.05
MgO	0.81	0.80	0.78	0.80	0.80	0.81	0.82	0.82	0.80	0.81	0.80	0.01
CaO	1.87	1.92	1.98	1.84	1.87	1.94	1.94	1.93	1.91	1.94	1.92	0.04
Na2O	8.76	8.76	8.76	8.76	8.76	8.76	8.76	8.76	8.76	8.76	8.76	0.00
K2O	5.55	5.45	5.90	5.49	5.54	5.37	5.41	5.51	5.58	5.45	5.53	0.15
P2O5	0.28	0.22	0.22	0.18	0.25	0.22	0.21	0.29	0.31	0.19	0.24	0.04
F (ppm)	806	2521	2653	1807	2907	703	907	1800	2403	1612	1812	807
SO2	0.09	0.06	0.05	0.07	0.07	0.11	0.09	0.09	0.10	0.06	0.08	0.02
Cl (ppm)	1411	1412	1429	1305	1403	1507	1410	1100	1402	1108	1349	137
Total	100.03	100.01	99.98	100.01	100.03	100.00	100.02	100.01	100.01	100.01	100.01	

Table C3.57.1 Raw microprobe data for sample BIT-288

Analysis	1	2	3	4	5	6	7	8	9	10
SiO2	55.65	55.72	54.74	55.30	55.76	54.89	55.77	55.37	55.93	54.65
TiO2	0.96	0.92	0.92	0.94	0.99	1.01	0.94	0.91	0.92	0.98
Al2O3	19.50	19.52	19.49	19.46	19.50	19.38	19.53	19.34	19.39	19.36
FeO	5.76	5.81	5.83	5.77	5.69	5.91	5.88	6.02	5.74	5.95
MnO	0.24	0.23	0.31	0.20	0.25	0.25	0.23	0.30	0.28	0.28
MgO	0.82	0.82	0.78	0.83	0.84	0.82	0.79	0.76	0.81	0.75
CaO	1.93	1.92	1.83	1.91	1.90	1.97	1.93	1.97	1.96	1.91
Na2O	8.54	8.43	8.35	8.45	8.64	8.42	8.42	8.26	8.51	8.67
K2O	5.55	5.59	5.45	5.56	5.54	5.43	5.46	5.43	5.43	5.49
P2O5	0.30	0.24	0.30	0.24	0.31	0.33	0.21	0.25	0.22	0.24
F (ppm)	1500	1800	2500	1600	1700	1100	800	3400	300	3200
SO2	0.07	0.12	0.16	0.07	0.08	0.10	0.07	0.05	0.09	0.07
Cl (ppm)	1400	1300	1300	1700	1600	1200	1000	1400	1400	1500
Total	99.60	99.63	98.54	99.07	99.82	98.74	99.42	99.15	99.43	98.81

Table C3.57.2 Microprobe data for sample BIT-288 corrected to 100%

Analysis	1	2	3	4	5	6	7	8	9*	10
SiO2	55.87	55.93	55.55	55.82	55.86	55.59	56.10	55.84	56.16	55.31
TiO2	0.96	0.92	0.93	0.95	0.99	1.02	0.95	0.92	0.92	0.99
Al2O3	19.58	19.59	19.78	19.64	19.54	19.63	19.64	19.51	19.47	19.59
FeO	5.78	5.83	5.92	5.82	5.70	5.99	5.91	6.07	5.76	6.02
MnO	0.24	0.23	0.31	0.20	0.25	0.25	0.23	0.30	0.28	0.28
MgO	0.82	0.82	0.79	0.84	0.84	0.83	0.79	0.77	0.81	0.76
CaO	1.94	1.93	1.86	1.93	1.90	2.00	1.94	1.99	1.97	1.93
Na2O	8.57	8.46	8.47	8.53	8.66	8.53	8.47	8.33	8.54	8.77
K2O	5.57	5.61	5.53	5.61	5.55	5.50	5.49	5.48	5.45	5.56
P2O5	0.30	0.24	0.30	0.24	0.31	0.33	0.21	0.25	0.22	0.24
F (ppm)	1506	1807	2537	1615	1703	1114	805	3429	1968	3239
SO2	0.07	0.12	0.16	0.07	0.08	0.10	0.07	0.05	0.09	0.07
Cl (ppm)	1406	1305	1319	1716	1603	1215	1006	1412	1406	1518
Total	100.01	100.00	100.00	99.99	100.01	100.00	99.99	99.99	100.02	100.01

*Flourine corrected to an average of 1956 ppm

Table C3.57.3 Microprobe data for sample BIT-288 corrected for sodium loss

Analysis	1	2	3	4	5	6	7	8	9	10	Mean	StdDev
Correction	0.998595	0.9974695	0.99759	0.99815	0.99941	0.99813	0.99755	0.99617	0.99830	1.000595		
SiO2	55.79	55.79	55.42	55.72	55.83	55.49	55.96	55.63	56.06	55.34	55.70	0.23
TiO2	0.96	0.92	0.93	0.95	0.99	1.02	0.94	0.91	0.92	0.99	0.95	0.04
Al2O3	19.55	19.54	19.73	19.61	19.52	19.59	19.60	19.43	19.44	19.60	19.56	0.09
FeO	5.78	5.82	5.90	5.81	5.70	5.97	5.90	6.05	5.75	6.03	5.87	0.12
MnO	0.24	0.23	0.31	0.20	0.25	0.25	0.23	0.30	0.28	0.28	0.26	0.04
MgO	0.82	0.82	0.79	0.84	0.84	0.83	0.79	0.76	0.81	0.76	0.81	0.03
CaO	1.94	1.92	1.85	1.92	1.90	1.99	1.94	1.98	1.96	1.93	1.93	0.04
Na2O	8.72	8.72	8.72	8.72	8.72	8.72	8.72	8.72	8.72	8.72	8.72	0.00
K2O	5.56	5.60	5.52	5.60	5.55	5.49	5.48	5.46	5.44	5.56	5.53	0.06
P2O5	0.30	0.24	0.30	0.24	0.31	0.33	0.21	0.25	0.22	0.24	0.27	0.04
F (ppm)	1504	1802	2531	1612	1702	1112	803	3416	1965	3240	1969	854
SO2	0.07	0.12	0.16	0.07	0.08	0.10	0.07	0.05	0.09	0.07	0.09	0.03
Cl (ppm)	1404	1302	1316	1713	1602	1213	1003	1407	1403	1519	1388	200
Total	100.02	100.02	100.02	100.01	100.02	100.02	100.01	100.02	100.03	100.00	100.02	

Appendix 4

Table C4.1 Microprobe glass standards for 3/5/99

VG568	SiO2	TiO2	Al2O3	FeO	MnO	MgO	CaO	Na2O	K2O	P2O5	F (ppm)	SO2	Cl (ppm)	Total	98% cutoff
1	75.74	0.07	12.44	1.07	0.00	0.00	0.47	3.13	3.13	0.02	3600	0.01	1070	98.36	
2	75.32	0.07	12.40	1.20	0.04	0.00	0.46	3.25	3.25	0.00	1900	0.03	850	98.07	
3	75.62	0.05	12.51	1.07	0.00	0.02	0.46	3.31	3.31	0.00	3280	0.00	990	98.47	
4	76.27	0.04	12.49	1.10	0.01	0.01	0.43	3.30	3.30	0.00	2790	0.03	1180	98.20	
5	75.19	0.08	12.58	1.11	0.00	0.02	0.48	3.72	3.72	0.02	1160	0.01	1020	98.39	
6	73.35	0.07	12.40	1.22	0.00	0.02	0.41	3.24	3.24	0.04	0	0.03	920	95.88	
Mean	75.63	0.06	12.48	1.11	0.01	0.01	0.46	3.34	3.34	0.01	2546	0.02	1022	98.50	
StdDev	0.42	0.02	0.07	0.05	0.02	0.01	0.02	0.22	0.22	0.01	1006	0.01	120		

KN18	SiO2	TiO2	Al2O3	FeO	MnO	MgO	CaO	Na2O	K2O	P2O5	F (ppm)	SO2	Cl (ppm)	Total	97% cutoff
1	72.94	0.17	10.94	3.69	0.06	0.00	0.19	3.62	3.62	0.00	3810	0.00	2810	96.75	
2	72.77	0.14	10.88	3.42	0.06	0.00	0.16	4.58	4.58	0.01	7630	0.00	3090	97.73	
3	73.35	0.14	11.00	3.47	0.00	0.00	0.16	4.57	4.57	0.00	6640	0.04	3030	98.12	
4	73.47	0.16	10.91	3.47	0.02	0.00	0.17	3.41	3.41	0.00	5160	0.02	3150	97.04	
5	71.74	0.15	10.70	3.47	0.04	0.00	0.12	5.48	5.48	0.00	7570	0.02	2930	97.37	
6	72.79	0.22	10.97	3.48	0.03	0.00	0.15	4.46	4.46	0.00	5670	0.00	3190	97.60	
Mean	72.83	0.16	10.89	3.46	0.03	0.00	0.15	4.50	4.50	0.00	6534	0.01	3078	97.57	
StdDev	0.68	0.04	0.12	0.02	0.02	0.00	0.02	0.74	0.74	0.00	1109	0.02	103		

KE12	SiO2	TiO2	Al2O3	FeO	MnO	MgO	CaO	Na2O	K2O	P2O5	F (ppm)	SO2	Cl (ppm)	Total	97% cutoff
1	69.86	0.33	7.78	8.44	0.33	0.00	0.41	5.10	5.10	0.01	2770	0.04	2970	97.29	
2	69.05	0.28	7.77	8.52	0.25	0.02	0.40	3.65	3.65	0.00	3720	0.05	3140	95.08	
3	69.93	0.35	7.78	8.49	0.30	0.00	0.38	4.25	4.25	0.02	5190	0.03	3160	96.77	
4	69.27	0.32	7.81	8.52	0.29	0.00	0.38	6.17	6.17	0.00	3780	0.04	3110	97.80	
5	68.82	0.34	7.65	8.39	0.16	0.04	0.38	7.29	7.29	0.05	3350	0.07	3010	98.13	
6	68.52	0.30	7.76	8.43	0.28	0.00	0.39	7.77	7.77	0.05	3990	0.04	3010	98.44	
Mean	69.12	0.32	7.75	8.44	0.27	0.01	0.39	6.58	6.58	0.03	3473	0.05	3025	97.91	
StdDev	0.58	0.02	0.07	0.06	0.07	0.02	0.02	1.20	1.20	0.02	539	0.02	60		

Table C4.2 Microprobe glass standards for 3/17/99

VG568	SiO2	TiO2	Al2O3	FeO	MnO	MgO	CaO	Na2O	K2O	P2O5	F (ppm)	SO2	Cl (ppm)	Total	99% cutoff
1	75.15	0.10	12.48	1.04	0.00	0.00	0.40	4.09	4.09	0.00	1770	0.02	1050	98.64	
2	76.01	0.05	12.37	1.20	0.00	0.02	0.47	4.42	4.42	0.00	2020	0.01	1100	99.83	
3	75.77	0.11	12.44	1.19	0.08	0.27	0.47	4.27	4.27	0.00	1710	0.00	1230	99.89	
4	75.85	0.10	12.28	1.09	0.03	0.01	0.46	4.57	4.57	0.01	680	0.02	1220	99.68	
5	75.56	0.09	12.42	1.18	0.09	0.08	0.47	3.91	3.91	0.00	2710	0.00	950	99.38	
6	76.35	0.10	12.50	1.12	0.05	0.57	0.41	3.76	3.76	0.00	0	0.03	970	100.08	
Mean	75.91	0.09	12.40	1.16	0.05	0.19	0.46	4.18	4.18	0.00	1424	0.01	1094	99.77	
StdDev	0.30	0.02	0.08	0.05	0.04	0.24	0.02	0.34	0.34	0.00	1081	0.01	133		

KN18	SiO2	TiO2	Al2O3	FeO	MnO	MgO	CaO	Na2O	K2O	P2O5	F (ppm)	SO2	Cl (ppm)	Total	99% cutoff
1	74.14	0.19	10.82	3.60	0.06	0.00	0.12	4.87	4.87	0.04	6300	0.01	3040	99.48	
2	73.77	0.23	10.91	3.57	0.07	0.00	0.16	5.17	5.17	0.02	5780	0.02	3060	99.35	
3	73.69	0.19	10.76	3.49	0.00	0.00	0.16	4.86	4.86	0.00	4740	0.02	2820	98.66	
4	74.44	0.16	10.90	3.50	0.01	0.10	0.11	5.58	5.58	0.02	3870	0.02	3430	100.12	
5	74.11	0.19	10.93	3.64	0.00	0.01	0.16	5.23	5.23	0.00	6130	0.01	2720	99.78	
6	73.71	0.14	10.76	3.50	0.03	0.03	0.18	5.29	5.29	0.00	5550	0.01	2800	99.12	
Mean	74.04	0.18	10.86	3.56	0.03	0.03	0.15	5.23	5.23	0.01	5526	0.01	3010	99.57	
StdDev	0.30	0.03	0.07	0.06	0.03	0.04	0.03	0.26	0.26	0.02	971	0.00	277		

KE12	SiO2	TiO2	Al2O3	FeO	MnO	MgO	CaO	Na2O	K2O	P2O5	F (ppm)	SO2	Cl (ppm)	Total	99% cutoff
1	69.56	0.27	7.71	8.55	0.26	0.01	0.35	7.33	7.33	0.00	3970	0.04	2920	99.11	
2	68.66	0.23	7.79	8.50	0.26	0.09	0.37	7.25	7.25	0.02	3320	0.05	2630	98.17	
3	68.35	0.27	7.83	8.68	0.29	0.03	0.35	7.46	7.46	0.00	3160	0.01	2760	98.31	
4	69.70	0.31	7.87	8.66	0.24	0.01	0.38	7.65	7.65	0.03	4160	0.03	2960	99.96	
5	68.62	0.27	7.85	8.56	0.15	0.01	0.38	7.53	7.53	0.03	3880	0.05	2800	98.55	
6	69.79	0.31	7.80	8.58	0.29	0.03	0.34	7.47	7.47	0.00	1910	0.01	2890	99.43	
Mean	69.68	0.30	7.79	8.60	0.26	0.02	0.36	7.49	7.49	0.01	3346.667	0.03	2923	99.50	
StdDev	0.12	0.02	0.08	0.06	0.02	0.01	0.02	0.16	0.16	0.02	1248	0.01	35		

Table C4.3 Microprobe glass standards for 3/18/99

VG568	SiO2	TiO2	Al2O3	FeO	MnO	MgO	CaO	Na2O	K2O	P2O5	F (ppm)	SO2	Cl (ppm)	Total	99% cutoff
1	74.75	0.12	12.48	1.15	0.04	0.02	0.46	3.40	3.40	0.00	1640	0.03	880	97.99	
2	76.14	0.03	12.42	1.18	0.00	0.04	0.44	3.99	3.99	0.00	450	0.00	1130	99.47	
3	76.32	0.08	12.41	1.10	0.06	0.03	0.39	4.05	4.05	0.04	2040	0.01	1170	99.87	
4	75.87	0.07	12.21	1.27	0.00	0.04	0.47	4.03	4.03	0.01	820	0.00	980	99.28	
5	75.28	0.08	12.39	1.14	0.00	0.02	0.42	3.71	3.71	0.00	410	0.03	990	98.29	
6	75.26	0.09	12.46	1.16	0.09	0.00	0.52	4.09	4.09	0.04	700	0.00	1000	98.90	
Mean	76.11	0.06	12.35	1.18	0.02	0.04	0.43	4.02	4.02	0.02	1103	0.01	1093	99.54	
StdDev	0.22	0.02	0.12	0.08	0.03	0.01	0.04	0.03	0.03	0.02	832	0.01	100		

KN18	SiO2	TiO2	Al2O3	FeO	MnO	MgO	CaO	Na2O	K2O	P2O5	F (ppm)	SO2	Cl (ppm)	Total	98.5% cutoff
1	71.79	0.16	10.88	3.50	0.03	0.00	0.17	5.42	5.42	0.02	630	0.00	3170	96.97	
2	71.81	0.16	10.76	3.44	0.03	0.00	0.16	6.06	6.06	0.00	4720	0.01	2960	97.93	
3	73.60	0.17	10.83	3.23	0.00	0.03	0.17	5.21	5.21	0.03	5210	0.01	3300	98.83	
4	73.87	0.16	11.03	3.59	0.01	0.01	0.12	5.21	5.21	0.03	5400	0.01	3100	98.63	
5	72.66	0.20	10.75	3.44	0.03	0.00	0.16	6.32	6.32	0.01	4260	0.00	3250	98.85	
6	72.48	0.15	10.82	3.49	0.00	0.00	0.16	5.84	5.84	0.00	4940	0.00	3390	98.32	
Mean	73.37	0.18	10.87	3.42	0.01	0.01	0.15	5.58	5.58	0.02	4956.667	0.01	3217	99.10	
StdDev	0.64	0.02	0.14	0.18	0.02	0.01	0.03	0.64	0.64	0.01	611	0.01	104		

KE12	SiO2	TiO2	Al2O3	FeO	MnO	MgO	CaO	Na2O	K2O	P2O5	F (ppm)	SO2	Cl (ppm)	Total	98% cutoff
1	68.01	0.30	7.69	8.44	0.23	0.00	0.38	7.04	7.04	0.01	1150	0.05	2850	97.03	
2	68.71	0.35	7.72	8.55	0.24	0.00	0.43	7.01	7.01	0.00	3590	0.02	2710	98.08	
3	69.86	0.26	7.84	8.27	0.29	0.02	0.39	6.15	6.15	0.01	0	0.05	2830	97.91	
4	69.53	0.28	7.86	8.43	0.26	0.00	0.39	7.50	7.50	0.00	3590	0.04	2900	99.39	
5	68.16	0.28	7.90	8.56	0.17	0.00	0.36	6.51	6.51	0.04	2170	0.01	2790	96.92	
6	68.33	0.28	7.75	8.71	0.27	0.03	0.38	7.17	7.17	0.00	4360	0.03	3080	98.10	
Mean	68.86	0.30	7.78	8.56	0.26	0.01	0.40	7.23	7.23	0.00	3846.667	0.03	2897	98.52	
StdDev	0.62	0.04	0.07	0.14	0.02	0.01	0.02	0.25	0.25	0.00	445	0.01	185		

Table C4.4 Microprobe glass standards for 3/30/99

VC568	SiO2	TiO2	Al2O3	FeO	MnO	MgO	CaO	Na2O	K2O	P2O5	F (ppm)	SO2	Cl (ppm)	Total	99% cutoff
1	75.19	0.08	9.50	1.19	0.08	0.05	0.38	3.88	3.88	0.00	2220	0.00	1080	95.69	
2	73.35	0.10	12.13	1.00	0.06	0.01	0.45	2.13	2.13	0.00	2190	0.00	1120	94.64	
3	75.11	0.09	10.74	1.12	0.03	0.03	0.42	3.99	3.99	0.02	2730	0.00	1060	96.84	
4	74.66	0.06	12.45	1.08	0.00	2.31	0.39	3.72	3.72	0.00	2050	0.05	800	100.08	
5	74.05	0.13	12.23	1.12	0.00	0.00	0.43	3.41	3.41	0.00	1770	0.00	880	96.60	
6	75.44	0.09	12.34	1.17	0.00	0.00	0.47	4.23	4.23	0.00	3470	0.02	1160	99.16	
Mean	75.05	0.08	12.39	1.13	0.00	1.16	0.43	3.98	3.98	0.00	2760	0.04	980	99.62	
StdDev	0.55	0.02	0.08	0.07	0.00	1.64	0.06	0.37	0.37	0.00	1004	0.02	255		

KN18	SiO2	TiO2	Al2O3	FeO	MnO	MgO	CaO	Na2O	K2O	P2O5	F (ppm)	SO2	Cl (ppm)	Total	98% cutoff
1	72.80	0.20	10.70	3.47	0.15	0.00	0.10	5.53	5.53	0.00	4850	0.00	3040	98.28	
2	74.10	0.17	10.58	3.45	0.11	0.00	0.15	4.60	4.60	0.00	4820	0.00	3270	98.72	
3	71.85	0.19	10.94	3.45	0.00	0.00	0.19	4.42	4.42	0.02	3160	0.00	2890	96.46	
4	70.98	0.20	10.48	3.45	0.00	0.04	0.12	4.85	4.85	0.00	6040	0.01	3160	95.66	
5	71.58	0.19	10.86	3.64	0.00	0.00	0.13	5.20	5.20	0.00	6700	0.02	3170	97.70	
6	73.18	0.18	10.79	3.52	0.07	0.00	0.14	4.98	4.98	0.00	4790	0.01	3120	98.12	
Mean	73.36	0.18	10.69	3.48	0.11	0.00	0.13	5.04	5.04	0.00	4820	0.00	3143	98.37	
StdDev	0.67	0.02	0.11	0.04	0.04	0.00	0.03	0.47	0.47	0.00	30	0.00	117		

KE12	SiO2	TiO2	Al2O3	FeO	MnO	MgO	CaO	Na2O	K2O	P2O5	F (ppm)	SO2	Cl (ppm)	Total	98% cutoff
1	69.33	0.28	7.72	8.42	0.31	0.01	0.38	7.10	7.10	0.03	4590	0.05	3080	98.76	
2	67.57	0.26	7.74	8.39	0.27	0.01	0.41	7.02	7.02	0.00	3250	0.02	3110	96.62	
3	67.03	0.27	7.85	8.33	0.22	0.02	0.34	7.30	7.30	0.03	4280	0.04	3020	96.54	
4	69.02	0.28	7.48	8.42	0.14	0.01	0.40	7.74	7.74	0.04	3490	0.05	2800	98.52	
5	68.84	0.30	7.71	8.65	0.19	0.00	0.38	7.25	7.25	0.01	2780	0.04	2780	98.26	
6	69.13	0.29	7.67	8.43	0.36	0.00	0.38	6.99	6.99	0.00	4280	0.07	3190	98.38	
Mean	69.08	0.29	7.64	8.48	0.25	0.00	0.39	7.27	7.27	0.02	3785	0.05	2963	98.48	
StdDev	0.21	0.01	0.11	0.11	0.10	0.01	0.01	0.33	0.33	0.02	814	0.01	204		

Table C4.5 Microprobe glass standards for 4/30/99

VG568	98.5% cutoff													
	SiO2	TiO2	Al2O3	FeO	MnO	MgO	CaO	Na2O	K2O	P2O5	F (ppm)	SO2	Cl (ppm)	Total
1	75.37	0.10	12.06	1.07	0.00	0.03	0.44	4.39	4.39	0.04	2500	0.00	950	98.80
2	75.11	0.05	12.11	0.99	0.00	0.02	0.47	3.85	3.85	0.00	2210	0.00	1090	97.98
3	75.55	0.08	11.84	1.17	0.05	0.01	0.44	4.20	4.20	0.00	1600	0.01	1070	98.64
4	75.48	0.10	12.00	1.16	0.10	0.01	0.44	3.97	3.97	0.00	1440	0.01	1240	98.37
5	76.21	0.08	12.16	1.13	0.00	0.01	0.42	3.85	3.85	0.04	1360	0.00	790	99.10
6	75.72	0.04	12.16	1.18	0.00	0.02	0.40	3.93	3.93	0.00	1890	0.00	950	98.68
Mean	75.71	0.08	12.05	1.14	0.01	0.02	0.42	4.09	4.09	0.02	1838	0.00	940	98.80
StdDev	0.36	0.02	0.15	0.05	0.03	0.01	0.02	0.25	0.25	0.02	492	0.00	115	

KN18	98% cutoff													
	SiO2	TiO2	Al2O3	FeO	MnO	MgO	CaO	Na2O	K2O	P2O5	F (ppm)	SO2	Cl (ppm)	Total
1	73.28	0.20	10.63	3.59	0.06	0.00	0.20	4.16	4.16	0.00	5040	0.02	3130	97.60
2	73.18	0.18	10.53	3.63	0.05	0.00	0.15	3.66	3.66	0.02	5900	0.00	3120	96.80
3	73.35	0.17	10.51	3.67	0.00	0.00	0.15	4.71	4.71	0.00	6070	0.01	2890	97.98
4	73.41	0.22	10.35	3.59	0.02	0.01	0.10	5.39	5.39	0.00	5700	0.03	2670	98.43
5	72.92	0.11	10.55	3.69	0.00	0.00	0.16	5.32	5.32	0.00	5880	0.00	3020	98.18
6	73.41	0.20	10.35	3.58	0.05	0.01	0.14	5.43	5.43	0.00	4780	0.01	2900	98.45
Mean	73.25	0.18	10.42	3.62	0.02	0.00	0.13	5.38	5.38	0.00	5453.333	0.01	2863	98.35
StdDev	0.29	0.06	0.12	0.06	0.02	0.00	0.03	0.05	0.05	0.00	590	0.01	178	

KE12	98% cutoff													
	SiO2	TiO2	Al2O3	FeO	MnO	MgO	CaO	Na2O	K2O	P2O5	F (ppm)	SO2	Cl (ppm)	Total
1	68.71	0.28	7.66	8.42	0.23	0.01	0.33	7.18	7.18	0.03	4940	0.02	2820	98.01
2	69.25	0.34	7.63	8.63	0.18	0.01	0.36	6.99	6.99	0.00	3310	0.06	2810	98.37
3	68.86	0.33	7.65	8.64	0.22	0.02	0.36	7.48	7.48	0.03	4070	0.03	2740	98.57
4	68.95	0.26	7.51	8.58	0.18	0.03	0.35	7.15	7.15	0.00	2890	0.03	2750	97.80
5	69.10	0.28	7.48	8.49	0.27	0.02	0.38	7.09	7.09	0.00	4010	0.03	3270	98.10
6	68.81	0.23	7.58	8.72	0.25	0.01	0.37	7.07	7.07	0.00	2450	0.04	2960	97.89
Mean	68.98	0.31	7.60	8.54	0.23	0.02	0.35	7.19	7.19	0.02	4083	0.03	2910	98.26
StdDev	0.24	0.03	0.08	0.11	0.04	0.01	0.02	0.21	0.21	0.02	668	0.01	243	

Table C4.6 Microprobe glass standards for 5/1/99

VG568	99%-101% cutoff													
	SiO2	TiO2	Al2O3	FeO	MnO	MgO	CaO	Na2O	K2O	P2O5	F (ppm)	SO2	Cl (ppm)	Total
1	76.45	0.10	12.17	1.03	0.01	0.02	0.42	3.79	3.79	0.01	2260	0.00	970	99.14
2	76.01	0.12	12.13	1.15	0.04	0.03	0.43	3.51	3.51	0.02	2180	0.01	950	98.66
3	76.21	0.09	12.19	1.07	0.00	0.01	0.44	3.74	3.74	0.02	3090	0.00	1010	99.06
4	76.36	0.07	12.26	1.26	0.05	0.01	0.47	3.07	3.07	0.00	1350	0.01	1000	98.59
5	76.23	0.12	12.14	1.12	0.00	0.00	0.40	3.60	3.60	0.00	940	0.00	760	98.73
6	76.15	0.05	12.27	1.13	0.04	0.03	0.36	3.88	3.88	0.01	16890	0.01	840	100.61
Mean	76.27	0.08	12.21	1.08	0.01	0.02	0.41	3.81	3.81	0.01	7413	0.00	940	99.61
StdDev	0.16	0.03	0.05	0.05	0.02	0.01	0.04	0.07	0.07	0.01	8218	0.01	89	

KN18	99%-101% cutoff													
	SiO2	TiO2	Al2O3	FeO	MnO	MgO	CaO	Na2O	K2O	P2O5	F (ppm)	SO2	Cl (ppm)	Total
1	75.85	0.20	10.88	3.65	0.03	0.00	0.07	4.81	4.81	0.02	9220	0.01	3130	101.10
2	76.53	0.13	10.98	3.68	0.05	0.00	0.09	1.48	1.48	0.00	7240	0.00	3410	97.90
3	73.82	0.24	10.81	3.63	0.05	0.00	0.27	4.99	4.99	0.02	6200	0.01	3170	99.14
4	76.25	0.17	10.86	3.57	0.04	0.00	0.10	3.10	3.10	0.01	4360	0.00	3080	99.39
5	74.30	0.20	10.92	3.40	0.04	0.01	0.07	4.94	4.94	0.00	3640	0.02	2900	98.88
6	75.28	0.19	11.11	3.55	0.08	0.00	0.13	5.01	5.01	0.00	6680	0.02	3370	100.71
Mean	75.11	0.20	10.93	3.58	0.06	0.00	0.17	4.37	4.37	0.01	5747	0.01	3207	99.75
StdDev	1.22	0.03	0.16	0.04	0.02	0.00	0.09	1.10	1.10	0.01	1225	0.01	148	

KE12	99%-101% cutoff													
	SiO2	TiO2	Al2O3	FeO	MnO	MgO	CaO	Na2O	K2O	P2O5	F (ppm)	SO2	Cl (ppm)	Total
1	71.68	0.34	8.14	8.58	0.21	0.00	0.33	4.66	4.66	0.06	2770	0.05	2950	98.82
2	72.55	0.32	7.98	8.51	0.23	0.03	0.37	6.83	6.83	0.04	3270	0.04	3000	101.78
3	70.86	0.29	8.14	8.56	0.25	0.00	0.34	6.10	6.10	0.02	3990	0.04	2730	99.55
4	71.81	0.34	8.03	8.47	0.28	0.00	0.38	6.67	6.67	0.07	3820	0.04	2750	101.00
5	71.77	0.29	7.85	8.48	0.30	0.01	0.39	6.87	6.87	0.00	4060	0.03	3190	100.97
6	71.84	0.26	7.95	8.75	0.23	0.00	0.39	6.61	6.61	0.02	3280	0.01	2940	100.88
Mean	71.57	0.30	7.99	8.57	0.26	0.00	0.37	6.56	6.56	0.03	3788	0.03	2903	100.60
StdDev	0.48	0.03	0.12	0.13	0.03	0.01	0.02	0.33	0.33	0.03	353	0.02	214	

Table C4.7 Microprobe glass standards for 5/5/99

VG568	SiO2	TiO2	Al2O3	FeO	MnO	MgO	CaO	Na2O	K2O	P2O5	F (ppm)	SO2	Cl (ppm)	Total	99% cutoff
1	76.27	0.08	12.06	1.32	0.02	0.02	0.40	3.69	3.69	0.00	2400	0.00	880	99.18	
2	76.50	0.06	12.00	0.97	0.00	0.00	0.41	3.76	3.76	0.00	1100	0.00	780	98.73	
3	76.72	0.09	11.98	1.15	0.00	0.01	0.41	3.46	3.46	0.00	2030	0.00	1210	99.17	
4	75.03	0.07	12.02	1.12	0.06	0.01	0.41	4.01	4.01	0.00	0	0.01	1020	97.66	
5	75.74	0.06	12.06	1.02	0.00	0.04	0.36	4.17	4.17	0.00	4280	0.00	1110	99.05	
6	76.46	0.07	11.96	1.22	0.00	0.01	0.42	3.77	3.77	0.03	720	0.00	910	98.92	
Mean	76.25	0.08	12.03	1.16	0.01	0.02	0.39	3.77	3.77	0.00	2903	0.00	1067	99.14	
StdDev	0.49	0.02	0.05	0.15	0.01	0.02	0.03	0.36	0.36	0.00	1206	0.00	169		

KN18	SiO2	TiO2	Al2O3	FeO	MnO	MgO	CaO	Na2O	K2O	P2O5	F (ppm)	SO2	Cl (ppm)	Total	99% cutoff
1	74.49	0.14	10.63	3.62	0.00	0.00	0.12	5.27	5.27	0.03	2460	0.01	3040	99.23	
2	74.38	0.22	10.50	3.74	0.00	0.00	0.15	5.15	5.15	0.00	4930	0.01	2770	99.20	
3	74.06	0.17	10.40	3.48	0.00	0.00	0.14	6.62	6.62	0.02	5210	0.00	3120	100.05	
4	74.88	0.14	10.74	3.59	0.00	0.00	0.12	5.12	5.12	0.06	6990	0.00	3160	100.13	
5	74.52	0.16	10.70	3.73	0.05	0.00	0.17	5.19	5.19	0.00	4450	0.01	2980	99.68	
6	74.88	0.20	10.65	3.57	0.07	0.00	0.12	5.20	5.20	0.00	5530	0.01	2860	99.92	
Mean	74.54	0.17	10.60	3.62	0.02	0.00	0.14	5.43	5.43	0.02	4928	0.01	2988	99.70	
StdDev	0.31	0.03	0.13	0.10	0.03	0.00	0.02	0.59	0.59	0.02	1484	0.01	151		

KE12	SiO2	TiO2	Al2O3	FeO	MnO	MgO	CaO	Na2O	K2O	P2O5	F (ppm)	SO2	Cl (ppm)	Total	99% cutoff
1	70.53	0.33	7.73	8.63	0.27	0.01	0.35	7.11	7.11	0.00	4870	0.05	3070	100.09	
2	69.75	0.27	7.65	8.75	0.16	0.00	0.35	7.01	7.01	0.00	5050	0.03	3070	99.02	
3	69.47	0.27	7.66	8.85	0.26	0.00	0.34	6.98	6.98	0.00	4140	0.05	2890	98.88	
4	70.06	0.25	7.74	8.43	0.26	0.00	0.34	7.30	7.30	0.01	3390	0.03	3410	99.44	
5	70.48	0.25	7.64	8.53	0.24	0.00	0.36	6.91	6.91	0.01	4210	0.04	2880	99.44	
6	70.92	0.24	7.78	8.70	0.29	0.00	0.36	5.62	5.62	0.00	2200	0.03	3080	98.81	
Mean	70.20	0.27	7.69	8.58	0.23	0.00	0.35	7.08	7.08	0.01	4380	0.04	3108	99.50	
StdDev	0.37	0.04	0.05	0.14	0.05	0.00	0.01	0.17	0.17	0.01	752	0.01	221		

Table C4.8 Microprobe glass standards for 10/7/99

VG568	99%-101% cutoff													
	SiO2	TiO2	Al2O3	FeO	MnO	MgO	CaO	Na2O	K2O	P2O5	F (ppm)	SO2	Cl (ppm)	Total
1	75.10	0.03	12.47	1.09	0.00	0.01	0.42	3.93	3.93	0.04	50	0.05	1000	98.27
2	76.66	0.10	12.55	0.94	0.02	0.09	0.40	4.07	4.07	0.00	1520	0.00	1090	100.07
3	75.63	0.10	12.49	1.13	0.03	0.02	0.43	4.21	4.21	0.00	1680	0.01	1150	99.43
4	75.23	0.05	12.50	1.23	0.02	0.01	0.45	3.97	3.97	0.04	1040	0.03	1110	98.77
5	76.32	0.03	12.51	1.18	0.00	0.01	0.42	3.63	3.63	0.02	2060	0.01	1030	99.40
6	76.76	0.05	12.44	1.08	0.00	0.02	0.40	3.73	3.73	0.00	1820	0.04	1120	99.71
Mean	76.34	0.07	12.50	1.08	0.01	0.03	0.41	3.91	3.91	0.01	1770	0.01	1098	99.65
StdDev	0.51	0.04	0.04	0.10	0.01	0.04	0.02	0.27	0.27	0.01	229	0.02	51	

KN18	99%-101% cutoff													
	SiO2	TiO2	Al2O3	FeO	MnO	MgO	CaO	Na2O	K2O	P2O5	F (ppm)	SO2	Cl (ppm)	Total
1	74.35	0.20	10.99	3.35	0.03	0.00	0.15	5.30	5.30	0.03	5040	0.02	3100	99.80
2	73.08	0.15	11.08	3.48	0.06	0.00	0.15	5.28	5.28	0.00	6470	0.00	2920	98.83
3	74.00	0.16	10.91	3.46	0.05	0.00	0.13	6.01	6.01	0.00	4780	0.00	2910	100.03
4	74.73	0.18	11.04	3.58	0.11	0.00	0.17	5.38	5.38	0.02	6170	0.02	3020	100.71
5	73.58	0.17	11.11	3.45	0.00	0.00	0.13	5.82	5.82	0.05	6490	0.05	3160	99.95
6	74.82	0.15	11.04	3.52	0.00	0.00	0.13	5.22	5.22	0.02	5710	0.00	3020	100.39
Mean	74.29	0.17	11.02	3.47	0.04	0.00	0.14	5.55	5.55	0.02	5638	0.02	3042	100.18
StdDev	0.51	0.02	0.07	0.09	0.05	0.00	0.02	0.35	0.35	0.02	726	0.02	94	

KE12	99% cutoff													
	SiO2	TiO2	Al2O3	FeO	MnO	MgO	CaO	Na2O	K2O	P2O5	F (ppm)	SO2	Cl (ppm)	Total
1	69.74	0.38	7.76	8.37	0.33	0.04	0.37	8.00	8.00	0.00	3300	0.02	2840	99.98
2	68.59	0.29	7.84	8.38	0.25	0.06	0.38	8.78	8.78	0.00	4280	0.04	2890	99.53
3	68.84	0.29	7.75	8.35	0.28	0.00	0.39	7.67	7.67	0.03	3910	0.02	2820	98.65
4	70.11	0.28	7.80	8.31	0.26	0.01	0.40	7.11	7.11	0.02	1650	0.08	3020	99.07
Mean	69.48	0.32	7.80	8.35	0.28	0.03	0.39	7.96	7.96	0.01	3077	0.05	2917	99.52
StdDev	0.79	0.06	0.04	0.04	0.04	0.02	0.02	0.84	0.84	0.01	1329	0.03	93	

Table C4.9 Microprobe glass standards for 10/14/99

VG568	SiO2	TiO2	Al2O3	FeO	MnO	MgO	CaO	Na2O	K2O	P2O5	F (ppm)	SO2	Cl (ppm)	Total
1	75.84	0.06	12.41	1.13	0.09	0.03	0.44	5.08	5.08	0.05	1600	0.01	1100	100.53
2	76.60	0.11	12.44	1.12	0.00	0.02	0.42	3.95	3.95	0.00	1200	0.04	900	100.00
3	77.06	0.10	12.55	1.15	0.00	0.03	0.43	3.96	3.96	0.00	1000	0.01	800	100.48
4	76.93	0.07	12.62	1.20	0.03	0.02	0.45	4.09	4.09	0.02	2600	0.00	1100	100.82
Mean	76.61	0.09	12.51	1.15	0.03	0.03	0.44	4.27	4.27	0.02	1600	0.02	975	100.45
StdDev	0.55	0.02	0.10	0.04	0.04	0.01	0.01	0.54	0.54	0.02	712	0.02	150	

9951%

KN18	SiO2	TiO2	Al2O3	FeO	MnO	MgO	CaO	Na2O	K2O	P2O5	F (ppm)	SO2	Cl (ppm)	Total
1	73.54	0.12	11.03	3.64	0.06	0.02	0.15	5.40	5.40	0.00	6400	0.03	3000	99.51
2	74.52	0.18	11.00	3.63	0.12	0.00	0.17	5.43	5.43	0.00	57100	0.00	3000	105.73
3	74.53	0.16	10.91	3.52	0.02	0.00	0.16	5.86	5.86	0.02	3500	0.00	2700	100.46
4	73.99	0.21	10.82	3.57	0.12	0.00	0.13	6.37	6.37	0.02	6500	0.02	2500	100.63
5	74.34	0.15	10.84	3.60	0.02	0.00	0.11	5.36	5.36	0.00	5800	0.02	3200	99.80
6	74.58	0.17	11.04	3.68	0.06	0.00	0.12	5.41	5.41	0.01	4700	0.04	3300	100.32
Mean	74.20	0.16	10.93	3.60	0.06	0.00	0.13	5.68	5.68	0.01	5380	0.02	2940	100.14
StdDev	0.43	0.03	0.10	0.06	0.04	0.01	0.02	0.44	0.44	0.01	1272	0.01	336	

99%-101% cutoff

KE12	SiO2	TiO2	Al2O3	FeO	MnO	MgO	CaO	Na2O	K2O	P2O5	F (ppm)	SO2	Cl (ppm)	Total
1	68.44	0.31	7.82	8.61	0.26	0.00	0.37	8.89	8.89	0.00	3600	0.02	2800	99.62
2	69.61	0.36	7.80	8.48	0.11	0.00	0.35	8.69	8.69	0.00	4700	0.04	2500	100.52
3	68.11	0.32	7.66	8.16	0.19	0.01	0.34	10.51	10.51	0.00	5100	0.02	2900	100.45
4	69.91	0.26	7.95	8.60	0.33	0.00	0.35	7.59	7.59	0.04	4000	0.04	3000	100.10
5	69.20	0.32	7.84	8.52	0.31	0.02	0.34	7.77	7.77	0.04	3200	0.07	2700	99.37
6	68.21	0.26	7.81	8.75	0.21	0.01	0.34	7.15	7.15	0.03	5200	0.07	2900	98.03
Mean	69.05	0.31	7.81	8.47	0.24	0.01	0.35	8.69	8.69	0.02	4120	0.04	2780	100.01
StdDev	0.76	0.04	0.10	0.18	0.09	0.01	0.01	1.16	1.16	0.02	779	0.02	192	

99%-101% cutoff

Table C4.10 Accepted concentrations for glass standards used.

VG568	SiO2	TiO2	Al2O3	FeO	MnO	MgO	CaO	Na2O	K2O	P2O5	F (ppm)	SO2	Cl (ppm)	Total
VG568	76.71	0.12	12.06	1.23	0.03		0.5	2.62	0.19	0.2				99.46
KN18	74.6	0.18	10.53	3.45	0.15	0.01	0.06	5.68	4.39		6400		3700	100.16
KE12	70.33	0.33	7.26	8.36	0.35	0.02	0.026	7.28	4.27		4200		3300	99.31

Appendix 5

Table C5.1 Feldspar data for sample EBT-1

Analysis	11	12	13	14
SiO ₂	62.21	61.48	61.56	62.19
Al ₂ O ₃	22.74	23.05	22.73	22.58
FeO	0.34	0.34	0.30	0.30
SrO	0.24	0.31	0.32	0.24
BaO	0.32	0.20	0.32	0.29
CaO	3.00	3.49	3.08	3.04
Na ₂ O	7.53	8.10	7.44	8.20
K ₂ O	3.26	1.91	3.00	2.38
Total	99.63	98.88	98.76	99.22
An	14.5	17.0	15.2	14.6
Ab	66.7	72.0	67.2	71.8
Or	18.8	11.0	17.6	13.6

Table C5.2 Feldspar data for sample EBT-3

Analysis	11	12	13	14
SiO ₂	57.92	61.59	61.47	61.32
Al ₂ O ₃	26.05	23.14	22.08	22.64
FeO	0.25	0.26	0.23	0.25
SrO	0.36	0.26	0.22	0.30
BaO	0.09	0.24	0.18	0.31
CaO	6.84	3.62	2.90	3.14
Na ₂ O	6.64	7.44	7.63	7.43
K ₂ O	1.09	2.84	3.16	3.03
Total	99.23	99.38	97.87	98.41
An	33.7	17.5	14.1	15.4
Ab	59.9	66.1	67.7	66.8
Or	6.4	16.4	18.2	17.7

Table C5.3 Feldspar data for sample EBT-4

Analysis	11	12	13	14
SiO ₂	62.07	61.68	62.83	63.31
Al ₂ O ₃	23.71	23.31	22.56	22.60
FeO	0.27	0.25	0.19	0.26
SrO	0.34	0.31	0.33	0.27
BaO	0.24	0.26	0.24	0.36
CaO	4.18	3.65	2.98	3.21
Na ₂ O	7.56	7.62	7.52	7.67
K ₂ O	2.38	2.77	3.39	2.97
Total	100.74	99.85	100.04	100.65
An	20.1	17.5	14.3	15.5
Ab	66.4	66.8	66.2	67.5
Or	13.6	15.8	19.5	17.0

Table C5.4 Feldspar data for sample EBT-5

Analysis	11	12	13	14
SiO2	63.48	63.34	60.37	58.62
Al2O3	22.50	22.59	23.34	26.06
FeO	0.23	0.28	0.34	0.59
SrO	0.28	0.24	0.33	0.48
BaO	0.26	0.25	0.22	0.26
CaO	3.03	2.97	3.71	6.91
Na2O	7.45	7.68	7.74	6.68
K2O	3.50	3.18	2.68	1.15
Total	100.73	100.53	98.75	100.76
An	14.5	14.3	17.6	33.7
Ab	65.5	67.6	67.2	59.6
Or	20.0	18.2	15.2	6.7

Table C5.5 Feldspar data for sample EBT-6

Analysis	11	12	13	14
SiO2	63.22	54.44	61.53	52.98
Al2O3	22.46	28.81	23.31	30.16
FeO	0.22	0.46	0.32	0.29
SrO	0.23	0.38	0.36	0.37
BaO	0.29	0.07	0.30	0.07
CaO	2.88	10.05	3.86	11.67
Na2O	7.69	5.03	7.37	4.36
K2O	3.15	0.65	2.67	0.47
Total	100.12	99.89	99.72	100.38
An	13.9	50.2	18.8	57.8
Ab	68.0	46.0	65.7	39.5
Or	18.1	3.9	15.5	2.8

Table C5.6 Feldspar data for sample EBT-7

Analysis	11	12	13	14
SiO2	62.12	63.19	62.14	61.98
Al2O3	22.34	23.04	22.84	22.86
FeO	0.24	0.23	0.20	0.26
SrO	0.27	0.33	0.27	0.29
BaO	0.31	0.30	0.29	0.26
CaO	2.81	3.32	3.29	3.41
Na2O	7.59	7.52	7.50	7.51
K2O	3.27	2.96	3.00	2.99
Total	98.96	100.88	99.51	99.55
An	13.6	16.1	16.0	16.5
Ab	67.5	66.8	66.7	66.3
Or	18.9	17.1	17.4	17.2

Table C5.7 Feldspar data for sample EBT-8

Analysis	11	12	13	14
SiO ₂	62.61	62.10	61.35	61.71
Al ₂ O ₃	22.76	23.02	22.55	22.63
FeO	0.32	0.26	0.31	0.25
SrO	0.31	0.28	0.28	0.31
BaO	0.35	0.24	0.31	0.31
CaO	3.10	3.29	3.27	2.80
Na ₂ O	7.41	7.58	7.59	7.62
K ₂ O	3.11	3.04	3.04	3.29
Total	99.96	99.81	98.70	98.92
An	15.2	15.9	15.7	13.6
Ab	66.6	66.8	66.9	67.5
Or	18.2	17.4	17.4	19.0

Table C5.8 Feldspar data for sample EBT-9

Analysis	11	12	13	14
SiO ₂	63.16	65.07	62.53	63.25
Al ₂ O ₃	21.59	21.59	21.40	21.36
FeO	0.23	0.20	0.19	0.20
SrO	0.16	0.04	0.17	0.17
BaO	0.27	0.07	0.22	0.22
CaO	2.12	1.68	2.28	2.09
Na ₂ O	7.33	9.92	7.53	7.36
K ₂ O	4.58	1.27	4.17	4.41
Total	99.45	99.85	98.49	99.06
An	10.1	7.9	10.8	10.1
Ab	63.9	85.0	65.6	64.7
Or	26.0	7.1	23.6	25.2

Table C5.9 Feldspar data for sample EBT-10

Analysis	11	12	13	14
SiO ₂	56.48	61.57	61.85	63.63
Al ₂ O ₃	20.69	22.86	22.68	22.35
FeO	5.61	0.31	0.24	0.28
SrO	0.07	0.31	0.31	0.25
BaO	0.00	0.30	0.32	0.30
CaO	1.84	3.07	3.02	2.48
Na ₂ O	6.38	8.70	7.87	9.24
K ₂ O	5.62	1.45	2.78	1.27
Total	96.69	98.56	99.07	99.79
An	9.1	14.8	14.6	11.9
Ab	57.7	76.8	69.5	80.9
Or	33.1	8.3	15.9	7.2

Table C5.10 Feldspar data for sample EBT-12

Analysis	11	12	13	14
SiO ₂	61.69	62.52	62.12	62.38
Al ₂ O ₃	23.00	22.98	22.97	22.44
FeO	0.24	0.20	0.22	0.26
SrO	0.34	0.31	0.30	0.26
BaO	0.30	0.31	0.29	0.30
CaO	3.67	3.39	3.68	3.04
Na ₂ O	7.64	7.70	7.72	7.74
K ₂ O	2.89	3.00	2.84	3.35
Total	99.76	100.42	100.14	99.77
An	17.4	16.1	17.3	14.3
Ab	66.3	66.9	66.7	66.8
Or	16.3	17.0	16.0	18.8

Table C5.11 Feldspar data for sample EBT-16

Analysis	12	13
SiO ₂	62.48	61.88
Al ₂ O ₃	22.31	23.47
FeO	0.40	0.31
SrO	0.27	0.32
BaO	0.31	0.29
CaO	2.71	3.79
Na ₂ O	7.39	7.50
K ₂ O	3.86	2.57
Total	99.72	100.12
An	13.0	18.4
Ab	65.0	66.7
Or	22.0	14.9

Table C5.12 Feldspar data for sample EBT-17

Analysis	11	12	13	14
SiO ₂	59.43	60.24	61.71	62.66
Al ₂ O ₃	23.15	22.82	22.62	22.88
FeO	0.26	0.24	0.26	0.26
SrO	0.30	0.34	0.32	0.31
BaO	0.26	0.33	0.34	0.31
CaO	3.71	3.76	3.37	3.21
Na ₂ O	7.45	7.41	7.54	7.56
K ₂ O	2.53	2.66	2.80	2.90
Total	97.08	97.81	98.97	100.08
An	18.2	18.4	16.4	15.7
Ab	66.9	66.2	67.3	67.5
Or	14.8	15.5	16.2	16.8

Table C5.13 Feldspar data for sample EBT-18

Analysis	11	12	13	14
SiO ₂	61.41	63.39	60.31	61.75
Al ₂ O ₃	23.34	22.02	23.53	22.12
FeO	0.27	0.22	0.24	0.26
SrO	0.28	0.15	0.34	0.27
BaO	0.29	0.32	0.26	0.31
CaO	3.63	2.08	4.01	2.71
Na ₂ O	7.54	8.55	7.56	7.96
K ₂ O	2.89	2.59	2.36	2.90
Total	99.63	99.33	98.60	98.26
An	17.4	10.0	19.4	13.1
Ab	66.2	75.2	67.0	70.3
Or	16.5	14.8	13.6	16.6

Table C5.14 Feldspar data for sample EBT-19

Analysis	11
SiO ₂	60.28
Al ₂ O ₃	23.43
FeO	0.30
SrO	0.35
BaO	0.28
CaO	4.02
Na ₂ O	7.42
K ₂ O	2.31
Total	98.37
An	19.7
Ab	66.7
Or	13.5

Table C5.15 Feldspar data for sample EBT-21

Analysis	11	12	13	14
SiO ₂	62.14	61.46	62.81	61.05
Al ₂ O ₃	22.74	22.95	22.60	23.52
FeO	0.20	0.19	0.19	0.37
SrO	0.21	0.29	0.28	0.33
BaO	0.27	0.35	0.26	0.26
CaO	3.22	3.44	3.16	4.05
Na ₂ O	7.78	7.58	8.07	7.50
K ₂ O	3.26	3.04	3.22	2.58
Total	99.82	99.30	100.59	99.66
An	15.1	16.4	14.5	19.4
Ab	66.7	66.3	67.9	65.8
Or	18.2	17.3	17.6	14.7

Table C5.16 Feldspar data for sample EBT-22

Analysis	11	12	13	14
SiO2	59.14	62.83	61.51	62.08
Al2O3	25.07	22.43	23.21	23.07
FeO	0.31	0.23	0.23	0.27
SrO	0.33	0.29	0.33	0.30
BaO	0.11	0.31	0.27	0.26
CaO	5.85	3.12	3.76	3.63
Na2O	7.37	7.50	7.62	7.66
K2O	1.43	3.33	2.77	2.80
Total	99.60	100.04	99.69	100.06
An	27.8	15.0	17.9	17.3
Ab	64.1	66.0	66.4	66.8
Or	8.1	19.0	15.7	15.9

Table C5.17 Feldspar data for sample EBT-23a

Analysis	11	12	13	14
SiO2	61.67	62.66	62.25	63.02
Al2O3	23.32	22.59	23.00	22.31
FeO	0.29	0.42	0.27	0.25
SrO	0.35	0.26	0.36	0.25
BaO	0.27	0.30	0.30	0.30
CaO	3.87	3.32	3.84	2.83
Na2O	7.51	7.61	7.69	7.61
K2O	2.70	3.27	2.63	3.54
Total	99.98	100.44	100.34	100.10
An	18.6	15.7	18.2	13.5
Ab	65.9	65.9	66.9	66.4
Or	15.5	18.4	14.9	20.1

Table C5.18 Feldspar data for sample EBT-23b

Analysis	11	12	13	14
SiO2	63.22	62.25	61.63	63.28
Al2O3	22.54	22.83	22.89	22.48
FeO	0.32	0.25	0.24	0.18
SrO	0.28	0.36	0.33	0.25
BaO	0.35	0.32	0.30	0.34
CaO	2.92	3.35	3.44	2.96
Na2O	8.41	7.63	7.62	7.70
K2O	3.44	3.13	2.95	3.52
Total	101.47	100.11	99.41	100.70
An	13.0	15.9	16.5	13.9
Ab	68.7	66.4	66.7	66.3
Or	18.2	17.7	16.8	19.7

Table C5.19 Feldspar data for sample EBT-30

Analysis	11	12	13	14
SiO ₂	62.51	61.45	61.58	61.29
Al ₂ O ₃	22.92	23.27	23.08	22.97
FeO	0.29	0.26	0.18	0.27
SrO	0.36	0.34	0.32	0.33
BaO	0.26	0.29	0.29	0.27
CaO	3.43	3.62	3.66	3.50
Na ₂ O	7.68	7.60	7.61	7.68
K ₂ O	2.96	2.81	2.81	2.76
Total	100.40	99.65	99.52	99.08
An	16.3	17.3	17.5	16.8
Ab	66.9	66.6	66.6	67.4
Or	16.8	16.0	16.0	15.8

Table C5.20 Feldspar data for sample EBT-33

Analysis	11	12	13	14
SiO ₂	62.17	63.09	61.55	62.82
Al ₂ O ₃	22.33	23.64	22.20	22.46
FeO	0.20	0.24	0.31	0.31
SrO	0.29	0.31	0.28	0.26
BaO	0.28	0.33	0.40	0.47
CaO	3.02	3.27	2.54	2.73
Na ₂ O	7.54	7.66	7.85	7.66
K ₂ O	3.37	2.97	3.37	3.25
Total	99.19	101.52	98.50	99.96
An	14.5	15.7	12.1	13.2
Ab	66.3	67.3	68.7	68.0
Or	19.3	17.0	19.2	18.8

Table C5.21 Feldspar data for sample EBT-34

Analysis	11	12	13	14
SiO ₂	61.11	61.47	61.82	62.38
Al ₂ O ₃	23.23	23.26	22.45	22.34
FeO	0.25	0.31	0.22	0.26
SrO	0.32	0.27	0.27	0.27
BaO	0.27	0.23	0.36	0.34
CaO	3.53	3.32	2.77	2.97
Na ₂ O	7.61	7.76	7.76	7.61
K ₂ O	2.75	2.89	3.36	3.25
Total	99.07	99.50	99.00	99.42
An	17.0	15.8	13.2	14.3
Ab	67.2	67.8	67.7	67.1
Or	15.8	16.4	19.1	18.6

Table C5.22 Feldspar data for sample EBT-34a

Analysis	11	12	13	14
SiO2	62.14	61.83	61.38	61.70
Al2O3	23.47	23.08	23.22	22.91
FeO	0.26	0.21	0.32	0.21
SrO	0.33	0.29	0.36	0.31
BaO	0.25	0.34	0.33	0.29
CaO	3.75	3.53	3.72	3.53
Na2O	7.75	7.77	7.59	7.77
K2O	2.56	2.77	2.78	2.69
Total	100.51	99.82	99.69	99.41
An	17.9	16.8	17.8	16.9
Ab	67.6	67.6	66.4	67.9
Or	14.6	15.7	15.8	15.3

Table C5.23 Feldspar data for sample EBT-34b

Analysis	11	12	13	14
SiO2	64.74	63.27	61.96	60.88
Al2O3	19.33	22.72	23.36	23.45
FeO	0.40	0.24	0.19	0.20
SrO	0.03	0.31	0.29	0.32
BaO	0.02	0.26	0.24	0.27
CaO	0.32	3.41	3.93	3.97
Na2O	5.56	7.54	7.57	7.46
K2O	8.54	2.98	2.55	2.54
Total	98.93	100.73	100.08	99.09
An	1.5	16.4	18.9	19.2
Ab	49.2	66.4	66.5	66.1
Or	49.2	17.1	14.6	14.7

Table C5.24 Feldspar data for sample EBT-34c

Analysis	11	12	13	14
SiO2	62.79	64.17	64.09	62.88
Al2O3	23.16	22.41	21.76	23.66
FeO	0.26	0.30	0.53	0.28
SrO	0.36	0.29	0.21	0.36
BaO	0.29	0.35	0.34	0.20
CaO	3.67	2.77	2.29	4.12
Na2O	7.64	7.74	7.64	7.75
K2O	2.99	3.73	4.34	2.62
Total	101.15	101.76	101.19	101.87
An	17.3	13.0	10.7	19.2
Ab	65.9	66.3	65.2	66.2
Or	16.8	20.8	24.1	14.6

Table C5.25 Feldspar data for sample EBT-34d

Analysis	11	12	13	14
SiO ₂	62.86	60.13	63.50	62.51
Al ₂ O ₃	22.94	19.24	22.28	22.98
FeO	0.26	4.91	0.18	0.21
SrO	0.33	0.01	0.26	0.34
BaO	0.28	0.00	0.27	0.31
CaO	3.36	1.96	2.83	3.46
Na ₂ O	7.54	6.87	7.48	7.56
K ₂ O	2.82	5.16	3.66	2.84
Total	100.39	98.28	100.46	100.21
An	16.4	9.5	13.5	16.7
Ab	67.3	60.8	65.6	66.9
Or	16.3	29.7	20.9	16.3

Table C5.26 Feldspar data for sample EBT-35

Analysis	11	12	13	14
SiO ₂	62.21	61.92	60.39	61.26
Al ₂ O ₃	23.70	23.93	23.74	23.42
FeO	0.20	0.24	0.27	0.27
SrO	0.35	0.37	0.33	0.27
BaO	0.32	0.21	0.28	0.29
CaO	3.84	4.17	3.99	3.82
Na ₂ O	7.61	7.64	7.58	7.68
K ₂ O	2.63	2.35	2.50	2.53
Total	100.86	100.84	99.07	99.54
An	18.4	19.9	19.2	18.3
Ab	66.6	66.7	66.6	67.3
Or	15.0	13.4	14.3	14.4

Table C5.27 Feldspar data for sample EBT-35a

Analysis	11	12	14
SiO ₂	63.69	62.95	61.11
Al ₂ O ₃	22.16	23.04	23.14
FeO	0.23	0.27	0.27
SrO	0.30	0.26	0.36
BaO	0.37	0.27	0.28
CaO	2.70	3.41	3.42
Na ₂ O	7.54	7.76	7.55
K ₂ O	3.58	2.84	2.88
Total	100.55	100.79	99.01
An	13.0	16.2	16.5
Ab	66.5	67.7	66.8
Or	20.5	16.1	16.6

Table C5.28 Feldspar data for sample EBT-35b

Analysis	11	12	14
SiO ₂	61.79	61.11	61.55
Al ₂ O ₃	22.62	23.32	24.04
FeO	0.21	0.27	0.31
SrO	0.29	0.33	0.30
BaO	0.33	0.32	0.22
CaO	3.20	3.59	4.28
Na ₂ O	7.76	7.67	7.55
K ₂ O	3.19	2.75	2.20
Total	99.38	99.35	100.43
An	15.1	17.2	20.6
Ab	67.0	67.2	66.7
Or	17.9	15.6	12.6

Table C5.29 Feldspar data for sample EBT-36

Analysis	11	12	13	14
SiO ₂	62.13	57.59	60.87	62.90
Al ₂ O ₃	23.23	25.91	23.26	23.33
FeO	0.25	0.35	0.23	0.25
SrO	0.35	0.34	0.38	0.32
BaO	0.30	0.09	0.29	0.27
CaO	3.32	6.37	3.65	3.61
Na ₂ O	8.00	7.09	7.67	7.67
K ₂ O	2.93	1.17	2.72	2.73
Total	100.50	98.91	99.05	101.08
An	15.5	30.7	17.5	17.3
Ab	68.3	62.6	67.1	67.2
Or	16.3	6.7	15.5	15.6

Table C5.30 Feldspar data for sample EBT-37

Analysis	11	12	13	14
SiO ₂	61.42	60.69	61.62	62.25
Al ₂ O ₃	23.28	23.00	23.31	22.61
FeO	0.23	0.28	0.22	0.23
SrO	0.29	0.35	0.27	0.30
BaO	0.27	0.33	0.35	0.28
CaO	3.48	3.36	3.78	3.37
Na ₂ O	7.73	7.63	7.73	7.84
K ₂ O	2.89	2.97	2.94	3.18
Total	99.58	98.60	100.23	100.06
An	16.5	16.1	17.7	15.7
Ab	67.2	67.0	66.0	66.7
Or	16.3	16.9	16.3	17.6

Table C5.31 Feldspar data for sample EBT-38

Analysis	12	13
SiO ₂	62.54	60.13
Al ₂ O ₃	22.84	23.04
FeO	0.29	0.26
SrO	0.35	0.32
BaO	0.31	0.29
CaO	3.22	3.32
Na ₂ O	7.61	7.67
K ₂ O	3.23	3.00
Total	100.37	98.02
An	15.3	15.9
Ab	66.4	67.1
Or	18.3	17.1

Table C5.32 Feldspar data for sample EBT-39

Analysis	11	12	13	14
SiO ₂	62.81	62.89	62.06	62.27
Al ₂ O ₃	23.12	23.34	23.46	22.95
FeO	0.29	0.26	0.23	0.26
SrO	0.38	0.25	0.31	0.32
BaO	0.27	0.29	0.30	0.28
CaO	3.47	3.49	3.73	3.30
Na ₂ O	7.42	7.43	7.50	7.63
K ₂ O	2.80	3.07	2.78	3.01
Total	100.56	101.01	100.36	100.03
An	17.0	16.8	17.9	15.8
Ab	66.6	65.6	66.1	67.0
Or	16.4	17.6	15.9	17.2

Table C5.33 Feldspar data for sample EBT-40

Analysis	11	12	13
SiO ₂	62.85	62.42	62.51
Al ₂ O ₃	22.68	22.43	22.73
FeO	0.28	0.29	0.30
SrO	0.20	0.26	0.25
BaO	0.27	0.34	0.34
CaO	3.14	2.76	3.00
Na ₂ O	7.61	7.63	8.59
K ₂ O	3.36	3.48	1.99
Total	100.38	99.60	99.69
An	14.9	13.2	14.2
Ab	66.1	66.9	74.5
Or	19.0	19.9	11.2

Table C5.34 Feldspar data for sample EBT-40a

Analysis	11	12	13	14
SiO ₂	62.68	62.67	61.68	61.98
Al ₂ O ₃	22.92	23.00	23.14	22.47
FeO	0.28	0.27	0.30	0.27
SrO	0.23	0.29	0.31	0.29
BaO	0.37	0.28	0.30	0.30
CaO	3.33	3.52	3.55	2.98
Na ₂ O	7.68	7.71	7.60	7.66
K ₂ O	2.99	2.93	2.89	3.30
Total	100.47	100.68	99.76	99.24
An	15.9	16.7	17.0	14.3
Ab	67.1	66.8	66.5	67.0
Or	17.0	16.5	16.5	18.8

Table C5.35 Feldspar data for sample EBT-40b

Analysis	11	12	13	14
SiO ₂	62.45	60.89	60.90	62.79
Al ₂ O ₃	22.72	23.18	23.30	22.94
FeO	0.30	0.32	0.30	0.25
SrO	0.35	0.36	0.32	0.28
BaO	0.34	0.33	0.29	0.29
CaO	3.23	3.45	3.53	3.26
Na ₂ O	7.55	7.77	7.65	7.72
K ₂ O	3.14	2.90	2.82	3.12
Total	100.08	99.19	99.13	100.63
An	15.5	16.3	16.9	15.5
Ab	66.5	67.3	67.0	66.9
Or	18.0	16.4	16.1	17.6

Table C5.36 Feldspar data for sample EBT-40c

Analysis	11	12	13	14
SiO ₂	62.89	62.26	59.88	62.60
Al ₂ O ₃	22.60	22.93	23.74	22.67
FeO	0.22	0.26	0.24	0.20
SrO	0.28	0.35	0.33	0.31
BaO	0.35	0.34	0.31	0.44
CaO	3.15	3.30	4.03	3.09
Na ₂ O	7.60	7.73	7.40	7.76
K ₂ O	3.22	3.06	2.53	3.16
Total	100.31	100.23	98.45	100.23
An	15.1	15.6	19.6	14.7
Ab	66.6	67.1	65.8	67.5
Or	18.4	17.3	14.6	17.9

Table C5.37 Feldspar data for sample EBT-40d

Analysis	11	12	13	14
SiO2	62.85	63.74	63.41	60.68
Al2O3	22.14	22.60	22.80	23.79
FeO	0.23	0.24	0.26	0.31
SrO	0.28	0.26	0.27	0.30
BaO	0.31	0.30	0.31	0.26
CaO	2.53	2.80	3.15	4.11
Na2O	7.80	7.72	7.72	7.72
K2O	3.92	3.52	3.41	2.49
Total	100.05	101.18	101.32	99.64
An	11.8	13.3	14.8	19.4
Ab	66.5	66.9	66.2	66.7
Or	21.7	19.9	19.0	14.0

Table C5.38 Feldspar data for sample EBT-41

Analysis	11	12	13
SiO2	61.90	64.35	63.81
Al2O3	23.47	22.32	22.68
FeO	0.23	0.23	0.24
SrO	0.34	0.24	0.30
BaO	0.32	0.33	0.30
CaO	3.57	2.60	2.89
Na2O	7.65	7.74	7.78
K2O	2.94	3.93	3.65
Total	100.41	101.75	101.65
An	16.9	12.1	13.5
Ab	66.5	66.1	66.3
Or	16.6	21.8	20.2

Table C5.39 Feldspar data for sample EBT-43

Analysis	11	12	13	14
SiO2	62.64	61.17	61.19	61.85
Al2O3	22.43	23.07	22.78	22.78
FeO	0.17	0.26	0.21	0.24
SrO	0.23	0.34	0.32	0.25
BaO	0.24	0.30	0.34	0.25
CaO	2.77	3.47	3.31	3.03
Na2O	7.72	7.54	7.50	7.63
K2O	3.40	2.73	2.83	3.02
Total	99.61	98.87	98.47	99.04
An	13.2	16.9	16.2	14.7
Ab	67.4	67.3	67.3	67.8
Or	19.3	15.8	16.5	17.5

Table C5.40 Feldspar data for sample EBT-44

Analysis	11	12	13	14
SiO ₂	63.95	63.67	63.12	63.35
Al ₂ O ₃	22.64	22.84	23.15	23.53
FeO	0.20	0.21	0.25	0.24
SrO	0.28	0.28	0.34	0.32
BaO	0.27	0.27	0.33	0.32
CaO	2.76	3.13	3.60	3.66
Na ₂ O	7.70	7.54	7.65	7.72
K ₂ O	3.36	3.13	2.70	2.62
Total	101.17	101.06	101.13	101.77
An	13.2	15.1	17.3	17.5
Ab	67.6	66.8	67.3	67.6
Or	19.2	18.0	15.4	14.9

Table C5.41 Feldspar data for sample EBT-47

Analysis	11	12	13	14	15
SiO ₂	63.79	62.51	62.09	62.20	63.59
Al ₂ O ₃	22.66	22.79	23.73	23.65	22.45
FeO	0.20	0.25	0.31	0.31	0.29
SrO	0.31	0.27	0.37	0.36	0.27
BaO	0.31	0.28	0.27	0.21	0.27
CaO	3.06	3.16	4.32	4.23	3.04
Na ₂ O	7.58	7.89	7.61	7.61	7.78
K ₂ O	3.43	3.42	2.41	2.49	3.49
Total	101.34	100.55	101.11	101.04	101.18
An	14.5	14.6	20.4	20.0	14.2
Ab	66.0	66.6	66.0	66.0	66.4
Or	19.4	18.8	13.6	14.0	19.4

Table C5.42 Feldspar data for sample EBT-48

Analysis	11	12	13	14
SiO ₂	62.76	62.53	62.84	62.86
Al ₂ O ₃	23.20	23.90	23.34	23.56
FeO	0.23	0.26	0.27	0.31
SrO	0.32	0.29	0.29	0.31
BaO	0.34	0.26	0.26	0.32
CaO	3.48	4.37	4.00	3.89
Na ₂ O	7.92	7.60	7.57	7.66
K ₂ O	3.02	2.56	2.83	2.75
Total	101.26	101.76	101.41	101.67
An	16.1	20.5	18.9	18.4
Ab	67.2	65.2	65.3	66.2
Or	16.7	14.3	15.9	15.5

Table C5.43 Feldspar data for sample EBT-49

Analysis	11	12	13	14	15
SiO ₂	63.67	62.69	62.17	62.88	62.66
Al ₂ O ₃	22.57	22.80	23.51	23.54	23.29
FeO	0.27	0.28	0.23	0.22	0.19
SrO	0.28	0.29	0.34	0.32	0.33
BaO	0.30	0.29	0.33	0.29	0.27
CaO	2.98	3.25	4.01	3.87	3.80
Na ₂ O	7.77	7.73	7.52	7.68	7.61
K ₂ O	3.65	3.31	2.79	2.93	2.85
Total	101.48	100.64	100.90	101.74	101.00
An	13.8	15.2	19.0	18.1	18.0
Ab	66.0	66.3	65.2	65.6	66.0
Or	20.2	18.5	15.8	16.3	16.1

Table C5.44 Feldspar data for sample EBT-50

Analysis	11	12	13
SiO ₂	62.72	64.08	62.82
Al ₂ O ₃	23.23	22.47	23.32
FeO	0.28	0.25	0.30
SrO	0.35	0.28	0.26
BaO	0.32	0.35	0.29
CaO	3.74	2.77	3.60
Na ₂ O	7.76	7.75	7.67
K ₂ O	2.87	3.77	3.01
Total	101.26	101.70	101.28
An	17.5	12.9	17.0
Ab	66.5	66.2	66.1
Or	16.0	20.9	16.9

Table C5.45 Feldspar data for sample EBT-51

Analysis	12	13	14	15
SiO ₂	63.12	63.34	63.40	61.71
Al ₂ O ₃	23.05	22.83	22.81	23.96
FeO	0.26	0.28	0.31	0.57
SrO	0.25	0.29	0.31	0.32
BaO	0.26	0.29	0.32	0.21
CaO	3.55	3.22	3.13	4.65
Na ₂ O	7.64	7.83	7.58	7.48
K ₂ O	3.13	3.30	3.50	2.23
Total	101.26	101.37	101.36	101.13
An	16.7	15.0	14.8	22.2
Ab	65.8	66.7	65.5	65.2
Or	17.5	18.3	19.7	12.6

Table C5.46 Feldspar data for sample EBT-52

Analysis	11	12	13	14
SiO ₂	62.75	62.17	62.86	60.48
Al ₂ O ₃	23.06	23.40	22.83	24.62
FeO	0.28	0.28	0.25	0.24
SrO	0.31	0.31	0.28	0.34
BaO	0.28	0.24	0.25	0.31
CaO	3.45	3.94	3.25	4.95
Na ₂ O	7.80	7.59	7.61	7.54
K ₂ O	2.86	2.79	3.28	1.91
Total	100.79	100.72	100.61	100.39
An	16.3	18.6	15.4	23.5
Ab	67.6	65.7	66.0	65.6
Or	16.1	15.7	18.5	10.8

Table C5.47 Feldspar data for sample EBT-53

Analysis	11	12	13	14
SiO ₂	62.53	63.10	62.08	62.83
Al ₂ O ₃	23.32	22.58	22.75	22.91
FeO	0.27	0.23	0.25	0.31
SrO	0.31	0.24	0.27	0.31
BaO	0.34	0.32	0.26	0.29
CaO	3.72	3.18	3.07	3.30
Na ₂ O	7.61	7.59	7.66	7.72
K ₂ O	2.89	3.34	3.41	3.11
Total	100.97	100.56	99.75	100.78
An	17.6	15.1	14.5	15.6
Ab	66.1	66.0	66.3	66.8
Or	16.3	18.9	19.2	17.5

Table C5.48 Feldspar data for sample EBT-54

Analysis	11	12	13	14	15
SiO ₂	62.71	62.96	62.44	60.70	62.92
Al ₂ O ₃	23.25	22.63	22.61	24.46	22.64
FeO	0.26	0.27	0.26	0.29	0.25
SrO	0.31	0.27	0.21	0.27	0.27
BaO	0.29	0.33	0.35	0.20	0.27
CaO	3.55	2.80	2.90	5.01	2.92
Na ₂ O	7.89	8.87	8.80	7.53	7.71
K ₂ O	2.95	1.78	1.83	1.81	3.48
Total	101.21	99.89	99.40	100.26	100.44
An	16.5	13.2	13.7	23.9	13.8
Ab	67.1	76.8	76.0	65.8	66.6
Or	16.3	10.0	10.3	10.3	19.6

Table C5.49 Feldspar data for sample EBT-56

Analysis	11	12
SiO ₂	61.13	61.53
Al ₂ O ₃	23.28	23.08
FeO	0.31	0.34
SrO	0.28	0.29
BaO	0.30	0.38
CaO	3.79	3.49
Na ₂ O	7.53	7.44
K ₂ O	2.66	2.81
Total	99.28	99.36
An	18.3	17.1
Ab	66.4	66.6
Or	15.3	16.3

Table C5.50 Feldspar data for sample EBT-62

Analysis	11	12	13
SiO ₂	62.78	62.85	62.85
Al ₂ O ₃	22.13	22.15	22.44
FeO	0.31	0.31	0.30
SrO	0.31	0.23	0.26
BaO	0.49	0.29	0.35
CaO	2.53	2.75	2.59
Na ₂ O	7.59	7.41	8.49
K ₂ O	3.67	3.77	2.42
Total	99.81	99.76	99.69
An	12.2	13.2	12.3
Ab	66.8	65.2	74.0
Or	21.0	21.6	13.7

Table C5.51 Feldspar data for sample BIT-42

Analysis	11	12	13	14
SiO ₂	62.26	63.18	63.44	62.98
Al ₂ O ₃	23.00	22.56	22.26	22.02
FeO	0.29	0.23	0.29	0.30
SrO	0.29	0.27	0.22	0.18
BaO	0.31	0.26	0.38	0.34
CaO	3.28	3.01	2.64	2.57
Na ₂ O	7.73	7.69	7.71	7.67
K ₂ O	2.99	3.23	3.59	3.74
Total	100.16	100.43	100.53	99.80
An	15.6	14.4	12.6	12.2
Ab	67.4	67.2	67.1	66.7
Or	17.0	18.4	20.3	21.1

Table C5.52 Feldspar data for sample BIT-272

Analysis	11	12	13	14
SiO2	62.96	62.74	62.29	61.92
Al2O3	21.89	22.10	22.26	22.63
FeO	0.22	0.22	0.29	0.22
SrO	0.27	0.28	0.30	0.32
BaO	0.35	0.36	0.32	0.31
CaO	2.74	2.74	3.03	3.45
Na2O	7.39	7.47	7.35	7.29
K2O	3.62	3.58	3.42	3.06
Total	99.45	99.50	99.27	99.20
An	13.3	13.3	14.7	16.9
Ab	65.7	66.1	65.4	65.3
Or	20.9	20.6	19.8	17.8

Table C5.53 Feldspar data for sample BIT-288

Analysis	11	12	13	14
SiO2	61.58	62.54	62.43	63.39
Al2O3	22.04	21.90	22.36	21.19
FeO	0.23	0.23	0.25	0.22
SrO	0.29	0.23	0.27	0.25
BaO	0.30	0.26	0.34	0.27
CaO	2.82	2.71	2.97	2.13
Na2O	7.31	7.45	7.39	7.34
K2O	3.61	3.50	3.41	4.19
Total	98.18	98.83	99.40	98.98
An	13.8	13.2	14.4	10.4
Ab	65.3	66.5	65.8	65.4
Or	21.0	20.3	19.8	24.3

Appendix 6

Table C6.1 Microprobe feldspar standards for 3/5/99

Ortho	SiO2	Al2O3	CaO	FeO	SrO	BaO	Na2O	K2O	Total	99% cutoff
1	64.30	16.61	0.03	1.75	0.02	0.07	1.00	15.41	99.19	
2	64.65	16.65	0.01	1.79	0.01	0.02	0.96	15.42	99.51	
3	63.24	16.77	0.00	1.79	0.04	0.05	1.00	15.55	98.42	
4	64.03	16.61	0.01	1.79	0.02	0.07	0.95	15.42	98.90	
5	64.32	16.72	0.01	1.73	0.02	0.08	0.91	15.43	99.21	
6	63.42	16.64	0.01	1.75	0.02	0.08	0.98	15.33	98.23	
Mean	64.42	16.66	0.02	1.76	0.02	0.06	0.96	15.42	99.30	
StdDev	0.20	0.05	0.01	0.032	0.008	0.029	0.045	0.013		

Albite	SiO2	Al2O3	CaO	FeO	SrO	BaO	Na2O	K2O	Total	99% cutoff
1	67.33	20.24	0.02	0.00	0.01	0.03	11.91	0.03	99.58	
2	67.97	20.03	0.04	0.02	0.00	0.02	11.93	0.03	100.04	
3	68.15	19.96	0.01	0.01	0.01	0.00	11.92	0.01	100.07	
4	68.07	20.07	0.02	0.02	0.02	0.02	11.85	0.02	100.09	
5	67.11	20.19	0.03	0.00	0.00	0.03	11.94	0.02	99.32	
6	67.80	20.20	0.02	0.04	0.01	0.00	11.92	0.02	100.02	
Mean	67.74	20.11	0.02	0.02	0.01	0.02	11.91	0.02	99.85	
StdDev	0.42	0.11	0.01	0.02	0.01	0.01	0.03	0.01		

Table C6.2 Microprobe feldspar standards for 3/17/99

Ortho									99% cutoff
	SiO2	Al2O3	CaO	FeO	SrO	BaO	Na2O	K2O	Total
1	64.27	16.86	0.01	1.80	0.00	0.04	0.96	15.52	99.45
2	64.93	16.69	0.01	1.75	0.02	0.04	1.00	15.51	99.94
3	63.41	16.77	0.00	1.74	0.02	0.10	0.99	15.55	98.57
4	64.32	16.69	0.00	1.75	0.02	0.10	1.03	15.48	99.39
5	64.94	16.77	0.00	1.77	0.01	0.06	1.04	15.77	100.36
6	63.67	16.79	0.02	1.81	0.00	0.08	0.97	15.62	98.95
Mean	64.37	16.76	0.01	1.76	0.01	0.07	1.00	15.57	99.54
StdDev	0.63	0.07	0.01	0.02	0.01	0.03	0.03	0.12	

Albite									101% cutoff
	SiO2	Al2O3	CaO	FeO	SrO	BaO	Na2O	K2O	Total
1	69.07	20.34	0.02	0.00	0.03	0.01	12.10	0.01	101.57
2	67.99	20.28	0.02	0.01	0.00	0.00	12.09	0.01	100.40
3	68.71	20.24	0.03	0.00	0.02	0.00	11.99	0.01	101.00
4	67.84	20.21	0.01	0.01	0.03	0.01	12.06	0.00	100.18
5	68.80	20.08	0.02	0.00	0.00	0.00	12.16	0.02	101.09
6	69.19	20.31	0.03	0.00	0.04	0.00	11.99	0.00	101.56
Mean	68.18	20.25	0.02	0.01	0.02	0.00	12.05	0.01	100.53
StdDev	0.47	0.04	0.01	0.01	0.01	0.01	0.05	0.01	

Table C6.3 Microprobe feldspar standards for 3/18/99

Ortho									99% cutoff
	SiO2	Al2O3	CaO	FeO	SrO	BaO	Na2O	K2O	Total
1	64.76	16.76	0.00	1.75	0.02	0.08	0.93	15.78	100.07
2	64.60	16.78	0.01	1.75	0.00	0.09	1.05	15.77	100.04
3	64.91	16.71	0.01	1.72	0.01	0.06	1.01	15.89	100.32
4	64.84	16.85	0.01	1.74	0.01	0.04	1.02	15.66	100.16
5	63.99	16.81	0.01	1.80	0.03	0.05	0.97	15.55	99.20
6	62.96	16.72	0.00	1.76	0.04	0.07	0.91	15.53	98.00
Mean	64.62	16.78	0.01	1.75	0.01	0.06	0.99	15.73	99.96
StdDev	0.37	0.05	0.01	0.03	0.01	0.02	0.05	0.13	

Albite									99% cutoff
	SiO2	Al2O3	CaO	FeO	SrO	BaO	Na2O	K2O	Total
1	68.56	20.29	0.04	0.03	0.00	0.01	12.00	0.00	100.92
2	68.36	20.09	0.02	0.03	0.04	0.00	11.88	0.02	100.44
3	67.19	20.06	0.01	0.00	0.03	0.00	11.85	0.03	99.16
4	68.36	20.01	0.00	0.00	0.00	0.00	11.94	0.02	100.34
5	68.34	20.28	0.01	0.00	0.04	0.01	12.02	0.00	100.69
6	68.15	20.03	0.02	0.00	0.03	0.00	12.02	0.02	100.27
Mean	68.16	20.13	0.02	0.01	0.02	0.00	11.95	0.02	100.30
StdDev	0.49	0.12	0.01	0.01	0.02	0.00	0.08	0.01	

Table C6.4 Microprobe feldspar standards for 3/30/99

Ortho	99%-101% cutoff									
	SiO2	Al2O3	CaO	FeO	SrO	BaO	Na2O	K2O	Total	
1	64.43	16.70	0.01	1.74	0.00	0.04	0.97	15.67	99.55	
2	63.87	16.66	0.01	1.79	0.04	0.03	1.06	15.46	98.91	
3	64.64	16.71	0.00	1.70	0.02	0.08	0.97	15.44	99.55	
4	65.10	17.04	0.00	1.74	0.00	0.06	5.42	15.44	104.79	
Mean	64.53	16.71	0.00	1.72	0.01	0.06	0.97	15.55	99.55	
StdDev	0.14	0.01	0.01	0.03	0.01	0.03	0.00	0.16		

Albite	99.5% cutoff									
	SiO2	Al2O3	CaO	FeO	SrO	BaO	Na2O	K2O	Total	
1	67.54	20.17	0.01	0.00	0.01	0.01	12.00	0.01	99.74	
2	67.49	20.19	0.02	0.02	0.00	0.00	12.03	0.01	99.76	
3	68.40	20.03	0.02	0.00	0.02	0.03	11.91	0.00	100.41	
4	68.40	20.09	0.02	0.00	0.02	0.00	11.95	0.03	100.51	
Mean	67.96	20.12	0.02	0.01	0.01	0.01	11.97	0.01	100.11	
StdDev	0.51	0.07	0.00	0.01	0.01	0.02	0.05	0.01	0.00	

Table C6.5 Microprobe feldspar standards for 4/30/99

Ortho							98% cutoff		
	SiO2	Al2O3	CaO	FeO	SrO	BaO	Na2O	K2O	Total
1	63.60	16.71	0.00	1.78	0.03	0.04	0.96	15.50	98.62
2	63.56	16.51	0.00	1.78	0.04	0.08	0.97	15.30	98.24
3	63.86	16.59	0.02	1.83	0.02	0.06	0.90	15.35	98.62
4	63.09	16.45	0.00	1.81	0.02	0.06	0.93	15.39	97.74
5	62.52	16.44	0.01	1.82	0.00	0.08	0.94	15.17	96.96
6	64.20	16.74	0.00	1.75	0.02	0.09	0.98	15.22	99.00
Mean	63.81	16.64	0.00	1.79	0.03	0.07	0.95	15.34	98.62
StdDev	0.29	0.11	0.01	0.03	0.01	0.02	0.04	0.12	

Albite							99% cutoff		
	SiO2	Al2O3	CaO	FeO	SrO	BaO	Na2O	K2O	Total
1	67.55	19.94	0.00	0.01	0.00	0.00	11.61	0.01	99.11
2	67.82	19.95	0.03	0.04	0.00	0.00	11.65	0.01	99.51
3	67.44	20.24	0.03	0.00	0.02	0.01	11.62	0.02	99.38
4	67.94	20.13	0.01	0.00	0.00	0.00	11.73	0.02	99.83
5	67.32	20.46	0.05	0.01	0.03	0.00	11.85	0.01	99.73
6	67.25	19.87	0.00	0.00	0.02	0.00	11.73	0.02	98.89
Mean	67.61	20.14	0.02	0.01	0.01	0.00	11.69	0.02	99.51
StdDev	0.26	0.22	0.02	0.02	0.01	0.00	0.10	0.01	

Table C6.6 Microprobe feldspar standards for 5/1/99

Ortho							98% cutoff			
	SiO2	Al2O3	CaO	FeO	SrO	BaO	Na2O	K2O	Total	
1	64.35	16.59	0.02	1.83	0.01	0.07	0.95	15.05	98.86	
2	63.84	16.65	0.00	1.82	0.05	0.05	0.96	14.90	98.27	
3	64.61	16.48	0.00	1.78	0.00	0.06	0.95	15.06	98.96	
4	63.38	16.55	0.00	1.88	0.01	0.05	0.97	14.96	97.79	
5	63.76	16.75	0.00	1.77	0.01	0.06	0.99	15.11	98.44	
6	63.46	16.81	0.00	1.78	0.00	0.06	0.95	14.99	98.04	
Mean	64.00	16.66	0.00	1.80	0.01	0.06	0.96	15.02	98.51	
StdDev	0.47	0.13	0.01	0.03	0.02	0.00	0.02	0.08		

Albite							99% cutoff			
	SiO2	Al2O3	CaO	FeO	SrO	BaO	Na2O	K2O	Total	
1	67.99	20.26	0.00	0.01	0.03	0.00	11.00	0.01	99.30	
2	66.34	19.80	0.04	0.00	0.01	0.01	11.45	0.01	97.65	
3	68.06	19.90	0.02	0.00	0.04	0.01	11.83	0.02	99.88	
4	67.02	20.11	0.03	0.00	0.00	0.02	11.74	0.02	98.95	
5	65.97	20.26	0.04	0.00	0.03	0.01	11.89	0.00	98.19	
6	67.57	19.94	0.03	0.01	0.00	0.00	11.75	0.02	99.32	
Mean	67.88	20.04	0.02	0.01	0.02	0.00	11.53	0.01	99.50	
StdDev	0.27	0.20	0.01	0.00	0.02	0.01	0.46	0.01		

Table C6.7 Microprobe feldspar standards for 5/5/99

Ortho	99% cutoff							Total	
	SiO2	Al2O3	CaO	FeO	SrO	BaO	Na2O		K2O
1	64.62	16.98	0.00	1.82	0.01	0.03	0.95	15.16	99.58
2	63.59	16.76	0.00	1.87	0.00	0.06	0.97	14.90	98.16
3	64.31	16.78	0.02	1.76	0.01	0.09	0.93	15.30	99.19
4	64.40	16.86	0.02	1.83	0.02	0.04	0.93	15.29	99.40
5	64.82	16.76	0.01	1.79	0.00	0.07	0.99	15.27	99.71
6	65.07	16.74	0.00	1.80	0.01	0.08	0.95	15.10	99.74
Mean	64.64	16.83	0.01	1.80	0.01	0.06	0.95	15.22	99.52
StdDev	0.31	0.10	0.01	0.03	0.01	0.03	0.02	0.09	

Albite	100% cutoff							Total	
	SiO2	Al2O3	CaO	FeO	SrO	BaO	Na2O		K2O
1	68.08	20.39	0.01	0.00	0.02	0.00	11.51	0.02	100.03
2	68.40	20.19	0.02	0.00	0.00	0.01	11.60	0.01	100.23
3	68.06	20.30	0.03	0.04	0.00	0.00	11.65	0.01	100.10
4	68.75	20.36	0.03	0.00	0.00	0.00	11.64	0.00	100.80
5	68.34	20.20	0.03	0.00	0.03	0.00	11.76	0.01	100.37
6	68.99	20.29	0.01	0.02	0.00	0.00	11.66	0.01	100.98
Mean	68.44	20.29	0.02	0.01	0.01	0.00	11.64	0.01	100.42
StdDev	0.37	0.08	0.01	0.02	0.01	0.00	0.08	0.01	

Table C6.8 Microprobe feldspar standards for 10/7/99

Ortho	SiO2	Al2O3	CaO	FeO	SrO	BaO	Na2O	K2O	Total	99% cutoff
1	65.06	16.66	0.00	1.69	0.00	0.10	0.98	15.47	99.95	
2	64.98	16.72	0.01	1.71	0.00	0.07	1.02	15.62	100.12	
3	64.71	16.70	0.00	1.73	0.03	0.04	1.00	15.60	99.80	
4	65.09	16.80	0.00	1.67	0.00	0.08	0.99	15.66	100.30	
5	63.89	16.69	0.00	1.75	0.00	0.10	1.01	15.16	98.59	
6	64.19	16.49	0.00	1.71	0.00	0.02	0.94	15.16	98.52	
Mean	64.96	16.72	0.00	1.70	0.01	0.07	1.00	15.59	100.04	
StdDev	0.17	0.06	0.01	0.03	0.01	0.02	0.02	0.08		

Albite	SiO2	Al2O3	CaO	FeO	SrO	BaO	Na2O	K2O	Total	101.5% cutoff
1	68.97	20.07	0.03	0.00	0.02	0.00	11.93	0.02	101.05	
2	68.72	20.16	0.01	0.02	0.00	0.03	11.89	0.01	100.84	
3	69.18	20.21	0.00	0.00	0.00	0.01	12.06	0.01	101.48	
4	69.10	20.20	0.05	0.03	0.00	0.00	12.01	0.02	101.40	
5	69.23	20.14	0.01	0.00	0.00	0.00	11.82	0.00	101.19	
6	67.67	20.36	0.01	0.03	0.01	0.00	12.01	0.02	100.11	
Mean	68.81	20.19	0.02	0.01	0.01	0.01	11.95	0.01	101.01	
StdDev	0.59	0.10	0.02	0.01	0.01	0.01	0.09	0.01		

Table C6.9 Microprobe feldspar standards for 10/14/99

Ortho	SiO2	Al2O3	CaO	FeO	SrO	BaO	Na2O	K2O	Total
1	64.22	16.52	0.00	1.64	0.00	0.10	0.91	15.55	98.95
2	64.40	16.64	0.02	1.78	0.02	0.06	0.98	15.49	99.39
3	64.59	16.68	0.00	1.80	0.03	0.07	0.97	15.57	99.71
4	64.26	16.62	0.00	1.75	0.00	0.05	0.97	15.56	99.21
5	64.77	16.80	0.00	1.79	0.00	0.04	0.93	15.05	99.38
6	64.70	16.81	0.01	1.75	0.00	0.03	0.96	15.29	99.54
Mean	64.54	16.71	0.01	1.77	0.01	0.05	0.96	15.39	99.45
StdDev	0.21	0.09	0.01	0.02	0.01	0.02	0.02	0.22	

99% cutoff

Table C6.10 Accepted values for feldspar standards

	SiO2	Al2O3	CaO	FeO	SrO	BaO	Na2O	K2O	Total
Albite	68.24	19.90	0.03				11.94	0.04	100.15
Ortho	64.79	16.72		1.88		0.05	0.91	15.49	100.00

Appendix 7

Table C7-Matrix of D values for electron microprobe geochemistry.

Sample	EBT-1	EBT-3	EBT-4	EBT-5	EBT-6	EBT-7	EBT-8	EBT-9	EBT-10	EBT-12	EBT-16	EBT-17	EBT-18
EBT-1	3.1	4.8	7.4	6.7	5.9	5.8	3.7	2.0	7.3	4.2	5.9	3.4	2.9
EBT-3	4.3	7.4	4.8	7.9	5.1	3.9	2.8	7.1	6.4	6.5	6.7	4.0	7.7
EBT-4	7.7	5.4	3.3	7.9	3.5	4.2	7.6	7.1	3.6	7.2	8.2	7.5	5.8
EBT-5	3.6	4.4	2.0	3.6	7.5	3.7	4.5	6.5	2.5	8.8	4.9	5.4	7.7
EBT-6	4.4	3.4	4.6	7.5	3.7	4.2	8.9	8.6	8.1	2.6	3.5	7.5	5.8
EBT-7	3.4	1.1	4.6	7.9	5.1	3.9	4.5	6.5	2.5	8.8	4.9	5.4	7.7
EBT-8	1.1	3.5	3.6	7.9	3.5	4.2	8.9	8.6	8.1	2.6	3.5	7.5	5.8
EBT-9	0.9	2.6	3.8	7.5	3.7	4.2	7.8	6.5	6.0	2.1	3.7	7.5	8.4
EBT-10	7.7	7.2	6.7	3.6	7.3	7.3	6.7	9.0	8.4	3.1	5.3	9.2	9.7
EBT-12	6.6	5.7	7.3	3.4	6.8	7.1	4.1	10.6	9.9	4.1	3.9	7.1	8.1
EBT-16	3.8	3.7	3.6	7.3	5.4	3.5	2.6	6.5	3.6	6.5	1.4	5.2	5.9
EBT-17	1.9	2.4	3.8	7.7	4.2	4.7	6.0	7.1	1.5	7.2	2.4	5.5	5.8
EBT-18	2.5	4.3	3.6	9.2	4.7	3.6	8.0	7.1	2.5	8.8	2.4	5.5	5.8
EBT-19	8.5	7.6	7.7	3.8	7.8	8.9	6.6	6.5	8.1	2.6	5.4	6.4	6.9
EBT-21	6.5	5.5	5.6	3.4	6.4	6.6	6.0	9.0	6.0	3.1	4.6	4.6	5.7
EBT-22	8.8	7.8	8.3	3.5	8.1	8.9	9.3	10.6	9.9	4.1	3.9	7.1	8.1
EBT-23a	10.4	9.0	9.7	4.6	10.0	10.5	8.4	8.2	7.9	1.9	1.4	5.2	5.9
EBT-23b	8.2	8.0	7.3	2.6	7.4	7.5	5.8	6.6	5.7	3.7	1.4	5.2	5.9
EBT-30	6.0	5.0	6.4	3.2	6.3	6.4	5.6	6.8	5.8	3.6	2.4	5.5	5.8
EBT-32	6.2	4.8	6.4	3.5	6.4	6.8	6.4	8.3	7.6	5.2	5.4	6.4	6.9
EBT-32a	8.1	5.8	7.3	6.3	8.8	8.4	5.1	6.7	6.0	4.5	4.6	4.6	5.7
EBT-33	6.6	4.8	5.4	5.2	6.9	6.4	6.4	6.2	6.2	3.7	4.4	5.1	6.0
EBT-34	6.7	5.6	5.5	5.4	6.9	6.2	6.2	6.0	5.7	2.7	3.8	4.8	5.8
EBT-34a	6.0	5.8	5.0	3.8	6.1	4.9	6.8	5.9	5.9	3.4	4.4	4.8	6.2
EBT-34b	6.3	6.3	4.7	4.4	6.2	4.4	5.8	6.6	5.7	3.4	2.9	5.7	5.6
EBT-34c	6.0	5.2	6.4	3.0	5.9	7.0	6.5	6.7	6.4	5.0	5.2	5.2	6.0
EBT-34d	6.9	5.3	5.8	6.2	7.7	6.3	6.5	6.7	6.5	3.4	3.9	5.4	6.1
EBT-35	6.9	5.5	6.0	4.4	7.2	6.7	6.5	7.0	7.5	2.6	3.8	6.5	7.1
EBT-35a	7.9	6.6	7.3	4.0	7.9	8.0	7.2	8.1	4.7	5.5	5.4	3.6	4.8
EBT-35b	5.1	4.8	3.7	6.4	5.7	4.1	5.6	4.3	4.7	5.5	5.4	3.6	4.8

Table C7 continued-Matrix of D values for electron microprobe geochemistry.

Sample	EBT-1	EBT-3	EBT-4	EBT-5	EBT-6	EBT-7	EBT-8	EBT-9	EBT-10	EBT-12	EBT-16	EBT-17	EBT-18
EBT-37	7.3	5.6	6.5	5.9	8.0	7.1	6.9	7.1	6.9	5.1	4.7	5.5	6.5
EBT-38	8.9	8.0	8.0	2.8	8.5	8.4	8.7	9.0	8.5	2.3	3.8	7.7	8.5
EBT-39	2.4	2.9	3.6	7.5	3.7	5.0	2.5	3.1	1.9	7.4	7.0	3.8	1.7
EBT-40	4.7	5.1	3.2	5.7	4.0	5.0	5.0	4.3	4.2	4.9	6.2	4.4	4.1
EBT-40a	4.2	4.8	2.6	6.2	3.8	4.6	4.7	3.6	3.8	5.5	6.4	4.0	3.8
EBT-40b	5.0	5.1	3.9	4.4	4.8	4.9	5.5	4.8	4.6	3.4	4.8	4.4	4.5
EBT-40c	5.9	4.9	4.3	4.9	5.9	5.6	5.0	5.6	5.2	3.5	4.8	4.6	5.1
EBT-40d	5.9	5.4	4.7	4.3	5.7	5.8	5.6	5.8	5.4	2.4	4.5	4.8	5.1
EBT-41	3.5	4.4	2.5	6.3	3.5	4.4	4.3	3.0	3.1	5.6	6.3	3.8	3.0
EBT-43	5.0	6.6	3.9	9.2	6.2	2.1	6.9	3.9	4.9	8.6	8.6	5.0	5.6
EBT-44	6.3	7.8	6.0	12.5	7.9	6.2	7.2	5.8	6.2	12.2	12.0	7.7	6.6
EBT-45	5.4	6.8	4.2	8.1	6.3	2.6	7.3	4.5	5.4	7.8	7.6	5.1	6.0
EBT-47	6.3	5.8	5.8	3.9	6.3	6.0	6.5	6.2	5.9	2.0	3.3	5.3	5.9
EBT-48	7.2	6.2	6.2	3.9	7.1	7.2	6.5	7.3	6.7	2.0	4.3	6.1	6.4
EBT-49	9.5	8.1	8.8	4.9	8.9	9.8	8.3	9.6	9.0	3.5	5.2	8.2	8.6
EBT-50	8.8	7.6	8.0	3.8	8.3	8.9	8.0	8.9	8.3	2.4	4.4	7.4	8.0
EBT-51	7.4	6.1	6.3	4.2	7.1	7.5	6.2	7.4	6.9	2.7	4.3	6.2	6.6
EBT-52	8.6	7.3	7.3	3.9	8.1	8.3	7.6	8.6	8.0	2.5	4.6	7.2	7.8
EBT-53	8.2	7.3	6.8	3.9	7.7	7.9	7.5	8.1	7.7	2.0	4.9	6.8	7.5
EBT-54	7.3	6.7	6.1	3.6	6.6	7.0	6.8	7.2	6.8	1.9	4.5	6.1	6.7
EBT-56	2.6	3.1	4.2	6.4	3.4	5.0	3.5	3.2	2.3	6.0	5.6	3.6	2.1
EBT-61	69.7	70.0	71.3	72.7	69.8	71.7	71.0	70.1	70.0	73.8	72.2	71.4	70.0
EBT-62	5.3	5.7	5.2	8.3	5.9	6.1	6.7	4.9	5.1	7.8	8.0	5.7	4.8
BIT-42	5.3	6.0	5.1	3.8	4.5	5.1	6.7	5.3	5.2	4.2	4.2	5.1	5.6
BIT-272	5.4	7.4	7.3	6.9	4.5	6.8	8.0	6.3	5.8	8.5	7.4	7.6	6.7
BIT-288	4.9	6.4	6.3	5.6	3.0	6.7	6.7	5.8	5.0	7.2	6.4	6.8	5.7

Table C7 continued-Matrix of D values for electron microprobe geochemistry.

Sample	EBT-19	EBT-21	EBT-22	EBT-23a	EBT-23b	EBT-30	EBT-32	EBT-32a	EBT-33	EBT-34	EBT-34a	EBT-34b	EBT-34c
EBT-21	9.9	2.5	3.3	2.6	4.4	3.7	1.3	3.6	2.9	3.4	3.8	1.6	
EBT-22	7.7	2.7	4.3	3.0	5.1	4.0	4.6	3.0	4.2	3.9	4.7	3.3	4.5
EBT-23a	10.3	3.0	3.2	4.7	4.5	6.3	3.6	3.7	5.5	3.4	2.5	4.6	4.7
EBT-23b	11.8	3.6	2.7	3.7	5.5	5.2	3.9	3.2	6.3	3.9	2.6	3.4	4.0
EBT-30	9.4	4.4	2.2	3.6	6.1	3.1	2.9	4.2	4.8	4.2	3.7	3.7	4.6
EBT-32	7.5	3.8	2.2	5.2	5.9	3.3	3.7	2.0	3.6	3.3	3.1	4.4	3.7
EBT-32a	7.7	4.8	3.9	4.7	4.8	3.9	2.2	4.1	4.8	4.2	4.7	3.3	4.6
EBT-33	9.0	4.8	3.1	5.2	6.8	5.8	4.5	2.6	3.6	3.4	2.5	4.6	4.7
EBT-34	7.4	4.8	3.1	4.7	5.0	6.3	3.6	3.0	4.2	4.2	4.7	3.3	4.5
EBT-34a	7.3	5.1	3.2	5.1	6.1	4.5	3.9	3.7	5.5	3.9	2.5	4.6	4.7
EBT-34b	6.9	4.5	2.7	4.4	5.9	3.1	2.9	3.2	6.3	4.4	2.6	3.4	4.0
EBT-34c	6.8	5.5	3.6	5.2	6.7	3.3	3.7	4.2	4.8	4.4	3.7	3.7	4.6
EBT-34d	7.7	3.2	2.3	3.6	4.8	3.9	2.2	2.0	3.1	3.3	3.1	4.4	3.7
EBT-35	7.2	6.1	4.1	6.5	6.8	5.8	4.5	4.1	6.1	4.5	3.1	4.4	3.7
EBT-35a	7.8	4.1	2.3	4.6	5.0	4.2	3.1	2.6	3.6	3.7	2.8	5.1	5.2
EBT-35b	9.2	2.8	2.3	3.1	3.3	3.5	3.1	2.4	5.2	4.9	4.6	3.9	4.4
EBT-36	5.0	7.0	4.6	7.1	8.4	5.9	4.9	5.1	7.2	5.6	6.5	5.8	6.3
EBT-37	7.9	5.8	3.9	6.0	6.4	5.7	4.3	4.1	6.5	4.6	4.9	4.1	4.2
EBT-38	10.1	2.9	2.9	2.7	2.9	2.0	3.6	3.6	6.8	4.8	4.9	4.5	4.5
EBT-39	3.4	7.7	5.9	8.3	9.7	8.1	6.0	5.9	5.6	4.0	3.7	2.7	3.0
EBT-40	5.3	5.6	4.0	6.5	7.9	5.6	5.2	5.1	7.2	4.6	4.9	4.1	4.2
EBT-40a	4.6	6.3	4.5	7.0	8.5	6.1	5.5	5.4	6.8	4.8	4.9	4.5	4.5
EBT-40b	5.8	4.5	2.6	5.4	6.7	4.1	3.9	3.8	5.6	4.0	3.7	2.7	3.0
EBT-40c	6.7	4.3	2.4	4.6	5.8	4.4	3.7	3.4	4.4	2.4	3.3	3.0	3.3
EBT-40d	6.9	3.5	1.8	4.3	5.4	3.6	3.4	3.1	4.6	3.1	3.3	2.2	3.1
EBT-41	4.1	6.3	4.5	7.2	8.7	6.3	5.4	5.4	6.9	5.1	5.2	4.5	4.6
EBT-43	3.5	10.3	8.1	10.4	12.1	8.8	8.0	8.4	10.0	8.1	7.4	6.5	5.8
EBT-44	4.6	13.2	11.1	13.6	15.0	12.8	11.2	11.3	12.3	10.6	10.9	10.1	9.9
EBT-45	4.5	9.5	7.3	9.5	11.2	7.9	7.2	7.8	9.6	7.8	6.8	5.8	5.0
EBT-47	7.4	3.9	2.2	3.9	5.2	2.8	2.6	2.7	4.8	3.9	2.7	1.9	2.6
EBT-48	8.4	2.2	1.5	3.2	3.8	3.4	3.4	2.8	4.0	3.5	4.0	2.9	4.0

Table C7 continued-Matrix of D values for electron microprobe geochemistry.

Sample	EBT-19	EBT-21	EBT-22	EBT-23a	EBT-23b	EBT-30	EBT-32	EBT-32a	EBT-33	EBT-34	EBT-34a	EBT-34b	EBT-34c
EBT-49	10.8	2.4	3.7	2.6	2.1	4.3	4.7	4.0	4.2	4.6	5.1	5.4	6.3
EBT-50	10.1	1.5	2.6	2.0	2.3	3.2	4.0	3.4	4.3	4.2	4.7	4.3	5.2
EBT-51	8.6	2.8	2.0	2.9	3.6	3.7	3.5	2.7	3.5	2.7	3.6	3.5	4.3
EBT-52	9.7	2.3	2.4	2.5	2.6	3.2	3.9	3.3	3.9	3.5	4.2	3.9	4.7
EBT-53	9.3	2.1	2.1	2.9	3.4	2.9	4.1	3.6	4.4	3.6	4.1	3.6	4.2
EBT-54	8.4	2.7	2.1	3.2	4.3	2.7	3.7	3.3	4.9	3.6	4.1	2.8	3.5
EBT-56	4.1	6.6	4.8	7.1	8.6	6.7	4.8	4.7	6.5	5.0	5.4	4.8	5.3
EBT-61	69.2	73.8	72.6	74.6	74.9	73.8	72.2	72.2	72.5	72.6	71.7	73.4	73.1
EBT-62	4.9	8.6	6.7	9.7	10.6	8.4	7.3	7.2	8.0	7.1	6.2	7.0	6.9
BIT-42	6.2	5.6	3.9	5.8	7.5	3.9	3.9	4.5	7.2	5.5	4.6	3.3	3.0
BIT-272	6.5	9.3	7.9	9.5	11.2	8.1	7.1	7.7	10.8	9.2	8.9	7.1	7.2
BIT-288	6.3	7.6	6.4	8.0	9.6	6.9	6.0	6.3	9.2	7.6	7.6	6.1	6.3

Table C7 continued-Matrix of D values for electron microprobe geochemistry.

Sample	EBT-34d	EBT-35	EBT-35a	EBT-35b	EBT-36	EBT-37	EBT-38	EBT-39	EBT-40	EBT-40a	EBT-40b	EBT-40c	EBT-40d
EBT-35	5.4	2.3	2.1	2.1	3.8	5.1	8.6	3.6	1.0	2.4	2.4	1.8	3.6
EBT-35a	3.5	3.9	4.4	5.9	6.4	7.1	6.4	3.4	1.9	2.4	1.8	3.7	3.6
EBT-35b	3.1	3.6	2.8	4.1	5.3	5.9	6.9	4.5	3.0	3.3	2.4	3.7	7.2
EBT-36	5.8	2.0	3.7	2.7	3.8	4.8	5.9	5.0	6.0	5.4	6.1	7.0	10.2
EBT-37	5.3	5.3	6.5	7.3	4.1	4.8	6.4	5.2	8.3	7.7	9.2	9.7	6.8
EBT-38	3.8	6.3	5.1	5.7	3.6	5.9	4.6	4.1	1.5	1.3	5.7	6.8	6.8
EBT-39	5.7	5.5	5.4	6.2	3.5	4.8	4.8	5.9	6.0	5.5	5.7	3.1	2.1
EBT-40	4.8	5.5	3.7	4.3	3.9	4.7	4.1	4.6	4.5	4.8	2.8	2.9	2.0
EBT-40a	3.6	4.4	3.6	3.8	4.4	4.7	4.1	4.6	3.0	3.3	3.4	4.8	4.4
EBT-40b	3.9	4.1	3.0	3.1	3.9	6.1	7.1	5.2	2.9	3.6	1.8	3.1	2.0
EBT-40c	3.0	4.2	5.4	6.3	3.9	8.4	9.9	5.9	6.0	5.5	5.7	6.8	6.8
EBT-41	5.0	5.7	8.2	9.6	4.9	8.4	9.9	5.9	6.0	5.5	5.7	6.8	6.8
EBT-43	8.5	7.6	11.4	12.7	8.7	11.6	13.5	6.4	4.5	4.8	2.8	3.1	2.1
EBT-44	11.2	10.8	7.5	8.9	4.5	7.8	8.8	6.4	4.5	4.8	2.8	2.9	2.0
EBT-45	7.8	7.2	2.8	2.8	4.3	4.3	3.3	6.2	4.6	5.3	3.4	2.9	2.0
EBT-47	3.0	3.9	3.0	2.2	5.8	5.0	3.1	6.5	4.6	5.3	5.8	4.8	4.4
EBT-48	2.6	4.8	4.4	2.5	7.6	5.8	3.4	8.6	6.8	7.4	5.8	4.8	4.4
EBT-49	4.3	6.0	3.6	1.9	6.9	5.3	2.4	8.1	6.0	6.7	4.8	4.3	3.6
EBT-50	3.5	5.5	3.1	2.2	5.6	4.7	3.4	6.6	4.8	5.3	3.8	2.4	2.4
EBT-51	3.3	4.5	3.3	2.0	6.3	5.0	2.4	7.8	5.6	6.2	4.5	3.4	3.2
EBT-52	3.8	5.0	3.4	2.4	6.0	5.0	2.6	7.4	4.9	5.5	3.8	3.0	2.6
EBT-53	3.7	5.1	3.6	2.7	5.5	5.3	3.1	6.5	4.0	4.7	3.0	2.5	1.7
EBT-54	3.3	5.4	5.4	6.1	4.6	6.0	7.3	2.1	3.0	3.0	3.4	4.3	4.0
EBT-56	4.5	5.4	72.0	73.2	70.4	70.4	73.7	70.2	71.2	70.8	71.6	72.7	72.8
EBT-61	72.5	65.6	8.0	8.0	4.6	6.0	8.8	5.2	4.9	4.5	5.0	6.4	6.3
EBT-62	7.4	5.6	4.7	5.4	3.9	5.5	5.0	5.7	3.8	3.9	2.7	4.4	3.8
BIT-42	4.1	5.3	8.6	9.3	7.5	9.4	9.1	6.5	6.6	6.6	6.5	8.2	7.7
BIT-272	6.9	8.2	7.2	7.8	6.7	8.3	7.9	5.3	5.1	5.2	5.1	6.7	6.2
BIT-288	5.4	7.2	7.2	7.8	6.7	8.3	7.9	5.3	5.1	5.2	5.1	6.7	6.2

Table C7 continued-Matrix of D values for electron microprobe geochemistry.

Sample	EBT-41	EBT-43	EBT-44	EBT-45	EBT-47	EBT-48	EBT-49	EBT-50	EBT-51	EBT-52	EBT-53	EBT-54	EBT-56
EBT-43	5.2	5.3	6.8	6.7	2.6	3.2	1.5	2.3	1.5	1.1	1.5	5.4	70.2
EBT-44	7.3	2.2	6.8	6.7	2.6	3.2	1.5	2.3	1.5	1.1	1.5	5.4	70.2
EBT-45	5.2	2.2	6.8	6.7	2.6	3.2	1.5	2.3	1.5	1.1	1.5	5.4	70.2
EBT-47	4.8	7.3	11.0	8.0	4.4	3.6	2.6	1.6	1.8	2.2	6.4	73.6	4.7
EBT-48	5.2	8.7	11.6	8.0	4.4	3.6	2.6	1.6	1.8	2.2	6.4	73.6	4.7
EBT-49	7.6	11.3	14.2	10.7	4.4	3.6	2.6	1.6	1.8	2.2	6.4	73.6	4.7
EBT-50	6.8	10.4	13.5	9.7	3.6	2.3	2.6	2.3	1.5	1.1	6.4	73.6	4.7
EBT-51	5.5	9.0	11.8	8.5	3.0	1.8	2.6	1.6	1.8	2.2	6.4	73.6	4.7
EBT-52	6.5	9.9	12.8	9.1	3.4	2.0	2.2	1.8	1.8	2.2	6.4	73.6	4.7
EBT-53	5.8	9.3	12.4	8.7	3.2	1.8	2.7	1.8	1.8	2.2	6.4	73.6	4.7
EBT-54	5.0	8.5	11.6	8.0	2.6	1.9	3.4	2.5	2.0	2.2	6.4	73.6	4.7
EBT-56	2.5	6.1	8.0	6.4	4.8	5.5	7.4	6.8	5.6	6.7	6.4	73.6	4.7
EBT-61	70.8	70.8	70.2	71.4	72.7	73.9	74.3	74.0	73.6	74.0	73.9	73.6	70.2
EBT-62	4.4	6.3	8.5	6.6	6.8	7.8	9.6	8.9	8.0	8.7	8.2	7.6	4.7
BIT-42	3.9	6.0	9.9	5.1	3.5	5.0	6.9	5.8	5.4	5.7	5.2	4.4	4.4
BIT-272	6.1	7.0	9.4	6.6	7.6	8.7	10.7	9.7	9.2	9.8	9.4	8.4	5.9
BIT-288	4.8	7.1	9.3	6.7	6.5	7.2	9.1	8.2	7.5	8.2	7.8	6.8	4.6

Table C7 continued-Matrix of D values for electron microprobe geochemistry.

Sample	EBT-61	EBT-62	BIT-42	BIT-272	BIT-288
EBT-62	67.1	5.6	4.9	2.3	2.3
BIT-42	71.0	7.2	4.0	2.3	2.3
BIT-272	69.1	6.6	4.0	2.3	2.3
BIT-288	69.7	6.6	4.0	2.3	2.3

Appendix 8

Table C8-List of samples and GPS locations

Sample	Latitude	Longitude	Elevation	Location
EBT-11	77.5426	166.8096	1242.8176	Middle Barne
EBT-12	77.5424	166.8087	1251.8929	Middle Barne
EBT-14	77.5423	166.8059	1242.4655	Middle Barne
EBT-15	77.5422	166.8066	1249.8802	Middle Barne
EBT-21	77.5254	166.8571	1587.5339	Hooper's Shoulder
EBT-22	77.5255	166.8572	1586.1150	Hooper's Shoulder
EBT-23	77.5254	166.8581	1590.6536	Hooper's Shoulder
EBT-24	77.5259	166.8577	1586.8962	Hooper's Shoulder
EBT-25	77.5259	166.8582	1591.0317	Hooper's Shoulder
EBT-26	77.5259	166.8583	1588.8192	Hooper's Shoulder
EBT-28	77.5261	166.8589	1589.8392	Hooper's Shoulder
EBT-29	77.5260	166.8597	1596.1178	Hooper's Shoulder
EBT-30	77.5261	166.8598	1595.9188	Hooper's Shoulder
EBT-32	77.5260	166.8605	1597.7251	Hooper's Shoulder
EBT-33	77.5260	166.8612	1598.6956	Hooper's Shoulder
EBT-33a	77.5261	166.8619	1597.3642	Hooper's Shoulder
EBT-34	77.5261	166.8619	1600.4095	Hooper's Shoulder
EBT-34a	77.5262	166.8624	1602.8158	Hooper's Shoulder
EBT-35	77.5262	166.8625	1602.3065	Hooper's Shoulder
EBT-39	77.5262	166.8638	1607.8531	Hooper's Shoulder
EBT-40	77.5255	166.8699	1636.2501	Hooper's Shoulder
EBT-40b	77.5256	166.8676	1628.5757	Hooper's Shoulder
EBT-40c	77.5259	166.8662	1620.8545	Hooper's Shoulder
EBT-40d	77.5260	166.8650	1619.4062	Hooper's Shoulder
EBT-40f	77.5262	166.8649	1612.3356	Hooper's Shoulder

Appendix 9

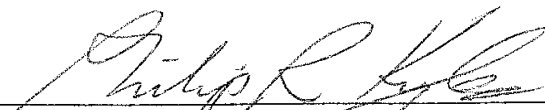
Table C9-Table of tephra stratigraphy and equivalent samples.

Sample	Equivalent	Location
EBT-19	EBT-20	Summit
EBT-41		Hooper's Shoulder
EBT-40		Hooper's Shoulder
EBT-40a		Hooper's Shoulder
EBT-40b		Hooper's Shoulder
EBT-40c		Hooper's Shoulder
EBT-40d	EBT-55	Hooper's Shoulder
EBT-40f		Hooper's Shoulder
EBT-39		Hooper's Shoulder
EBT-36		Hooper's Shoulder
EBT-35	EBT-38	Hooper's Shoulder
EBT-35a		Hooper's Shoulder
EBT-35b		Hooper's Shoulder
EBT-34c		Hooper's Shoulder
EBT-34a		Hooper's Shoulder
EBT-34	EBT-37	Hooper's Shoulder
EBT-33a		Hooper's Shoulder
EBT-33		Hooper's Shoulder
EBT-32a		Hooper's Shoulder
EBT-32		Hooper's Shoulder
EBT-31	EBT-54	Hooper's Shoulder
EBT-30	EBT-53	EBT-62 Hooper's Shoulder
EBT-29	EBT-52	Hooper's Shoulder
EBT-28	EBT-51	Hooper's Shoulder
EBT-27	EBT-50	Hooper's Shoulder
EBT-26	EBT-49	Hooper's Shoulder
EBT-25	EBT-48	Hooper's Shoulder
EBT-24	EBT-47	Hooper's Shoulder
EBT-23b	EBT-23	Hooper's Shoulder
EBT-23a	EBT-23	Hooper's Shoulder
EBT-22		Hooper's Shoulder
EBT-21		Hooper's Shoulder
EBT-9	EBT-10	EBT-18 Middle Barne
EBT-11	EBT-17	Middle Barne
EBT-12		Middle Barne
EBT-15		Middle Barne
EBT-14	EBT-16	Middle Barne
EBT-1	EBT-2	EBT-56 Terminus of the Barne
EBT-3		Terminus of the Barne
EBT-4		Terminus of the Barne
EBT-5		Terminus of the Barne
EBT-6		Terminus of the Barne
EBT-7	EBT-8	Terminus of the Barne
EBT-8		Terminus of the Barne


Table C9 continued-Table of tephra stratigraphy and equivalent samples.

Sample	Equivalent		Location
EBT-43	EBT-44	EBT-45	Terra Nova Saddle
EBT-44	EBT-45	EBT-46	Terra Nova Saddle
EBT-45	EBT-46		Terra Nova Saddle
EBT-46			Terra Nova Saddle
EBT-61			Terra Nova Summit
EBT-62			Terra Nova Summit
BIT-42			Manhaul Bay
BIT-272			Mt. DeWitt
BIT-288			Mt. DeWitt

This Thesis is accepted on behalf of the faculty
of the Institute by the following committee:



Academic Adviser



Research Advisor

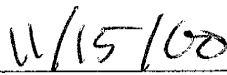


Committee Member



Committee Member

Committee Member



Date